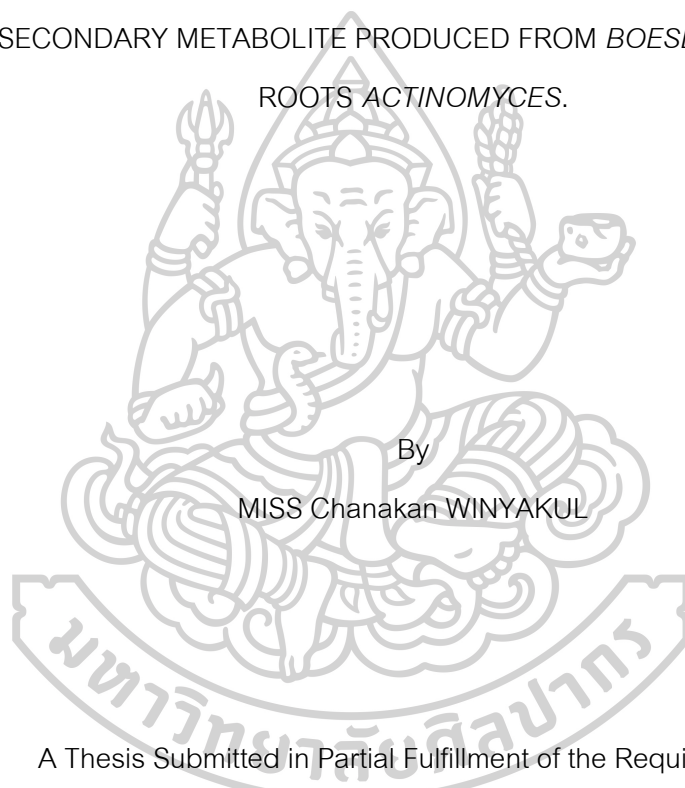




BIOLOGICAL ACTIVITIES OF SYNTHETIC HETEROCYCLIC COMPOUNDS AND
NATURAL SECONDARY METABOLITE PRODUCED FROM *BOESENBERGIA ROTUNDA*
ROOTS *ACTINOMYCES*.



By
MISS Chanakan WINYAKUL

A Thesis Submitted in Partial Fulfillment of the Requirements

for Doctor of Philosophy ORGANIC CHEMISTRY

Department of CHEMISTRY

Graduate School, Silpakorn University

Academic Year 2021

Copyright of Silpakorn University

ฤทธิ์ทางชีวภาพของสารประกอบเฮเทอโรไซคลิกที่สังเคราะห์ได้และสารทุติยภูมิที่ผลิต
จากแอคติโนมัยซีสจากรากกระชาย



วิทยานิพนธ์นี้เป็นส่วนหนึ่งของการศึกษาตามหลักสูตรปรัชญาดุษฎีบัณฑิต
สาขาวิชาเคมีอินทรีย์ แบบ 1.1 ปรัชญาดุษฎีบัณฑิต
ภาควิชาเคมี
บัณฑิตวิทยาลัย มหาวิทยาลัยศิลปากร
ปีการศึกษา 2564
ลิขสิทธิ์ของมหาวิทยาลัยศิลปากร

BIOLOGICAL ACTIVITIES OF SYNTHETIC HETEROCYCLIC COMPOUNDS
AND NATURAL SECONDARY METABOLITE PRODUCED FROM
BOESENBERGIA ROTUNDA ROOTS *ACTINOMYCES*.



A Thesis Submitted in Partial Fulfillment of the Requirements
for Doctor of Philosophy ORGANIC CHEMISTRY
Department of CHEMISTRY
Graduate School, Silpakorn University
Academic Year 2021
Copyright of Silpakorn University

Title Biological activities of synthetic heterocyclic compounds and natural
 secondary metabolite produced from *Boesenbergia rotunda* roots
 actinomyces.

By MISS Chanakan WINYAKUL

Field of Study ORGANIC CHEMISTRY

Advisor Assistant Professor Dr. Waya Phutdhawong

Graduate School Silpakorn University in Partial Fulfillment of the Requirements for
the Doctor of Philosophy

..... Dean of graduate school
(Associate Professor Jurairat Nunthanid, Ph.D.)

Approved by

..... Chair person
(Assistant Professor Dr. Kanok-on Rayanil)

..... Advisor
(Assistant Professor Dr. Waya Phutdhawong)

..... Committee
(Associate Professor Dr. Thongchai Taechowisan)

..... External Examiner
(Assistant Professor Dr. Anan Athipornchai)

60302801 : Major ORGANIC CHEMISTRY

Keyword : Heterocyclic, Diketopiperazine, Lansai A-D, Biological activities

MISS CHANAKAN WINYAKUL : BIOLOGICAL ACTIVITIES OF SYNTHETIC HETEROCYCLIC COMPOUNDS AND NATURAL SECONDARY METABOLITE PRODUCED FROM *BOESENBERGIA ROTUNDA* ROOTS *ACTINOMYCES*. THESIS ADVISOR : ASSISTANT PROFESSOR DR. WAYA PHUTDHAWONG

Heterocyclic compounds are often found to be part of the structure of many biologically active substances, including anticancer, antibacterial anti-inflammatory activities. It has also been found to be part of plant growth regulators. At present, heterocyclic compounds have been structurally developed through extensive synthesis in order to obtain better bioactive compounds. Herein, we synthesize heterocyclic derivatives in two synthetic routes. The substituent on the pyrrole and furan rings were selectively modified by substitution, reduction, Wittig and hydrolysis reactions. However, all synthetic routes of heterocyclic derivatives were not successful.

Moreover, *Actinomyces* crude extract was found many biological activities. *Boesenbergia rotunda Actinomyces* (*Streptomyces*, IP-M01) crude extract have an antibacterial, antioxidant and anticancer activities. Researcher was interested in studying the biological activity of purified active compound in this crude extract and further development the structure by chemical synthesis methods. This crude extract didn't have active purified compound which was identified by bioautography.

Lansai A-D (26-29) are 2,5-DKP derivatives that was isolated from *Streptomyces* sp. SUC1. The cytotoxicity of lansai A-D (26-29) were low toxicity against Hela and LLC-MK2 cell lines, which lansai C and D (28-29) were displayed an anti-inflammatory effect on RAW 264.7 cells. In this study, we synthesized lansai C and D derivatives by formation of 2,5 DKP ring from dipeptide and modified C-substituent by using one-pot Aldol condensation and substituent at *N*-position of DKP ring. The lansai C and D (28-29) and its derivatives were evaluated in influenza virus (H5N2) propagation inhibition by using hemagglutination assay. Lansai C (28) and derivatives

63, 65, 74a-74d, 296c were showed negative results. The molecular docking study was found that lansai C (28) and compound 74d can form H-bonds with the amino acids in the active site of the enzymes, HGPRT, H5N2, SARS-CoV-2 3CLpro and SARS-CoV-2 RBD with ACE2, with low binding energy than favipiravir. Lansai C (28), lansai D (29) and its derivatives (63-66, 74a-e, 74g, 296a-c) were evaluated the antibacterial activity which showed low activities against *S. aureus* and *E. coli* (MIC > 512 µg/mL).



ACKNOWLEDGEMENTS

I would like to take this opportunity to thank all the people who have supported me during my education. I could not have performed my work without their help.

First of all, I would like to express my sincere appreciation to Assistant Professor Dr. Waya S. Phutdhawong, my advisor for her guidance and support throughout my graduate studies including the revision of this thesis and valuable suggestions in my life.

To Associate Professor Dr. Weerachai Phutdhawong for the financial support.

To Associate Professor Dr. Thongchai Taechowisan for his helpful support and suggestion throughout my study.

To Associate Professor Dr. Jitnapa Sirirak for her helpful support and suggestion throughout my study.

To committee members, Assistant Professor Dr. Kanok-on Rayanil and Assistant Professor Dr. Anan Athipornchai for their time, helpful comments, and suggestions.

I would like to thank the Department of Chemistry, Faculty of Science, Silpakorn University, and all staff for their help as well.

To the Department of Microbiology, Faculty of Science, Silpakorn University, and all staff for their help with the facility, equipment, and chemicals that used to test the biological activity.

Finally, I would like to thank my dad and mom, my sister for their love and support.

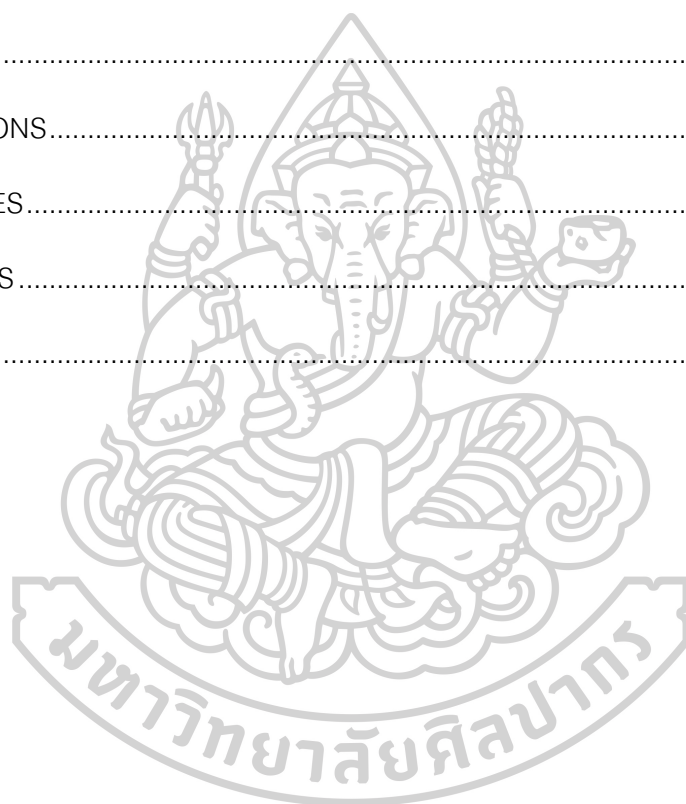
MISS Chanakan WINYAKUL

TABLE OF CONTENTS

	Page
ABSTRACT	D
ACKNOWLEDGEMENTS.....	F
TABLE OF CONTENTS.....	G
LIST OF TABLES.....	J
LIST OF FIGURES	K
LIST OF SCHEMES.....	M
CHAPTER 1	1
INTRODUCTION.....	1
1. Heterocyclic compounds	1
1.1 Furans.....	1
1.2 Pyrroles.....	1
1.3 Indoles.....	2
1.4 2,5-diketopiperazines.....	4
2. <i>Boesenbergia rotunda</i> (L.) Actinomyces.....	5
3. Lansai compound	6
Figure 5. Lansai compounds from <i>Streptomyces sp.</i> SUC1 crude extract.....	6
4. Objective of this study	7
5. Scope of this study	7
6. Synthetic plan of this study.....	7
6.1 Synthetic plan of heterocyclic compound derivatives.....	7
6.2 Synthetic 2,5-diketopiperazine derivatives	9

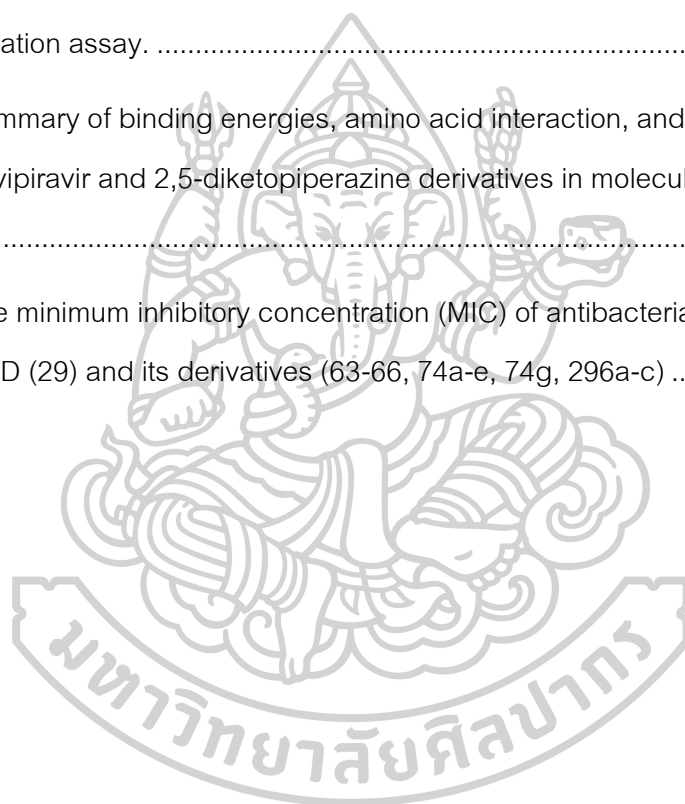
CHAPTER 2	12
LITERATURE REVIEW	12
1. Previous study of discover and synthesis of substituted of heterocyclic compounds.	12
CHAPTER 3	46
EXPERIMENTAL	46
1. General methods for the synthesis.....	46
2. Synthesis of pyrrole and furan derivatives	46
3. Identification of <i>Boesenbergia rotunda Actinomyces</i> crude extract.....	65
4. Lansai C and D derivatives.....	66
4.1 Extraction, purification and structure elucidation of Lansai compounds	66
4.2 Synthesis of Lansai C and D derivatives	66
5. Identification of <i>Boesenbergia rotunda Actinomyces</i> crude extract.....	85
6. Biological activities	85
6.1 Cytotoxicity activity.....	85
6.2 Antiviral activity.....	87
6.3 Antibacterial activity	87
CHAPTER 4	89
RESULTS AND DISCUSSION	89
1. The first synthetic route of pyrrole derivatives.....	89
2. The second synthetic route of pyrrole and furan derivatives	95
3. Results of Identification of <i>Boesenbergia rotunda Actinomyces</i> crude extract.....	96
4. Results of the synthesis of Lansai C and D derivatives	97

4.1 Extraction, purification and structure elucidation of Lansai compounds.	97
4.2 The synthesis of Lansai C and D derivatives.	97
5. Results of the Biological activities	101
5.1 Cytotoxicity activity.....	101
5.2 Antiviral activity.....	102
5.3 Antibacterial activity	108
CHAPTER 5	110
CONCLUSIONS.....	110
REFERENCES.....	113
APPENDIXES	120
VITA	172



LIST OF TABLES

	Page
Table 1. The cytotoxicity of Lansai A-D (26-29) against Hela cancer cell line and LLC-MK2 normal cell line.	102
Table 2. Summary of influenza virus (H5N2) propagation inhibition in embryonated chicken eggs of Lansai C (28), Lansai D (29), and its derivatives detected by hemagglutination assay.	103
Table 3. Summary of binding energies, amino acid interaction, and hydrogen bond length of Favipiravir and 2,5-diketopiperazine derivatives in molecular docking studies.	105
Table 4. The minimum inhibitory concentration (MIC) of antibacterial activity of Lansai C (28), Lansai D (29) and its derivatives (63-66, 74a-e, 74g, 296a-c)	109



LIST OF FIGURES

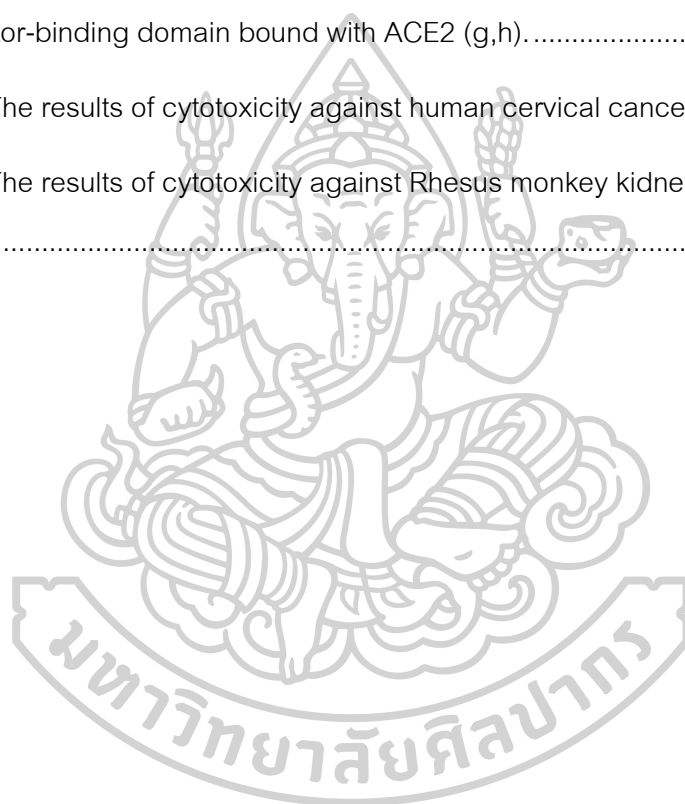
	Page
Figure 1. Structure of furan derivative.....	1
Figure 2. Structure of pyrrole derivative.....	2
Figure 3. Structure of indole derivatives.	3
Figure 4. Structure of 2,5-DKP derivatives.....	4
Figure 5. Lansai compounds from <i>Streptomyces</i> sp. SUC1 crude extract.	6
Figure 6 Structure of endostemonines A-J (107-116) (Zhao et al., 2020).....	16
Figure 7. Structure of all isolated prenylated 2,5-DKPs from a co-culture of <i>Penicillium</i> sp. DT-F29 with <i>Bacillus</i> sp. B31. (Yu et al., 2017)	27
Figure 8. Structure of rosellin A (175) and rosellin B (176) (Lohmann et al., 2018).....	28
Figure 9. Structure of botryosulfuranols A (177), B (178) and C (179) isolated from the endophytic fungus <i>Botryosphaeria mamani</i> E224 from the fresh leaves of <i>Bixa Orellana</i> (Bixaceae) (Barakat et al., 2019).	29
Figure 10. Structure of (-)-(S)-variecolortide D (180a), (+)-(R)-variecolortide D (180b) and brevicompanine I (182) and three known 2,5-DKP alkaloids (181, 183, 184) (Shan et al., 2020).....	29
Figure 11. Structure of Lansai A-D.....	43
Figure 12. Structural elucidation of Lansai A-D (26-29).	97
Figure 13. Zimmerman–Traxler model.	100
Figure 14. NOEDIFF and NOE contracts for stereoisomers of compounds 73e, 74d, and 296c.....	101
Figure 15. Comparison of the binding position of Favipiravir (green), Lansai C (28) (pink), compound 64 (brown), compound 66 (purple), compound 74a (orange),	

compound 74b (red), compound 74c (yellow), and compound 74d (blue) in the cavity of
 (a) human hypoxanthine-guanine phosphoribosyltransferase (HGPRT), (b)
 neuraminidase from H5N2 avian influenza virus, (c) SARS-CoV-2 3CL main protease,
 and (d) SARS-CoV-2 spike receptor-binding domain bound with ACE2. 104

Figure 16. Hydrogen bond interactions of compound 74d (blue) and Lansai C (28)
 (pink) in the cavity of human hypoxanthine-guanine phosphoribosyltransferase (a,b),
 Avian influenza virus H5N2 (c,d), COVID-19 3CL main protease (e,f), and SARS-CoV-2
 spike receptor-binding domain bound with ACE2 (g,h). 108

Figure 17. The results of cytotoxicity against human cervical cancer cells (HeLa)..... 167

Figure 18. The results of cytotoxicity against Rhesus monkey kidney cells (LLC-MK2).
 167

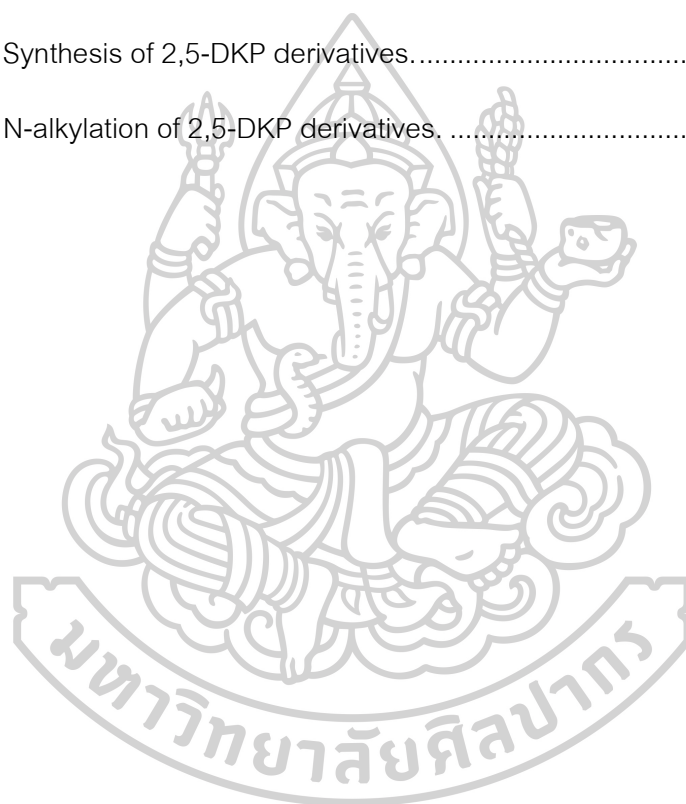


LIST OF SCHEMES

	Page
Scheme 1. The first synthetic plan of plant growth regulators as pyrrole derivatives.	8
Scheme 2. The second synthetic plan of 2,4-disubstituted pyrrole and furan derivatives.	9
Scheme 3. The first synthetic plan of 2,5-DKP derivatives.....	10
Scheme 4. The second synthetic route of 2,5-DKP derivatives.	11
Scheme 5. Synthesis of pyrroloazepinone 81 (Martínez & Villarreal, 2010).	13
Scheme 6. Synthesis of azepinone derivative 94 and 95 (Martínez & Villarreal, 2010)...	14
Scheme 7. Synthesis of pyrrolyl-indomethacin derivatives 101 and 102 (Serra Moreno et al., 2012).....	15
Scheme 8. Synthesis of indomethacin derivative 106 (Serra Moreno et al., 2012).	16
Scheme 9. Synthesis of tolmetin derivatives 121a-f, 122a-c, 123a-c, and 124a-c (Kassab et al., 2021).....	18
Scheme 10. Synthesis of aroyl-pyrrolyl-hydroxy-amides (APHAs) 133a-i and 134a-i as a HDAC inhibitors. (Mai et al., 2009).....	20
Scheme 11. Synthesis of 3,5-diaryl-1H-pyrrole-2-carboxamide derivatives (compounds 140a-f). (Zubia et al., 2009).....	22
Scheme 12. Synthesis of pyrrole-based hydroxamate (compound 146a-g and 147a-g) as HDAC inhibitor. (Valente et al., 2009)	24
Scheme 13. Synthesis of 4-substituted 6-(3-acetyl-2-methyl-1H-pyrrol-1-yl)-N-hydroxyhexanamide derivatives (151a-z) (Singh et al., 2021).	25

Scheme 14. Synthesis of 4-substituted spiro[(dihydropyrazin2,5-dione)-6,3'-(2',3'-dihydrothieno[2,3-b]naphtho-4',9'-dione)] derivatives (188a-p) (Gomez-Monterrey et al., 2008).....	30
Scheme 15. Synthesis of oxyprenylated diketopiperazine derivatives (192, 196 and 202) (Mollica et al., 2014).	32
Scheme 16. Synthesis of 2,5-diketopiperazine derivatives 205a-k, 206a-k and 207a-k (Liao et al., 2016).....	33
Scheme 17. Synthesis of compound 212a-h (Fu et al., 2018).	34
Scheme 18. Synthesis of plinabulin derivatives (217a-h, 218 and 219) (Fu et al., 2018).	35
Scheme 19. Synthesis of 2,5-DKP derivatives (222, 223 and 224) (Labriere et al., 2018).	37
Scheme 20. Synthesis of compound 227 (Labriere et al., 2018).	37
Scheme 21. Preparation of compound 229, 230 and 231 (Labriere et al., 2018).....	38
Scheme 22. Preparation of tetrasubstituted 2,5-DKP derivatives 234 and 236 (Labriere et al., 2018).....	39
Scheme 23. Synthesis of piperazine-2,5-dione derivatives 244 and 245 (Jassem et al., 2020).....	40
Scheme 24. Synthesis of Neoechinulin B (250a) (Nishiuchi et al., 2022).	41
Scheme 25. Synthesis of Deprenylneoechinulin B (250b) (Nishiuchi et al., 2022).	41
Scheme 26. Synthesis of 3-arylmethylene-6-methylenepiperazine-2,5-diones (250c-q) (Nishiuchi et al., 2022).....	42
Scheme 27. Total synthesis of (-)-Lansai B (Wang & Reisman, 2014).....	45
Scheme 28. Acylation of pyrrole (3).....	89
Scheme 29. Preparation of N-substituted pyrrole keto-ester derivatives.....	90

Scheme 30. Reduction of pyrrole keto-ester derivatives.....	91
Scheme 31. Reductive elimination of pyrrole keto-ester derivatives.....	93
Scheme 32. Methylation of compound 276.	94
Scheme 33. Preparation of pyrrole-2-acetic acid.....	95
Scheme 34. Preparation of 2,4-disubstituted heterocyclic derivatives.	96
Scheme 35. Synthesis of tetrasubstituted 2,5-DKP derivatives 63-66.	98
Scheme 36. Synthesis of 2,5-DKP derivatives.....	99
Scheme 37. N-alkylation of 2,5-DKP derivatives.....	100



CHAPTER 1

INTRODUCTION

1. Heterocyclic compounds

Heterocyclic compound is a cyclic molecule that have three to more than 10 carbon atoms and have the hetero atom such as oxygen, nitrogen and sulfur atom at least one atom in the ring. The heterocyclic compound containing oxygen atom such as furan, nitrogen atom such as pyrrole, pyridine and indole and sulfur atom such as thiophene.

1.1 Furans

Furan (1) is a five-membered heterocyclic ring which was contained with one oxygen atom. Many furan compounds were found in several biological activity such as Mumiamicin (2) (Kimura et al., 2018) (Figure 1) which was extracted from *Actinomyces, Mumia* sp. (YSP-2-79), from marine sponge in Kagoshima district, Japan. Mumiamicin showed the biological activity, antioxidation and antibacterial such as *B. subtilis*, *K. rhizophila* and *E. coli*.

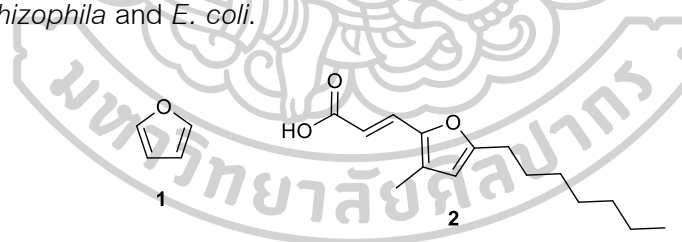


Figure 1. Structure of furan derivative.

1.2 Pyrroles

pyrrole (3) is a five-membered heterocyclic ring containing one nitrogen atom. Pyrrole compounds plays important roles in natural products such as proline (4), chlorophyll (5) and heme (6). Moreover, Rhazinilam (7) (David et al., 1997), pyrrole hydroxamic acid (8,9) (Zubia et al., 2009) Makaluvamine A (10) (Nijampatnam et al., 2014) and Prodigiosin (11) (Hu et al., 2016) were evaluated in biological activities as anticancer, antibacterial, antimalarial and antibiotic activity, respectively. T h e

phenylpyrrole (12,13) (Brindisi et al., 2016) showed enzyme inhibitory activity against HDAC1 and HDAC6 enzymes with IC_{50} values of 96.0 ± 11.8 and 36.0 ± 2.9 nM, respectively. The aroyl-pyrrolyl-hydroxy-amides (APHAs) (14-16) (Mai et al., 2009) were showed inhibitory activity against both maize HD2 enzyme with IC_{50} values of 0.05 and 0.23 μ M, respectively (Figure 2).

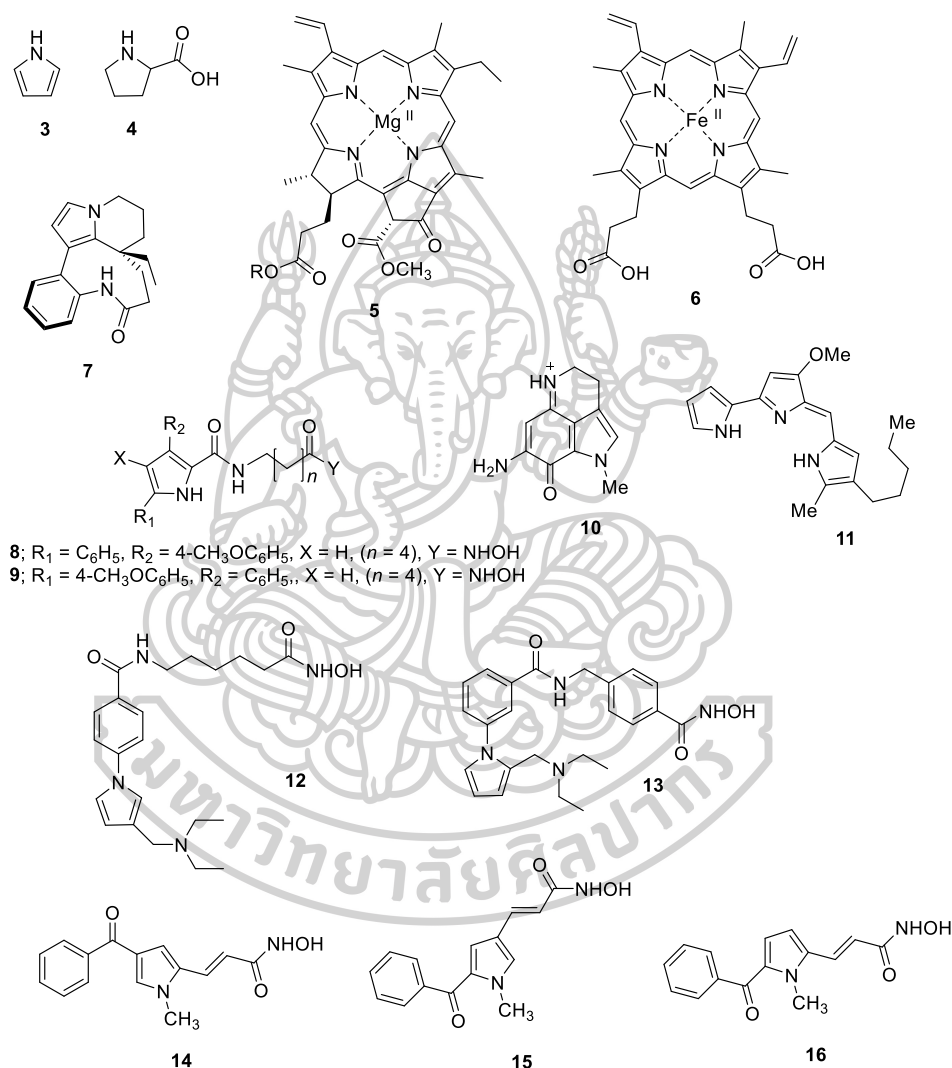


Figure 2. Structure of pyrrole derivative.

1.3 Indoles

Indole (17) is an aromatic heterocyclic compound that has bicyclic structure, consisting of pyrrole ring fused benzene ring. Indole is one of heterocyclic compound which was widely found in nature such as plants, fungi and marine organism.

Many indole derivatives have interesting biological activity such as 1-benzyl-indole-3-carbinol (**18**), apylsinopsin (**19**) and pityriacitin (**20**) which were processed as anti-breast cancer, anti-malarial and anti-prostate cancer activity, respectively. Moreover, some indole derivatives were currently used as medicine such as indomethacin (**21**) which was used as anti-inflammatory drug for treatment of rheumatoid disease, Panobinostat (**22**) (Singh et al., 2021) used as HDAC inhibitor drug. Furthermore, the 3-carboxylic substituted indole derivatives, indole-3-acetic acid (IAA) (**23**), indole-3-propionic acid (IPA) (**24**) and indole-3-butyric acid (IBA) (**25**) are used as plant growth regulator (Figure 3).

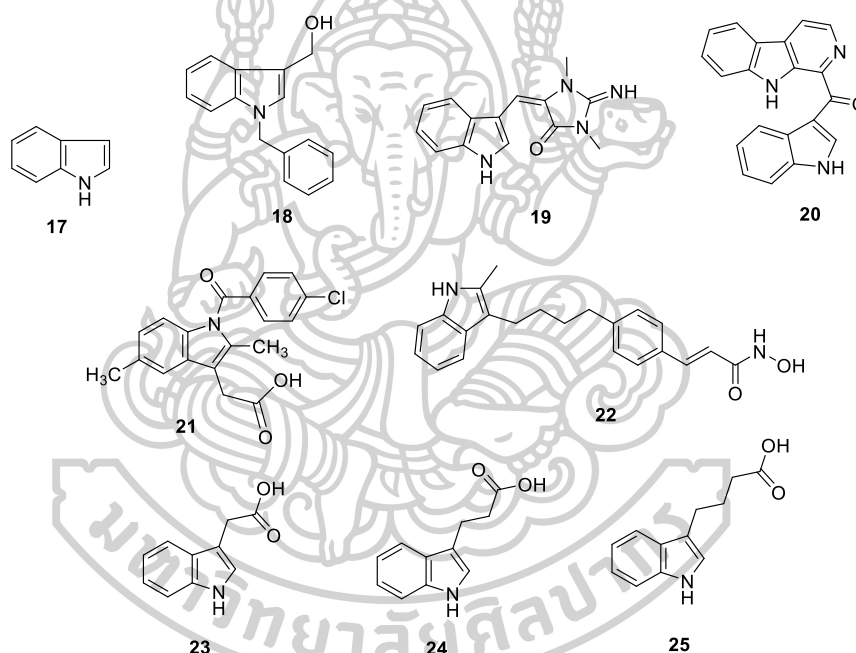


Figure 3. Structure of indole derivatives.

From the important of heterocyclic compound as described above which their derivatives have been found many biological activities. Therefore, in this study was interested in the synthesis of plant growth regulator by develop the target molecule by conversion of indole moiety to pyrrole compound as core structure as shown in synthetic plan scheme 1. This target molecule is assumed that it could have properties as plant growth regulators as well as IAA. Moreover, the synthesis of 2,4-disubstituted heterocyclic derivatives was proceeded for study their biological activity such as anticancer activity as shown in synthetic plan scheme 2.

1.4 2,5-diketopiperazines

2,5-diketopiperazine (2,5-DKP) (Figure 4) is a six-membered cyclic dipeptide that was often found alone or embedded as a part of compound in a variety of natural products from microorganisms, plants and animals. The unique 2,5-DKP structure with rigid structure, chiral nature and variety of side chain resulted in the ability in binding with a wide variety of receptors that makes 2,5-DKP scaffolds were employed to drug discovery. The bioactivity of both natural and synthetic 2,5-DKP have been found in decade year ago, inhibition of PDE5 and oxytocin, neuroprotective, anxiolytic, bioherbicide, anti-inflammatory, anti-tumor, anti-oxidative, anti-fungal, anti-bacterial, anti-hyperglycemic and anti-viral activities (Borthwick, 2012).

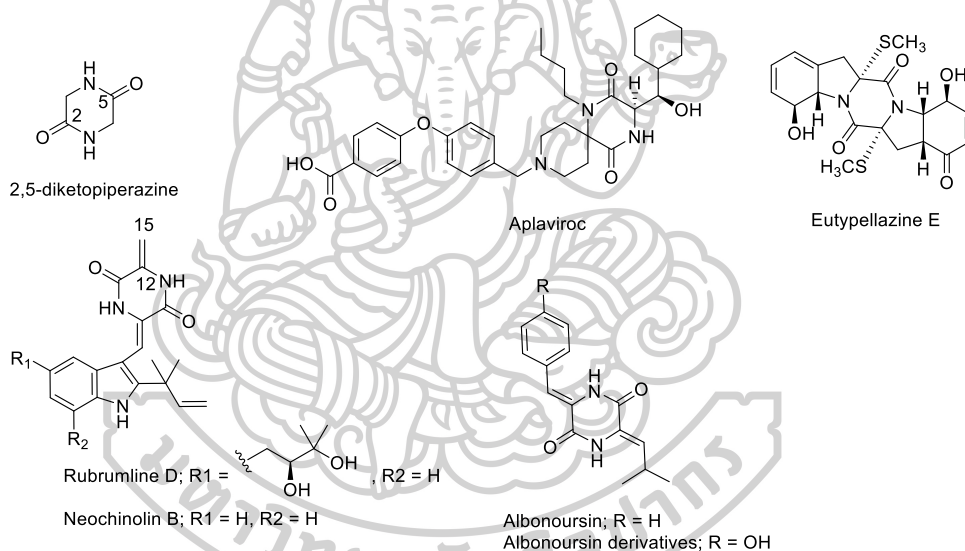


Figure 4. Structure of 2,5-DKP derivatives.

Many 2,5-DKP compounds have been found the antiviral activity. For instance, Aplaviroc (APL) (figure 10) was exhibited high-affinity binding to chemokine co-receptor 5 (CCR5) that was developed for treatment of patients with human immunodeficiency virus type 1 (HIV-1) [1]. Eutypellazine A-L (figure 10) were isolated from fungus *Eutypella* sp. MCCC 3A00281 could inhibit the replication of HIV-1 with low toxicity ($CC_{50} > 100$). Eutypellazine E was showed the most inhibitory effect at IC_{50} $3.2 + 0.4 \mu\text{M}$. The structure-activity relationship study was showed that the thiomethyl group at C-2/C-2' and double bond at C-6'/C-7' in Eutypellazine E enhancing the activity more

than those analogues (Niu et al., 2017). Rubrumlines D and Neoechinulin B (figure 10) were isolated from the fungus *Eurotium rubrum*, were exhibited antiviral activity against the influenza A/WSN/33 virus with the inhibitory rate 52.64% and 70.48% (IC_{50} 126.0, 27.4 μ M and CC_{50} >200 μ M), respectively. The presence of double bond at $\Delta^{12,15}$ unit of Rubrumlines D was significantly enhanced the antiviral activity. In addition, the absence of isoprenyl or oxygenated isoprenyl group at indole ring of Neoechinulin B was showed the most active in activity (Figure 4) (Chen et al., 2015). Wang and co-worker reported the Albonoursin and its derivative (R= OH, (3 Z,6 Z)-3 -(4 -hydroxybenzylidene)-6 -isobutylidenepiperazine-2,5-dione) were displayed influenza virus activity against H1N1 with IC_{50} at 41.5 ± 4.5 and 6.8 ± 1.5 μ M, respectively (Wang et al., 2013).

Heterocyclic compounds as described above were received by synthesis and nature. However, heterocyclic derivative compounds that have the new biological activity have been imported to develop for medicals and pharmaceuticals by using many new methodologies for the synthesis to afford the new heterocyclic compounds. Moreover, the isolation of heterocyclic compound from natural organisms have been always carried out especially from an *Actinomyces*.

2. *Boesenbergia rotunda* (L.) *Actinomyces*.

Boesenbergia rotunda (L.) is a common medicinal plant that useful in both food and health of consumer which the previous study was found that the crude extract of *Actinomyces* from root of *Boesenbergia rotunda* (L.) have an antibacterial activity against *B. cereus*, *B. subtilis*, *S. aureus*, and *C. albicans* with MIC 0.5, 0.5, 0.5 and 256 μ g/mL, respectively. This crude extract could be exhibited the antioxidant with IC_{50} value 259.27 μ g/mL and the total phenolic acid was observed in 0.216 ± 1.48 mg GAE/g. Moreover, crude extract was exhibited the anticancer activities against Hela, HepG2 and Huh 7 with IC_{50} value 5.28, 31.54 and 68.05 μ g/mL, respectively, and showed the toxicity with L929 cell line at IC_{50} 161.76 μ g/mL. (Sujanya)

From the biological activity of *Actinomyces* crude extract, the researcher was interested in studying the chemical composition of this crude extract and further

development of the structure by chemical synthesis methods and study the biological activity these chemical composition.

3. Lansai compound

The extraction of secondary metabolite from *Actinomyces*, *Streptomyces* sp. SUC1, endophytic on the aerial roots of *Ficus benjamina* in silpakorn university, Nakhonpathom, was afforded the crude extract which could be exhibited anticancer activity against BC and KB cell lines with IC_{50} of 3.41 and $> 20 \mu\text{g/mL}$, respectively. The crude extract possessed the antifungal activity against *Colletotrichum musae* (*C. musae*) with MIC of $15 \mu\text{g/mL}$. The identification of purify compound study was found that this crude extract was consisted of 4 purify compound, Lansai A (LS-A)(**26**), Lansai B (LS-B)(**27**), Lansai C (LS-C)(**28**) and Lansai D (LS-D)(**29**) which were 2,5-DKP as a core structure (figure 11). LS-B was only weakly active against BC cell line with IC_{50} of $15.03 \mu\text{g/mL}$ while another compound were inactive (Tuntiwachwuttikul et al., 2008). All Lansai compound were inactive against *C. musae* and LS-C and LS-D were displayed an anti-inflammatory effect on RAW 264.7 cells (Taechowisan et al., 2009, 2010).

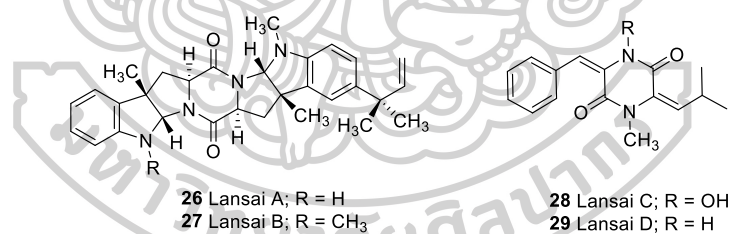


Figure 5. Lansai compounds from *Streptomyces* sp. SUC1 crude extract.

The structure of Lansai C and D (Figure 5) has benzylidene and alkyldene substituents at 3 and 6 positions of the 2,5-DKP core structure. In comparison with the presence of a double bond at positions C-3 and C-6 of Nеоechinulin, the structure of Lansai C and D would process an antiviral activity effect. In addition, the presence of substituents on α -carbon is in the opposite direction to *N*-substituents, which could orient the functionalized chain in the appropriate direction to receptors (Saavedra et al.,

2020). Therefore, in this research, 2,5-DKP derivatives have been designed by emulating Lansai C and D scaffolds and additionally substituted at the position of nitrogen atoms of the 2,5-DKP ring by *N*-alkylation reaction as shown in synthetic plan 3 and 4. These target compounds were used to study the evaluation of antiviral activity.

4. Objective of this study

1. To design and synthesize the heterocyclic compounds which possessed plant growth regulator activity.
2. To develop the heterocyclic compound which possessed biological activities.
3. To identify the bioactive compounds from crude extract of *Actinomyces* which was isolated from *Boesenbergia rotunda* root.
4. To evaluate the biological activities and plant growth regulators activity of the synthetic heterocyclic derivatives.

5. Scope of this study

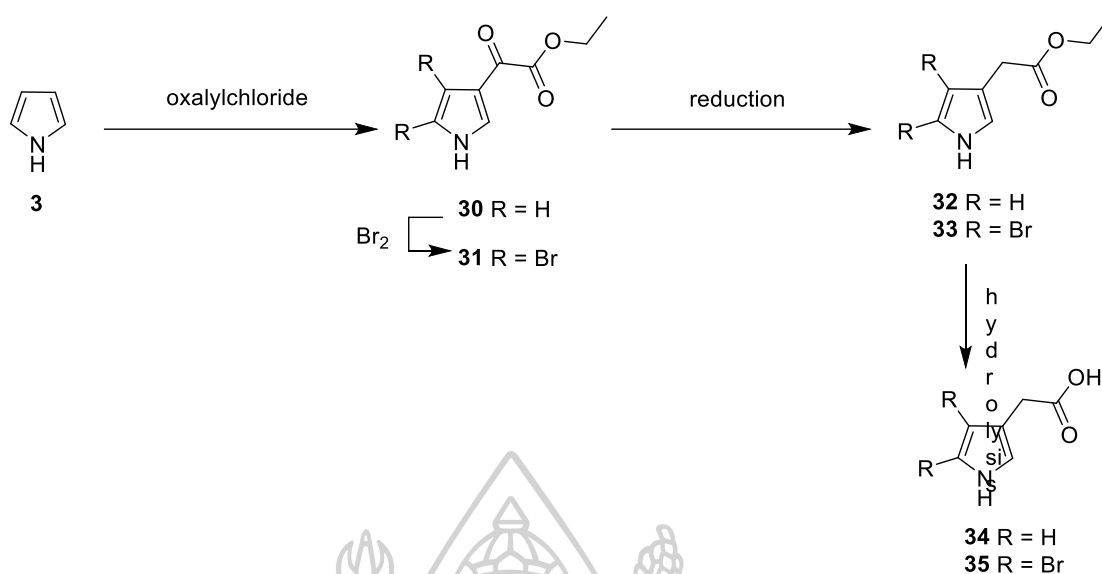
Identify the bioactive compounds from crude extract of *Actinomyces* which was isolated from *Boesenbergia rotunda* root. Synthesized, confirmed the structure of the heterocyclic derivatives and tested the biological activity.

6. Synthetic plan of this study

6.1 Synthetic plan of heterocyclic compound derivatives

6.1.1 Synthetic plan 1

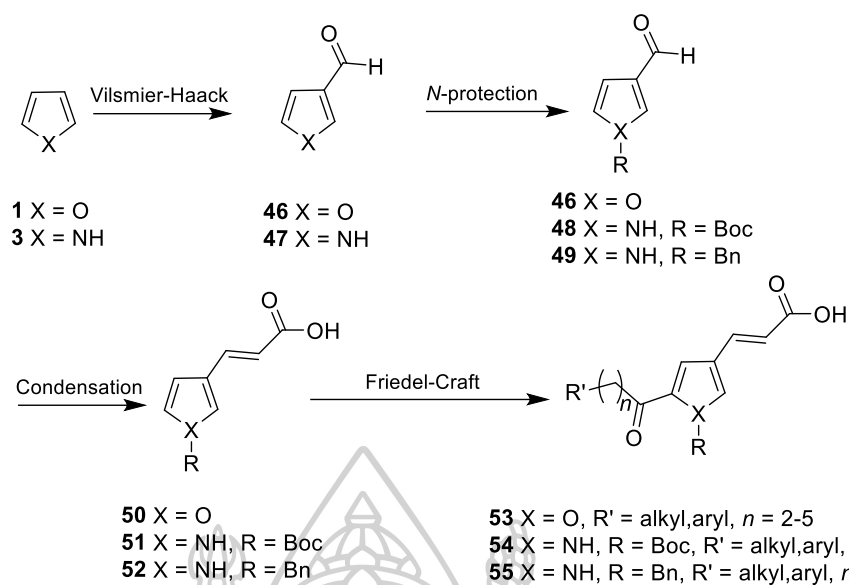
The first synthetic plan of heterocyclic compound derivatives is synthesis of plant growth regulators as pyrrole derivatives. Pyrrole derivative (34,35) would be synthesized from pyrrole (3) which was substituted with oxalylchloride and brominated with bromine. The *alpha* carbonyl of oxalyl group would be reduced to CH₂ to provide compound 32,33 followed by hydrolysis of ester moiety to carboxylic.



Scheme 1. The first synthetic plan of plant growth regulators as pyrrole derivatives.

6.1.2 Synthetic plan 2

The second synthetic plan of heterocyclic compound derivatives is synthesis of 2,4-disubstituted of five-membered heterocyclic derivatives, furan and pyrrole. The derivatives would be synthesized by using Vilsmier-Haack reaction of five-membered heterocyclic ring followed by *N*-protection. Then, condensation of aldehyde (46,48,49) with using Horner-Wadsworth-Emmons reaction to provide α,β -unsaturated carboxylic acid (50-52). The α,β -unsaturated carboxylic acid (50-52) would be second substituted via Friedel-Craft reaction to provide 2,4-disubstituted of five-membered heterocyclic derivatives (53-55).

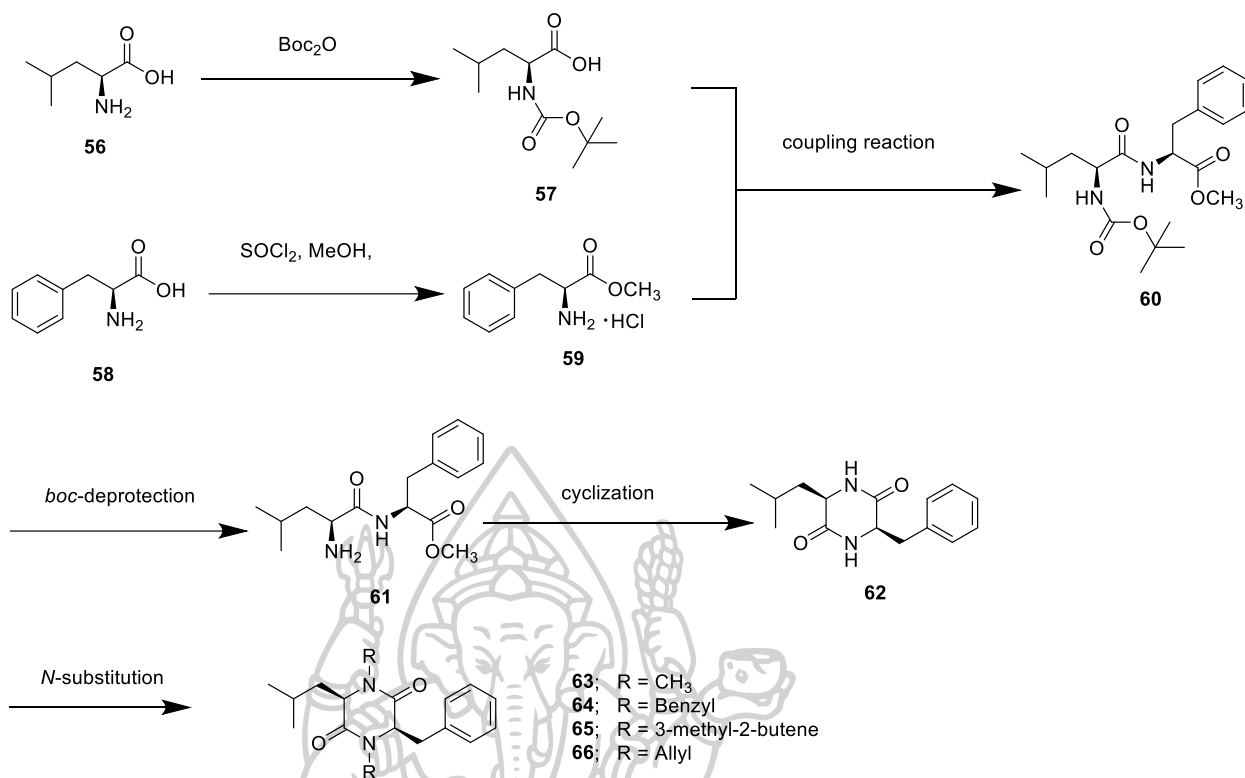


Scheme 2. The second synthetic plan of 2,4-disubstituted pyrrole and furan derivatives.

6.2 Synthetic 2,5-diketopiperazine derivatives

6.2.1 Synthetic plan 1

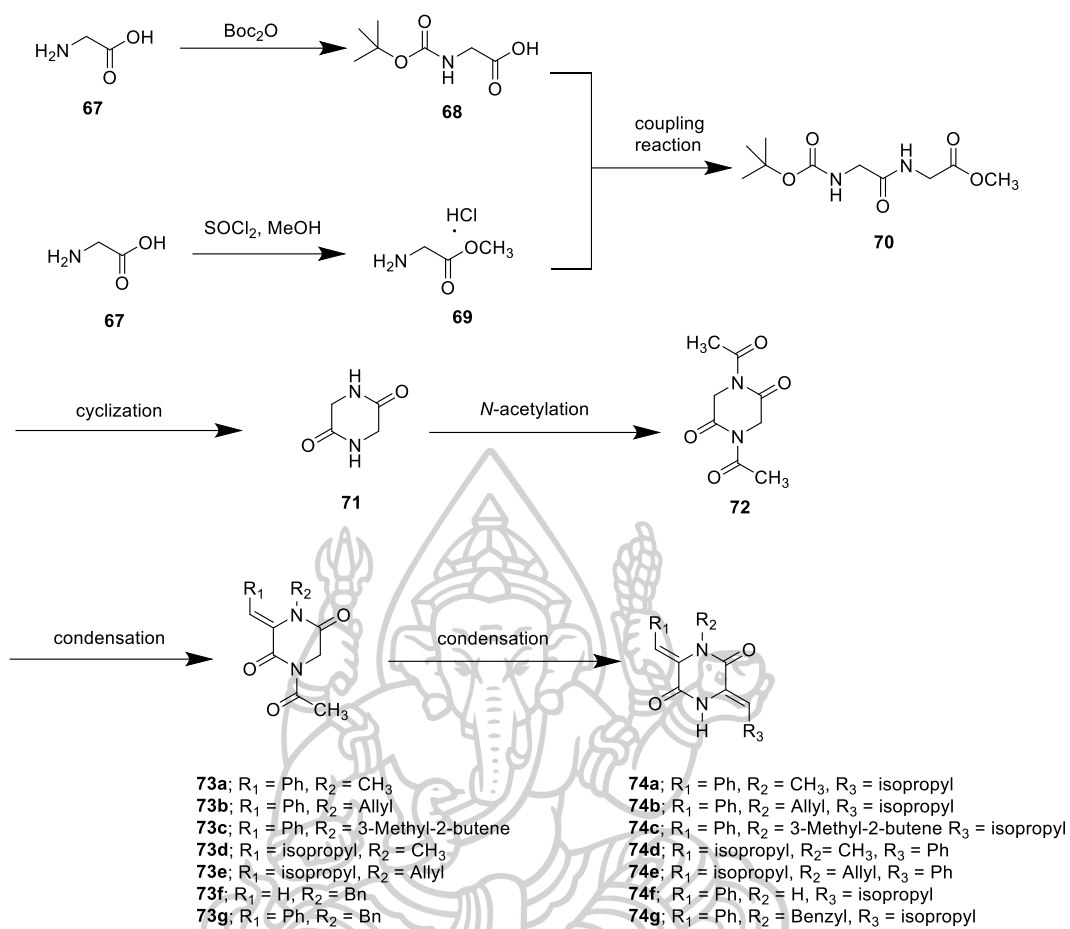
The first synthetic route of 2,5-diketopiperazine derivatives would be started from coupling reaction of protected amino acid, *N*-boc-leucine (**57**) and phenylalanine methyl ester hydrochloride (**59**). Then, *N*-deprotection of compound **60** followed by intramolecular cyclization to afford compound **62**. Finally, *N*-substitution with alkyl or aryl group would be provided compound **63-66**.



Scheme 3. The first synthetic plan of 2,5-DKP derivatives.

6.2.2 Synthetic plan 2

The second synthetic route of 2,5-diketopiperazine derivatives would be started from coupling reaction of protected amino acid, *N*-*boc*-glycine (68) and glycine methyl ester hydrochloride (69), *N*-deprotection followed by intramolecular cyclization of compound 70 would be performed to afford glycine anhydride (71). Compound 73a-g would be synthesized from *N*-acetylation of compound 71, condensed with the first aldehyde and deacetylation followed by *N*-alkylation, respectively. Compound 73a-g would be undergone a second condensation with another aldehyde to provide compound 74a-g.



Scheme 4. The second synthetic route of 2,5-DKP derivatives.

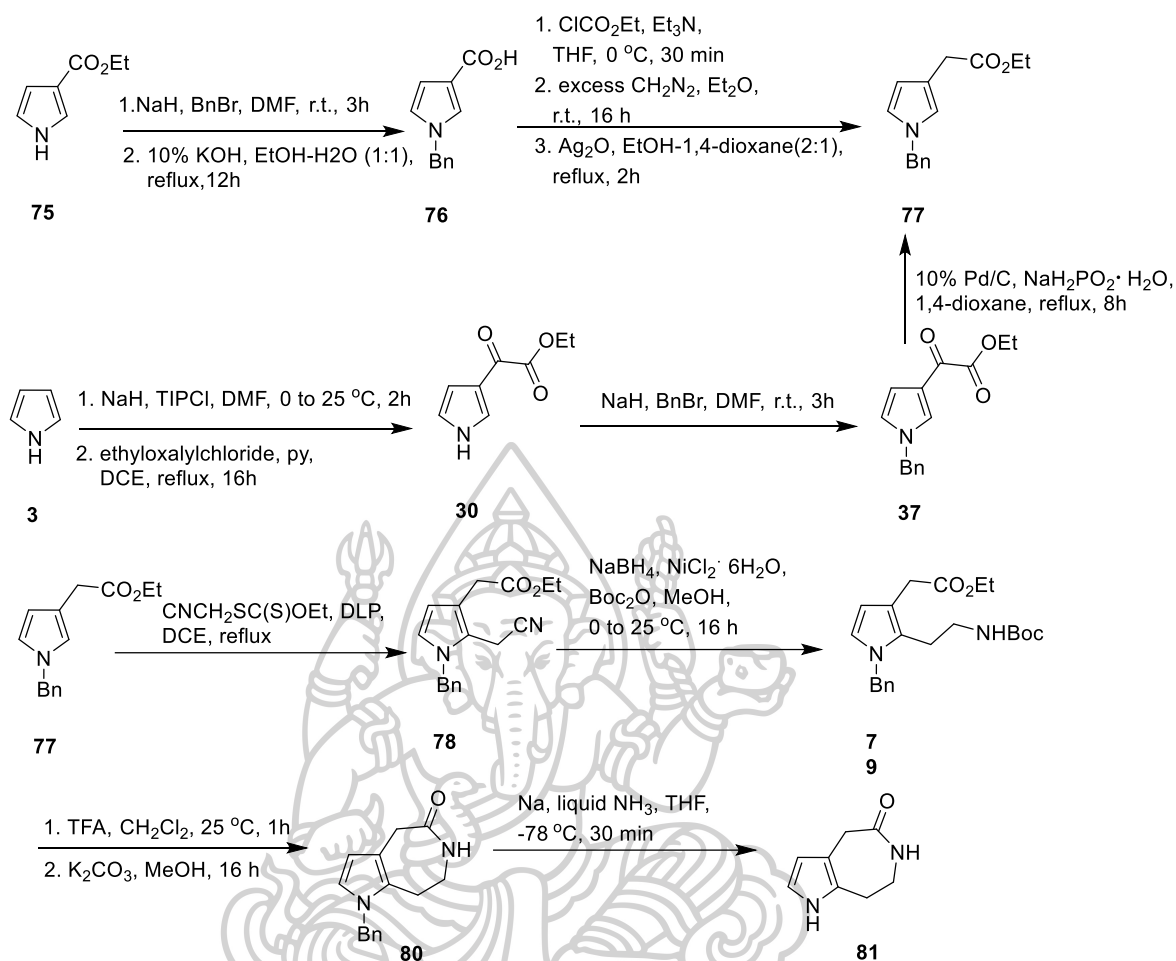
CHAPTER 2

LITERATURE REVIEW

1. Previous study of discover and synthesis of substituted of heterocyclic compounds.

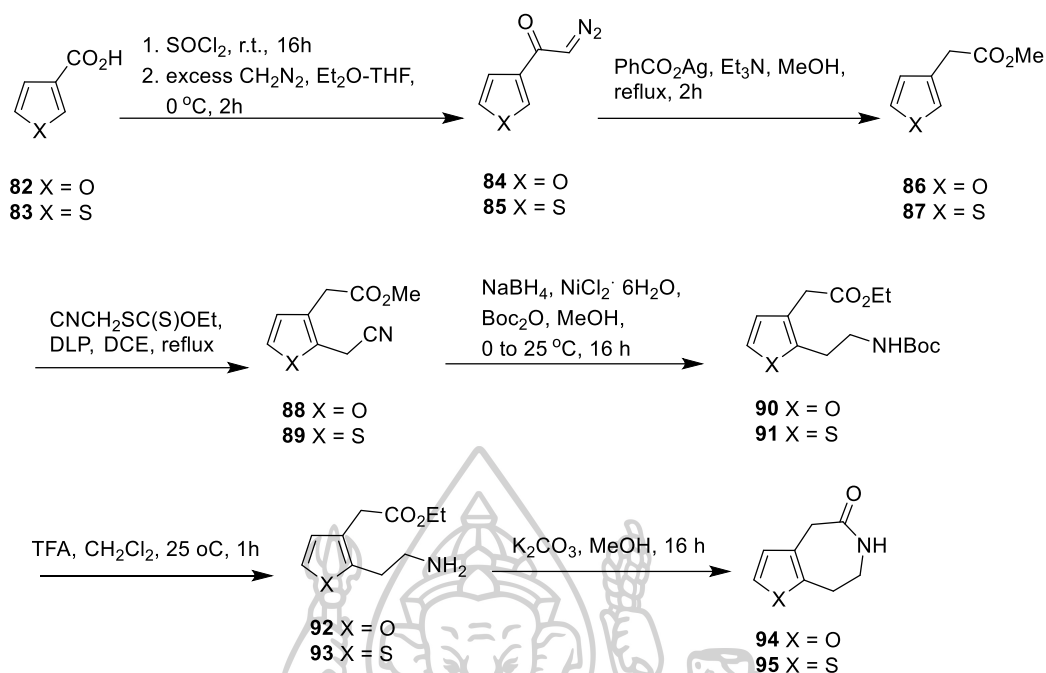
Heterocyclic compounds play role in pharmaceutical an important in a component of medicinal that using for the treatment several diseases. Many researchers are interested in the structure of heterocyclic compounds that have a wide variety of biological activities, whether of the core structures or components of those active compounds. In this research, we are interested in the synthesis of pyrrole and furan derivatives which we are expected that have a biological activity such as anti-bacterial, anti-cancer activities and plant growth regulators, which are reported in previous studies.

In 2010, Martínez & Villarreal (Martínez & Villarreal, 2010) synthesized the five-membered ring of heterocyclic 3-acetic acid derivatives which was started from protection of 1*H*-pyrrole-3-carboxylate (**75**) with benzyl bromide in the present of sodium hydride followed by alkaline hydrolysis to provide compound **76**. Ethyl 1-benzyl-1*H*-pyrrole-3-acetate (**77**) was achieved via conversion of compound **76** to diazo ketone using ethyl chloroformate followed by the reaction with ethereal diazomethane and treated with silver oxide, respectively. However, this method gave low yield of compound **77**. While compound **77** was received in better yield by hydrogenolysis with Pd/C/NaH₂PO₂·H₂O of compound **37** which was prepared from pyrrole by using the procedure of Bray and co-worker (Bray et al., 1990). Then, alkylation of compound **77** with S-(cyanomethyl) O-ethyl carbonodithioate in the presence of dilauroyl peroxide to afford compound **78**. Compound **78** was reduced in the presence of di-*tert*-butyl dicarbonate for prevention the dimerization and decomposition to provide *N*-Boc amine **79**. Compound **81** was obtained from *N*-Boc deprotection of **79** followed by the intramolecular lactamization and *N*-benzyl deprotection (Scheme 5).



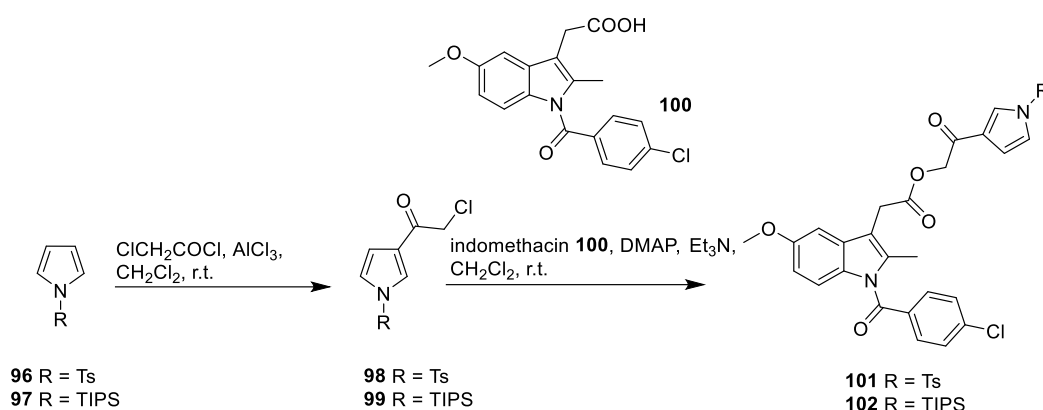
Scheme 5. Synthesis of pyrroloazepinone 81 (Martínez & Villarreal, 2010).

Furan and thiophene acetates **86** and **87** were prepared by using Arndt-Eistert homologation of compound **82** and **83**, respectively. The azepinone derivative **94** and **75** was achieved from compound **86** and **87** (Scheme 6) via the same procedure for the synthesis of compound **81** from compound **77**. The evaluation of pyrroloazepinone **81** and its derivatives **94** and **95** was found that these compounds was not inhibit the proliferation of PC3, U291, K562 and MCF7 cancer cell lines.



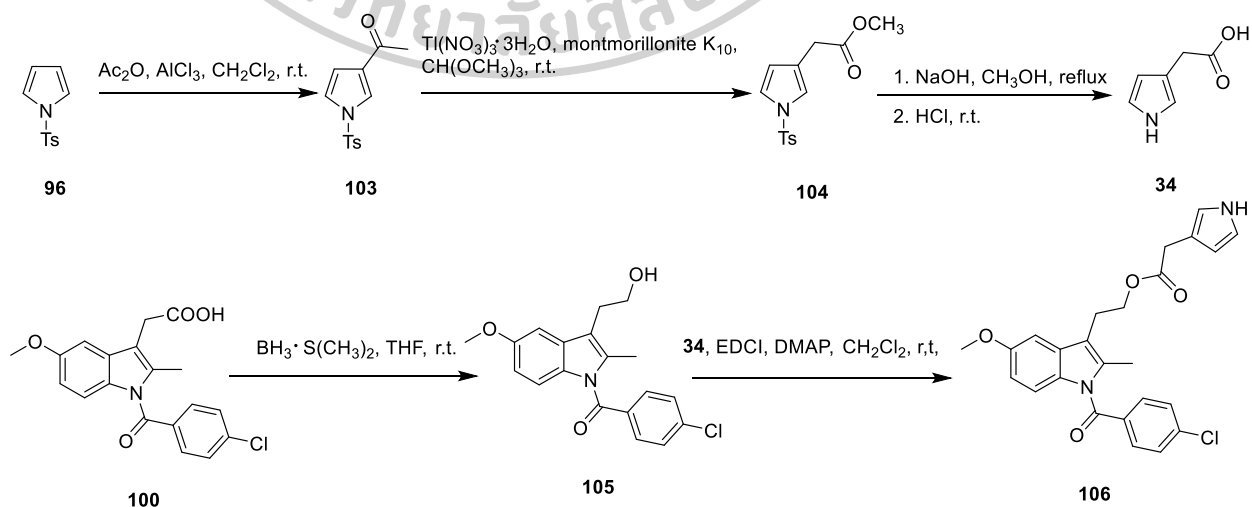
Scheme 6. Synthesis of azepinone derivative **94** and **95** (Martínez & Villarreal, 2010).

In 2012, the synthesis of a novel pyrrolyl-indomethacin derivatives was reported by Judith and co-worker (Serra Moreno et al., 2012). The indomethacin (**100**), a non-steroidal anti-inflammatory drug, was modified by binding with 3-position with pyrrole moiety. The synthesis was started from *N*-protected of pyrrole with tosyl chloride and triisopropylsilyl chloride then acetylation of *N*-protected pyrroles (**96,97**) with chloroacetyl chloride using AlCl_3 in dry dichloromethane. The *N*-protected-3-chloroacetyl pyrroles (**98,99**) were coupled with indomethacin (**100**) by using DMAP as the coupling agent and triethylamine as base to provide new indomethacin esters (**101,102**) as potential prodrugs. (Scheme 7).



Scheme 7. Synthesis of pyrrolyl-indomethacin derivatives **101** and **102** (Serra Moreno et al., 2012).

Then, researcher synthesized indomethacin derivative **106** by designing the different spacer chain of 3-position of pyrrole. The synthesis of key intermediate **34** was began by acetylation *N*-tosylpyrrole (**96**) and conversion of acetylate compound **103** into 3-acetic acid methyl ester (**104**) by using thallium-based oxidative trans position follow by hydrolysis of methyl ester was provided the target key intermediate **34**. The reduced indomethacin (**105**) was produced by using borane-methyl sulfide complex in THF. Then, condensation of compound **105** with 3-acetic acid pyrrole (**34**) employing EDCI and DMAP to give compound **106** (Scheme 8). The innovative monomers, compound **101**, **102**, **106** and indomethacin, showed no cytotoxic effects by using primary calvarial osteoblasts.



Scheme 8. Synthesis of indomethacin derivative **106** (Serra Moreno et al., 2012).

In 2020, Zhao and co-worker found ten novel pyrrole-2-carboxylic acids, endostemonines A-J (**107-116**) (Zhao et al., 2020) (Figure 6), which were extracted from actinomycete (*Streptomyces* sp.BS-1) that was isolated from *Stemona Sessilifolia*. The crude extract and the new compounds (**108-116**) were tested insecticidal activity against *Aphis gossypii* and *Tetranychus urticae* by using dipping method. The result showed that the crude extract of *Streptomyces* sp.BS-1 showed strong insect toxicity. All of the tested compound were less active than imidacoprid (IM) and bifenazate (BI), the positive control against *Aphis gossypii* with LC_{50} in range of 3.55-32.00 mg/L in 72 h and displayed moderate toxicities in *Tetranychus urticae* with LC_{50} in range of 3197.65-685.5 mg/L in 72 h.

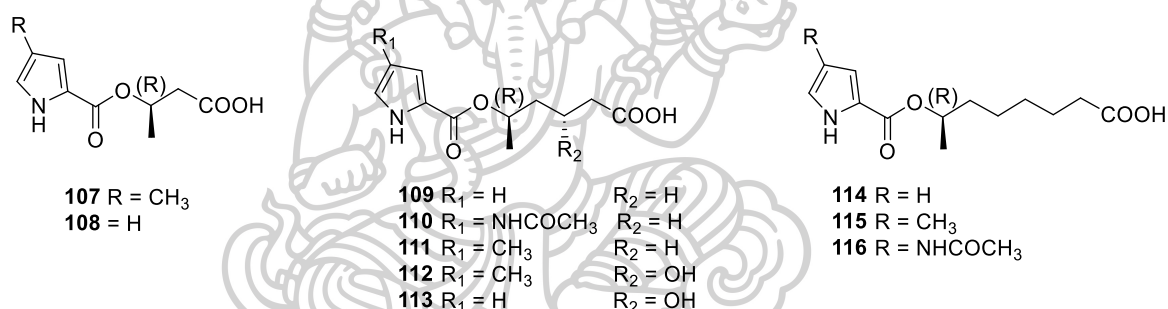
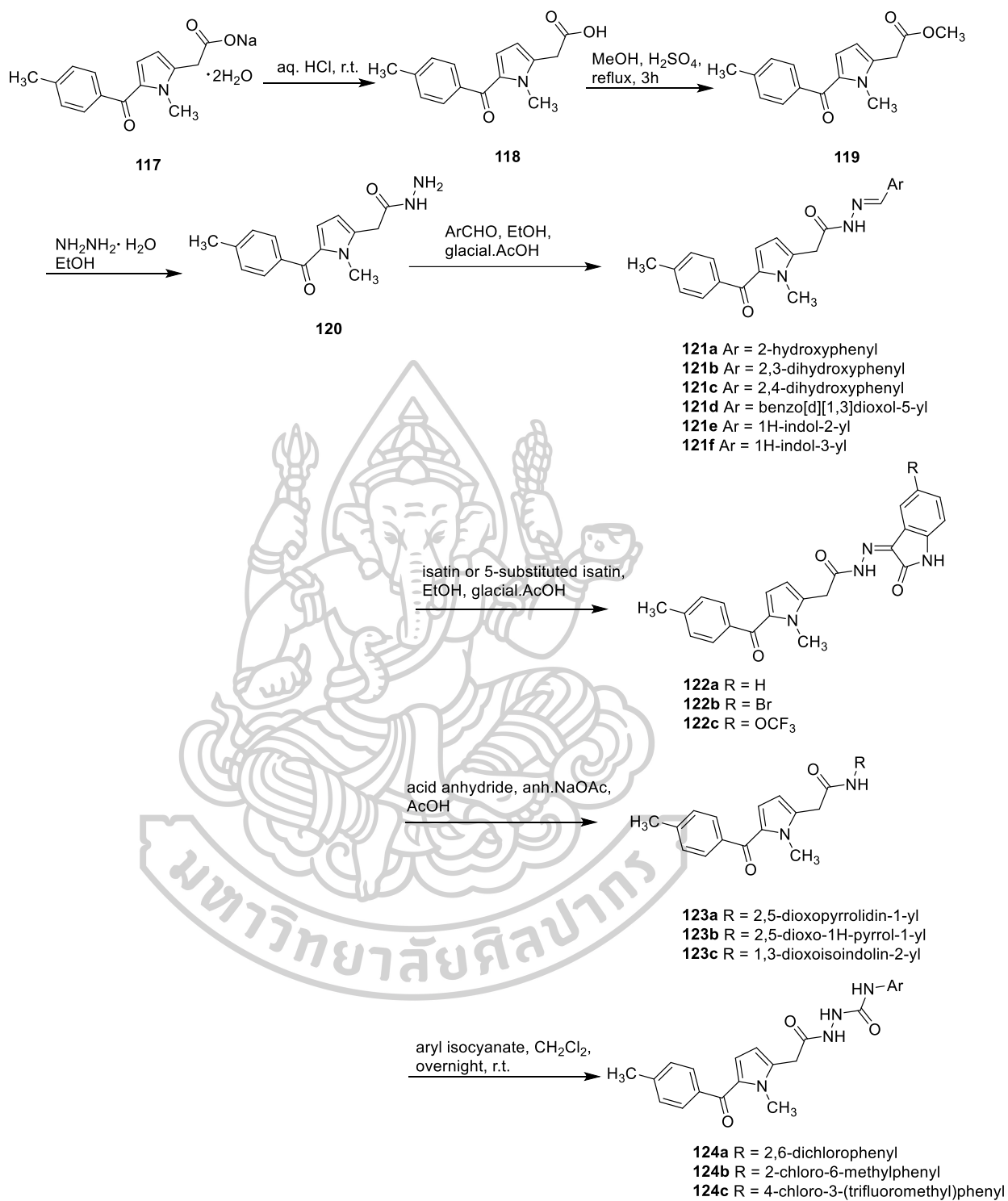


Figure 6 Structure of endostemonines A-J (**107-116**) (Zhao et al., 2020).

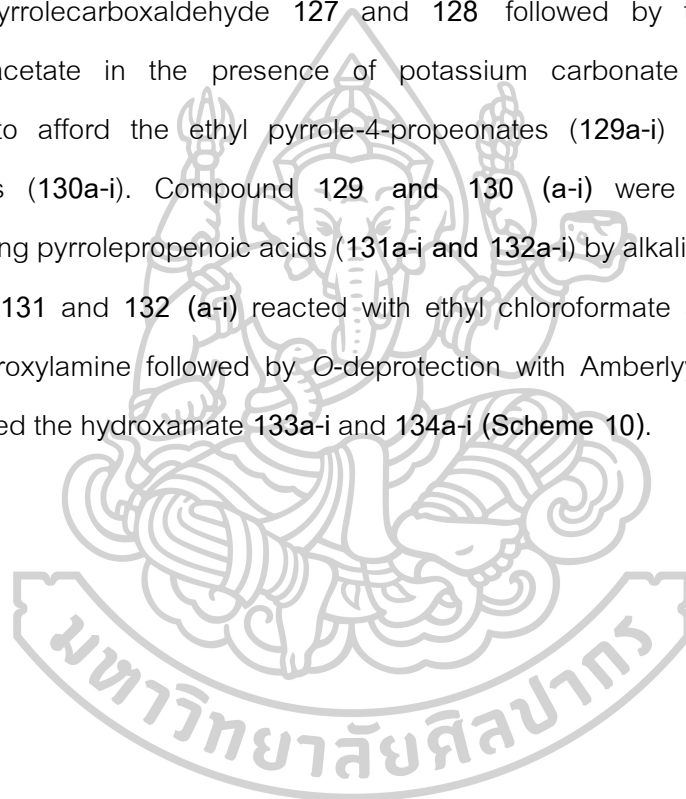
In 2021, Kassab and co-worker (Kassab et al., 2021) synthesized the novel tolmetin derivatives as potential VEGFE-2 inhibitors and apoptosis inducers of cancer cell lines. Fifteen novel tolmetin derivatives **121a-f**, **122a-c**, **123a-c**, and **124a-c** were synthesised from tolmetin hydrazide **120** which was prepared in three steps starting with commercial tolmetin sodium dihydrate **117**. Hydrolysis of compound **117** under aqueous acidic conditions at room temperature gave 2-(1-methyl-5-(4-methylbenzoyl)-1H-pyrrol-2-yl)acetic acid (tolmetin) (**118**). Esterification of Tolmetin **118** provided methyl 2-(1-methyl-5-(4-methylbenzoyl)-1H-pyrrol-2-yl)acetate (**119**). Tolmetin hydrazide **120** was prepared from the ester **119** via reflux with 80% hydrazine hydrate in methanol for 3 h. Tolmetin derivatives **121a-f** and **122a-c** were prepared by the reaction of tolmetin

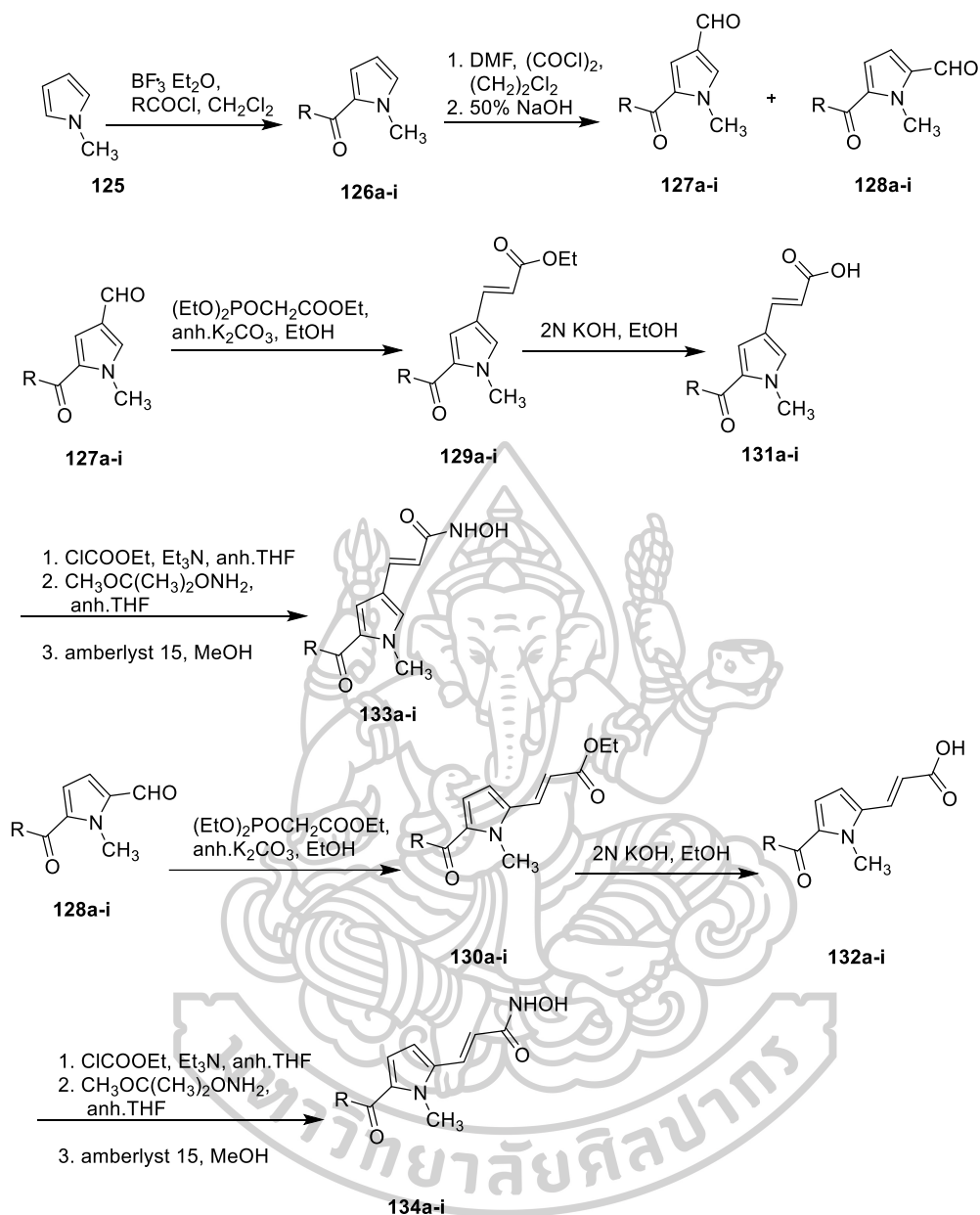
hydrazide **120** with different aryl or heteroaryl aldehydes and isatin or 5-substituted isatin, respectively. While Tolmetin derivatives **123a-c** were prepared from the reaction of tolmetin hydrazide **120** with acid anhydride in presence of anhydrous sodium acetate and acetic acid as solvent. Finally, tolmetin semicarbazide derivatives **124a-c** were prepared by stirring tolmetin hydrazide **120** with aryl isocyanate in methylene chloride for overnight at room temperature (Scheme 9). The study of antiproliferative activity against NCI 60 cell-lines of fifteen newly synthesized compounds were found that compound **121b** exhibited activity against 58 cancer cell lines with GI% in range 10.3 to 95.9% while compound **121c** exhibited activity against 60 cancer cell lines with GI% in range 12.6 to 95.5%. The structure relationship of the newly synthesized derivatives with their antiproliferative activity was revealed that grafting azomethane spacer between acetamide linker and the terminal hydrophobic moiety was provided a good impact on anticancer activity. The tolmetin derivatives incorporating acylhydrazone linker directly connected to a phenyl ring bearing with hydroxyl group at ortho position (**121a-c**) or indole ring with a nearby NH group (**121e,f**) was showed potent antiproliferative activity. Compounds **121a-c** bearing ortho hydroxyl group showed more potent broad-spectrum anticancer activity than compound **121e,f** with NH moiety. The additional of hydroxyl group on the phenyl ring in compounds **121b** and **121c** improved the anticancer activity which compound **121b**, additional hydroxyl group of phenyl ring at position 3, showed more potent anticancer activity than compound **121c** with the additional hydroxyl group of phenyl ring at position 4. Moreover, The pyrrole ring on derivatives **123a,b** was more tolerated for anticancer activity than *iso*-indoline moiety in compound **123c**. Compound **124c** which has the terminal 4-chloro-3-trifluoromethylphenyl moiety was possessed more potent the activity than compound **124a,b**.



Scheme 9. Synthesis of tolmetin derivatives **121a-f**, **122a-c**, **123a-c**, and **124a-c** (Kassab et al., 2021).

In 2009, Mai and co-worker (Mai et al., 2009) reported the synthesis of aroyl-pyrrolyl-hydroxy-amides (APHAs) as a class of HDAC inhibitor. The key intermediates 2-aroyle-1-methyl-1*H*-pyrrol-4-yl (**127a-i**) and 2-aroyle-1-methyl-1*H*-pyrrol-5-yl (**128a-i**) were synthesized through a two-step synthesis, Friedel-Craft and Vilsmeier-Haack reaction from methylpyrrole. The synthesis started from 1-methyl-1*H*-pyrrole and the aroyl chloride in the presence of boron trifluoride diethyl etherate. Then, the reaction of 2-aroyle-1-methyl-1*H*-pyrroles (**126a-i**) with oxalyl chloride and *N,N*-dimethylformamide provided pyrrolecarboxaldehyde **127** and **128** followed by treating with triethyl phosphonoacetate in the presence of potassium carbonate under Wittig-Honor conditions to afford the ethyl pyrrole-4-propeonates (**129a-i**) and ethyl pyrrole-4-propeonates (**130a-i**). Compound **129** and **130** (**a-i**) were converted into the corresponding pyrrolepropenoic acids (**131a-i** and **132a-i**) by alkaline hydrolysis. Finally, Compound **131** and **132** (**a-i**) reacted with ethyl chloroformate and *O*-(2-methoxy-2-propyl) hydroxylamine followed by *O*-deprotection with Amberlyst 15 ion-exchange resin provided the hydroxamate **133a-i** and **134a-i** (Scheme 10).



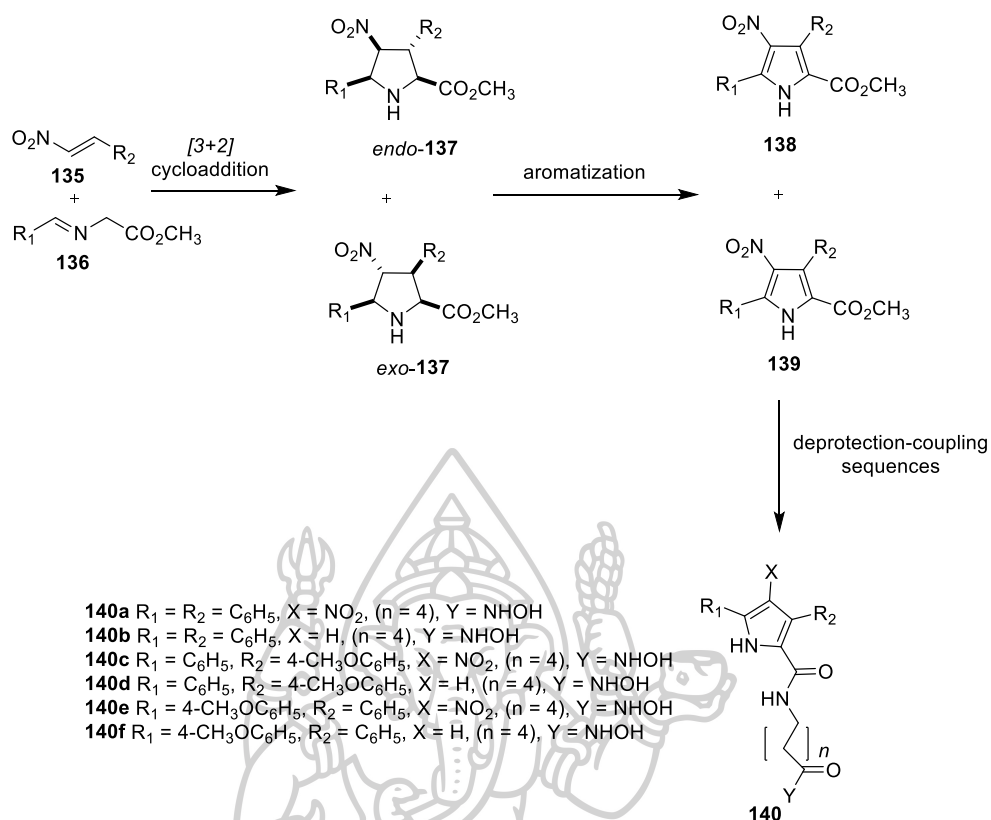


Scheme 10. Synthesis of aroyl-pyrrolyl-hydroxy-amides (APHAs) 133a-i and 134a-i as a HDAC inhibitors. (Mai et al., 2009)

The novel derivatives 133a-i and 134a-i were tested against maize deacetylases HD2, HD1-B (class I HDAC homologue) and HD1-A (class II HDAC homologue). It was found that compounds 133g, 133i and 134g were low class I selectivity while compound 133a, 133b, 133e, 134c and 134e were preferentially inhibited the class II enzyme.

Compound **133b**, **133i**, and **134g** were selected to test against human HDAC1 and HDAC4 IPs obtained from human leukaemia U937 and breast cancer ZR-75.1 cell lysates, respectively. At 5 μM , compound **133b** and **133i** showed HDAC1 inhibition similar to that of SAHA and MS-275, used as reference drugs, whereas **134g** was less effective. The inhibitory effects of the tested iso-APHAs against HDAC4 were much less noticeable, **133b** being totally inactive and **133i** and **134g** showing just a marginal inhibition.

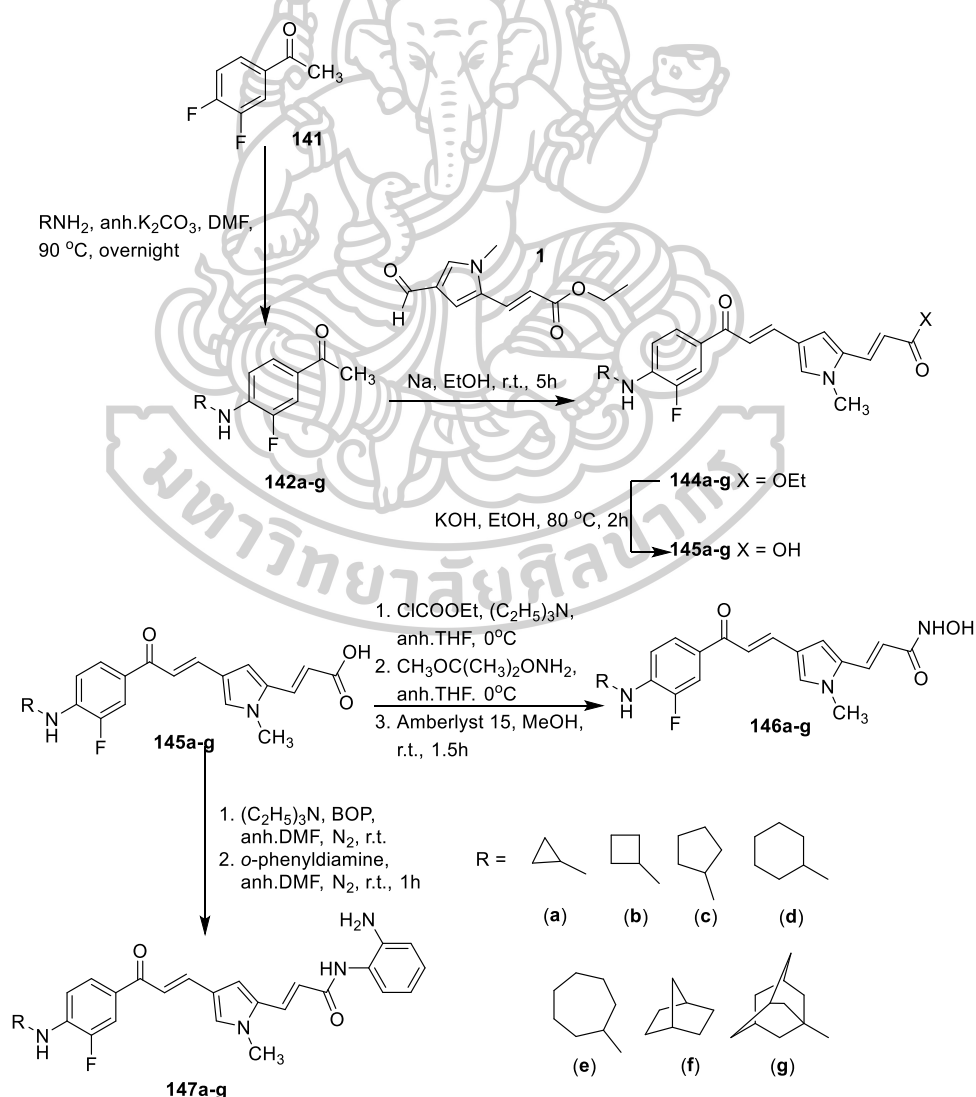
In the same year, Zubia and co-worker (Zubia et al., 2009) reported the synthesis of 3,5-diaryl-1*H*-pyrrole-2-carboxamide derivatives (**140a-f**). The key step in this synthesis is a (3 + 2) thermal cycloaddition between nitroalkenes **135** and the azomethine ylides derived from imines **136** (Vivanco et al., 2000). A mixture of *endo*- and *exo*-**137** cycloadducts was aromatized in the presence of MnO_2 to yield the corresponding (1*H*)-pyrroles **138** and **139** in 1:2 ratio. Deprotection of the methyl ester groups and coupling with the appropriate α -amino ester yielded the corresponding amides **140a-f** (Scheme 11). These compounds were tested the inhibition of HDAC enzymatic activity in nuclear extracts from the colon cancer cell line, HCT116, and in the T-cell leukemia, MOLT-4. Compound **140h** and **140i** showed inhibited HDAC enzymes at 1 μM and both of compound **140h** and **140i** inhibited cancer-cell growth with IC_{50} values of 0.47 ± 0.15 and 0.39 ± 0.06 μM , respectively, whereas for HCT116 cells IC_{50} values were 0.6 ± 0.07 and 0.62 ± 0.02 μM , respectively. Interestingly, the sensitivity to compounds **140h** and **140i** was similar to that observed for SAHA: IC_{50} values of 0.44 ± 0.09 (MOLT4) and 0.82 ± 0.11 μM (HCT-116), respectively.



Scheme 11. Synthesis of 3,5-diaryl-1H-pyrrole-2-carboxamide derivatives (compounds 140a-f). (Zubia et al., 2009)

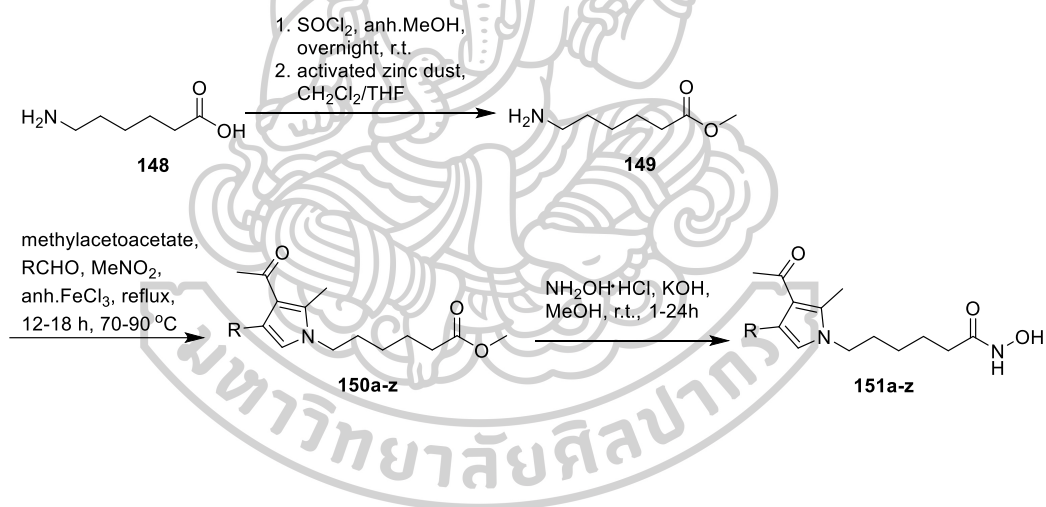
In the same year, Valente and co-worker (Valente et al., 2009) reported the synthesis of pyrrole-based hydroxamate (146a-g and 147a-g) as HDAC inhibitor. The synthesis started from the reaction of 3,4-difluoroacetophenone (141) with the corresponding cycloalkylamine in the presence of K_2CO_3 to obtain the intermediate 142a-g. Further condensation of 142a-g with the ethyl-3-(4-formyl-1-methyl-1H-pyrrol-2-yl)-2-propenoate (143) under basic conditions furnished the ethyl 3-(4-(3-(4-(cycloalkylamino)-3-fluorophenyl)-3-oxoprop-1-enyl)-1-methyl-1H-pyrrol-2-yl)-acrylates (144a-g) which underwent alkaline hydrolysis to yield the corresponding acrylic acids 145a-g, key intermediate for the synthesis of the final compounds. These key intermediates 145a-g reacted with ethyl chloroformate, followed by addition of *O*-(2-methoxy-2-propyl)-hydroxylamine and further cleavage in the presence of the Amberlyst 15 ion exchange resin furnished the desired 3-(4-(3-(4-(cycloalkylamino)-3-fluorophenyl)-3-oxoprop-1-enyl)-1-methyl-1H-pyrrol-2-yl)-N-hydroxyacrylamides 146a-g.

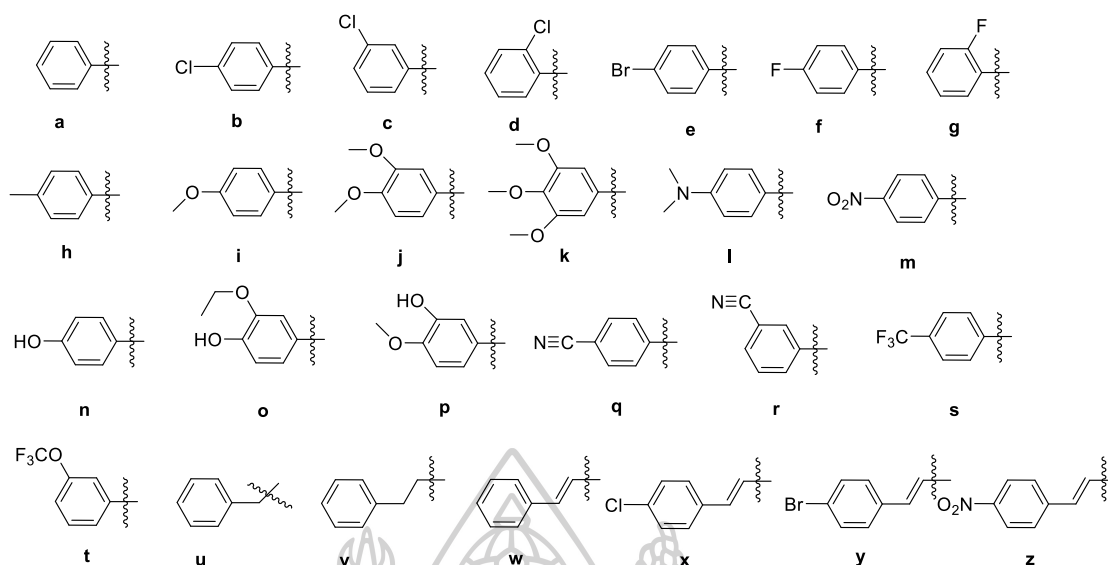
The 2-aminoanilide derivatives **147a-g** was synthesized from **145a-g**, by treatment with benzotriazole-1-yloxytris(dimethylamino)phosphonium hexafluorophosphate (Bop) and the *o*-phenyldiamine in the presence of triethylamine (Scheme 12). These synthesized compounds were tested against HDAC1, HDAC4 and HDAC6. The results showed that the cyclopropylamino and cyclobutylamino hydroxamates **146a** and **146b** showed the highest HDAC1/HDAC6 inhibitory activities, with IC_{50} values of 0.02 and 0.03 μm (against HDAC1) and 1.1 and 0.8 μm (HDAC6), respectively. When tested in U937 leukemia cells (caspase 3–7 method, 1 μm , 30 h), **146a** and **146b** induced apoptosis (28.8 and 28.3%, respectively) more effective than SAHA (16.3% at 5 μm) as reference drug.



Scheme 12. Synthesis of pyrrole-based hydroxamate (compound **146a-g** and **147a-g**) as HDAC inhibitor. (Valente et al., 2009)

In 2021, Singh and co-worker (Singh et al., 2021) reported the synthesis of pyrrole hydroxamic acid as HDAC inhibitors. These analogs were synthesized through three step sequences started from esterification of 6-aminocaproic acid (**148**) using thionyl chloride in methanol followed by reacting with zinc dust to provide aminocaproic acid methyl ester (**149**). Then, cyclization of, aminocaproic acid methyl ester (**149**) with aromatic aldehyde, nitromethane and methylacetoacetate afforded 4-substituted methyl 6-(3-acetyl-2-methyl-1*H*-pyrrol-1-yl)-hexanoate derivatives (**150a-z**). Finally, conversion of ester derivatives (**150a-z**) to 4-substituted 6-(3-acetyl-2-methyl-1*H*-pyrrol-1-yl)-*N*-hydroxyhexanamide derivatives (**151a-z**) were achieved by using potassium hydroxide and hydroxylamine hydrochloride in dry methanol (Scheme 13).





Scheme 13. Synthesis of 4-substituted 6-(3-acetyl-2-methyl-1H-pyrrol-1-yl)-N-hydroxyhexanamide derivatives (**151a-z**) (Singh et al., 2021).

These analogs were evaluated for their anticancer activity *in-vitro* against leukemia (K-562), lung (A-549), breast (MCF7), and cervical (HeLa) human cancer cell lines using Sulforhodamine B (SRB) assay method. The *in-vitro* studies of compound **150a-z** indicated that substitution with electron donating groups produces active or moderately active compounds. Interestingly, *p*-nitro-substituted molecule produced a most active derivative in the series. The *in-vitro* anticancer study of compound **151a-z** indicated that the unsubstituted phenyl derivative, 6-(3-acetyl-2-methyl-4-phenyl-1H-pyrrol-1-yl)-N-hydroxy-hexanamide (**151a**) have moderate antitumor activity against K-562 human leukemia cell line. Substitution at 4-phenyl ring with weak and moderate electron withdrawing groups, such as fluoro, chloro, and bromo potentiated the cytotoxic activity. Moreover, the *in-vitro* anticancer evaluation of selected 4-substituted methyl 6-(3-acetyl-2-methyl-1H-pyrrol-1-yl)-hexanoate (**150i**, **150m**, **150z**) and 4-substituted 6-(3-acetyl-2-methyl-1H-pyrrol-1-yl)-N-hydroxyhexanamide derivatives (**151i**, **151m**) against lung (A-549), breast (MCF-7), and cervical (HeLa) cancer cell lines. The result indicates that all five derivatives were active against lung (A-549), breast (MCF-7), and cervical (HeLa) human cancer cell lines at <10 µg/ml concentration. The

compounds with promising anticancer activity during *in-vitro* cell line studies were subjected to HDAC1 and HDAC6 inhibitory assay. Among these compounds, **151i** exhibited outstanding HDAC1 and HDAC6 inhibitory potential with IC_{50} value of 0.024 and 0.034 μ M, respectively, although that is lesser than SAHA.

2,5-DKP ring has been found in many natural compounds isolated from fungus, actinomycetes, mushroom, plant, lichen and etc. Recently, the reports of 2,5-DKP natural products were widely interested.

In 2017, Yu and co-worker (Yu et al., 2017) reported the isolation of 2,5-DKP from a co-culture of *Penicillium* sp. DT-F29 with *Bacillus* sp. B31. It was found that most of 13 compounds as known 2,5-DKPs (verruculogen TR-2 (**152**), 12-hydroxyverruculogen TR-2 (**153**), 12 β -hydroxy-13 α -methoxyverruculogen TR-2 (**154**), 12 α -hydroxy-13 α -prenylverruculogen TR-2 (**157**), spirotryprostatin (**158**), cycloprostatin C (**159**), 12,13-dihydroxyfunitremorgin C (**160**), cyclotryprostatin B (**161**), funitremorgin B (**165**), prenylcycloprostatin B (**166**), 13-prenyl funitremorgin B (**168**), funitremorgin A (**171**)) and 10 compounds as a new 2,5-DKPs, 12 β -hydroxy-13 α -ethoxyverruculogen TR-2 (**155**), 12 β -hydroxy-13 α -butoxyethoxyverruculogen TR-2 (**156**), hydrocycloprostatin A (**162**), hydrocycloprostatin B (**163**), 25-hydroxyfunitremorgin B (**167**), 12 β -hydroxy-13 α -butoxyethoxyfunitremorgin B (**169**), 12 β -hydroxy-13 α -methoxyverruculogen (**170**), 25-hydroxyfunitremorgin A (**172**), 26 α -hydroxyfunitremorgin A (**173**), diprostatin A (**174**), (Figure 13) . However, the new compounds (**155-156**, **162-163**, **167**, **169-170**, **172-174**) have the core structure as cyclo(Trp-Pro) 2,5-DKPs. These pure compounds were analyzed the inhibitory activity of BRD4 protein which was a target protein for BET inhibitor, important to therapeutic cancer. The results showed that compounds **153**, **157**, **158**, **164**, **165**, **166**, **168**, **169**, **171** and **174** exhibited BRD4 protein inhibitory activity at the concentration 20 μ M. Compounds **164** and **165** showed the most BRD4 inhibitory rate at 72.7% and 80.4%, respectively as well as the control (+)-JQ1 at 85.7%. Moreover, compound **165** could be affected with BRD4 protein inhibitory activity at 6.54 μ M of IC_{50} while (+)-JQ1 showed at 0.24 μ M.

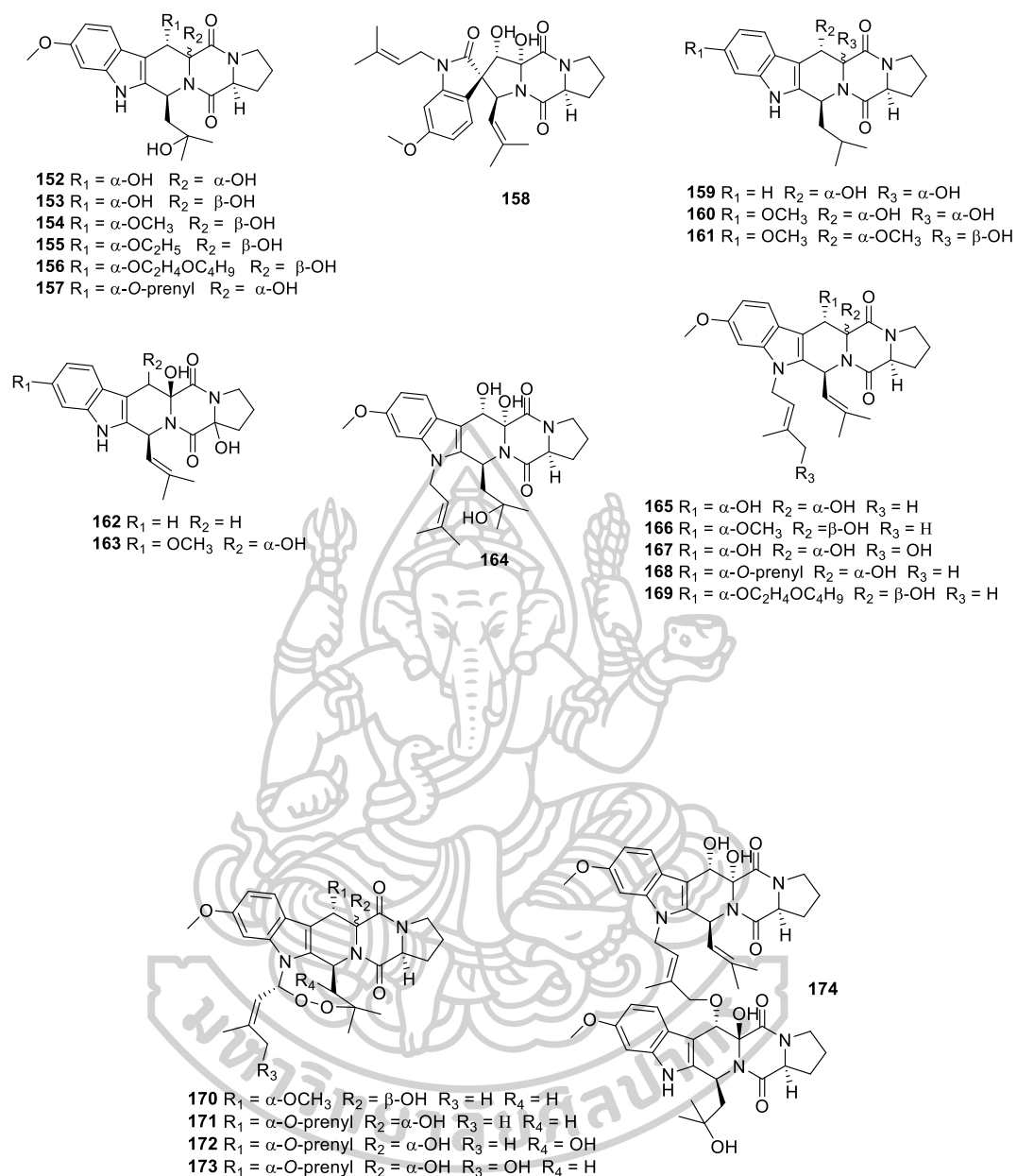


Figure 7. Structure of all isolated prenylated 2,5-DKPs from a co-culture of *Penicillium* sp. DT-F29 with *Bacillus* sp. B31. (Yu et al., 2017)

In 2018, Lohmann and co-worker (Lohmann et al., 2018) reported the isolation of two red diketopiperazine alkaloids, rosellin A (175) and B (176) (Figure 8), from the fruiting bodies of the mushroom *Mycena rosella*. Rosellin A (175) and B (176) were evaluated for their bioactivities and their ecological roles. Both 175 and 176 were proved to be inactive against the bacteria *Escherichia coli*, *Bacillus subtilis* and

Staphylococcus capitis at up to 1 mmol per disc in an agar diffusion assay. Rosellin A (175) was also tested against the bacteria *Azoarcus toluyliticus*, *Azovibrio restrictus*, and *Azospirillum brasilense*, and the fungi *Mucor hiemalis*, *Penicillium notatum*, and *Spinellus fusiger*, but showed no activity at up to 1 mmol per disc in an agar diffusion assay. However, strong bleaching of the leaves of garden cress plants (*Lepidium sativum*) was observed after four weeks exposure via the roots to 1 mmol of 1 per test tube.

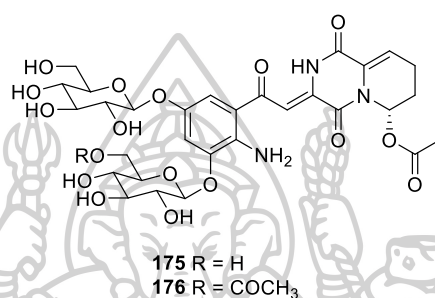


Figure 8. Structure of rosellin A (175) and rosellin B (176) (Lohmann et al., 2018).

In 2019, Barakat and co-worker (Barakat et al., 2019) reported the isolation of thiodiketopiperazines with two spirocyclic center from the endophytic fungus *Botryosphaeria mamani* E224 from the fresh leaves of *Bixa Orellana* (Bixaceae). The isolation provided three thiodiketopiperazine, botryosulfuranols A (177), B (178) and C (179) (Figure 9) which compound 179 was identified as the disulfur-bridged derivative of 177. Compounds 177-179 were evaluated for cell-growth inhibition of four cancer cell lines (human hepatocellular carcinoma HepG2, human colon adenocarcinoma HT29, human colorectal adenocarcinoma Caco-2 and human cervical adenocarcinoma HeLa) and two healthy cell lines (monkey kidney epithelial Vero and rat small intestine epithelial IEC6). The result shows that the cytotoxicities of 177-179 are weak to moderate but botryosulfuranol A (177) is always the most active in all these the cell line that tested here, thus, the α,β -unsaturated ketone and an open sulfur bridge have effective to the tested cell line.

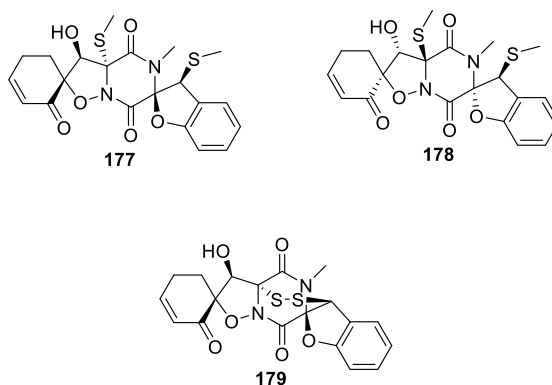


Figure 9. Structure of botryosulfuranols A (177), B (178) and C (179) isolated from the endophytic fungus *Botryosphaeria mamani* E224 from the fresh leaves of *Bixa Orellana* (Bixaceae) (Barakat et al., 2019).

In 2020, Shan and co-worker (Shan et al., 2020) reported the isolation of three new alkaloids, (-)-(S)-variecolortide D (180a), (+)-(R)-variecolortide D (180b) and brevicompanine I (182) and three known alkaloids (181, 183, 184) (Figure 16), from ethylacetate crude extract of the fungus *Aspergillus ruber* WH4-1. All the compounds were investigated for their anti-inflammatory properties. However, only compound 181 showed weak inhibitory activity against the production of nitric oxide with inhibitory rate of $53.2 \pm 3.8\%$ at $30 \mu\text{M}$.

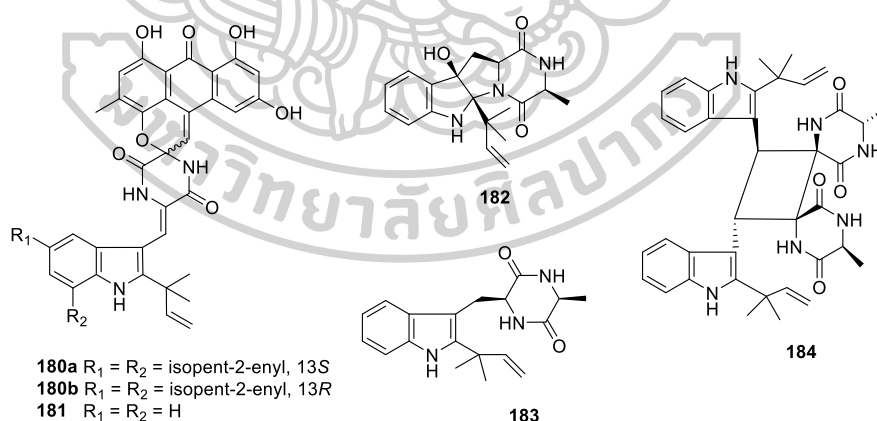
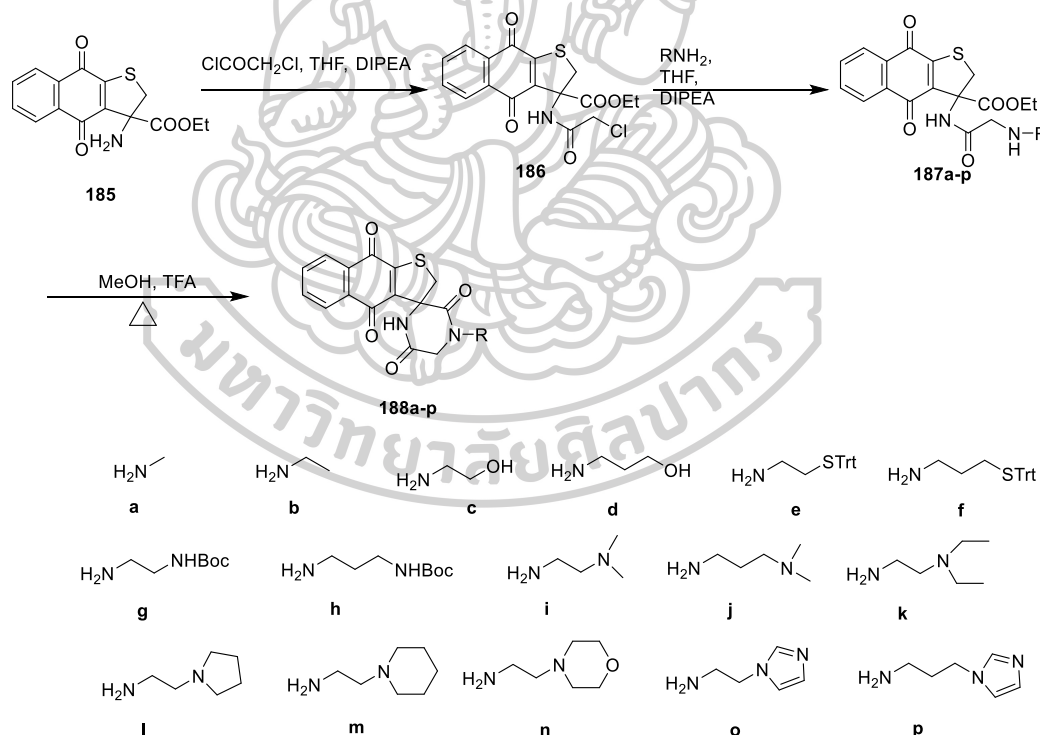


Figure 10. Structure of (-)-(S)-variecolortide D (180a), (+)-(R)-variecolortide D (180b) and brevicompanine I (182) and three known 2,5-DKP alkaloids (181, 183, 184) (Shan et al., 2020).

The synthesis of 2,5-DKP was also well reported. In 2008, Monterrey and co-worker (Gomez-Monterrey et al., 2008) reported the synthesis of 4-substituted

spiro[(dihydropyrazin2,5-dione)-6,3'-(2',3'-dihydrothieno[2,3-*b*]naphtho-4',9'-dione)] derivatives (**188a-p**) as cytotoxic agent. The synthesis started from condensation of 3-amino-3-ethoxycarbonyl-2,3-dihydrothieno[2,3-*b*]naphtho-4,9-dione (**185**, DTNQ) with chloroacetyl chloride in THF, using diisopropylethylamine as base, afforded the derivatives (**186**) with 90% yield. Then, nucleophilic displacement of the chloride functionality with a variety of amine derivatives (**a-p**), in THF and diisopropylethylamine at reflux, provided the corresponding compound **187a-p**. Finally, the complete lactamization of derivatives **187a-p** in MeOH at reflux using TEA as base afforded the corresponding final 4-*N*-substituted spirodiketopiperazine derivatives (**188a-d**, **188i-p**) in 40–55% overall yields. The final thioethyl (**188e**), thiopropyl (**188f**), aminoethyl (**188g**), and aminopropyl (**188h**) derivatives were obtained after S-Trt or NH-Boc deprotection using 20% TFA in dichloromethane in quantitative yields (Scheme 14).

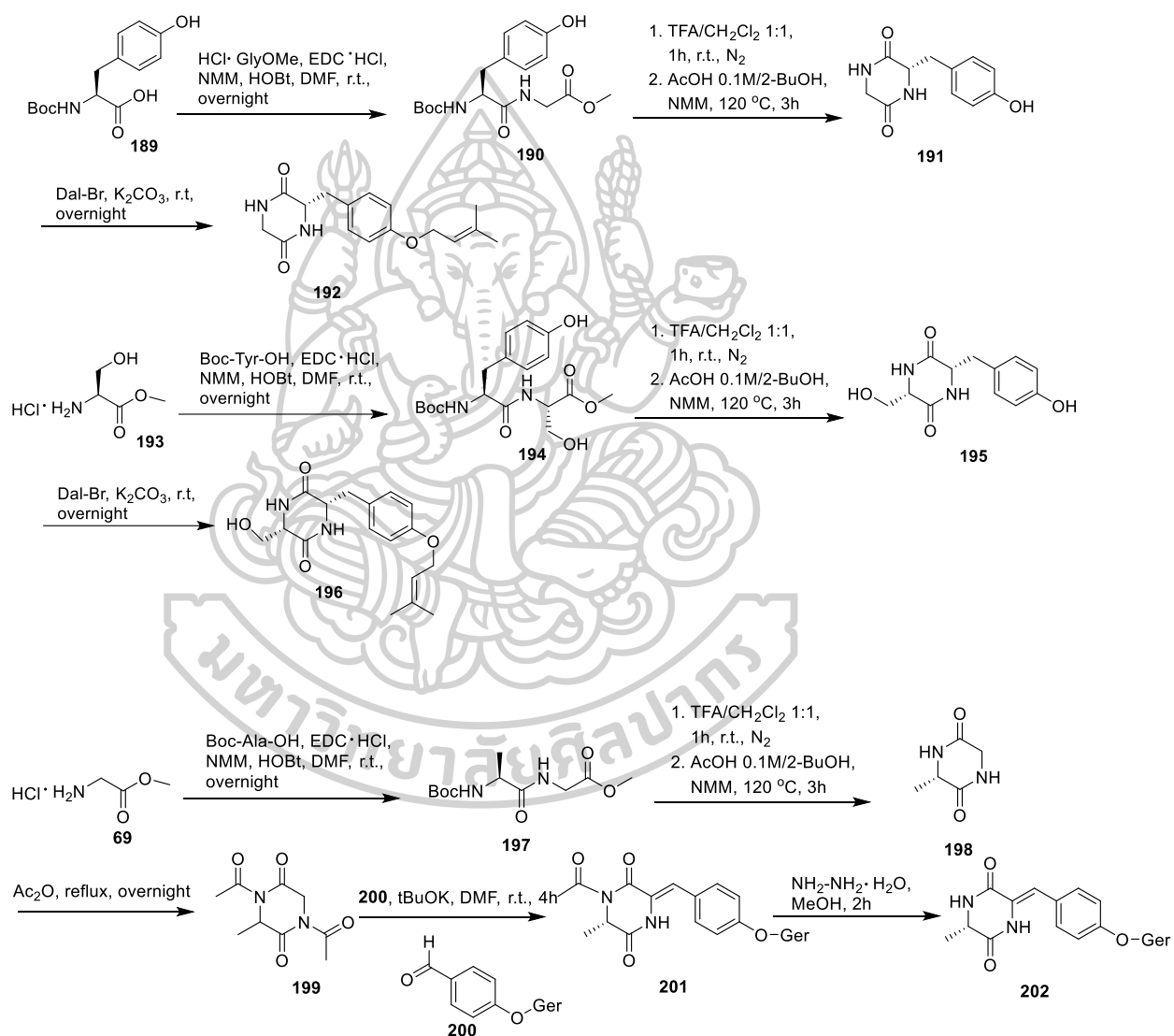


Scheme 14. Synthesis of 4-substituted spiro[(dihydropyrazin2,5-dione)-6,3'-(2',3'-dihydrothieno[2,3-*b*]naphtho-4',9'-dione)] derivatives (**188a-p**) (Gomez-Monterrey et al., 2008).

The *in vitro* activity was evaluated against the MCF-7 human breast carcinoma and SW 620 human colon carcinoma cell lines. Compounds **188i** and **188l** show the most potent compounds of this series, with a cytotoxic activity of **188i** and **188l** ($IC_{50} = 0.031 \pm 0.012$, 0.040 ± 0.010 μM , MCF-7; 0.112 ± 0.020 , 0.119 ± 0.005 μM , SW 620) comparable to that of doxorubicin ($IC_{50} = 0.022 \pm 0.008$ μM , MCF-7 and 0.178 ± 0.003 μM , SW 620). This result indicated that the side-chain length, determined by the number of methylene groups separating the chromophore and the remote protonatable amine groups in the pendant arm, appeared to have an important effect upon cytotoxicity and the aromatic nature of the heterocyclic side chain, relatively rigid and more electron-rich when compared to the alkylcyclic pyrrolidine, is not well-tolerated in the molecular target.

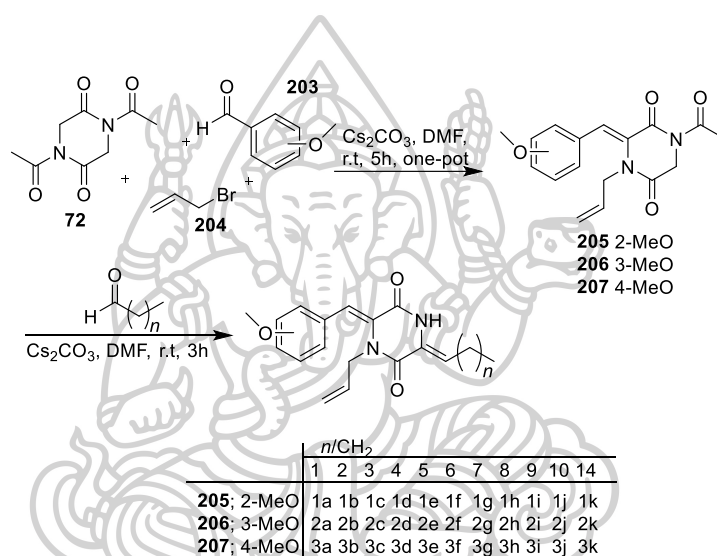
In 2014, Mollica and co-worker (Mollica et al., 2014) synthesized three naturally occurring oxyprenylated diketopiperazine (**192**, **196** and **202**). The higher lipophilicity of the diketopiperazine was observed the higher anti-cancer activity. The synthesis of oxyprenylated diketopiperazine derivatives (**192**, **196** and **202**) started from coupling reaction of *N*-Boc amino acid with amino acid methyl ester hydrochloride provided dipeptide Boc-Tyr-Gly-OMe (**190**), Boc-Tyr-Ser-OMe (**194**) and Boc-Ala-Gly-OMe (**197**) in case of compound **192**, **196** and **202**, respectively. The dipeptide was *N*-Boc deprotection by treatment with TFA followed by cyclization by using reflux reaction under AcOH-2-butanol and NMM to provide compound **191**, **195** and **198**, respectively. In case of product **192** and **196**, *O*-alkylation was performed with 3,3-dimethylallylbromide (Dal-Br) or geranyl bromide (Ger-Br), respectively. In the synthesis of compound **202** was undergone acetylation of compound **198** by using acetic anhydride. Then, compound **199** was condensed with compound **200** using *t*-BuOK as base. Finally, compound **201** was removed acetyl group by using hydrazine monohydrate in methanol (Scheme 15). The three oxyprenylated diketopiperazines (**192**, **196** and **202**) were studied the growth inhibitory activity against six human cancer cell lines (Hs683, A549, MCF-7, SKMEL-28, B16F10 and U373) by using the MTT colorimetric assay. The result shows that compounds (**192**) and (**196**) display weak or

no ($IC_{50} > 100 \mu\text{M}$) inhibitory activities, while deoxymycelianamide (**202**) was found as the only effective compound with a mean IC_{50} value of $11 \mu\text{M}$. The presence of the shorter isopentenylloxy side chains led to decrease the growth inhibitory activity. It can be hypothesized that not only the presence of an *O*-geranyl chain like in (**202**) is a determinant for the observed effects but also, the carbon–carbon double bond exocyclic to the DKP ring may play a key role to this regard.



Scheme 15. Synthesis of oxyprenylated diketopiperazine derivatives (**192**, **196** and **202**) (Mollica et al., 2014).

In 2016, the synthesis of a novel 2,5-diketopiperazine derivatives was reported by Liao and co-worker (Liao et al., 2016). The intermediates **205**, **206**, and **207** were synthesized by combining the aromatic aldehydes, allyl bromide, 1,4-diacetyl-DKP, and Cs_2CO_3 in one pot reaction. Then, the intermediates **205**, **206**, and **207** were treated with various alkyl aldehydes in the presence of Cs_2CO_3 at room temperature to afford the target compounds 2,5-diketopiperazine derivatives in moderate yield, but unfortunately compound **206d** could not be obtained after several trials because it is unstable (Scheme 16).

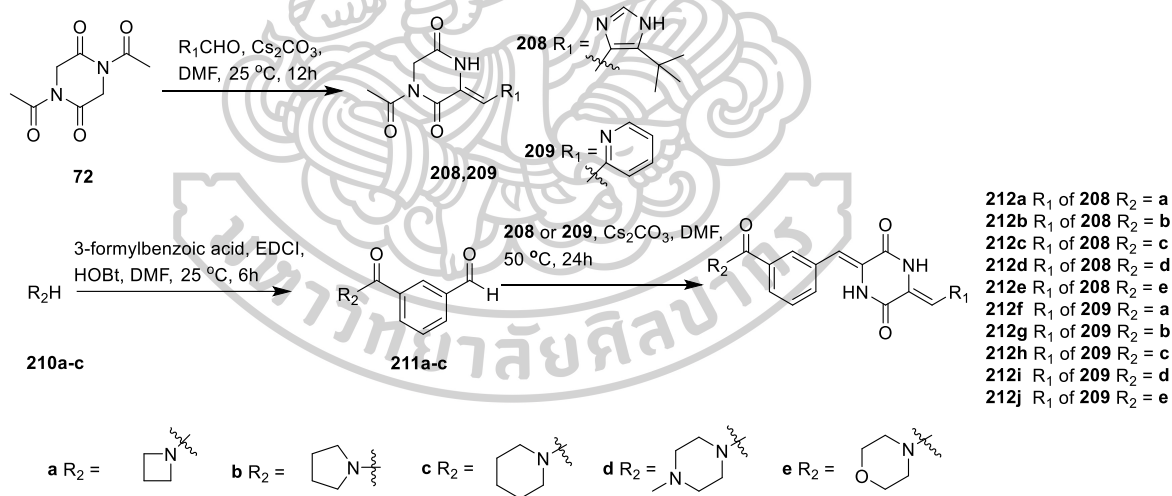


Scheme 16. Synthesis of 2,5-diketopiperazine derivatives **205a-k**, **206a-k** and **207a-k** (Liao et al., 2016).

All synthetic compound **205a-k**, **206a-k** and **207a-k** were tested the cytotoxic activity against eight cancer cell lines (U937, K562, HL60, A549, MCF-7, Hela, DU145 and HT29). The result shows that compounds **205b-e** and **205h** showed strong activity against the cell lines with their IC_{50} values ranged from 0.5 to 28.9 μM . Compound **205c** with a pentylidene chain ($n = 3$) displayed good cytotoxic effects against all the cancer cell lines (the strongest activity against the cancer cell line HL60 with an IC_{50} value of 0.5 μM). Compounds **206a-k** had activity which indicated that the position of the methoxy moiety on the phenyl ring was important for the cytotoxic activity of the 2,5-diketopiperazine derivatives. This result was supported by strong activity for most of the compounds **207a-h** against the cancer cell lines. Compound **207c** with a pentylidene

chain ($n = 3$) exhibited significant cytotoxic activity ($IC_{50} = 0.36-1.9 \mu\text{M}$) to all of the cancer cell lines. Similar to compounds **205a-k**, the derivatives with longer (**207d-k**) or shorter (**207a-b**) alkyl side chains had weaker activity, and the n -value for the bioactive compounds could not be more than eight.

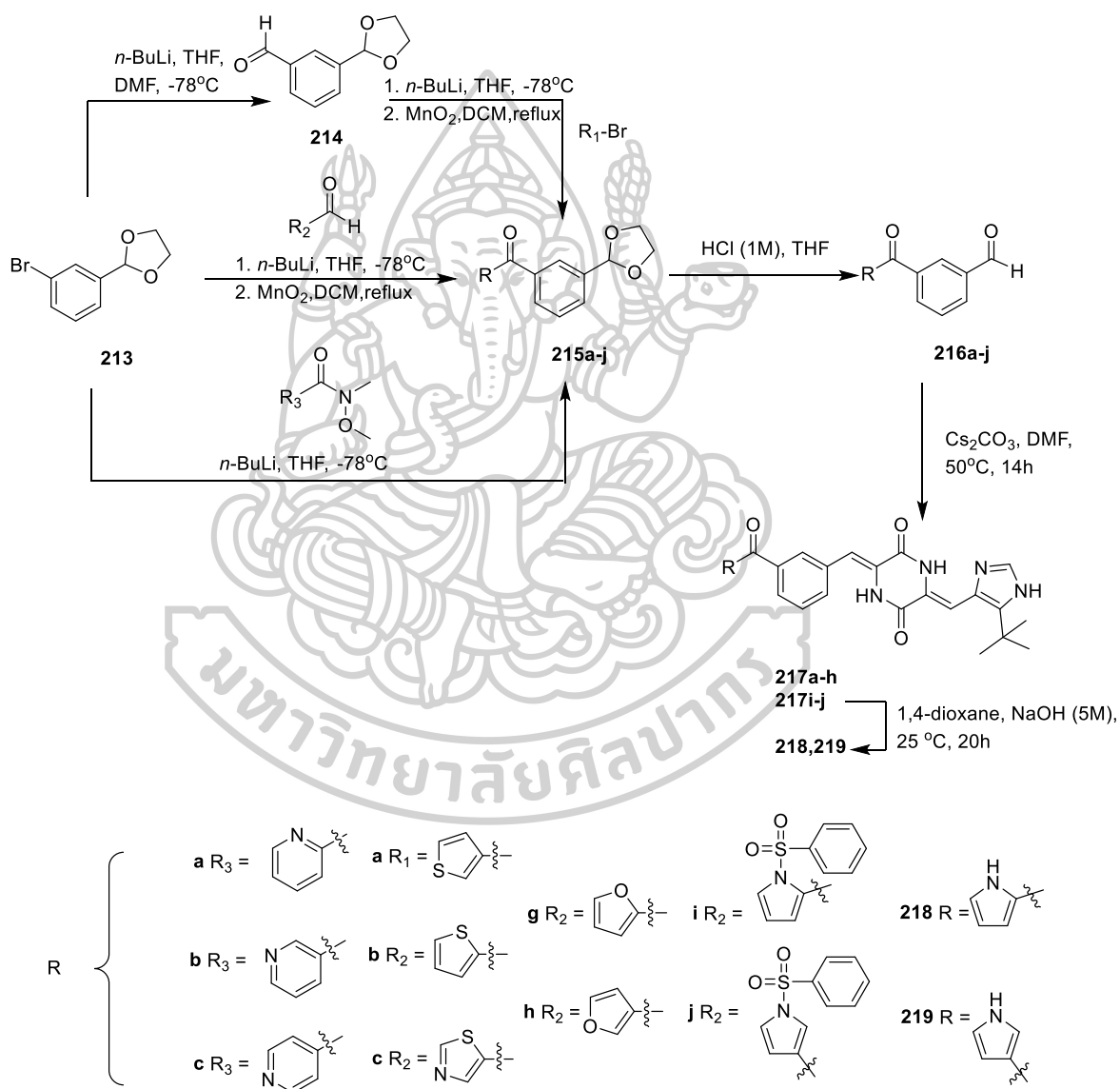
In 2018, the plinabulin derivatives were synthesized by Fu and co-worker (Fu et al., 2018). The synthesis was started from the reaction of *N,N*-diacetyl-piperazine-2,5-dione (**72**) with 5-(*tert*-butyl)-1*H*-imidazole-4-carbaldehyde or 2-formylpyridine in presence of Cs_2CO_3 in DMF under N_2 atmosphere to afford the intermediates **208** or **209**, respectively. In parallel, the adducts **211a-e** were obtained through the carbodiimide mediated coupling reaction between 3-formylbenzoic acid and a saturated *N*-heterocyclic group **210a-e**. The final products **212a-h** were obtained via treatment of **211a-e** with intermediate **208** or **209** under Aldol condensation conditions (Scheme 17).



Scheme 17. Synthesis of compound **212a-h** (Fu et al., 2018).

The intermediates **216a-j** were obtained by the conversion of 1-bromo-3-(1,3-dioxolan-2-yl) benzene (**213**) into the corresponding secondary alcohols via bromo-lithium exchange reaction. Subsequently, the secondary alcohols were oxidized by MnO_2 to afford Compounds (**215a-j**). Then, Compounds (**215a-j**) were converted to

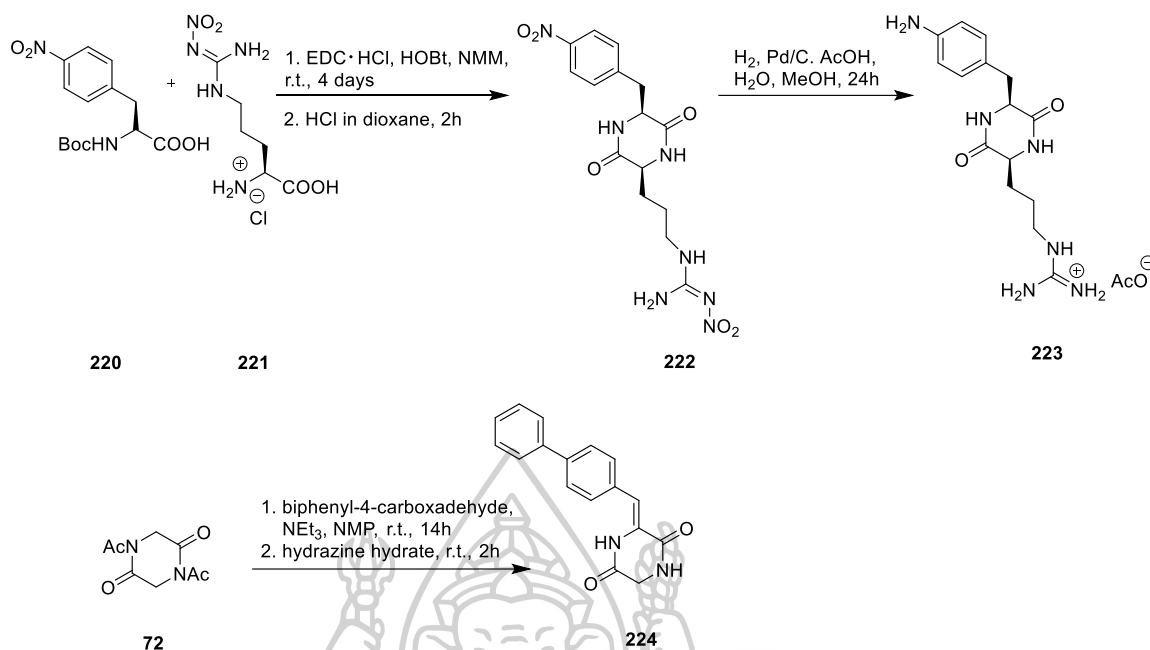
aldehydes (**216a-j**) via hydrochloric acid hydrolysis. In other hand, Compound **213** was reacted with Weinreb amides to give Compounds **214a-c**. Compounds **214a-c** was treated with dilute hydrochloric acid in THF to provide the aldehydes **216a-c**. Finally, the substituted heteroaromatic compounds (**217a-j**) were obtained through Aldol reaction between **216a-j** and the intermediate **208**. Compounds **217i-j** were subsequently hydrolyzed under basic (5 M NaOH) conditions to give **218** and **219** (Scheme 18).



Scheme 18. Synthesis of plinabulin derivatives (**217a-h**, **218** and **219**) (Fu et al., 2018).

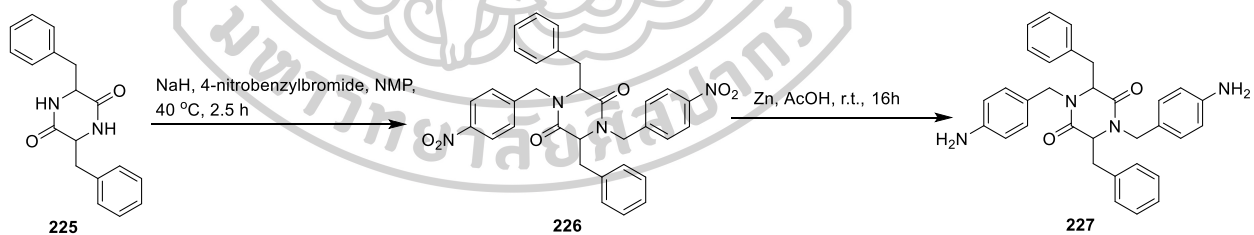
The activities of the synthesized derivatives against BxPC-3 cell line were evaluated by sulforhodamine B assay (SRB). Compound **212a-h** showed weakly activity by comparing with plinabulin. The activity decreased when replacement of the tert-butyl imidazole ring with pyridine ring. These results indicated that the tert-butyl imidazole ring was superior to the pyridine ring for the biological activity. Compound **217d** and **217e** were exhibited strong inhibitory activities against BxPC-3 cell line with IC₅₀ of 1.56 nM and 1.72 nM, respectively. Compound **217f** displayed less activity, the IC₅₀ value was 17.11 nM. In addition, Compounds **217g-h** exhibited moderate inhibitory activities (IC₅₀ at 9.23 and 9.41 nM, respectively). In contrast, the pyrrole substituent derivatives, Compounds **218** and **219**, led to decrease in activity (both IC₅₀ >100 nM). The results indicated that bioisosteric replacement of sulfur atom with -NH or oxygen atom on thiophene derivatives were detrimental to antiproliferative activity.

In the same year, Labrière and co-worker (Labriere et al., 2018) developed the 2,5-diketopiperazine as antimicrobial agents. The development was started from the preparation of compound **222** and **223** from coupling reaction of boc-4-nitrophenylalanine (**220**) and nitro protected arginine methyl ester (**221**) by using EDC and HOBt. The Boc protecting group was removed with HCl in dioxane to yield **222** by using *N*-methylmorpholine (NMM) and AcOH. Reduction of the nitro groups was carried out by using catalytic hydrogenation in AcOH to afford **223** (Scheme 19). The preparation of compound **224** was proceeded through condensation of 1,4-diacetylpiperazine-2,5-dione **72** with biphenyl-4-carboxaldehyde to obtain monoacetyl derivative followed by deacetylation by using hydrazine hydrate (Scheme 19).



Scheme 19. Synthesis of 2,5-DKP derivatives (222, 223 and 224) (Labriere et al., 2018).

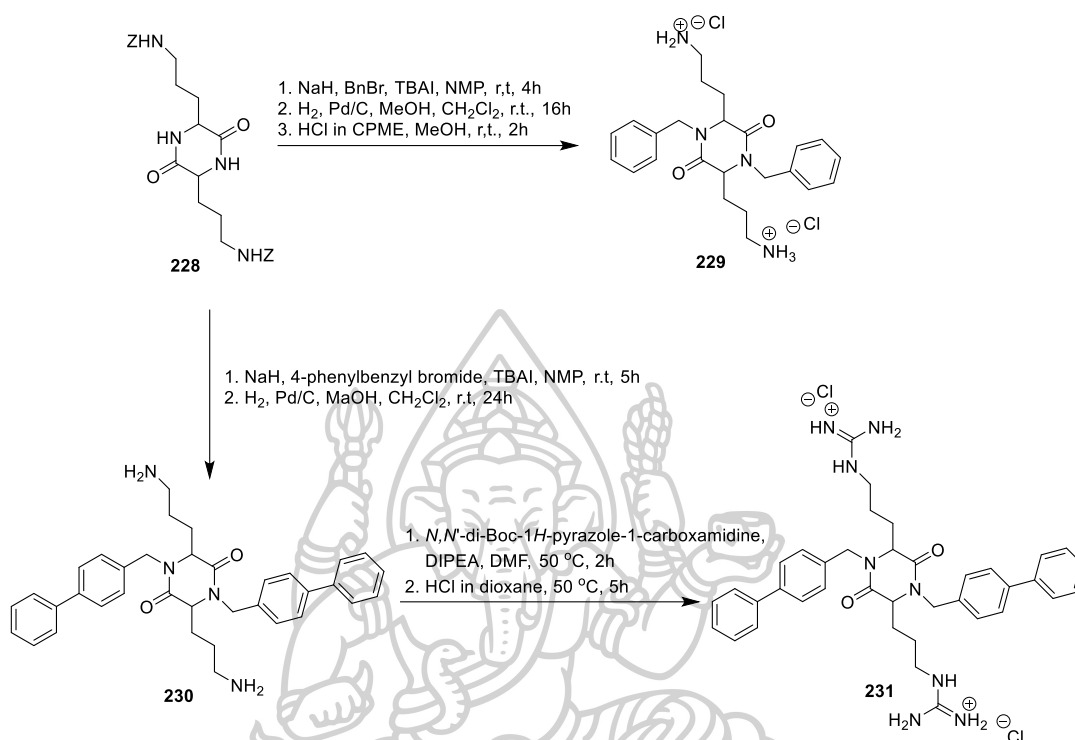
The tetrasubstituted compounds 226 and 227 were prepared from 3,6-dibenzylpiperazine-2,5-dione 225 via the deprotonation with NaH and further alkylated with 4-nitrobenzyl bromide. Reduction of the nitro groups was done by using zinc in AcOH to generate 227 (Scheme 20).



Scheme 20. Synthesis of compound 227 (Labriere et al., 2018).

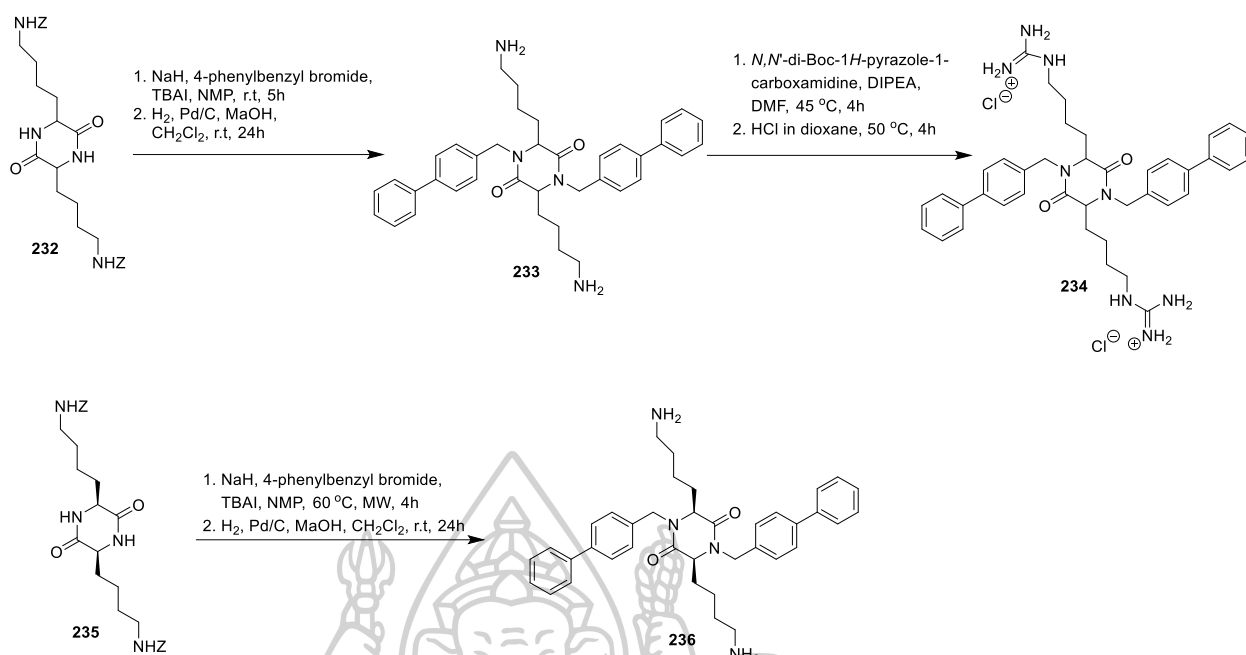
Compound 229 was prepared from mono-condensation of *Z*-ornithine of compound 228. Then, deprotonation with NaH and further alkylated with benzyl bromide followed by deprotection of the *Z* groups via hydrogenation and the amine was converted to its corresponding hydrochloride salt to afford tetrasubstituted 2,5-DKP 229. Compound 231 was obtained by the alkylation of 10 with 4-phenylbenzyl bromide. Then,

amine **230** was reacted with *N,N'*-di-Boc-1*H*-pyrazole-1-carboxamidine and further deprotection of the Boc groups with HCl in dioxane to finally obtain **231** (Scheme 21).



Scheme 21. Preparation of compound **229**, **230** and **231** (Labriere et al., 2018).

Compound **231** was synthesized, in analogy to compound **228**, by mono-condensation of *Z*-lysine. Deprotonation of **232** with NaH and further alkylation with 4-phenylbenzyl bromide yielded **233** after deprotection of the *Z* groups. The primary amines were bis-guanidinylated with *N,N'*-di-Boc-1*H*-pyrazole-1-carboxamidine to generate **234** after deprotection of the Boc groups with HCl in dioxane (Scheme 22). To study the potential impact of stereochemistry on the biological activity, the pure *cis* enantiomer (of **232**) **235** was alkylated with 4-phenylbenzyl bromide using the phosphazene base BEMP to afford **236** (Scheme 22).

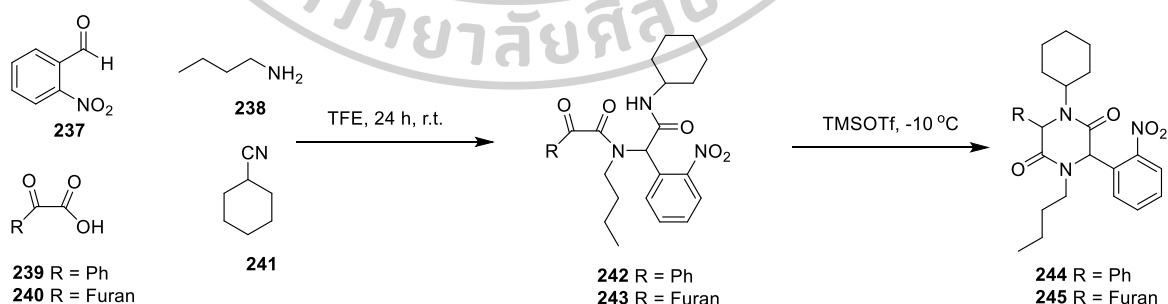


Scheme 22. Preparation of tetrasubstituted 2,5-DKP derivatives 234 and 236 (Labriere et al., 2018).

The prepared compounds were initially screened against a selection of human pathogenic bacteria including both Gram-negative and positive strains (*S.aureus*, *MRSA*, *E.coli*, *E.faecalis*, *P.aeruginosa* and *S.epidermidis*). The result showed that compound 222, 223, 224, 226, 227 and 229 were inactive in the bacterial strain. Compounds 230, 231, 233 and 234 were highly potent antimicrobials with a broad and high activity at low $\mu\text{g/mL}$ concentrations (2 to 32 $\mu\text{g/mL}$). Moreover, Compound 227, 230, 231, 233, 234 and 236 were evaluated in antifungal activity against *C.albicans*, *C.glabrata*, *C.perapsilosis*, *C.krusei* and *C.tropicalis*. The result showed that compound 227 was also inactive against the fungal strain. The remaining five compounds displayed high antifungal activities in the 2 to 16 $\mu\text{g/mL}$ range.

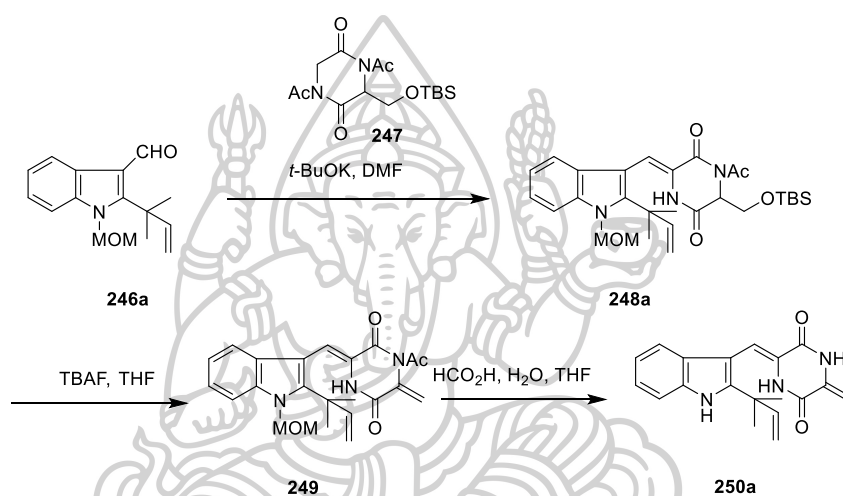
In 2020, Jassem and co-worker (Jassem et al., 2020) reported the synthesis of drug-like piperazine-2,5-dione by using Ugi/tandem process catalyzed by TMSOTf procedure. The products 242 and 243 were prepared from Ugi four-component reaction of 2-nitrobenzaldehyde 237 with butyl amine (238) various keto carboxylic acids 239, 240 and cyclohexyl isocyanide (241) in 2,2,2-trifluoroethanol (TFE). The cyclization of

compound **242** and **243** under condition of TMSOTf (40 mol %) led to compound **244** and **245** with the quantitative yield (Scheme 23). The derivatives **244** and **245** was used to molecular docking analysis with various anticancer target proteins: human androgen receptor (AR) (PDB ID: 1E3G), human steroidogenic cytochrome P450 17A1 (PDB ID: 4NKV), epidermal growth factor receptor 2 HER2 (PDB ID: 3PP0), and estrogen receptor alpha (ER α) (PDB ID: 1A52). The result show that in the proteins HER2 and alpha Er α , compounds **244** and **245** had no H-bonding with amino acids but have a few Van der Waals interactions with the amino acid residues. The calculated binding energies indicated that the compounds **244** and **245** could participate in selective and efficient binding with active sites of the proteins HER2 and alpha ER α binding pockets which was provided a good binding affinity with proteins HER2 and alpha Er α . In the protein receptors 1E3G and 4NKV, compounds **244** and **245** showed interaction with nine amino acid residues of the protein receptor PDB ID:1E3G and fourteen amino acid residues of the protein receptor PDB ID: 4NKV. Piperazine-2,5-dione backbones of the compounds **244** and **245** were suited in the middle of the binding pockets and the most of their substituents anchored in favourable positions of the amino acid residues. Thus, theoretically the synthesized compounds **244** and **245** can provide a high binding affinity with the protein receptors (1E3G and 4NKV) and enhance their inhibitory potency.



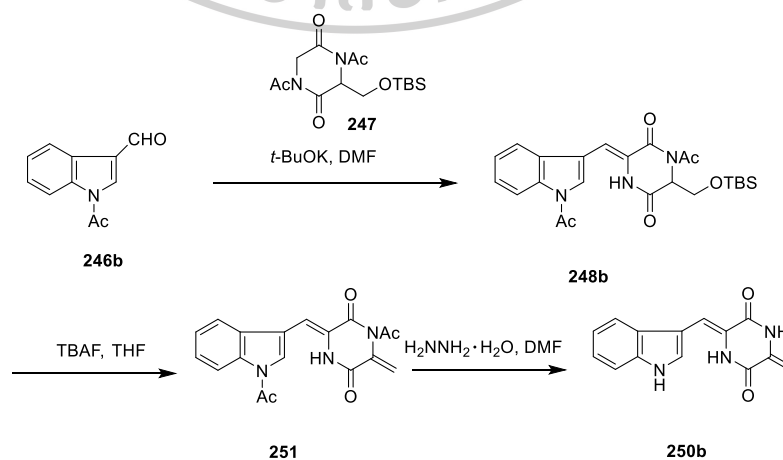
Scheme 23. Synthesis of piperazine-2,5-dione derivatives **244** and **245** (Jassem et al., 2020).

In 2021, Nishiuchi and co-worker (Nishiuchi et al., 2022) reported the synthesis of neoechinulin B and its derivatives as prenylated indole diketopiperazine alkaloids that shows antiviral activities against hepatitis C virus (HCV). Neoechinulin B (**250a**) was obtained from removal of the MOM of intermediate **249** which was synthesized from the coupling of aldehydes **246a** and 1,4-diacetyl-3-(Martínez & Villarreal)piperazine-2,5-dione (**247**) followed by the TBAF treatment of the coupling products **248a** as shown in scheme 24.



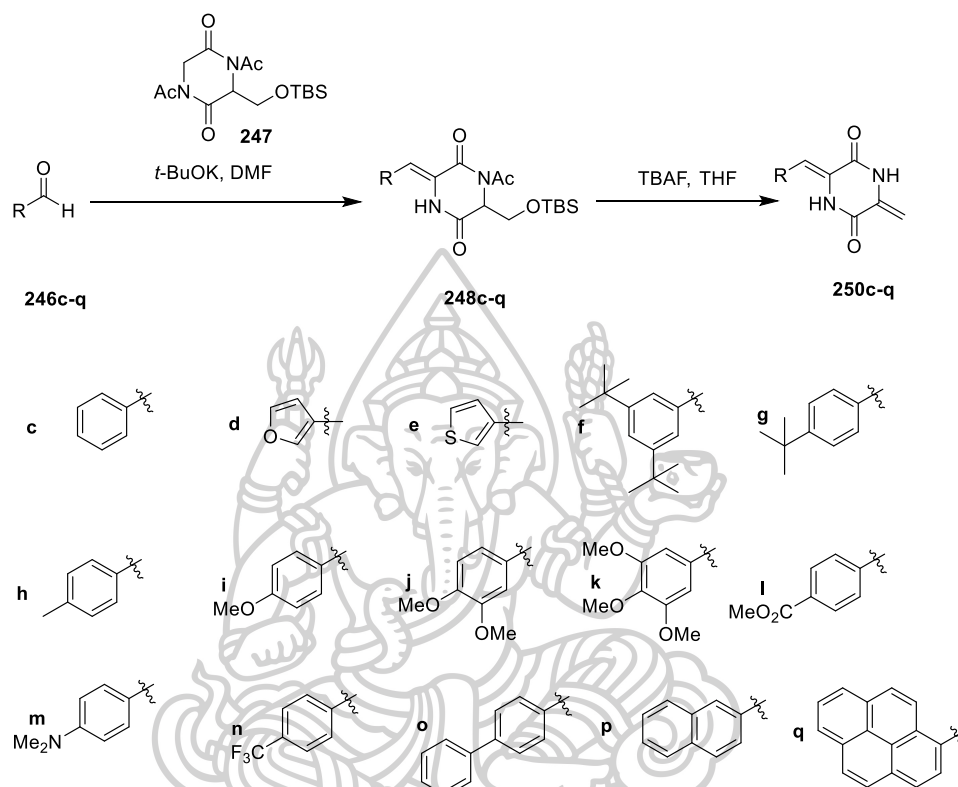
Scheme 24. Synthesis of Neoechinulin B (**250a**) (Nishiuchi et al., 2022).

Deprenylneoechinulin B (**250b**) was synthesized from coupling reaction of compound **246b** with compound **247** followed by treatment with TBAF and deacetylation by using hydrazine monohydrate in DMF as shown in scheme 25.



Scheme 25. Synthesis of Deprenylneoechinulin B (**250b**) (Nishiuchi et al., 2022).

The another 3-arylmethylene-6-methylenepiperazine-2,5-diones (**250c-q**) were obtained through two step synthesis, coupling reaction and TBAF treatment as shown in scheme 26.



Scheme 26. Synthesis of 3-arylmethylene-6-methylenepiperazine-2,5-diones (**250c-q**) (Nishiuchi et al., 2022).

Compound **250a-q** were evaluated antiviral activities against HCV and SARS-CoV-2. Neoechinulin B (**250a**) showed antiviral activities against HCV and SARS-CoV-2 with IC_{50} 4.7 ± 1.4 and 32.9 ± 13.2 μ M, respectively. These results indicated that the exomethylene moiety in compound **250a** was important for the antiviral activities against both HCV and SARS-CoV-2. Among the neoechinulin B derivatives tested in this study, compounds **250l**, **250n**, and **250p** showed more potent anti-HCV activity than **250a** with IC_{50} 1.2 ± 0.16 , 1.6 ± 0.32 and 0.26 ± 0.11 μ M, respectively, without exhibiting any serious cytotoxicity. Furthermore, compound **250c**, **250d**, **250h**, **250j**, **250l**, and **250o** exhibited anti-SARS-CoV-2 activity. Particularly, **250c**, **250d**, **250h**, **250j**, and **250l** exhibited more

potent anti-SARS-CoV-2 activity than **250a** with IC_{50} 13.6±3.2, 9.3±6.2, 6.0±2.4, 10.3±3.7 and 8.4±2.1 μ M, respectively.

In 2008, Tuntiwachwuttikul and co-worker (Tuntiwachwuttikul et al., 2008) reported the isolation of four novel secondary metabolites, Lansai A-D (**26-29**) as a 2,5-DKP derivative, which were isolated from ethyl acetate extract of the culture of *Streptomyces* sp. SUC1, endophytic on the aerial roots of *Ficus benjamina*. The crude ethyl acetate extract of the culture of *Streptomyces* sp. SUC1 showed *in vitro* anticancer activity (BC and KB cell lines) with IC_{50} of 3.41 and >20 mg/ml, respectively. The crude extract also possessed antifungal activity against *Colletotrichum musae* with an MIC of 15 mg/ml. Unfortunately, compound **27** was only weakly active against the BC cell line (IC_{50} =15.03 mg/ml); compounds **26**, **28**, and **29** were inactive (IC_{50} >20 mg/ml). Compounds **26-29** were also inactive against *C. musae* (MIC>100 mg/ml).

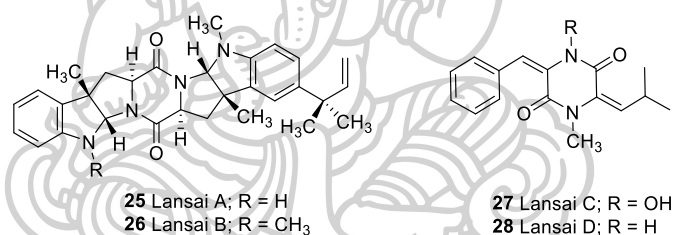
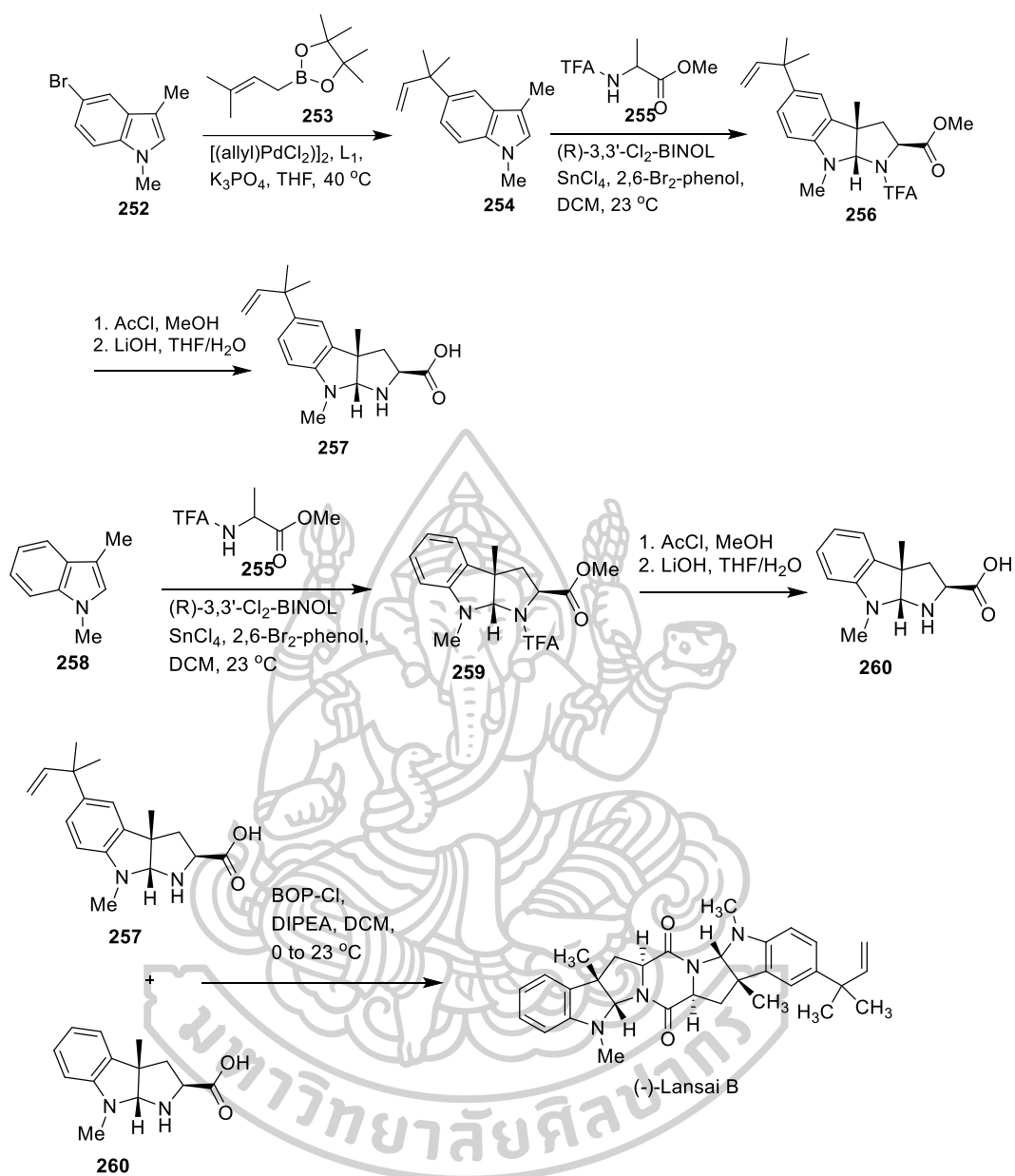


Figure 11. Structure of Lansai A-D.

In 2009, Taechowisan and co-worker (Taechowisan et al., 2009) reported the study of *in vitro* anti-inflammatory action of Lansai A (**26**) and C (**28**) in 1, 2.5 and 5 mg/mL concentrations. The result show that Lansai C was inhibited the formation of nitric oxide (NO), prostaglandin E2 (PGE2), tumour necrosis factor (TNF- α), interleukin (IL-1 α), IL-6 and IL-10 and expression of NO synthase and cyclooxygenase-2 (COX-2) in lipopolysaccharide (LPS)-induced murine macrophage RAW 264.7 cells. In addition, cytotoxic effect of Lansai C (**28**) was evaluated in the absence or presence of LPS. When treated alone, Lansai A (**26**) and C (**28**) did not affect the cell viability at all concentrations. Therefore, Lansai C (**28**) would be useful for the treatment of inflammatory diseases that show the increased expression of COX-2.

In 2010, Taechowisan and co-worker (Taechowisan et al., 2010) reported the investigation of the effects of Lansai C (**28**) and D (**29**) on NO production in lipopolysaccharide-induced RAW 264.7 cells, and evaluation of the mechanisms of action of the compounds. Lansai C (**28**) and D (**29**) were tested cytotoxic effects by MTT assay. These compounds were not toxic to RAW 264.7 cells at concentration 5 µg/ml. Lansai C (**28**) and D (**29**) were tested the effects to NO production, iNOS protein and iNOS mRNA expression, NF-kB and STAT-1 activations. The results show that Lansai C (**28**) and D (**29**) inhibited NO production with IC₅₀ 2.63 and 3.42 µg/ml, respectively. These compounds inhibited LPS-induced iNOS protein and iNOS mRNA expression. Lansai C (**28**) and D (**29**) inhibited the LPS-induced activation of transcription factors for iNOS by more than 80 and 70% inhibition, respectively of NF-kB and 70 and 55% inhibition, respectively of STAT-1. Therefore, both of Lansai C (**28**) and D (**29**) are implicated in their effects on iNOS expression. The mechanism of Lansai C (**28**) and D (**29**) to STAT-1 inhibition are not known, but may be associated with inhibition of phosphorylation of STAT-1 or its up-stream kinase JAK2. Because NF-kB and STAT-1 are involved in the activation of several inflammatory genes, Lansai C and D could be inhibited the activation of NF-kB and STAT-1, therefore, Lansai C (**28**) and D (**29**) exhibited the pharmacological efficacy as anti-inflammatory compounds.

In 2014, Wang and co-worker (Wang & Reisman, 2014) reported the total synthesis of (-)-Lansai B. The synthesis was started from bromoindole **252** reacted with prenylboronate **253** via Suzuki-Miyaura coupling to furnish the reverse-prenylated indole **254**. Compound **254** reacted with methyl 2-trifluoroacetamidoacrylate via (3+2) cycloaddition provided the pyrroloindoline **256** in 85% yield and 92% ee. Compound **259** could be prepared from 1,3-dimethyl indole **258** and acrylate **255** in 79% yield, 12:1 d.r. and 93% ee. Compounds **256** and **259** were undergone TFA deprotection and saponification to provide compound **260** and **257**, respectively. Finally, treatment of the mixture of compounds **260** and **259** with BOPCl delivered (-)-Lansai B in 20 % overall yield from commercially available materials in 6 steps synthesis (Scheme 27).



Scheme 27. Total synthesis of (-)-Lansai B (Wang & Reisman, 2014).

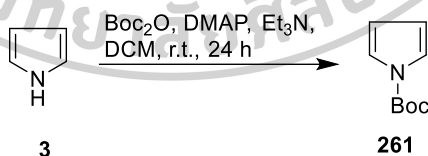
CHAPTER 3

EXPERIMENTAL

1. General methods for the synthesis

All reactions sensitive to air or moisture were carried out under anhydrous conditions, unless otherwise stated. Solvents and reagents were used with further purification, which were purchased from Sigma–Aldrich (Darmstadt, Germany), Tokyo Chemical Industry (Tokyo, Japan) and Fluka Chemical (Buchs, Switzerland) Companies. ^1H and ^{13}C NMR spectra were measured in CDCl_3 , Methanol- d_4 and DMSO-d_6 on a Bruker Avance 300 spectrometer (Bruker, Massachusetts, Germany; 300 MHz for ^1H , 75 MHz for ^{13}C). Melting points were uncorrected and measured using a Stuart Scientific SMP 2 melting point apparatus (Cole-Parmer Ltd., Staffordshire, UK). Mass spectra were measured using micrOTOF (Bruker, MA, USA). The reaction was monitored by thin-layer chromatography (TLC) and by using an aluminum sheet precoated with silica gel 60 F₂₅₄ (Darmstadt, Germany). Column chromatography was conducted on Merck Kieselgel 60 (Darmstadt, Germany).

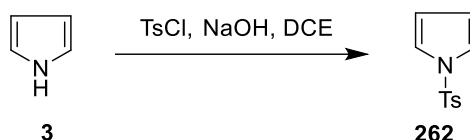
2. Synthesis of pyrrole and furan derivatives

Synthesis of *tert*-butyl 1*H*-pyrrole-1-carboxylate (261)

A mixture of catalytic amount of DMAP (0.2 g, 1.6 mmol), pyrrole (3) (1 mL, 14 mmol), triethylamine (2.6 mL, 18 mmol) and Boc_2O (4.3 mL, 4.08 g, 18 mmol) was dissolved in DCM (50 mL) under argon atmosphere. The reaction mixture was stirred for 24 h at room temperature and then quenched with saturated. NH_4Cl (30 mL). The organic layer was washed with brine and water, respectively. The combined organic layers were dried over with anhydrous Na_2SO_4 and concentrated under reduced pressure to give colorless solid (2.09 g) which used in the following step without further

purification. ^1H NMR (300 MHz, CDCl_3) δ 7.27 (t, $J = 2.4$ Hz, 2H), 6.24 (t, $J = 2.4$ Hz, 2H), 1.63 (2, 9H) ppm.

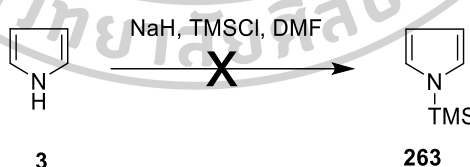
Synthesis of 1-tosyl-1H-pyrrole (262)



Pyrrole (1 mL, 0.96 g, 14 mmol) was added to well-agitated NaOH (1.73 g, 43 mmol) in DCE 10 mL. The mixture was then cooled to 0 °C and stirred for 10 min. The solution of TsCl (3.3 g, 17 mmol) in DCE 2 mL was added dropwise over 20 min. After 30 min, the mixture was allowed to come to room temperature and stirred for overnight. Then, the reaction was quenched by pouring to distilled water 30 mL and extracted with DCM (3 x 20 mL). The combined organic layer was washed with water and dried over with anhydrous Na_2SO_4 and concentrated under reduced pressure to give white solid (2.78 g, 87 %yield) which used in the following step without further purification. ^1H NMR (300 MHz, CDCl_3) δ 7.73 (d, $J = 8.4$ Hz, 2H), 7.28 (d, $J = 8.1$ Hz, 2H), 7.15 (t, $J = 2.4$ Hz, 2H), 6.28 (t, $J = 2.4$ Hz, 2H), 2.39 (s, 3H) ppm.

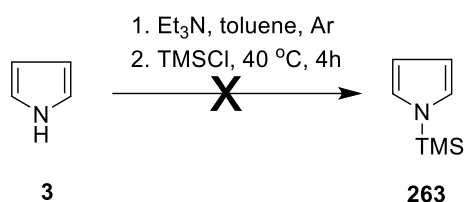
Synthesis of 1-(trimethylsilyl)-1H-pyrrole (263)

Procedure 1



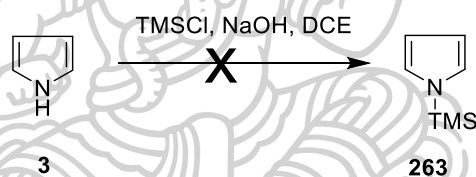
Pyrrole (2.5 mL, 2.4 g, 36 mmol) was dissolved in DMF 50 mL. NaH (1.6 g, 40 mmol) was added portionwise to a solution of pyrrole at 0 °C. The mixture was stirred for 45 min. Then, TMSCl (4.6 mL, 3.9 g, 36 mmol) was added dropwise to a solution. The mixture was allowed to reach room temperature and stirred for 2 h. The mixture was diluted with water 50 mL and extracted with Et_2O (2 x 20 mL). The combined organic extracts were dried with anhydrous Na_2SO_4 and concentrated under reduced pressure. The crude mixture contained no required product when check NMR spectroscopy.

Procedure 2

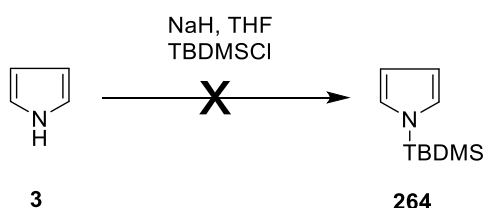


TMSCl (1.9 mL, 1.6 g, 15 mmol) was added to a solution of pyrrole (1 mL, 0.96 g, 14 mmol) with triethylamine (2.4 mL, 1.7 g, 17 mmol) and toluene 14 mL. The mixture was stirred at 40 °C for 4 h. Then the mixture was cooled to room temperature and diluted with 14 mL of hexane:ether (1:1). The mixture was filtered through celite and the filtrate was concentrated in vacuo. The crude mixture contained no required product when check NMR spectroscopy.

Procedure 3



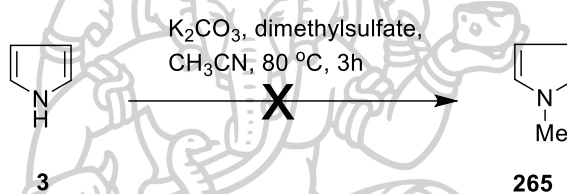
Pyrrole (1 mL, 0.96 g, 14 mmol) was dissolved in DCE 10 mL. NaOH (1.7 g, 43 mmol) was added to a solution of pyrrole at 0 °C and stirred for 10 min. The solution of TMSCl (2.2 mL, 1.88 g, 17 mmol) in DCE 2 mL was added dropwise to a mixture over 20 min. After 30 min, the reaction was allowed to reach room temperature and stirred for overnight. The mixture was diluted with water 50 mL. The reaction was extracted with EtOAc (3 x 20 mL). The combined organic layer was dried over with anhydrous Na₂SO₄ and concentrated under reduced pressure. The crude mixture contained no required product when check NMR spectroscopy.

Synthesis of 1-(*tert*-butyldimethylsilyl)-1*H*-pyrrole (264)

The solution of pyrrole (0.52 mL, 0.5 g, 7 mmol) in dry THF 15 mL was added to solution of NaH (1.24 g, 53 mmol) in dry THF 20 mL under argon atmosphere at room temperature. Then, a solution of TBDMSCl (3.1 g, 20 mmol) in THF 15 mL was added dropwise to the mixture. The reaction mixture was stirred at room temperature for 12 h. Then, water 15 mL was added cautiously to the mixture. The mixture was extracted with Et₂O (2 x 20 mL). The combined organic extracts were dried with anhydrous Na₂SO₄ and concentrated under reduced pressure. The crude mixture contained no required product when check NMR spectroscopy.

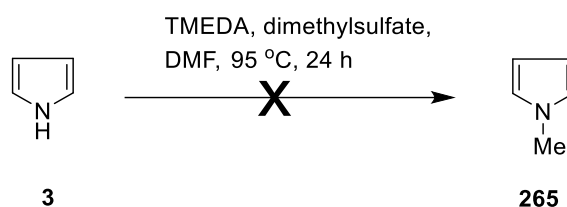
Synthesis of 1-methyl-1H-pyrrole (265)

Procedure 1



Pyrrole (0.5 mL, 0.46 g, 6.8 mmol) was dissolved in dry CH₃CN (20 mL). K₂CO₃ (1.4 g, 10 mmol) was added to a mixture and stirred for 30 min at 0 °C. Dimethylsulfate (0.8 mL, 1.01 g, 8 mmol) was added to the mixture and refluxed at 80 °C for 3 h. Then, solvent was evaporated under reduced pressure. The residue was dissolved with DCM 30 mL and washed water (3 x 30 mL). The DCM layer was dried with anhydrous Na₂SO₄ and concentrated under reduced pressure. However, the crude mixture contained no required product when check NMR spectroscopy.

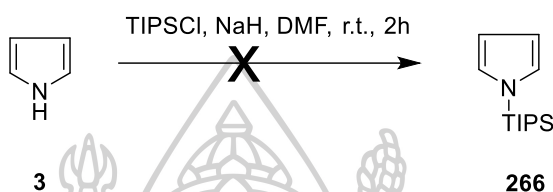
Procedure 2



Pyrrole (0.7 mL, 0.67 g, 10 mmol) was mixed with TMEDA (0.15 mL, 0.12 g, 1mmol) and dimethylsulfate (10 mL, 13.3 g, 105 mmol) in DMF 5 mL. The mixture was

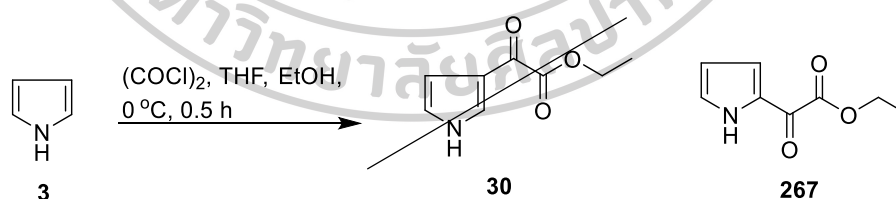
stirred and heated to 95 °C for 24 h. After completion, the mixture was cooled to room temperature and water was added 8 mL. The mixture was extracted with EtOAc (2 x 15 mL). The combined organic layer was washed with water (2 x 10 mL). The organic layer was dried with anhydrous Na₂SO₄ and concentrated under reduced pressure. However, the crude mixture contained no required product when check NMR spectroscopy.

Synthesis of 1-(triisopropylsilyl)-1*H*-pyrrole (266)



NaH (0.63 g, 27 mmol) was added portionwise to a solution of pyrrole (1 mL, 0.96 g, 14 mmol) in DMF 20 mL at 0 °C. The mixture was stirred for 45 min. TIPSCl (3.1 mL, 2.79 g, 14 mmol) was added dropwise to a mixture. The mixture was allowed to room temperature and stirred for 2 h. Then, the mixture was diluted with water 50 mL and extracted with Et₂O (2 x 20 mL). The organic layer was dried with anhydrous Na₂SO₄ and concentrated under reduced pressure. The crude mixture contained no required product when check NMR spectroscopy.

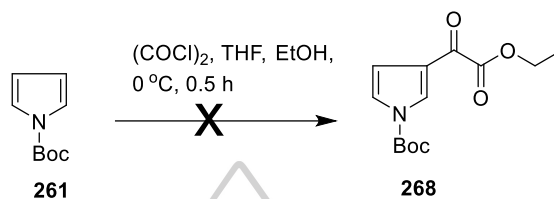
Synthesis of ethyl 2-oxo-2-(1*H*-pyrrol-3-yl)acetate (30)



Oxalyl chloride (1.4 mL, 11 mmol) was added dropwise to a solution of pyrrole (0.9 mL, 10 mmol) in THF 30 mL at 0 °C. When reaction was completed, EtOH 5 mL was added and stirred for 0.5 h at room temperature. The mixture was poured into ice water and extracted with DCM (2 x 20 mL). The organic phase was dried with anhydrous Na₂SO₄ and evaporated under reduced pressure. The crude product was purified by preparative TLC using 4:1 hexane:EtOAc as mobile phase to give only the undesired ethyl 2-oxo-2-(1*H*-pyrrol-2-yl)acetate (**267**) (1.51 g, 62 % yield) as colorless oil. ¹H NMR

(300 MHz, CDCl₃) δ 7.39 (dd, $J = 3.9, 1.2$ Hz, 1H), 7.20 (s, 1H), 6.35 (dd, $J = 3.6, 2.1$ Hz, 1H), 4.41 (q, $J = 7.2$ Hz, 2H), 1.41 (t, $J = 7.2$ Hz, 1H) ppm; ¹³C NMR (75 MHz, CDCl₃) δ 172.16, 162.40, 129.46, 128.65, 122.70, 112.22, 62.44, 14.05 ppm

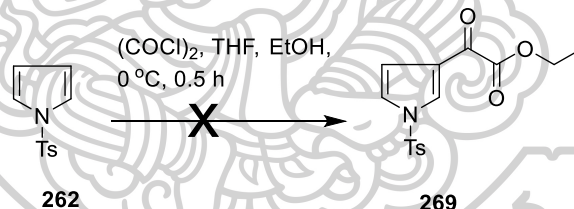
Synthesis of *tert*-butyl 3-(2-ethoxy-2-oxoacetyl)-1*H*-pyrrole-1-carboxylate (268)



The synthesis of *tert*-butyl 3-(2-ethoxy-2-oxoacetyl)-1*H*-pyrrole-1-carboxylate (268) was employed the same procedure in the synthesis of ethyl 2-oxo-2-(1*H*-pyrrol-3-yl)acetate (30). The product was not observed.

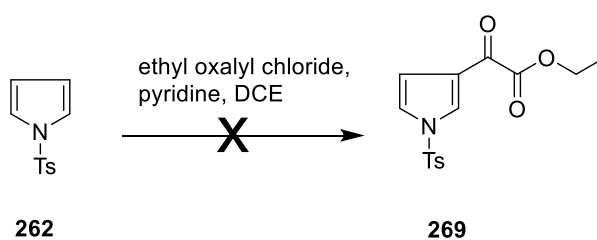
Synthesis of ethyl 2-oxo-2-(1-tosyl-1*H*-pyrrol-3-yl)acetate (269)

Procedure 1



The procedure 1 of ethyl 2-oxo-2-(1-tosyl-1*H*-pyrrol-3-yl)acetate (269) synthesis was used the same procedure in the synthesis of ethyl 2-oxo-2-(1*H*-pyrrol-3-yl)acetate (30). The product was not observed.

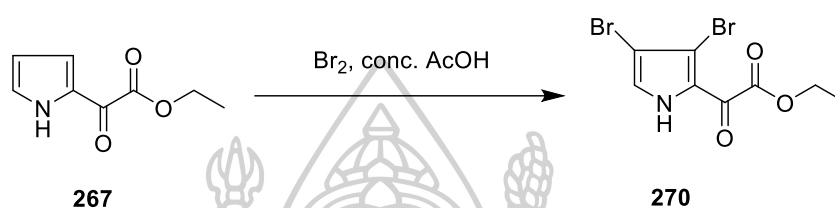
Procedure 2



The mixture of 1-tosyl-1*H*-pyrrole (262) (0.1g, 0.5 mmol), pyridine (0.11 mL, 0.1 g, 1.4 mmol) and ethyl oxalyl chloride (0.19 g, 1.4 mmol) in DCE 3 mL was refluxed at 75

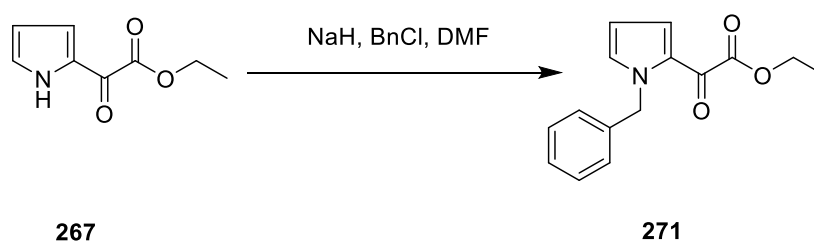
°C for 16 h. Then, the reaction was cooled to room temperature and poured into saturated aqueous NH_4Cl . The organic phase was separated and combined with a DCM extract of aqueous phase. The combined organic phase was washed with saturated aqueous NaCl , dried with anhydrous Na_2SO_4 and evaporated under reduced pressure. However, the product was not observed.

Synthesis of ethyl 2-(3,5-dibromo-1*H*-pyrrol-2-yl)-2-oxoacetate (270)



The bromine (0.3 mL, 1 g, 6 mmol) was added dropwise to a stirred solution of ethyl 2-oxo-2-(1*H*-pyrrol-3-yl)acetate (**267**) (0.46 g, 3 mmol) in AcOH 16 mL. The reaction mixture was stirred at room temperature for overnight. Then, the mixture was poured onto ice water, the precipitate was occurred. The precipitate was filtered and washed with water to give ethyl 2-(3,5-dibromo-1*H*-pyrrol-2-yl)-2-oxoacetate (**270**) (0.12 g, 62 %yield) as a white solid which used in the following step without further purification. ^1H NMR (300 MHz, CDCl_3) δ 7.38 (s, 1H), 4.40 (q, $J = 7.2$ Hz, 2H), 1.41 (t, $J = 7.2$ Hz, 3H) ppm; ^{13}C NMR (75 MHz, CDCl_3) δ 164.9, 161.5, 130.2, 124.4, 114.0, 102.2, 62.9, 14.05 ppm.

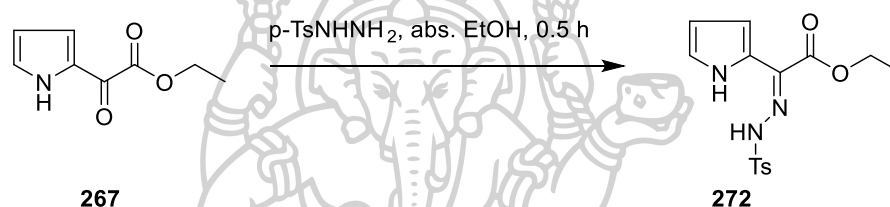
Synthesis of ethyl 2-(1-benzyl-1*H*-pyrrol-2-yl)-2-oxoacetate (271)



NaH (0.3 g, 13 mmol) was added to a solution of ethyl 2-oxo-2-(1*H*-pyrrol-3-yl)acetate (**267**) (1 g, 6 mmol) in DMF 5 mL at 0 °C and stirred for 45 min. Then, benzylchloride (0.9 mL, 1 g, 7.9 mmol) was added dropwise to a mixture. The reaction was allowed to warm to room temperature and stirred for 3 h. Then, water 50 mL was

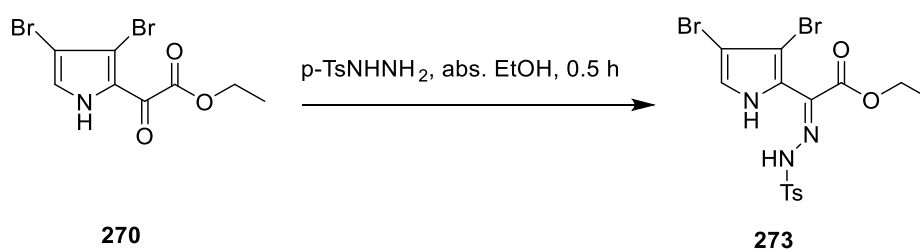
added to a reaction. The reaction was extracted with EtOAc (3 x 20 mL). The combined organic layer was dried over with anhydrous Na_2SO_4 and concentrated under reduced pressure to give colorless oil crude. The crude was purified on silica gel by column chromatography using 4:1 hexane:EtOAc as mobile phase. The ethyl 2-(1-benzyl-1*H*-pyrrol-2-yl)-2-oxoacetate (**271**) (0.86 g, 56 % yield) was obtained as colorless oil. ^1H NMR (300 MHz, CDCl_3) δ 7.32 (dd, $J = 4.2, 1.8$ Hz, 1H), 7.30-7.19 (m, 3H), 7.14-7.11 (m, 2H), 7.05 (t, $J = 2.1$ Hz, 1H), 6.25 (dd, $J = 4.5, 2.4$ Hz, 1H), 5.54 (s, 2H), 4.33 (q, $J = 7.2$ Hz, 2H), 1.35 (t, $J = 7.2$ Hz, 3H) ppm.

Synthesis of ethyl (*E*)-2-(1*H*-pyrrol-2-yl)-2-(2-tosylhydrazono)acetate (**272**)



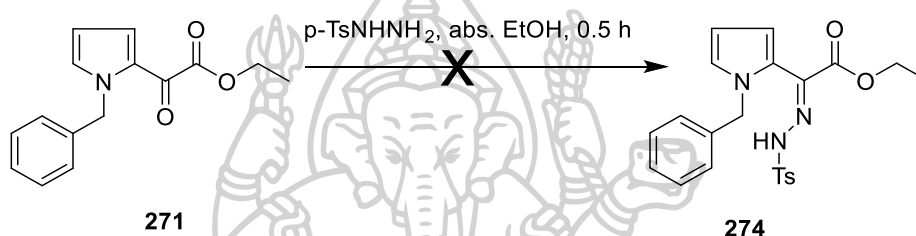
The mixture of ethyl 2-oxo-2-(1*H*-pyrrol-3-yl)acetate (**267**) (0.33 g, 2 mmol) and *p*-TsNHNH₂ (0.62 g, 3 mmol) in absolute EtOH 5 mL was refluxed for 30 min. When the reaction completed, solvent was removed under vacuo to give crude product. The crude product was purified by column chromatography using 4:1 hexane:EtOAc as eluent to give ethyl (*E*)-2-(1*H*-pyrrol-2-yl)-2-(2-tosylhydrazono)acetate (**272**) (0.062 g, 9 % yield) as a yellow solid. ^1H NMR (300 MHz, CDCl_3) δ 11.54 (s, 1H), 9.2 (br s, 1H), 7.84 (d, $J = 8.4$ Hz, 2H), 7.30 (d, $J = 7.8$ Hz, 2H), 6.86-6.84 (m, 1H), 6.73-6.71 (m, 1H), 6.20-6.17 (m, 1H), 4.40 (q, $J = 7.2$ Hz, 2H), 2.42 (s, 3H), 11.41 (t, $J = 7.2$ Hz, 3H) ppm.

Synthesis of ethyl (*E*)-2-(3,5-dibromo-1*H*-pyrrol-2-yl)-2-(2-tosylhydrazono)acetate (**273**)



The synthesis of ethyl (*E*)-2-(3,5-dibromo-1*H*-pyrrol-2-yl)-2-(2-tosylhydrazono)acetate (**273**) was used the same procedure for the synthesis of ethyl (*E*)-2-(1*H*-pyrrol-2-yl)-2-(2-tosylhydrazono)acetate (**272**). The crude product was purified by column chromatography using 4:1 hexane:EtOAc as eluent to provide the unstable product (0.046 g, 5 %yield) as a yellow oil. ^1H NMR (300 MHz, CDCl_3) δ 11.76 (s, 1H), 10.1 (br s, 1H), 7.82 (d, $J = 8.4$ Hz, 2H), 7.33 (d, $J = 8.1$ Hz, 2H), 6.67 (ds, $J = 3$ Hz, 1H), 4.39 (q, $J = 7.2$ Hz, 2H), 2.42 (s, 3H), 1.41 (t, $J = 7.2$ Hz, 3H) ppm.

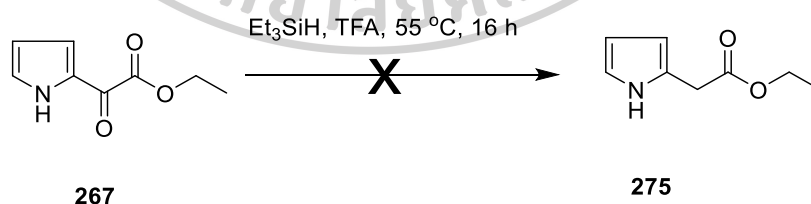
Synthesis of ethyl (*E*)-2-(1-benzyl-1*H*-pyrrol-2-yl)-2-(2-tosylhydrazono)acetate (**274**)



The synthesis of ethyl (*E*)-2-(1-benzyl-1*H*-pyrrol-2-yl)-2-(2-tosylhydrazono)acetate (**274**) was used the same procedure for the synthesis of ethyl (*E*)-2-(1*H*-pyrrol-2-yl)-2-(2-tosylhydrazono)acetate (**272**) but not provided the desired product.

Synthesis of ethyl 2-(1*H*-pyrrol-2-yl)acetate (**275**)

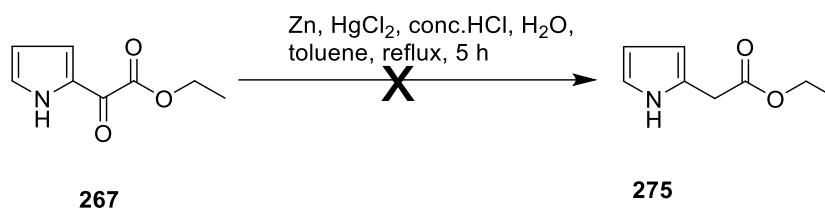
Procedure 1



Et_3SiH (5.12 mL, 3.69 g, 31 mmol) was added to a solution of ethyl 2-oxo-2-(1*H*-pyrrol-3-yl)acetate (**267**) (0.26 g, 1.5 mmol) in trifluoroacetic acid 4 mL. The reaction mixture was heated at 55 °C for 16 h. Then, the mixture was concentrated and the residue was diluted with saturated NaHCO_3 50 mL. The mixture was extracted with EtOAc (3 x 75 mL). The combined organic phase was dried with anhydrous Na_2SO_4 and

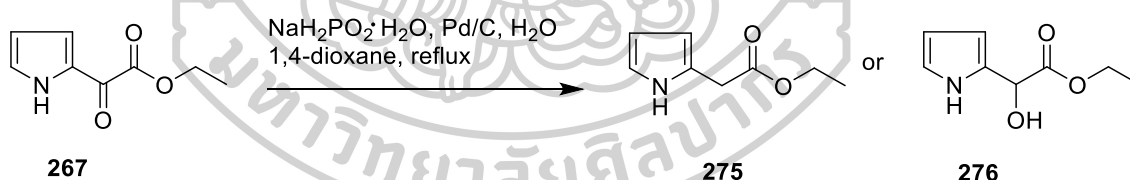
evaporated under reduced pressure. The crude mixture contained no required product when check NMR spectroscopy.

Procedure 2



A mixture of Zn (1.8 g, 27.5 mmol), Hg₂Cl₂ (0.18 g, 0.66 mmol), conc. HCl (0.1 mL) and water 3 mL was heated under reflux for 5 min. The mixture was filtered and the solid residue was treated with water 1 mL, conc. HCl 26 mL, toluene 1.5 mL and ethyl 2-oxo-2-(1*H*-pyrrol-3-yl)acetate (0.44 g, 2.63 mmol). The mixture was heated under reflux for 5 h. Then, the mixture was diluted with water 20 mL and extracted with Et₂O (3 x 20 mL). The combined organic layers were washed with water (20 mL) and dried with anhydrous Na₂SO₄ and evaporated under reduced pressure. However, the crude mixture contained no required product when check NMR spectroscopy.

Procedure 3



Reaction time	product
2 days	275
8 h	276

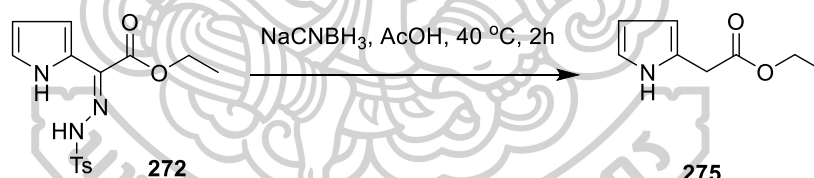
The solution of NaH₂PO₂·H₂O (78 mmol) in water 7.5 mL was added to the mixture of ethyl 2-oxo-2-(1*H*-pyrrol-3-yl)acetate (**267**) (15.5 mmol) and catalyst amount of

10 % Pd/C (mmol) in 1,4-dioxane 46 mL. The mixture was refluxed at 100 °C for the following reaction time. Then, the reaction mixture was cooled to room temperature. The mixture was filtered through celite and washed with EtOAc. The filtrate was concentrated under reduced pressure. The crude product was purified by column chromatography using 9:1 hexane:EtOAc as eluent to give the product.

Ethyl 2-(1*H*-pyrrol-2-yl)acetate (**275**) (0.01 g, 5 % yield) was given as colorless oil. ¹H NMR (300 MHz, CDCl₃) δ 8.74 (br s, 1H), 6.75 (dd, *J* = 3.9, 2.7 Hz, 1H), 6.14 (dd, *J* = 5.7, 3 Hz, 1H), 6.01 (s, 1H), 4.17 (q, *J* = 7.2 Hz, 2H), 3.66 (s, 2H), 1.27 (t, *J* = 7.2 Hz, 3H) ppm; ¹³C NMR (75 MHz, CDCl₃) δ 171.3, 123.3, 117.7, 108.3, 107.3, 61.1, 33.2, 14.2 ppm

Ethyl 2-hydroxy-2-(1*H*-pyrrol-2-yl)acetate (**276**) (0.17 g, 29 % yield) was given as colorless oil. ¹H NMR (300 MHz, CDCl₃) δ 8.67 (br s, 1H), 6.76 (s, 1H), 6.19-6.14 (m, 2H), 5.25 (s, 1H), 4.33-4.22 (m, 2H), 3.40 (br s, 1H), 1.28 (t, *J* = 7.2 Hz, 3H) ppm.

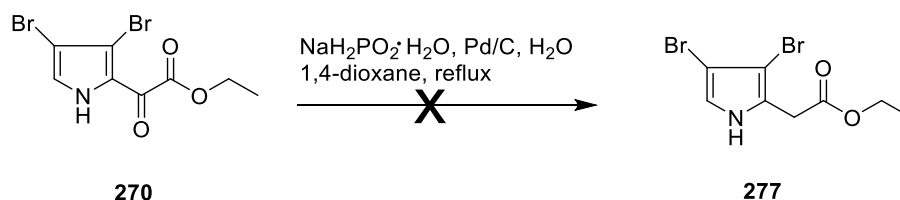
Procedure 4



NaCNBH₃ (0.5 g, 7.9 mmol) was added to a solution of (*E*)-2-(1*H*-pyrrol-2-yl)-2-(2-tosylhydrazono)acetate (**272**) (0.48 g, 1.4 mmol) in 3 mL of glacial AcOH. The reaction mixture was stirred at 40 °C for 2h. Then, the reaction mixture was quenched by pouring into 60 mL of ice-cold water and the mixture was extracted with DCM (2 x 30 mL). The DCM layer was washed with saturated NaHCO₃ and water, respectively, and dried with anhydrous Na₂SO₄ and evaporated under reduced pressure to provide crude product. The crude product was purified by preparative TLC using 6:1 hexane:EtOAc as mobile phase to give the Ethyl 2-(1*H*-pyrrol-2-yl)acetate (**275**) (0.013 g, 6 % yield) as colorless oil. ¹H NMR (300 MHz, CDCl₃) δ 8.74 (br s, 1H), 6.75 (dd, *J* = 3.9, 2.7 Hz, 1H), 6.14 (dd, *J* = 5.7, 3 Hz, 1H), 6.01 (s, 1H), 4.17 (q, *J* = 7.2 Hz, 2H), 3.66 (s, 2H), 1.27 (t, *J*

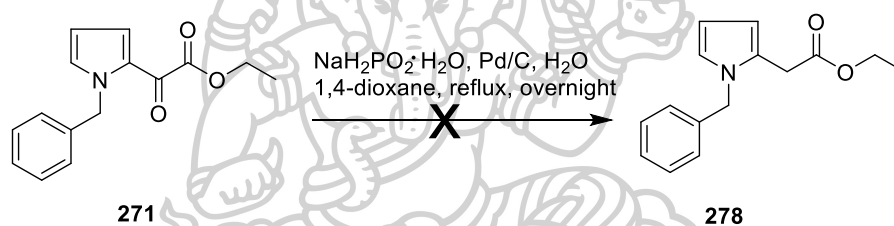
= 7.2 Hz, 3H) ppm; ^{13}C NMR (75 MHz, CDCl_3) δ 171.3, 123.3, 117.7, 108.3, 107.3, 61.1, 33.2, 14.2 ppm.

Synthesis of ethyl 2-(3,5-dibromo-1H-pyrrol-2-yl)acetate (277)



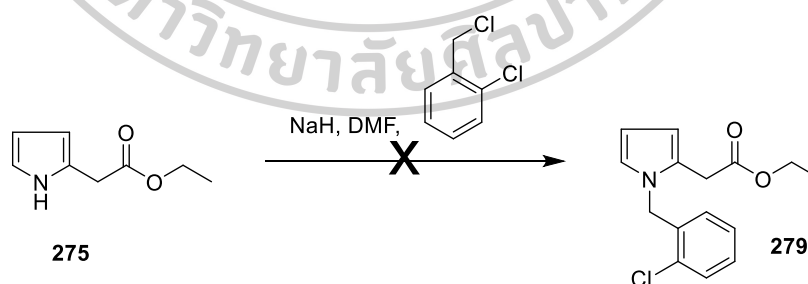
The synthesis was followed the procedure 3 of the synthesis of ethyl 2-(1H-pyrrol-2-yl)acetate (275) but the desired product was not observed.

Synthesis of ethyl 2-(1-benzyl-1H-pyrrol-2-yl)-2-oxoacetate (278)



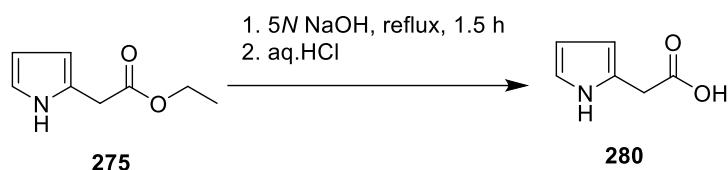
The synthesis was employed the procedure 3 of the synthesis of ethyl 2-(1H-pyrrol-2-yl)acetate (275) but the desired product was not observed.

Synthesis of ethyl 2-(1-(2-chlorobenzyl)-1H-pyrrol-2-yl)acetate (279)



The synthesis was employed using the procedure for the synthesis of ethyl 2-(1-benzyl-1H-pyrrol-2-yl)-2-oxoacetate (271) but using 1-chloro-2-(chloromethyl)benzene instead of benzylchloride as a *N*-substituted reagent. However, the desired product was not observed.

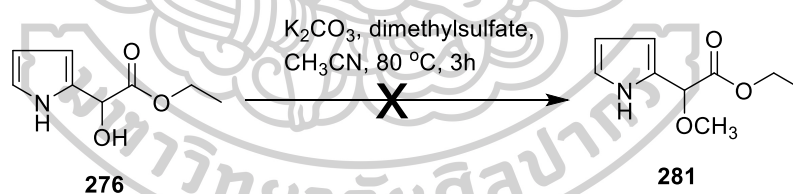
Synthesis of 2-(1*H*-pyrrol-2-yl)acetic acid (280)



5*N* NaOH 2 mL was added to a solution of ethyl 2-(1*H*-pyrrol-2-yl)acetate (275) (0.048 g, 0.4 mmol) in MeOH 5 mL. The reaction mixture was refluxed for 1.5 h. Then, the mixture was allowed to cool in ice bath and the aqueous HCl solution was added to the mixture until pH = 3. The mixture was extracted with EtOAc (3 x 10 mL). The organic layer was washed with saturated NaCl and dried with anhydrous Na₂SO₄ and evaporated under reduced pressure to provide 2-(1*H*-pyrrol-2-yl)acetic acid (0.0051 g, 10 %yield) as a colorless oil which without the further purification. ¹H NMR (300 MHz, CDCl₃) δ 8.60 (br s, 1H), 6.76 (s, 1H), 6.15 (dd, *J* = 5.4, 2.7 Hz, 1H), 6.05 (s, 1H), 3.72 (s, 2H) ppm; ¹³C NMR (75 MHz, CDCl₃) δ 171.8, 122.4, 118.0, 108.5, 107.9, 32.94 ppm.

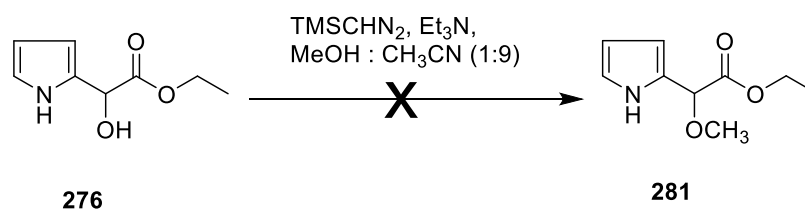
The synthesis of ethyl 2-methoxy-2-(1*H*-pyrrol-2-yl)acetate (281)

Procedure 1



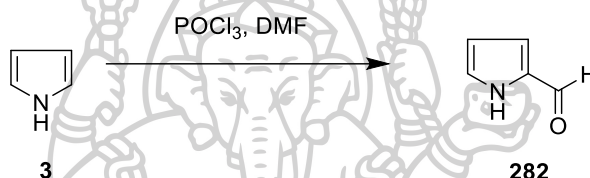
The synthesis was employed the procedure 1 for the synthesis of 1-methyl-1*H*-pyrrole (265) but the desired product was not observed.

Procedure 2



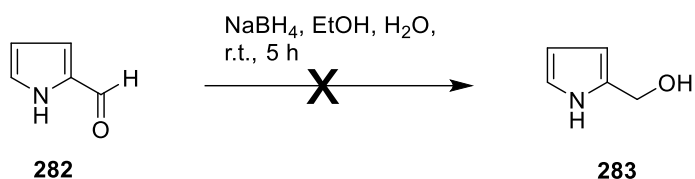
The solution of TMSCHN₂ (0.12 mL, 0.09 g, 0.78 mmol) in hexane 0.64 mL was added to a stirred solution of ethyl 2-hydroxy-2-(1*H*-pyrrol-2-yl)acetate (**276**) (0.1 g, 0.56 mmol) and Et₃N (0.11 mL, 0.08 g, 7.8 mmol) in MeOH:CH₃CN (1:9, 4 mL) at room temperature. The reaction mixture was stirred at room temperature for 15 h. Then, the mixture was concentrated in *vacuo* and the residue was worked up by extraction with DCM (3 x 10 mL). The combined DCM layers was dried over with anhydrous Na₂SO₄ and evaporated under reduced pressure. However, the desired product was not observed.

Synthesis of 1*H*-pyrrole-2-carbaldehyde (**282**)



POCl₃ (3.6 mL, 5.9 g, 38 mmol) was added dropwise to dry DMF 4.8 mL under argon atmosphere at 0 °C and stirred continue at room temperature for 5 min. Then, the solution of pyrrole (1.2 mL, 1.2 g, 17 mmol) in DMF 3 mL was added dropwise to this solution. The reaction mixture was stirred at room temperature for 1h. After the reaction completed, the mixture was poured into ice water and basic was adjusted with 20% NaOH. The mixture was extracted with DCM (3 X 20 mL). The combined organic phase was dried over with anhydrous Na₂SO₄ and evaporated under reduced pressure to provide crude product. The crude product was purified by column chromatography using 1:1 hexane:EtOAc as mobile phase to give the 1*H*-pyrrole-2-carbaldehyde (**282**) (1.4439 g, 88% yield) as yellow oil. ¹H-NMR (300 MHz, CDCl₃) δ 11.0 (br s, 1H), 9.49 (s, 1H), 7.19-7.17 (m, 1H), 7.02 -6.99 (m, 1H), 6.35-6.32 (m, 1H) ppm.

Synthesis of (1*H*-pyrrol-2-yl)methanol (283)



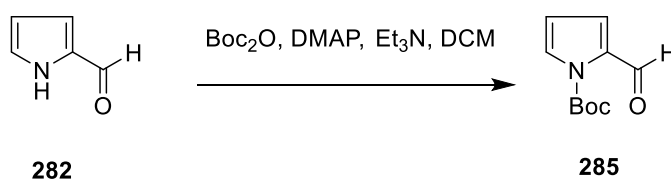
NaBH₄ (0.4 g, 10 mmol) was added to a solution of 1*H*-pyrrole-2-carbaldehyde (282) (0.85 g, 8.9 mmol) in MeOH 25 mL. The mixture was stirred for 1 h at room temperature. Then, the mixture was poured into ice water and concentrated in *vacuo*. The residue was extracted with DCM (3 x 20 mL). The combined organic layers were dried with anhydrous Na₂SO₄ and evaporated under reduced pressure. However, the desired product was not observed.

Synthesis of 1-benzyl-1*H*-pyrrole-2-carbaldehyde (284)



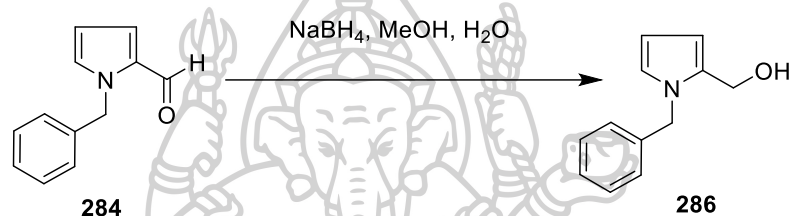
The synthesis was employed the procedure for the synthesis of ethyl 2-(1-benzyl-1*H*-pyrrole-2-yl)-2-oxoacetate (271). The crude product was purified by preparative TLC using 2:1 hexane:EtOAc as mobile phase to give the 1-benzyl-1*H*-pyrrole-2-carbaldehyde (284) (0.09 g, 11.9 % yield) as colorless oil. ¹H-NMR (300 MHz, CDCl₃) (Dudhe et al., 2020) δ 9.54 (s, 1H), 7.35-7.22 (m, 3H), 7.14-7.11 (m, 2H), 6.95 (d, *J* = 3.3 Hz, 2H), 6.25 (t, *J* = 3 Hz, 1H), 5.54 (s, 2H) ppm; ¹³C NMR (75 MHz, CDCl₃) δ 179.5, 137.5, 131.5, 131.3, 128.6, 127.6, 127.2, 124.7, 110.1, 51.9 ppm,

Synthesis of *tert*-butyl 2-formyl-1*H*-pyrrole-1-carboxylate (285)



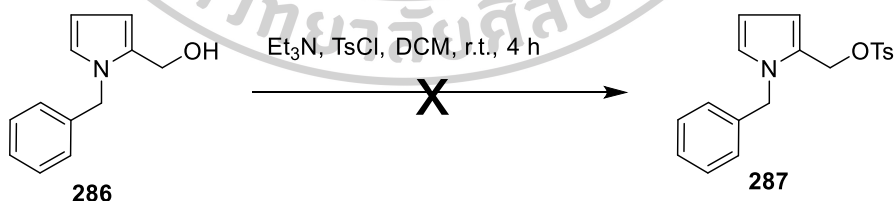
The synthesis was employed the procedure for the synthesis of *tert*-butyl 1*H*-pyrrole-1-carboxylate (**261**). The crude product was purified by preparative TLC using 4:1 hexane:EtOAc as mobile phase to give the *tert*-butyl 2-formyl-1*H*-pyrrole-1-carboxylate (**285**) (0.05 g, 27.5 %yield) as colorless oil. $^1\text{H NMR}$ (300 MHz, CDCl_3) δ 10.32 (s, 1H), 7.44 (dd, $J = 3, 1.8$ Hz, 1H), 7.19 (dd, $J = 3.6, 1.8$ Hz, 1H), 6.28 (t, $J = 3.3$ Hz, 1H), 1.64 (s, 9H) ppm.

Synthesis of (1-benzyl-1*H*-pyrrol-2-yl)methanol (**286**)



The synthesis was employed the procedure for the synthesis of (1*H*-pyrrol-2-yl)methanol (**283**). The product was achieved without further purified (0.17 g, 28 % yield) as colorless oil. $^1\text{H NMR}$ (300 MHz, CDCl_3) δ 7.33-7.24 (m, 2H), 7.07- 7.04 (m, 2H), 6.70 (dd, $J = 2.4, 2.1$ Hz, 1H), 6.17 (dd, $J = 3.3, 1.8$ Hz, 1H), 6.12 (t, $J = 3$ Hz, 1H), 5.19 (s, 2H), 4.50 (ds, $J = 5.1$ Hz, 2H) ppm

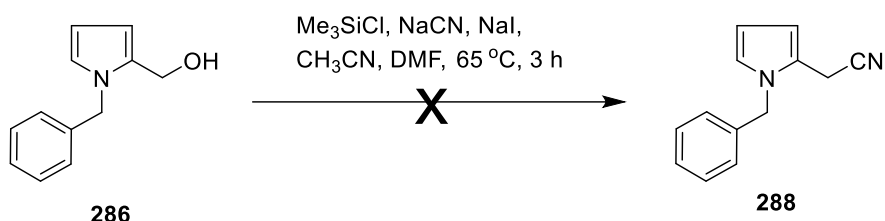
Synthesis of (1-benzyl-1*H*-pyrrol-2-yl)methyl 4-methylbenzenesulfonate (**287**)



(1-benzyl-1*H*-pyrrol-2-yl)methanol (**286**) (0.13 g, 0.7 mmol) in dry DCM (10 mL) was added Et_3N (0.15 mL, 0.11 g, 1.04 mmol) and stirred for 30 min at room temperature. TsCl (0.2 g, 1.04 mmol) was added to the mixture at 0 °C and stirred at room temperature for 4 h. Then, 20% NH_4Cl 5 mL was added to a mixture and extracted with DCM (3 x 30 mL). The DCM layer was washed with brine and dried with anhydrous

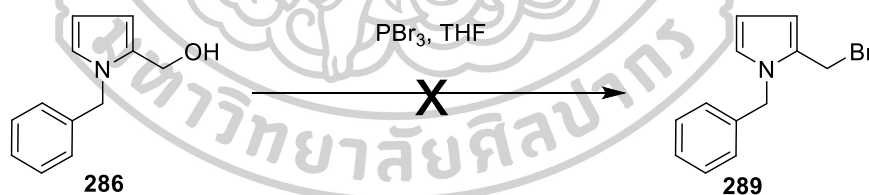
Na_2SO_4 and concentrated under reduced pressure. However, the desired product was not observed.

Synthesis of 2-(1-benzyl-1*H*-pyrrol-2-yl)acetonitrile (288)



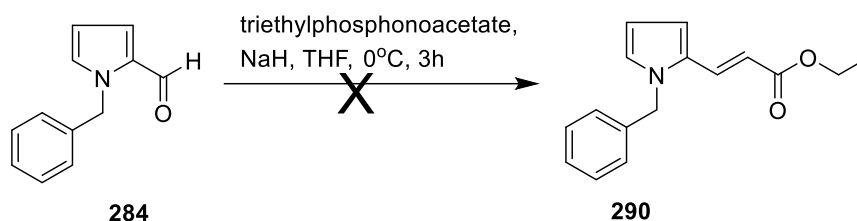
A mixture of NaCN (0.06 g, 1.2 mmol), NaI (0.002 g, 0.01 mmol) and CH_3CN 3 mL were added to a solution of (1-benzyl-1*H*-pyrrol-2-yl)methanol (286) (0.11 g, 0.6 mmol) in dry DMF (3 mL). The Me_3SiCl (0.15 mL, 0.13 g, 1.2 mmol) was added to a mixture at room temperature under Argon atmosphere. Then, the mixture was heated at 65 °C for 3 h. The mixture was poured into water 10 mL and extracted with Et_2O (2 x 30 mL). The organic phase was washed with water and brine, respectively. The organic phase was dried with anhydrous Na_2SO_4 and concentrated under reduced pressure. However, the desired product was not observed.

Synthesis of 1-benzyl-2-(bromomethyl)-1*H*-pyrrole (289)



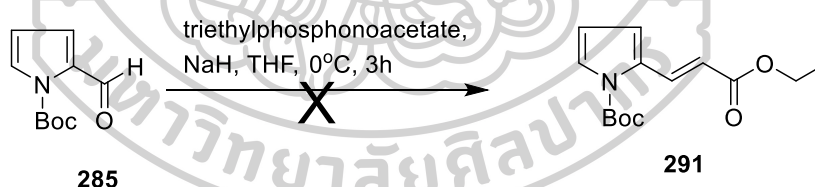
(1-benzyl-1*H*-pyrrol-2-yl)methanol (286) (0.14 g, 0.7 mmol) was dissolved in THF 20 mL. PBr_3 (0.28 mL, 3 mmol) was added slowly under ice bath cooling. The reaction mixture was stirred for 1 h at room temperature. Then, saturated NaHCO_3 was added until pH 8. The mixture was extracted with EtOAc (3 x 20 mL). The combined organic layers were dried over with anhydrous Na_2SO_4 and solvent was removed in *vacuo*. However, the desired product was not observed.

Synthesis of ethyl (*E*)-3-(1-benzyl-1H-pyrrol-2-yl)acrylate (290)



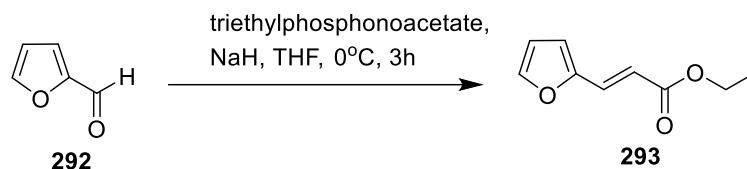
The mixture of NaH (0.025 g, 1 mmol) and triethyl phosphonoacetate (0.14 g, 0.6 mmol) in dry THF 3 mL was stirred at 0°C for 1 h under argon atmosphere. The solution of 1-benzyl-1H-pyrrole-2-carbaldehyde (284) (0.12 g, 0.6 mmol) in dry THF 9 mL was added to a mixture and stirred for 2 h at 0 °C. Then, the reaction mixture was poured into water and extracted with Et₂O (3 x 20 mL). The organic layer was dried over with anhydrous Na₂SO₄ and solvent was removed in vacuo to give crude product. The product was not purified by preparative TLC and column chromatography.

Synthesis of *tert*-butyl (*E*)-2-(3-ethoxy-3-oxoprop-1-en-1-yl)-1H-pyrrole-1-carboxylate (291)



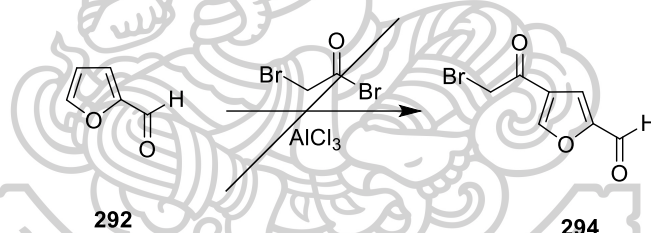
The synthesis was employed using the procedure for the synthesis of ethyl (*E*)-3-(1-benzyl-1H-pyrrol-2-yl)acrylate (290) which *tert*-butyl 2-formyl-1H-pyrrole-1-carboxylate (285) was used as starting material. The product was not purified by preparative TLC and column chromatography.

Synthesis of ethyl (*E*)-3-(furan-2-yl)acrylate (293)



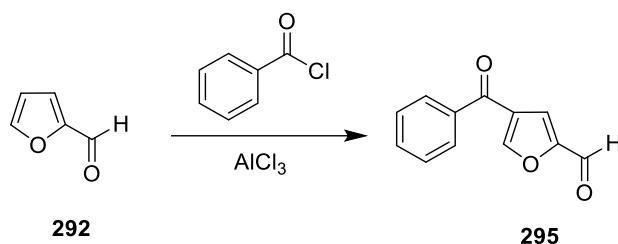
The synthesis was employed using the procedure for the synthesis of ethyl (*E*)-3-(1-benzyl-1H-pyrrol-2-yl)acrylate (**290**) which 2-furaldehyde (**292**) was used as starting material. The crude product was purified by preparative TLC using 4:1 hexane:EtOAc as mobile phase to give the ethyl (*E*)-3-(furan-2-yl)acrylate (**293**) (0.03 g, 30.9 % yield) as colorless oil. ¹H NMR (300 MHz, CDCl₃) δ 7.47 (s, 1H), 7.43 (d, *J* = 15.9 Hz, 1H), 6.60 (d, *J* = 3.3 Hz, 1H), 6.47 (dd, *J* = 3.6 Hz, 1.8 Hz, 1H), 6.30 (d, *J* = 15.9 Hz, 1H), 4.24 (q, *J* = 7.2 Hz, 2H), 1.32 (t, *J* = 7.2 Hz, 3H) ppm.

Synthesis of 4-(2-bromoacetyl)furan-2-carbaldehyde (294)



Bromoacetyl bromide (0.1 mL, 0.24 g, 1.2 mmol) was added to a suspension of AlCl₃ (0.22 g, 1.7 mmol) in dry DCM 2 mL at 0 °C under Argon atmosphere and stirred at room temperature for 10 min. The solution of 2-furaldehyde (**291**) (0.1 g, 1.2 mmol) in dry DCM 1 mL was added to a mixture and stirred at room temperature for 2 h. Then, the reaction mixture was poured into ice water and extracted with DCM (4 x 10mL). The combined DCM layers was washed with 1M NaOH and dried over with anhydrous Na₂SO₄ and solvent was removed in vacuo. The product was not observed in this reaction. However, the desired product was not observed.

Synthesis of 4-benzoylfuran-2-carbaldehyde (295)



The synthesis was employed using the procedure for the synthesis of 4-(2-bromoacetyl)furan-2-carbaldehyde (294) which 2-furaldehyde (292) and benzoyl chloride were used in this reaction. The crude product was purified by preparative TLC using 4:1 hexane:EtOAc as mobile phase to give the 4-benzoylfuran-2-carbaldehyde (295) (9.0 mg, 8.1 % yield) as colorless oil. $^1\text{H NMR}$ (300 MHz, CDCl_3) δ 9.67 (s, 1H), 8.11 (d, $J = 8.0$ Hz, 2H), 7.70 (s, 1H), 7.62 (t, $J = 6.8$ Hz, 1H), 7.48 (t, $J = 8.0$ Hz, 2H) 6.60 (s, 1H) ppm.

3. Identification of *Boesenbergia rotunda* Actinomyces crude extract.

The spores of *Boesenbergia rotunda* Actinomyces (IP-M01) were streaked on 200 petri dishes of ISP-2 agar medium and incubated at 30 °C for 14 days. Next, the culture medium was cut into small pieces which were extracted with EtOAc about 3 times or until the solvents were colorless. The organic extracts were filtrated through cotton and evaporated at 50 °C to provide a crude EtOAc extract. The EtOAc crude extract was evaluated the antibacterial activity against *B. subtilis* by using bioautography assay. The crude extract was dissolved in MeOH and spot on TLC. The TLC was developed by using 20 % EtOAc in hexane as eluent. Then, TLC was sterilized under UV lamp for 30 min. The TLC was put on nutrient agar petri dish which 1% melt agar with bacterial strain was poured and incubated at 37 °C for 24 h.

The crude extract was isolated by chromatography including column, preparative TLC and etc. The purified compounds were elucidated by NMR spectroscopy and mass spectrometry.

4. Lansai C and D derivatives

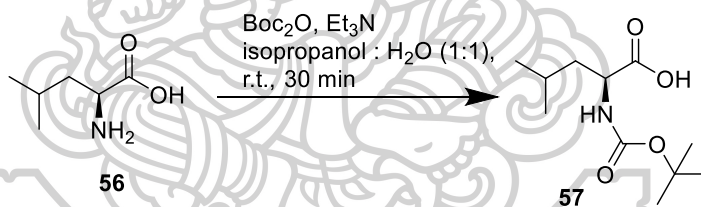
4.1 Extraction, purification and structure elucidation of Lansai compounds

The spores of *Streptomyces* sp. SUC1 were streaked on 108 petri dishes of ISP-2 agar medium and incubated at 30 °C for 14 days. Next, the culture medium was cut into small pieces which were extracted with EtOAc about 3 times or until the solvents were colorless. The organic extracts were filtrated through cotton and evaporated at 50 °C to provide a crude EtOAc extract.

The crude EtOAc extract was isolated by column chromatography by using 4:1 hexane:EtOAc as an eluent. The fractions were monitored by TLC and solvent was removed under reduced pressure. The purified compounds were elucidated by NMR spectroscopy.

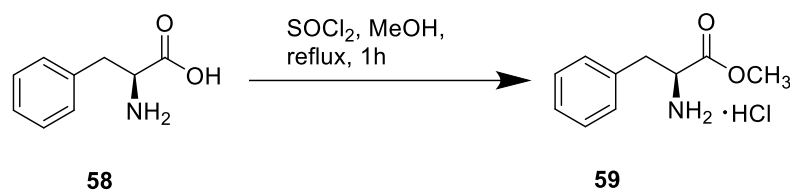
4.2 Synthesis of Lansai C and D derivatives

Synthesis of (*N*-tert-butoxycarbonyl)-*L*-leucine (57)



L-Leucine (1.00 g, 7.60 mmol) was suspended in 20.0 mL of water and isopropanol (1:1). Then, the suspension was treated with Et_3N (3.3 mL, 23.6 mmol) and Boc_2O (1.8 mL, 7.80 mmol). The mixture was stirred at room temperature for 30 min. After the reaction was completed, the alcohol was removed under vacuum (40 °C) and the residue was acidified with 1N H_2SO_4 to precipitate the product as white solid (1.41 g, 79% yield) which was filtered off and washed with water. m.p. (84.0-88.5 °C); ^1H NMR (300 MHz, CDCl_3) δ 0.96 (d, J = 6.3 Hz, 6H,) 1.45 (s, 9H,) 1.48-1.58 (m, 1H) 1.66-1.80 (m, 2H) 4.30 (s, 1H) 4.87 (s, 1H) ppm; ^{13}C NMR (300 MHz, CDCl_3) δ 177.8, 155.7, 80.2, 52.0, 41.4, 28.3, 24.8, 22.8, 21.7 ppm

Synthesis of *L*-Phenylalanine methyl ester hydrochloride (59)



L-phenylalanine (1.03 g, 6.20 mmol) was dissolved in methanol (13.0 mL). Thionyl chloride (0.5 mL, 6.90 mmol) was added to the mixture at 0 °C and the mixture was refluxed at 80 °C for 2 h. After the reaction was completed, solvent was evaporated under vacuum to afford *L*-Phenylalanine methyl ester hydrochloride as white solid (0.73 g, 54 %yield). m.p. 155-158 °C; ¹H NMR (300 MHz, MeOD) δ 7.42–7.33 (m, 3H), 7.32–7.27 (m, 2H), 4.35 (td, *J* = 6.9, 0.6 Hz, 1H), 3.82 (s, 3H), 3.29 (dd, *J* = 14.7, 6.5 Hz, 1H), 3.20 (dd, *J* = 14.4, 7.5 Hz, 1H) ppm; ¹³C NMR (300 MHz, MeOD) δ 169.0, 133.9, 129.1, 128.7, 127.5, 53.8, 52.2, 35.9 ppm

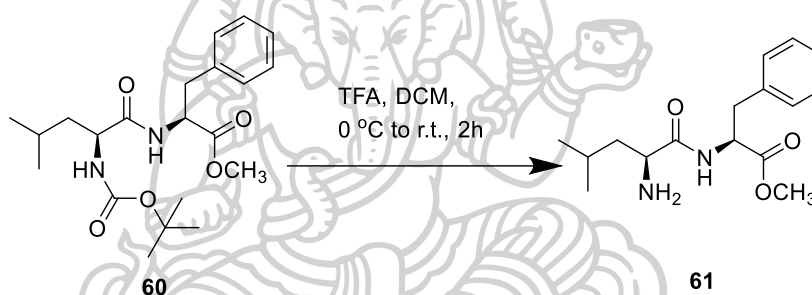
Synthesis of Methyl (*N*-*tert*-butoxycarbonyl)-*L*-leucyl-*L*-phenylalaninate (60)



(*N*-*tert*-butoxycarbonyl)-*L*-leucine (57) (0.11 g, 0.40 mmol) was dissolved in dry THF (3.0 mL) under argon atmosphere and cooled at 0 °C in ice bath. The solution was treated with HATU (0.25 g, 0.70 mmol) and DIPEA (0.11 mL, 0.60 mmol) and allowed to stir at 0 °C for 10 min. Then, *L*-phenylalanine methyl ester hydrochloride (2) (0.09 g, 0.50 mmol) was added, and the reaction was stirred at room temperature overnight. After completing the reaction, the solvent was removed under vacuum, and the residue was dissolved with EtOAc. The EtOAc solution was extracted with 2N HCl (2 × 20.0 mL) and saturated/undurated NaHCO₃ (2 × 20.0 mL). The organic phase was washed with brine (2 ×

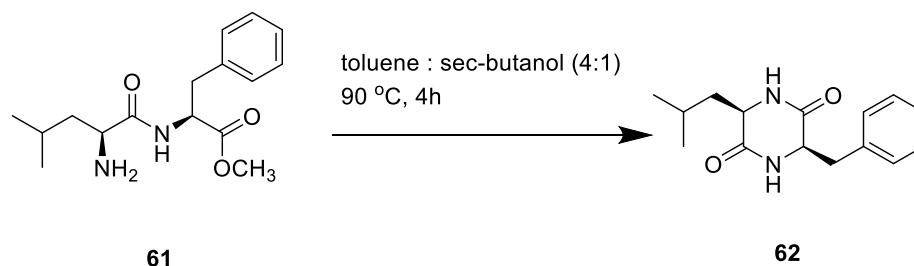
20.0 mL), dried with anhydrous Na_2SO_4 , and evaporated under reduced pressure to provide the crude product. The crude product was purified by column chromatography using Hexane:EtOAc (4:1) to obtain Methyl (N-tert-butoxycarbonyl)-L-leucyl-L-phenylalaninate (**60**) as a colorless oil (0.11 g, 84%yield); ^1H NMR (300 MHz, CDCl_3) δ 7.30–7.19 (m, 3H), 7.12–7.10 (m, 2H), 6.72 (m, 1H), 5.03 (s, 1H), 4.84 (dd, $J = 13.5, 6$ Hz, 1H), 4.10 (m, 1H), 3.68 (s, 1H), 3.14 (dd, $J = 13.8, 5.7$ Hz, 1H), 3.06 (dd, $J = 13.8, 6.3$ Hz, 1H), 1.69–1.25 (m, 2H), 1.49–1.39 (m, 1H), 1.43 (s, 3H), 0.91 (d, $J = 6.3$ Hz, 3H), 0.90 (d, $J = 6$ Hz, 3H) ppm; ^{13}C NMR (300 MHz, CDCl_3) δ 172.3, 171.7, 155.5, 135.8, 129.3, 128.5, 127.0, 80.0, 53.1, 52.2, 52.1, 41.2, 37.9, 28.2, 24.6, 22.8, 21.9 ppm

Synthesis of Methyl-L-leucyl-L-phenylalaninate (**61**)



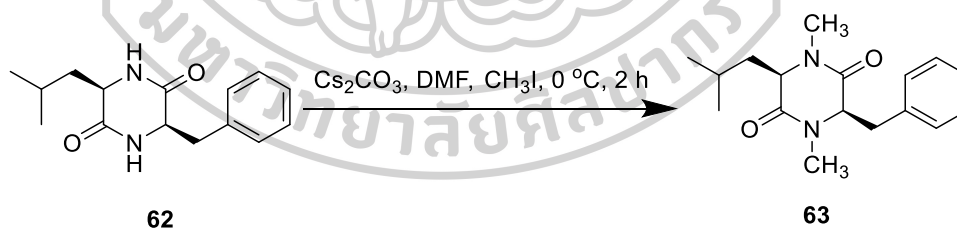
Methyl (tert-butoxycarbonyl)-L-leucyl-L-phenylalaninate (**60**) (0.54 g, 1.40 mmol) was dissolved in DCM (5.0 mL). Trifluoro acetic acid (0.2 mL, 2.60 mmol) was added to the solution at 0 °C. The reaction mixture was allowed at room temperature for 2 h. Then, the excess reagent and solvent were removed under reduced pressure. The resulting oil was neutralized by saturated NaHCO_3 and then extracted with DCM (2 × 30.0 mL), dried with anhydrous Na_2SO_4 , and evaporated under reduced pressure. The crude product was purified by column chromatography using 5% MeOH in DCM to obtain methyl-L-leucyl-L-phenylalaninate (**61**) as a colorless oil (0.28 g, 68%yield); ^1H NMR (300 MHz, CDCl_3) δ 7.72 (d, $J = 8.1$ Hz, 1H), 7.30–7.20 (m, 3H), 7.13–7.11 (m, 2H), 4.83 (dd, $J = 13.8, 7.5$ Hz, 1H), 3.70 (s, 3H), 3.36 (m, 1H), 3.16 (dd, $J = 13.8, 6.0$ Hz, 1H), 3.05 (dd, $J = 13.6, 6.9$ Hz, 1H), 1.70–1.55 (m, 1H), 1.60–1.52 (m, 1H), 1.25–1.17 (m, 1H), 0.92 (d, $J = 6.3$ Hz, 3H), 0.88 (d, 6.3 Hz, 3H) ppm; ^{13}C NMR (300 MHz, CDCl_3) δ 175.7, 172.3, 136.1, 129.2, 128.5, 127.0, 53.3, 52.8, 52.3, 43.9, 37.9, 24.7, 23.2, 21.4 ppm

Synthesis of (3*S*,6*S*)-3-Benzyl-6-isobutyl-2,5-diketopiperazine (62)



Methyl-*L*-leucyl-*L*-phenylalaninate (**61**) (0.31 g, 1.10 mmol) was dissolved in sec-buthanol:toluene (1:4, 12.0 mL). The solution was refluxed at 90 °C for 4 h. Then, the reaction was worked up by removing solvent under vacuum, and the residue was triturated with MTBE to obtain (3*S*,6*S*)-3-Benzyl-6-isobutyl-2,5-diketopiperazine (**62**) as a white solid (0.12 g, 46%yield); m.p. 258 °C–259 °C (Lit (Nitecki et al., 1968) 263 °C–264 °C); ¹H NMR (300 MHz, CDCl₃) δ 7.34–7.30 (m, 3H), 7.25–7.22 (m, 2H), 6.21 (s, 1H) 6.13 (s, 1H), 4.26–4.22 (m, 1H), 3.36–3.32 (m, 1H), 3.31 (dd, J = 13.9, 3.8 Hz, 1H), 3.05 (dd, J = 13.8, 7.8 Hz, 1H), 1.76–1.71 (m, 1H), 1.69–1.64 (m, 1H), 1.57–1.50 (m, 1H), 0.92 (d, J = 6.2 Hz, 3H, 0.83 (d, J = 6.2 Hz, 3H) ppm; ¹³C NMR (300 MHz, CDCl₃) δ 168.7, 167.7, 135.0, 129.7, 129.0, 127.6, 56.1, 52.7, 41.8, 39.8, 24.1, 23.1, 21.0 ppm

Synthesis of (3*S*,6*S*)-3-Benzyl-6-isobutyl-1,4-dimethyl-2,5-diketopiperazine (63)



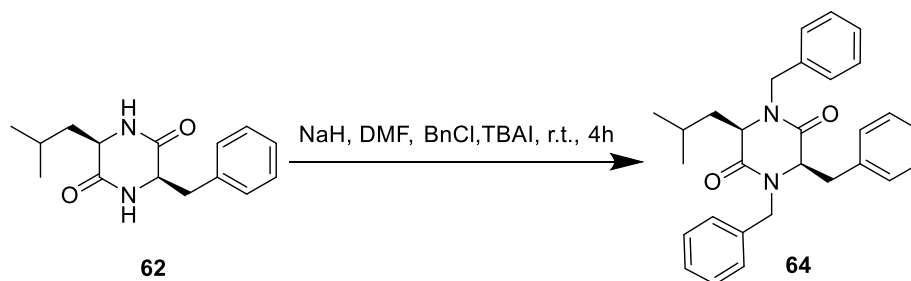
(3*S*,6*S*)-3-Benzyl-6-isobutyl-2,5-diketopiperazine (**62**) (0.08 g, 0.30 mmol) was dissolved in DMF (3.0 mL) under argon atmosphere. Cs₂CO₃ (0.32 g, 0.90 mmol), and methyl iodide (0.06 mL, 0.90 mmol) was added to the solution. The reaction mixture was stirred at 0 °C for 2 h. Then, the reaction was quenched with brine and extracted with EtOAc (2 × 20.0 mL). The organic layer was washed with brine (3 × 20.0 mL) and dried with anhydrous Na₂SO₄. The crude product was obtained by removing EtOAc solvent under reduced pressure and purified by preparative TLC using methanol in DCM (5%)

as a mobile phase to obtain (3*S*,6*S*)-3-Benzyl-6-isobutyl-1,4-dimethyl-2,5-diketopiperazine (**63**) as a colorless oil (0.01 g, 16% yield); ^1H NMR (300 MHz, CDCl_3) δ 7.32–7.24 (m, 3H), 7.12–7.09 (m, 2H), 4.18 (t, $J = 4.6$ Hz, 1H), 3.60 (dd, $J = 9.2, 4.2$ Hz, 1H), 3.30 (dd, $J = 13.9, 4.8$ Hz, 1H), 3.16 (dd, $J = 13.9, 4.5$ Hz, 1H), 2.95 (s, 3H), 2.86 (s, 3H), 1.76–1.63 (m, 1H), 0.82 (d, $J = 6.5$ Hz, 3H), 0.70 (d, $J = 6.6$ Hz, 3H), 0.69–0.60 (m, 1H), 0.29–0.19 (m, 1H) ppm; ^{13}C NMR (300 MHz, CDCl_3) δ 166.5, 165.1, 153.6, 130.0, 128.8, 127.6, 63.9, 60.0, 42.4, 37.6, 32.8, 32.5, 25.1, 22.7, 21.4 ppm; HRMS [ESI] $^+$ calculated for $\text{C}_{17}\text{H}_{24}\text{N}_2\text{O}_2$: 311.1730 [M + Na] $^+$; found: 311.1733).

General procedure for the synthesis of (3*S*,6*S*)-3-benzyl-1,4-disubstituted-6-isobutyl-2,5-diketopiperazine (**64-66**)

(3*S*,6*S*)-3-Benzyl-6-isobutyl-2,5-diketopiperazine (**62**) (0.40 mmol) was dissolved in DMF (3.0 mL) under argon atmosphere. The solution was cooled to 0 °C and added with NaH (2.2 eq), and the mixture was stirred at 0 °C for 15 min. Then, alkyl halide or aryl halide (2.0 eq) and TBAI (0.2 eq) were added to the solution. The reaction was allowed at room temperature and stirred for 4 h. The reaction was quenched with saturated NH₄Cl and extracted with EtOAc (3 × 20.0 mL). The organic layer was washed with water (3 × 20.0 mL) and then dried with anhydrous Na₂SO₄ and evaporated under reduced pressure. The crude product was purified by preparative TLC.

(3*S*,6*S*)-1,3,4-Tribenzyl-6-isobutyl-2,5-diketopiperazine (**64**)

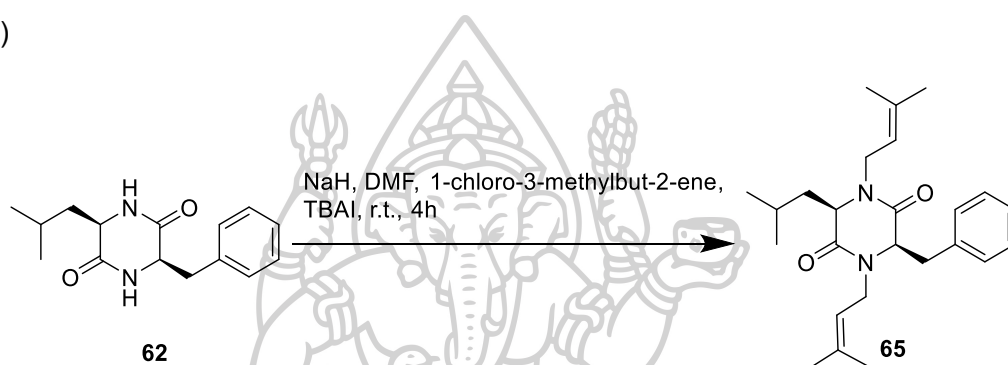


Following the general procedure, the product was obtained as a colorless oil (0.07 g, 34% yield); ^1H NMR (300 MHz, CDCl_3) δ 7.36–7.27 (m, 9H), 7.18–7.12 (m, 4H), 7.10–7.07 (m, 2H), 5.37 (d, $J = 15.4$ Hz, 1H), 5.32 (d, $J = 15.4$ Hz, 1H), 4.23 (dt, $J = 5.2,$

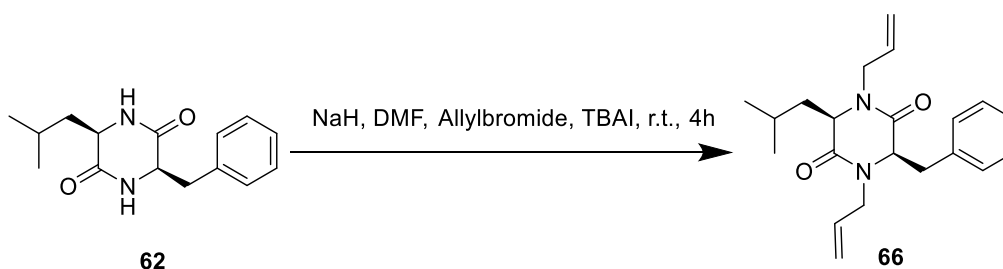
0.9 Hz, 1H), 3.78 (d, $J = 15$ Hz, 1H), 3.74 (dd, $J = 10.2, 3.9$ Hz, 1H), 3.57 (d, $J = 15$ Hz, 1H), 3.31 (dd, $J = 14.0, 4.7$ Hz, 1H), 3.23 (dd, $J = 14.1, 6.0$ Hz, 1H), 1.79–1.74 (m, 1H), 1.02–0.93 (m, 1H), 0.82 (d, $J = 6.3$ Hz, 3H), 0.76 (d, $J = 6.6$ Hz, 3H), 0.69–0.60 (m, 1H) ppm; ^{13}C NMR (300 MHz, CDCl_3) δ 166.9, 165.9, 136.0, 135.7, 135.6, 129.9, 128.9, 128.8, 128.1, 128.0, 127.9, 127.6, 60.6, 56.9, 47.1, 47.0, 42.7, 38.1, 25.2, 22.9, 21.4 ppm; HRMS [ESI] $^+$ calculated for $\text{C}_{29}\text{H}_{32}\text{N}_2\text{O}_2$: 463.2356 [M + Na] $^+$; found: 463.2362.

(3*S*,6*S*)-3-Benzyl-6-isobutyl-1,4-bis(3-methylbut-2-en-1-yl)-2,5-diketopiperazine

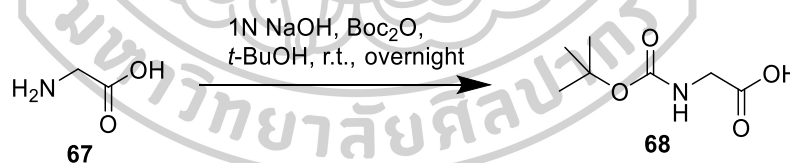
(65)



Following the general procedure, the product was obtained as a colorless oil (0.07 g, 47% yield); ^1H NMR (300 MHz, CDCl_3) δ 7.32–7.20 (m, 3H), 7.15–7.12 (m, 2H), 5.12–5.09 (m, 1H), 5.08–5.04 (m, 1H), 4.58 (dd, $J = 14.7, 5.7$ Hz, 1H), 4.40 (dd, $J = 14.9, 5.6$ Hz, 1H), 4.24 (t, $J = 4.9$ Hz, 1H), 3.72 (dd, $J = 10.1, 3.7$ Hz, 1H), 3.46 (dd, $J = 14.8, 8.2$ Hz, 1H), 3.37 (dd, $J = 14.8, 8.5$ Hz, 1H), 3.25 (dd, $J = 14.1, 5.1$ Hz, 1H), 3.14 (dd, $J = 14.1, 4.8$ Hz, 1H), 1.75–1.69 (m, 1H), 1.72 (s, 3H), 1.71 (s, 3H), 1.65 (s, 3H), 1.63 (s, 3H), 0.83–0.75 (m, 1H), 0.82 (d, $J = 6.5$ Hz, 3H), 0.70 (d, $J = 6.6$ Hz, 3H) ppm; ^{13}C NMR (300 MHz, CDCl_3) δ 166.4, 165.3, 137.8, 137.1, 136.0, 130.0, 128.7, 127.4, 118.5, 118.1, 60.3, 56.9, 42.2, 41.8, 41.5, 37.8, 25.8, 25.7, 24.9, 23.0, 21.2, 18.0, 17.9 ppm; HRMS [ESI] $^+$ calculated for $\text{C}_{25}\text{H}_{36}\text{N}_2\text{O}_2$: 419.2669 [M + Na] $^+$; found: 419.2673.

(3*S*,6*S*)-1,4-Diallyl-3-benzyl-6-isobutyl-2,5-diketopiperazine (66)

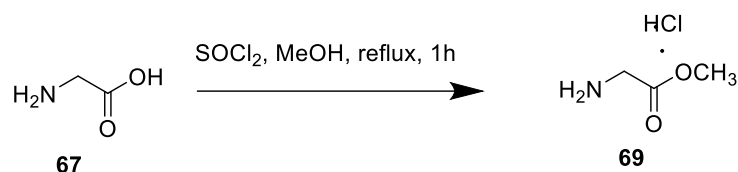
Following the general procedure, the product was obtained as a colorless oil (0.02 g, 15% yield); ^1H NMR (300 MHz, CDCl_3) δ 7.33–7.25 (m, 3H), 7.15–7.12 (m, 2H), 5.78–5.71 (m, 1H), 5.70–5.64 (m, 1H), 5.23 (ddd, $J = 10.2, 4.2, 0.9$ Hz, 2H), 5.14 (ddd, $J = 17.1, 9.6, 0.9$ Hz, 2H), 4.68 (tdd, $J = 15.0, 4.8, 1.5$ Hz, 1H), 4.54, (tdd, $J = 15.0, 4.8, 1.5$ Hz, 1H), 4.28 (t, $J = 5.0$ Hz, 1H), 3.75 (dd, $J = 9.8, 3.8$ Hz, 1H), 3.36 (dd, $J = 15.0, 7.5$ Hz, 1H), 3.27–3.15 (m, 1H), 3.22–3.18 (m, 2H), 1.80–1.64 (m, 1H), 0.90–0.81 (m, 1H), 0.84 (d, $J = 6.6$ Hz, 3H), 0.73 (d, $J = 6.6$ Hz, 3H), 0.53–0.40 (m, 1H) ppm; ^{13}C NMR (300 MHz, CDCl_3) δ 166.5, 165.3, 135.8, 131.8, 131.4, 130.0, 128.8, 127.5, 119.1, 118.8, 60.5, 57.0, 46.6, 42.6, 37.9, 25.2, 22.9, 21.3 ppm; HRMS [ESI] $^+$ calculated for $\text{C}_{21}\text{H}_{28}\text{N}_2\text{O}_2$: 341.2224 [M + H] $^+$; found: 341.2224.

Synthesis of (*N*-*tert*-butoxycarbonyl)-Glycine (68)

The solution of glycine (0.48 g, 6.39 mmol) in *t*-BuOH (5.0 mL) was treated with 1*N* NaOH (10.0 mL, 10.00 mmol) and Boc_2O (0.95 g, 4.40 mmol) and stirred at room temperature for overnight. Then, the mixture was concentrated to half of volume. The residue was extracted with hexane and hexane layer was extracted with saturated NaHCO_3 . The aqueous layers were combined and was acidified by using 1*M* H_2SO_4 until pH = 2. Then, the solution was extracted with Et_2O (3 x 10.0 mL) followed by drying with anhydrous Na_2SO_4 and evaporated under reduced pressure to provide the product as a white crystalline powder (0.62 g, 55 %yield); m.p. 88-89 $^\circ\text{C}$; ^1H NMR (300 MHz, CDCl_3)

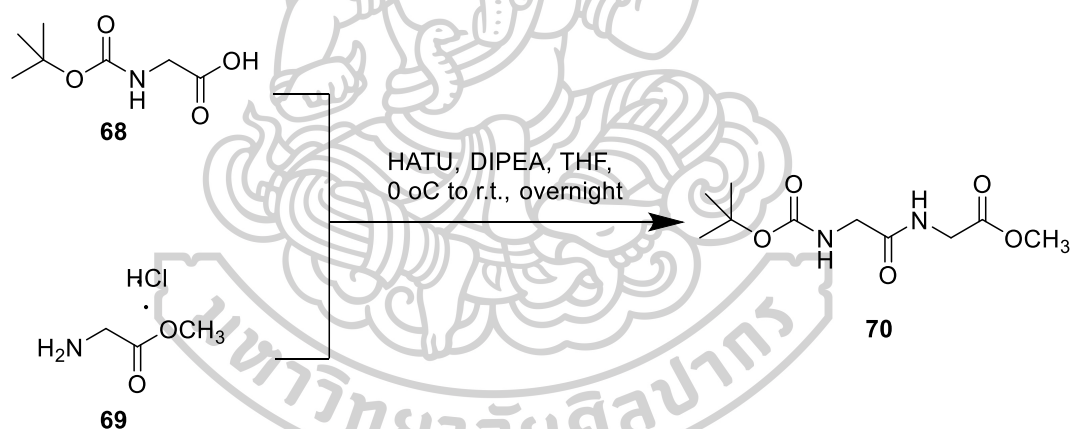
δ 8.76 (br s, 1H), 5.18 (br s, 1H), 3.91 (d, $J = 16.9$ Hz, 2H), 1.45 (s, 9H) ppm; ^{13}C NMR (300 MHz, CDCl_3) δ 174.6, 156.0, 80.4, 42.2, 28.2 ppm

Synthesis of glycine methyl ester hydrochloride (69)



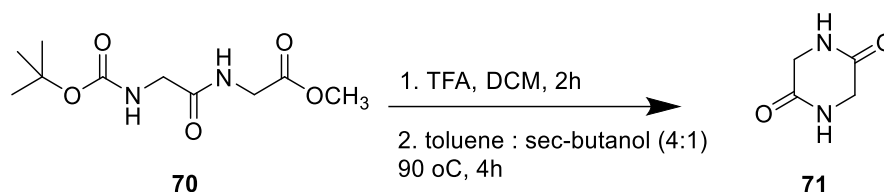
The synthesis of Glycine methyl ester hydrochloride (69) was followed condition of L-phenylalanine methyl ester hydrochloride (59). The product was afforded as a white solid (0.76 g, 65 %yield); m.p. 142-146 °C; ^1H NMR (300 MHz, CDCl_3) δ 4.87 (s, 3H), 3.83 (s, 2H) ppm; ^{13}C NMR (300 MHz, CDCl_3) δ 167.5, 52.1, 39.5 ppm

Synthesis of methyl (*tert*-butoxycarbonyl) glycyL glycinate (70)



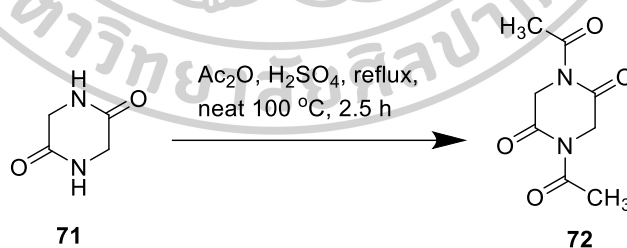
The synthesis of methyl (*tert*-butoxycarbonyl) glycyL glycinate (70) was followed condition of methyl (*N-tert*-butoxycarbonyl)-L-leucyl-L-phenylalaninate. The product was afforded as a colorless oil (0.16 g, 84 %yield); ^1H NMR (300 MHz, CDCl_3) δ 6.69 (br s, 1H), 5.20 (br s, 1H), 4.07 (d, $J = 5.4$ Hz, 2H), 3.85 (d, $J = 4.8$ Hz, 2H), 3.5 (s, 3H), 1.46 (s, 9H) ppm; ^{13}C NMR (300 MHz, CDCl_3) δ 170.3, 156.2, 80.0, 52.3, 43.9, 41.0, 28.2 ppm

Synthesis of 2,5-Diketopiperazine (71)



Methyl (*tert*-butoxycarbonyl) glycyl glycinate (**70**) (0.54 g, 1.40 mmol) was dissolved in DCM (5.0 mL). Trifluoro acetic acid (0.2 mL, 2.60 mmol) was added to the solution at 0 °C. The reaction mixture was allowed at room temperature for 2 h. Then, the excess reagent and solvent were removed under reduced pressure. The resulting oil was neutralized by saturated NaHCO_3 and then extracted with DCM (2 \times 30.0 mL), dried with anhydrous Na_2SO_4 , and evaporated under reduced pressure to obtain a colorless oil. Then, the crude product was dissolved in *sec*-butanol:toluene (1:4, 12.0 mL). The solution was refluxed at 90 °C for 4 h. Then, the reaction was worked up by removing solvent under vacuum, and the residue was triturated with MTBE to obtain 2,5-Diketopiperazine (**71**) as a white solid (0.25 g, 56% yield); m.p. 309 °C–310 °C (Lit [21] 311 °C–312 °C); ^1H NMR (300 MHz, CDCl_3) δ 4.04 (s, 2H) ppm; ^{13}C NMR (300 MHz, CDCl_3) δ 168.6, 43.9 ppm.

Synthesis of 1,4-Diacetyl-2,5-diketopiperazine (72)



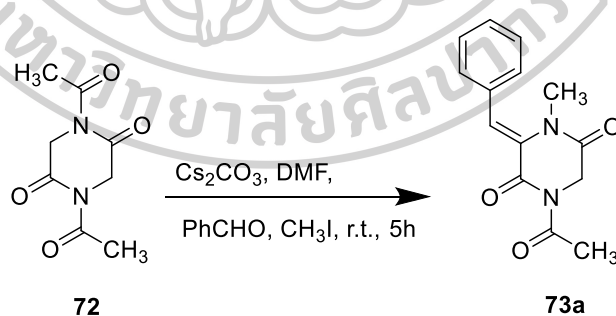
2,5-Diketopiperazine (**71**) (0.51 g, 4.5 mmol) was suspended in acetic anhydride (6.0 mL), and concentrated H_2SO_4 was added two drops. The reaction mixture was refluxed at 100 °C for 2.5 h. The reaction provided the red solution, which was diluted with EtOAc and filtered through celite. The filtrate was concentrated; thus, the crude product can obtain a yellow oil. The yellow oil was recrystallized with excess isopropanol and stored in a fridge. The pure product was precipitated as a colorless needle crystal.

The crystal was filtered and washed with cold isopropanol ((0.19 g, 21% yield); m.p. 99 –100 °C (Lit (Liao, Qin, Yao, et al., 2014) 102 –103 °C); ^1H NMR (300 MHz, CDCl_3) δ 4.60 (s, 2H), 2.59 (s, 3H) ppm; ^{13}C NMR (300 MHz, CDCl_3) δ 170.7, 165.8, 47.1, 26.7 ppm

General procedure for the synthesis of (3Z)-4-acetyl-3-benzylidene-1-substituted-2,5-diketopiperazine (73a–e)

A 10 mL round bottom flask, which was filled with argon atmosphere, contained 1,4-diacetyl piperazine-2,5-dione (**72**) (0.10 g, 0.54 mmol, 1.0 eq), aldehyde (1.40 mmol, 2.5 eq), alkyl halide (1.40 mmol, 2.5 eq), Cs_2CO_3 (1.40 mmol, 2.5 eq), and dry DMF (4.4 mL). The reaction mixture was stirred at room temperature for 4 h. Then, the mixture was poured into crush ice water. After the precipitate was formed, it was filtered and washed with water. If the precipitate was not formed, then the solution will be extracted with EtOAc (3 \times 15.0 mL). The organic layers were combined and washed with water (2 \times 15.0 mL). The organic layer was dried with anhydrous Na_2SO_4 and evaporated under reduced pressure to obtain the crude product. The product was purified by preparative TLC or column chromatography.

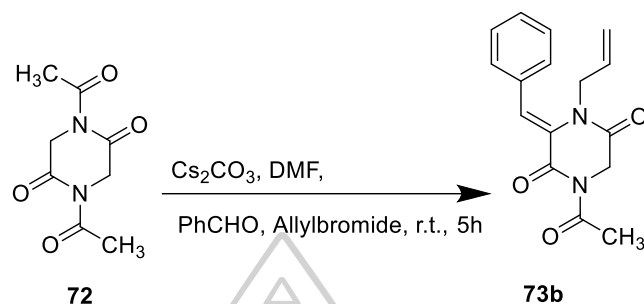
(3Z)-1-Acetyl-3-benzylidene-4-methyl-2,5-diketopiperazine (73a)



Following the general procedure, the product was obtained as a white solid (0.03 g, 23% yield); m.p. 160–161 °C; ^1H NMR (300 MHz, CDCl_3) δ 7.42–7.37 (m, 3H), 7.34–7.31 (m, 2H), 4.54 (s, 2H), 2.91 (s, 3H), 2.64 (s, 3H) ppm; ^{13}C NMR (300 MHz, CDCl_3)(Liao, Qin, Yao, et al., 2014) δ 171.5, 164.9, 163.8, 132.7, 131.6, 129.6, 129.4,

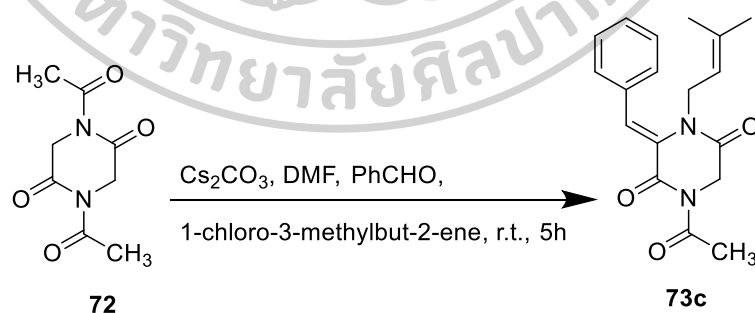
128.6, 125.5, 45.3, 34.4, 26.7; HRMS [ESI]⁺ calculated for C₁₄H₁₄N₂O₃: 281.0897 [M + Na]⁺; found: 281.0896.

(3Z)-1-Acetyl-4-allyl-3-benzylidene-2,5-diketopiperazine (73b)



Following the general procedure, the product was obtained as a white solid (0.02 g, 15% yield); m.p. 142–144 °C; ¹H NMR (300 MHz, CDCl₃) δ 7.44–7.34 (m, 5H), 7.31 (s, 1H), 5.57–5.46 (m, 1H), 5.03 (dd, J = 10.2, 1.2 Hz, 1H), 4.74 (dd, J = 16.8, 1.2 Hz, 1H), 4.54 (s, 2H), 4.11 (d, J = 5.6 Hz, 2H), 2.63 (s, 3H) ppm; ¹³C NMR (300 MHz, CDCl₃) (Liao, Qin, Yao, et al., 2014) δ 171.3, 164.8, 164.3, 132.6, 131.0, 129.7, 129.6, 129.3, 128.7, 126.6, 118.8, 46.4, 45.2, 26.6 ppm; HRMS [ESI]⁺ calculated for C₁₆H₁₆N₂O₃: 307.1053 [M + Na]⁺; found: 307.1050.

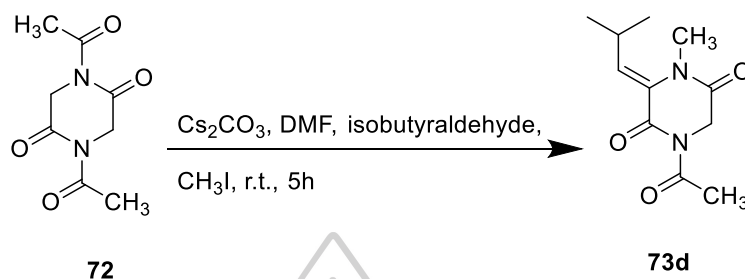
(3Z)-1-Acetyl-3-benzylidene-4-(3-methylbut-2-ene-1-yl)-2,5-diketopiperazine (73c)



Following the general procedure, the product was obtained as a colorless oil (0.11 g, 14% yield); ¹H NMR (300 MHz, CDCl₃) δ 7.43–7.36 (m, 5H), 7.29 (s, 1H), 4.87 (tq, J = 6.9, 1.2 Hz, 1H), 4.50 (s, 2H), 4.11 (d, J = 6.9 Hz, 2H), 2.62 (s, 3H), 1.57 (s, 3H), 1.20 (s, 3H); ¹³C NMR (300 MHz, CDCl₃) δ 171.4, 164.7, 164.4, 132.5, 131.2, 129.6,

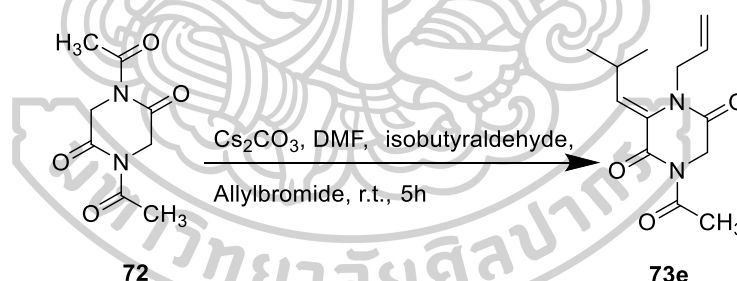
129.5, 129.3, 128.4, 121.5, 118., 46.0, 45.1, 26.6; HRMS [ESI]⁺ calculated for C₁₈H₂₀N₂O₃: 335.1366 [M + Na]⁺; found: 335.1352.

(6Z)-4-Acetyl-6-(2-methylpropylidene)-1-methyl-2,5-diketopiperazine (73d)



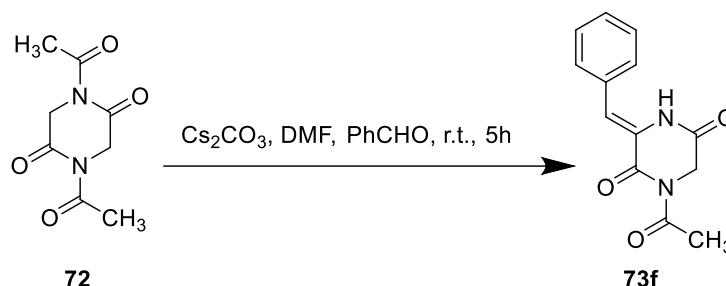
Following the general procedure, the product was obtained as a brown oil (0.08 g, 14% yield); ¹H NMR (300 MHz, CDCl₃) δ 6.17 (d, J = 11.1 Hz, 1H), 4.39 (s, 2H), 3.26 (s, 3H), 2.84–2.72 (m, 1H), 2.56 (s, 3H), 1.13 (d, J = 6.3 Hz, 6H) ppm; ¹³C NMR (300 MHz, CDCl₃) δ 171.4, 164.7, 164.0, 137.0, 131.1, 45.3, 34.8, 27.4, 26.6, 22.3 ppm; HRMS [ESI]⁺ calculated for C₁₁H₁₆N₂O₃: 247.1053 [M + Na]⁺; found: 247.1044.

(6Z)-4-Acetyl-1-allyl-6-(2-methylpropylidene)-2,5-diketopiperazine (73e)



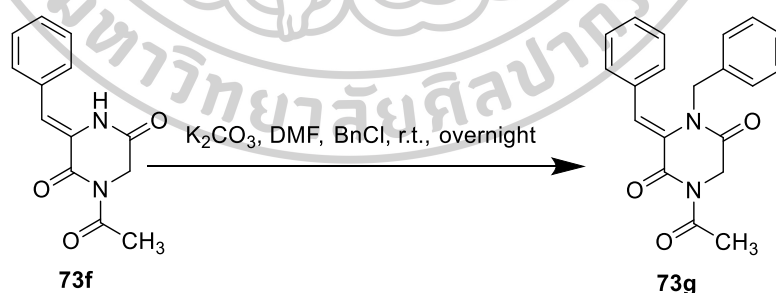
Following the general procedure, the product was obtained as a yellow oil (0.10 g, 18% yield); ¹H NMR (300 MHz, CDCl₃) δ 6.17 (d, J = 10.8 Hz, 1H), 5.88–5.75 (m, 1H), 5.18 (dq, J = 18.9, 1.2 Hz, 2 H), 4.38 (s, 2H), 4.28 (at, J = 5.7, 1.5 Hz, 2H), 2.77–2.69 (m, 1H), 2.56 (s, 3H), 1.08 (d, J = 6.6 Hz, 6H) ppm; ¹³C NMR (300 MHz, CDCl₃) δ 170.3, 163.6, 163.4, 137.0, 130.9, 128.9, 116.7, 48.1, 44.3, 26.2, 25.5, 20.9 ppm; HRMS [ESI]⁺ calculated for C₁₃H₁₈N₂O₃: 273.1210 [M + Na]⁺; found: 273.1207.

Synthesis of (3Z)-1-Acetyl-3-benzylidene-2,5-diketopiperazine (73f)



1,4-Diacetyl piperazine-2,5-dione (11) (0.50 g, 2.5 mmol) was dissolved in dry DMF (10.0 mL) under argon atmosphere. Cs_2CO_3 (0.80 g, 2.5 mmol) and benzaldehyde (0.2 mL, 1.8 mmol) were added into the solution. The mixture was stirred at room temperature for 3 h. After the reaction was completed, the mixture was poured into crush ice water. (3Z)-1-Acetyl-3-benzylidene-2,5-diketopiperazine was precipitated as a white solid, which was filtered and washed with excess water (0.28 g, 46% yield); m.p. 185–189 °C (Lit (Katritzky et al., 1988) 195–197 °C); ^1H NMR (300 MHz, CDCl_3) δ 7.93 (br s, 1H), 7.50–7.45 (m, 2H), 7.41–7.38 (m, 3H), 7.19 (s, 1H), 4.52 (s, 2H), 2.66 (s, 3H) ppm; ^{13}C NMR (300 MHz, CDCl_3) δ 172.5, 162.7, 159.9, 132.5, 1129.6, 129.4, 128.5, 125.7, 119.9, 46.1, 27.2 ppm.

Synthesis of (3Z)-1-Acetyl-4-benzyl-3-benzylidene-2,5-diketopiperazine (73g)



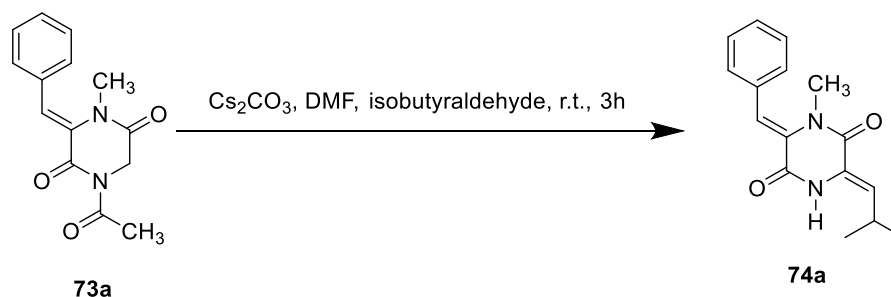
(3Z)-1-Acetyl-3-benzylidene-2,5-diketopiperazine (73f) (0.10 g, 0.4 mmol) was used to treat K_2CO_3 (0.11 g, 0.8 mmol) with dry DMF (3.0 mL). Benzyl chloride (0.06 g, 0.5 mmol) was added to the solution. The mixture was stirred at room temperature overnight. After the reaction was completed, the reaction mixture was poured into water and extracted with EtOAc (3 × 15.0 mL). The organic layer was washed with water and dried with anhydrous Na_2SO_4 . The organic solvent was removed under reduce pressure

to provide the crude product. (3*Z*)-1-Acetyl-4-benzyl-3-benzylidene-2,5-diketopiperazine (73g) was provided as a pale yellow solid by column chromatography using 4:1 hexane:EtOAc as an eluent (0.02 g, 17% yield); m.p. 117–120 °C; ¹H NMR (300 MHz, CDCl₃) δ 7.50–7.39 (m, 5H), 7.21–7.19 (m, 3H), 6.88–6.85 (m, 2H), 4.67 (s, 2H), 4.55 (s, 2H), 2.54 (s, 3H) ppm; ¹³C NMR (300 MHz, CDCl₃) δ 171.3, 165.1, 164.3, 135.8, 132.6, 129.9, 129.7, 129.6, 128.9, 128.6, 127.9, 127.8, 126.9, 47.2, 45.2, 26.5 ppm; HRMS [ESI]⁺ calculated for C₂₀H₁₈N₂O₃: 357.1210 [M + Na]⁺; found: 357.1205.

General procedure for the synthesis of (3*Z*,6*Z*)-3-benzylidene-6-(2-methyl propylidene)-4-substituted-2,5-diketopiperazine (74a-f)

The solution of intermediate (73a-f) (0.3 mmol, 1.0 eq) in dry DMF (3.0 mL) was treated with Cs₂CO₃ (0.4 mmol, 1.5 eq) and aldehyde (0.4 mmol, 1.5 eq) under argon atmosphere. The reaction mixture was stirred at room temperature for 3 h. Then, the mixture was poured into crush ice water. After the precipitate was formed, it was filtered and washed with water. If the precipitate was not formed, then the solution will be extracted with EtOAc (3 × 15.0 mL). The organic layers were combined and washed with water (2 × 15.0 mL). The organic layer was dried with anhydrous Na₂SO₄ and evaporated under reduced pressure to obtain the crude product. The product was purified by preparative TLC or column chromatography.

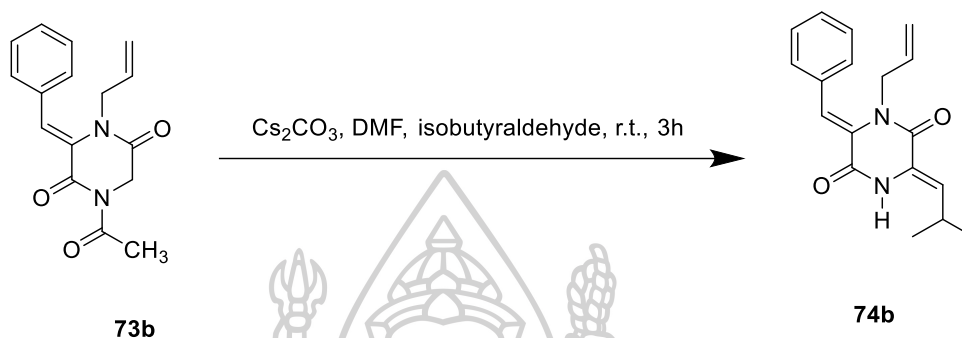
(3*Z*,6*Z*)-3-Benzylidene-6-(2-methylpropylidene)-4-methyl-2,5-diketopiperazine (74a)



Following the general procedure, the product was provided as a pale yellow solid (0.06 g, 55% yield); m.p. 139–142 °C; ¹H NMR (300 MHz, CDCl₃) δ 8.77 (br s, 1H), 7.43–7.31 (m, 3H), 7.28–7.25 (m, 3H), 6.05 (d, J = 10.2 Hz, 1H), 2.94 (s, 3H), 2.75–2.63

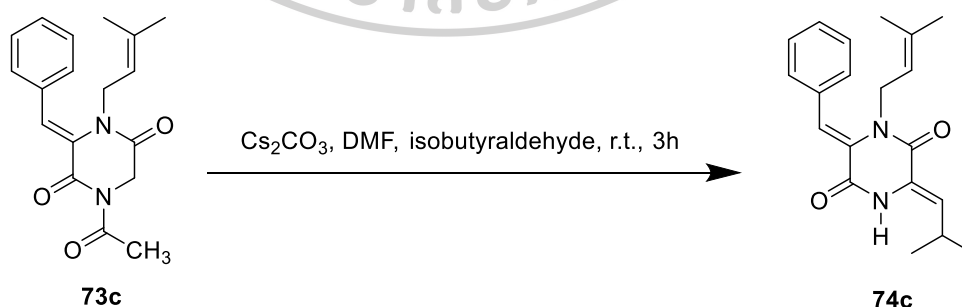
(m, 1H), 1.12 (d, $J = 6.6$ Hz, 6H) ppm; ^{13}C NMR (300 MHz, CDCl_3) δ 160.2, 159.7, 134.0, 130.4, 129.4, 128.4, 128.2, 128.0, 124.5, 120.5, 36.5, 25.5, 22.1 ppm; HRMS $[\text{ESI}]^+$ calculated for $\text{C}_{16}\text{H}_{18}\text{N}_2\text{O}_2$: 293.1260 $[\text{M} + \text{Na}]^+$; found: 293.1256.

(3Z,6Z)-4-Allyl-3-benzylidene-6-(2-methylpropylidene)-2,5-diketopiperazine (74b)



Following the general procedure, the product was obtained as a colorless oil ((0.05 g, 46% yield); ^1H NMR (300 MHz, CDCl_3) δ 9.53 (br s, 1H), 7.41–7.27 (m, 5H), 7.23 (s, 1H), 6.08 (d, $J = 10.2$ Hz, 1H), 5.59–5.45 (m, 1H), 5.00 (dd, $J = 10.2, 1.2$ Hz, 1H), 4.74 (dd, $J = 17.1, 1.2$ Hz, 1H), 4.23 (d, $J = 5.7$ Hz, 2H), 2.90–2.74 (m, 1H), 1.13 (d, $J = 6.6$ Hz, 6H); ^{13}C NMR (300 MHz, CDCl_3) δ 161.4, 159.9, 134.0, 131.6, 129.3, 129.1, 128.7, 128.4, 124.7, 121.5, 117.9, 47.7, 25.5, 22.2; HRMS $[\text{ESI}]^+$ calculated for $\text{C}_{18}\text{H}_{20}\text{N}_2\text{O}_2$: 319.1417 $[\text{M} + \text{Na}]^+$; found: 319.1410).

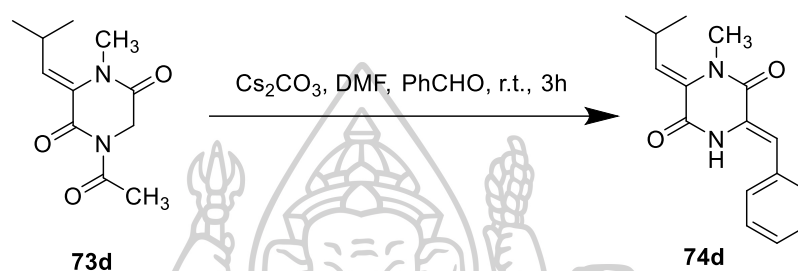
(3Z,6Z)-3-Benzylidene-6-(2-methylpropylidene)-4-(3-methyl but-2-en-1-yl)-2,5-diketo-piperazine (74c)



Following the general procedure, the product was obtained as a white solid (0.05 g, 45% yield); m.p. 175–178 °C; ^1H NMR (300 MHz, CDCl_3) δ 7.83 (br s, 1H), 7.40–7.27 (m, 5H), 7.23 (s, 1H), 6.03 (d, $J = 10.2$ Hz, 1H), 4.91 (tt, $J = 6.6, 1.5$ Hz, 1H),

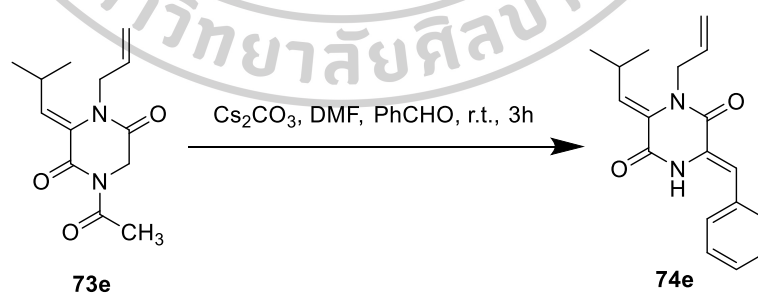
4.20 (d, $J = 6.6$ Hz, 2H), 2.59–2.52 (m, 1H), 1.56 (s, 3H), 1.21 (s, 3H), 1.12 (d, $J = 6.6$ Hz, 6H) ppm; ^{13}C NMR (300 MHz, CDCl_3) δ 161.1, 160.0, 136.9, 134.0, 129.4, 128.6, 128.5, 128.3, 128.1, 124.8, 121.6, 118.6, 44.0, 25.6, 25.5, 22.1, 17.7 ppm; HRMS [ESI]⁺ calculated for $\text{C}_{20}\text{H}_{24}\text{N}_2\text{O}_2$: 347.1730 [M + Na]⁺; found: 347.1723.

(3Z,6Z)-3-Benzylidene-6-(2-methylpropylidene)-1-methyl-2,5-diketopiperazine (74d)



Following the general procedure, the product was obtained as a colorless oil (0.006 g, 8% yield); ^1H NMR (300 MHz, CDCl_3) δ 8.05 (br s, 1H), 7.45–7.30 (m, 5H), 7.00 (s, 1H), 6.07 (d, $J = 11.1$ Hz, 1H), 3.43 (s, 3H), 3.01–2.89 (m, 1H), 1.13 (d, $J = 6.5$ Hz, 6H) ppm; ^{13}C NMR (300 MHz, CDCl_3) δ 159.6, 159.0, 133.0, 131.7, 129.3, 128.6, 128.5, 128.4, 125.9, 116.5, 35.5, 27.4, 23.0 ppm; HRMS [ESI]⁺ calculated for $\text{C}_{16}\text{H}_{18}\text{N}_2\text{O}_2$: 293.1260 [M + Na]⁺; found: 293.1251.

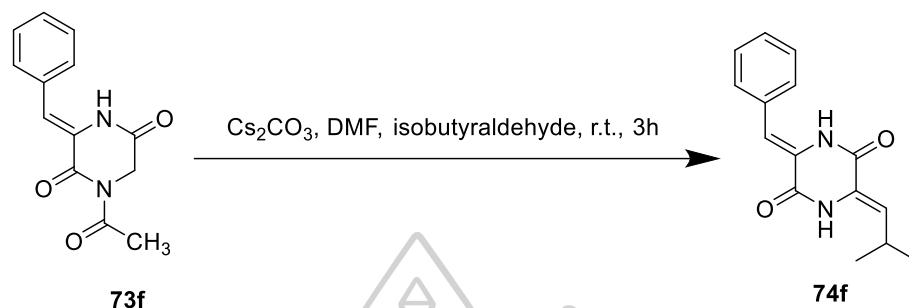
(3Z,6Z)-1-Allyl-3-benzylidene-6-(2-methylpropylidene)-2,5-diketopiperazine (74e)



Following the general procedure, the product was obtained as a pale yellow solid (0.02 g, 21% yield); m.p. 115–119 °C; ^1H NMR (300 MHz, CDCl_3) δ 7.95 (br s, 1H), 7.46–7.34 (m, 5H), 7.01 (s, 1H), 6.13 (d, $J = 11.4$ Hz, 1H), 5.99–5.89 (m, 1H), 5.24 (ddd, $J = 19.8, 10.5, 0.9$ Hz, 2H), 4.49 (dt, $J = 4.5, 1.8$ Hz, 2H), 2.93–2.89 (m, 1H), 1.10 (d, $J = 6.6$ Hz, 6H) ppm; ^{13}C NMR (300 MHz, CDCl_3) δ 159.4, 158.5, 133.1, 132.2, 131.7, 129.4,

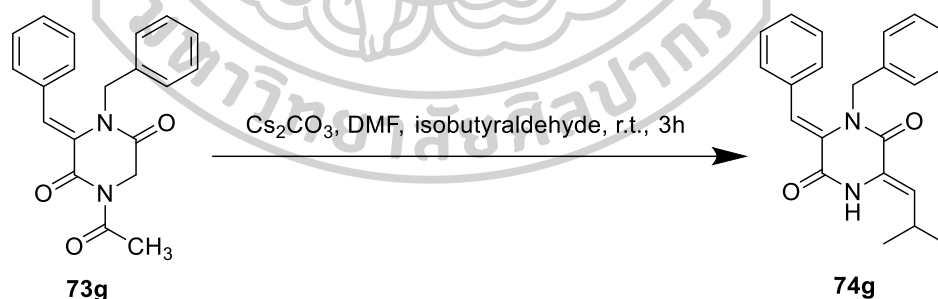
128.7, 128.4, 127.0, 125.8, 116.5, 116.3, 49.2, 27.0, 22.9 ppm; HRMS [ESI]⁺ calculated for C₁₈H₂₀N₂O₂: 319.1417 [M + Na]⁺; found: 319.1420.

(3Z,6Z)-3-Benzylidene-6-(2-methylpropylidene)-2,5-diketopiperazine (74f)



Following the general procedure, the product was obtained as a white solid (0.13 g, 82% yield); m.p. 243–246 °C (Lit (Shin et al., 1969) 271–271.5 °C); ¹H NMR (300 MHz, CDCl₃) δ 8.06 (br s, 1H), 7.81 (br s, 1H), 7.48–7.43 (m, 2H), 7.38–7.34 (m, 3H), 6.99 (s, 1H), 6.02 (d, J = 10.2 Hz, 1H), 2.59–2.51 (m, 1H), 1.12 (d, J = 6.6 Hz, 6H) ppm; ¹³C NMR (300 MHz, CDCl₃) δ 157.1, 157.0, 132.7, 129.5, 128.9, 128.3, 126.8, 124.3, 116.2, 29.7, 25.5, 22.0 ppm.

(3Z,6Z)-4-Benzyl-3-benzylidene-6-(2-methylpropylidene)-2,5-diketopiperazine (74g)



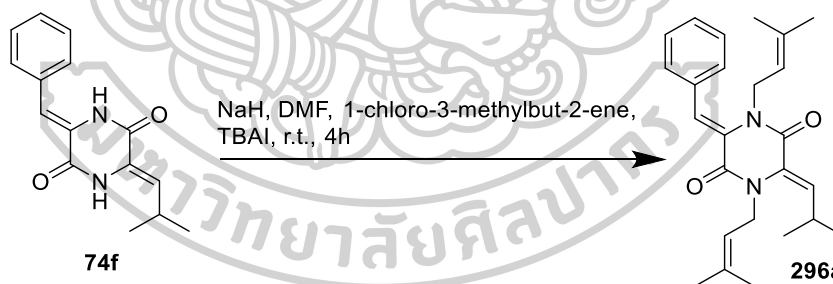
Following the general procedure, the product was obtained as a colorless oil (0.01 g, 12% yield); ¹H NMR (300 MHz, CDCl₃) δ 7.95 (br s, 1H), 7.44–7.32 (m, 4H), 7.30–7.27 (m, 1H), 7.21 (s, 1H), 7.19–7.16 (m, 3H), 6.92–6.83 (m, 2H), 6.05 (d, J = 10.5 Hz, 1H), 4.72 (s, 2H), 2.60–2.50 (m, 1H), 1.11 (d, J = 6.6 Hz, 6H) ppm; ¹³C NMR (300 MHz, CDCl₃) δ 160.6, 160.0, 136.2, 133.9, 129.5, 128.8, 128.6, 128.5, 128.4, 128.3,

127.5, 124.6, 122.0, 48.6, 29.7, 25.7, 22.1 ppm; HRMS [ESI]⁺ calculated for C₂₂H₂₂N₂O₂: 369.1573 [M + Na]⁺; found: 369.1567.

General procedure for the synthesis of (3Z,6Z)-3-benzylidene-6-(2-methylpropylidene)-1,4-disubstituted-2,5-diketopiperazine (296a–c)

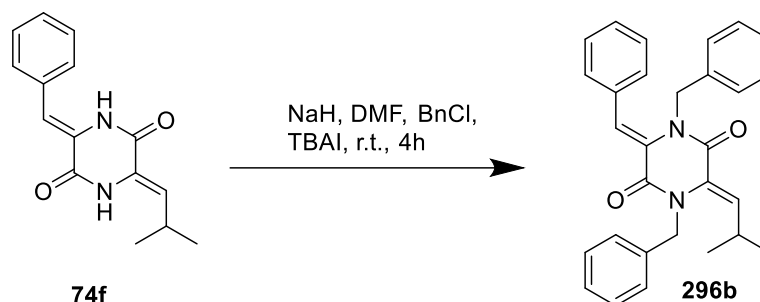
(3Z,6Z)-3-Benzylidene-6-(2-methylpropylidene)-2,5-diketopiperazine (**74f**) (0.40 mmol) was dissolved in DMF (3.0 mL) under argon atmosphere. The solution was cooled to 0 °C and added with NaH (2.2 eq), and the mixture was stirred at 0 °C for 15 min. Then, alkyl halide or aryl halide (2.0 eq) and TBAI (0.2 eq) were added to the solution. The reaction was allowed at room temperature and stirred for 4 h. The reaction was quenched with saturated NH₄Cl and extracted with EtOAc (3 × 20 mL). The organic layer was washed with water (3 × 20 mL) and then dried with anhydrous Na₂SO₄ and evaporated under reduced pressure. The crude product was purified by preparative TLC.

(3Z,6Z)-3-Benzylidene-6-(2-methylpropylidene)-1,4-bis(-3-methylbut-2-en-1yl)-2,5-diketopiperazine (296a)



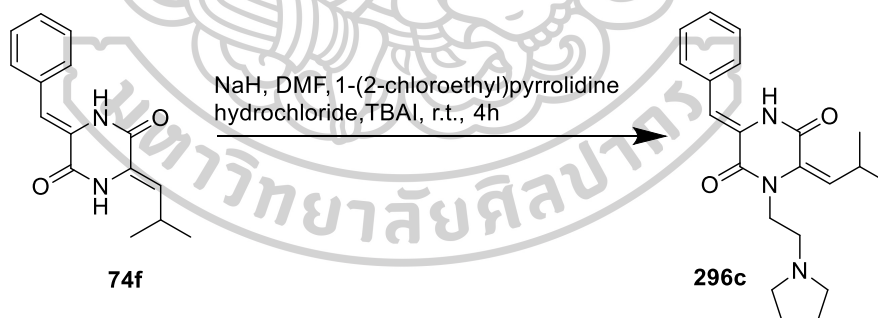
Following the general procedure, the product was obtained as a colorless oil (0.002 g, 2% yield); ¹H NMR (300 MHz, CDCl₃) δ 7.36–7.29 (m, 5H), 7.09 (s, 1H), 6.01 (d, J = 10.8 Hz, 1H), 5.23 (tq, J = 6.1, 1.5 Hz, 1H), 4.88 (tq, J = 6.8, 1.4 Hz, 1H), 4.35 (d, J = 6.1 Hz, 2H), 4.09 (d, J = 6.8 Hz, 2H), 2.80–2.68 (m, 1H), 1.71 (sd, J = 1.1 Hz, 3H), 1.68 (s, 3H), 1.55 (sd, J = 0.8 Hz, 3H), 1.25 (sd, J = 0.6 Hz, 3H), 1.09 (d, J = 6.5 Hz, 6H) ppm; ¹³C NMR (300 MHz, CDCl₃) δ 163.4, 162.9, 136.9, 136.0, 129.9, 129.5, 129.4, 128.6, 128.3, 122.2, 119.5, 118.7, 45.5, 43.3, 27.1, 25.6, 25.5, 22.5, 18.2, 17.6 ppm; HRMS [ESI]⁺ calculated for C₂₅H₃₂N₂O₂: 393.2537 [M + H]⁺; found: 393.2542.

(3Z,6Z)-1,4-Dibenzyl-3-benzylidene-6-(2-methylpropylidene)-2,5-diketo piperazine (296b)



Following the general procedure, the product was obtained as a pale yellow oil (0.02 g, 10% yield); ^1H NMR (300 MHz, CDCl_3) δ 7.44–7.27 (m, 5H), 7.25 (s, 1H), 7.23–7.18 (m, 3H), 7.16–7.10 (m, 3H), 7.08–7.01 (m, 2H), 6.79–6.76 (m, 2H), 6.04 (d, $J = 10.8$ Hz, 1H), 4.94 (s, 2H), 4.63 (s, 2H), 2.79–2.67 (m, 1H), 1.07 (d, $J = 6.6$ Hz, 6H) ppm; ^{13}C NMR (300 MHz, CDCl_3) δ 163.5, 163.0, 136.4, 134.4, 133.4, 129.9, 129.6, 129.3, 129.0, 128.6, 128.4, 127.7, 127.6, 127.5, 126.6, 122.9, 50.2, 48.3, 27.3, 22.2 ppm; HRMS [ESI]⁺ calculated for $\text{C}_{29}\text{H}_{28}\text{N}_2\text{O}_2$: 459.2043 [M + Na]⁺; found: 459.2052.

(3Z,6E)-3-Benzylidene-6-(2-methylpropylidene)-1-(1-ethylpyrrolidine)-2,5-diketopiperazine (296c)



Following the general procedure, the product was obtained as a pale yellow solid (0.01 g, 6% yield); m.p. 158–162 °C; ^1H NMR (300 MHz, CDCl_3) δ 8.16 (br s, 1H), 8.05 (d, $J = 7.2$ Hz, 2H), 7.40–7.28 (m, 3H), 7.27 (s, 1H), 5.56 (d, $J = 10.2$ Hz, 1H), 4.58 (t, $J = 6.0$ Hz, 2H), 3.04 (t, $J = 6.0$ Hz, 2H), 2.76 (m, 4H), 2.66–2.58 (m, 1H), 1.88 (sq, $J = 3.3$ Hz, 4H), 1.10 (d, $J = 6.6$ Hz, 6H) ppm; ^{13}C NMR (300 MHz, CDCl_3) δ 160.4, 153.6, 135.1, 131.5, 128.7, 128.3, 127.8, 123.0, 121.2, 121.1, 65.6, 54.6, 54.1, 25.0, 23.5, 22.3 ppm; HRMS [ESI]⁺ calculated for $\text{C}_{21}\text{H}_{27}\text{N}_2\text{O}_2$: 354.2103 [M + H]⁺; found: 354.2174.

5. Identification of *Boesenbergia rotunda Actinomyces* crude extract.

The spores of *Boesenbergia rotunda Actinomyces* (IPM-01) were streaked on 100 petri dishes of ISP-2 agar medium and incubated at 30 °C for 14 days. Next, the culture medium was cut into small pieces which were extracted with EtOAc about 3 times or until the solvents were colorless. The organic extracts were filtrated through cotton and evaporated at 50 °C to provide a crude EtOAc extract. The EtOAc crude extract was evaluated the antibacterial activity against *B. subtilis* by using bioautography assay. The crude extract was dissolved in MeOH and spot on TLC. The TLC was developed by using 20% EtOAc in hexane as eluent. Then, TLC was sterilized under UV lamp for 30 min. The TLC was put on nutrient agar petri dish which 1% melt agar with bacterial strain was poured and incubated at 37 °C for 24 h.

The crude extract was isolated by chromatography including column, preparative TLC and etc. The purified compounds were elucidated by NMR spectroscopy and mass spectrometry.

6. Biological activities

6.1 Cytotoxicity activity

The cytotoxicity activity studies were evaluated using MTT assay. The cancer cell lines, human cervical cancer cells (HeLa) were obtained from the Department of Microbiology, Faculty of Science (Silpakorn University, Nakhon pathom). The normal cell lines, Rhesus monkey kidney cells (LLC-MK2) were derived from the Department of Biology, Faculty of Science (Silpakorn University, Nakhon pathom).

Preparation of Dulbecco's Modified Eagle Medium (DMEM) for cell cultures

The 1,000 mL of sterile deionized water in 1,000 mL Duran bottle was autoclaved and cooled down to room temperature then added DMEM powder 10 g. The solution was stirred which was prepared under the vertical laminar air flow. The stock solution of DMEM was added with an antibiotic; penicillin (100 µg/mL) and streptomycin sulfate (100 µg/mL) and 10% Fetal Bovine Serum (FBS) then was adjusted pH to 7.1-7.2

with sterile solution of NaHCO_3 . The completed DMEM was filtered through 0.22 μm acrodisc filter.

Cell cultures

These cell lines were cultured as monolayer in Dulbecco's Modified Eagle's Medium (DMEM) containing 10% Fetal Bovine Serum (FBS) and antibiotic then incubated at 37 °C with 5% CO_2 atmosphere. The medium was changed every 2 days until cells increased to 80-90% confluent.

MTT assay for anticancer and cytotoxicity activity

Cells in cell culture flask were detached with enzyme trypsin then transferred to 96 well plates to a density of 2×10^5 cells per well containing 100 μL of DMEM medium with 10% FBS and incubated at 37 °C with 5% CO_2 for overnight. Then, Lansai compounds (26-29) were dissolved in DMSO for 1,024 $\mu\text{g}/\text{mL}$ as a stock solution. The various concentrations were diluted 2-fold from stock solution. Cells were treated with the reducing concentration of test compounds (512, 256, 128, 64, 32, 16, 8, 4, 2, 1 and 0.5 $\mu\text{g}/\text{mL}$) in medium without FBS for 24 h. The 5% and 20% of DMSO in medium without FBS were used as a control. Cells were once rinsed with phosphate buffer saline (PBS). The 3-(4,5-dimethylthiazol-2-yl)-2,5-diphenyl-2H-tetrazolium bromide (MTT) solution (20 μL of 5 mg/mL) was added to each well and incubated for 4 h at 37 °C. The MTT solution was removed. The resulting formazan crystal was dissolved with 100 μL of DMSO to each well. The absorbance was measured at 540 nm with microplate spectrometer. Percentage of cell viability was determined and calculated using the following formula.

$$\% \text{ cell viability} = \frac{\text{Abs sample} - \text{Abs blank}}{\text{Abs reference} - \text{Abs blank}} \times 100$$

The IC_{50} of each cell was calculated from the calibration curve with X-axis as a concentration and Y-axis as the percentage of cell viability.

6.2 Antiviral activity

6.2.1 Virus propagation inhibition assay

Virus propagation inhibition assays were examined by embryonated chicken egg inoculation. One hundred microliters of LS-C, LS-D, and its derivatives at various concentrations (25, 50, and 100 $\mu\text{g mL}^{-1}$) was incubated with 100 μL of virus suspension at 37 °C for 30 min. One hundred microliters of the mixture were inoculated into each embryonated chicken egg and incubated at 37 °C for 4 days. The allantoic fluid was investigated by HA assay (Au - Brauer & Au - Chen, 2015).

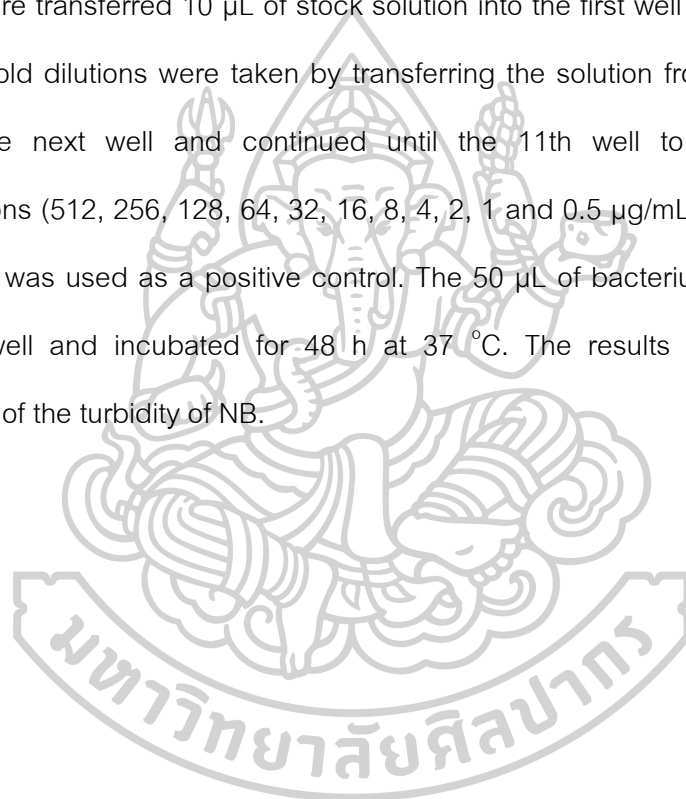
6.2.2 Molecular docking studies

Molecular docking studies were performed using iGEMDOCK v.2.1 to investigate the possible binding between enzymes involved in antiviral activities and our compounds (Lansai C (28), compound 64, compound 66, and compounds 74a-74d), which serve as virus propagation inhibitor. The following four enzymes were selected as the receptor: human hypoxanthine-guanine phosphoribosyltransferase (HGPRT, PDB ID: 4KN6), neuraminidase from H5N2 avian influenza virus (H5N2, PDB ID: 5HUK), SARS-CoV-2 3CL main protease (SARS-CoV-2 3CLpro, PDB ID: 6LU7), and SARS-CoV-2 spike receptor-binding domain bound with ACE2, (SARS-CoV-2 RBD with ACE2, PDB ID: 6M0J). Moreover, Favipiravir, which is an antiviral medication used to treat influenza [16], was docked into these four enzymes, and its result was compared with our potential antiviral drugs (Lansai C (28), compound 64, compound 66, and compounds 74a-74d). The resulted interactions of protein-ligands were analyzed with Discovery Studio 2017.

6.3 Antibacterial activity

The minimal inhibitory concentration (MIC) of antibacterial activity was studied with microbroth dilution method. The Lansai C (28), Lansai D (29) and its derivatives (63-66, 74a-e, 74g, 256a-c) were determined against gram-positive bacterial pathogens

(*Staphylococcus aureus*) and against gram-negative bacterial pathogens (*Escherichia coli*). Chloramphenicol was used as the standard antibiotic to compare the bacterial cultures. These bacterial were cultured in Nutrient broth (NB) with shaking incubation at 180 cycles/min for 24 h at 37 °C which was adjusted to the 0.5 McFarland standard (1×10^5 CFU / mL). The test compounds were dissolved in DMSO to prepare 1,024 µg/mL stock solution and chloramphenicol were dissolved in EtOH to 50 mg/mL. These stock solutions were transferred 10 µL of stock solution into the first well containing 190 µL of NB. The 2-fold dilutions were taken by transferring the solution from the first well (100 µL) into the next well and continued until the 11th well to obtain the various concentrations (512, 256, 128, 64, 32, 16, 8, 4, 2, 1 and 0.5 µg/mL). The NB containing 20% DMSO was used as a positive control. The 50 µL of bacterium in NB was added into each well and incubated for 48 h at 37 °C. The results were determined by comparison of the turbidity of NB.

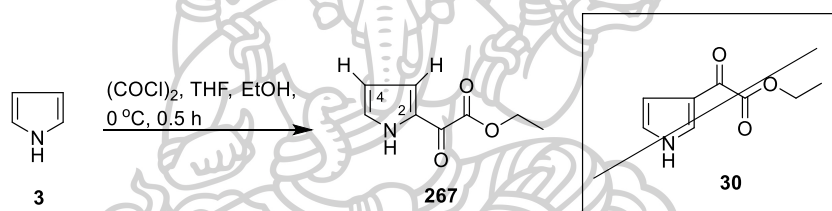


CHAPTER 4

RESULTS AND DISCUSSION

1. The first synthetic route of pyrrole derivatives

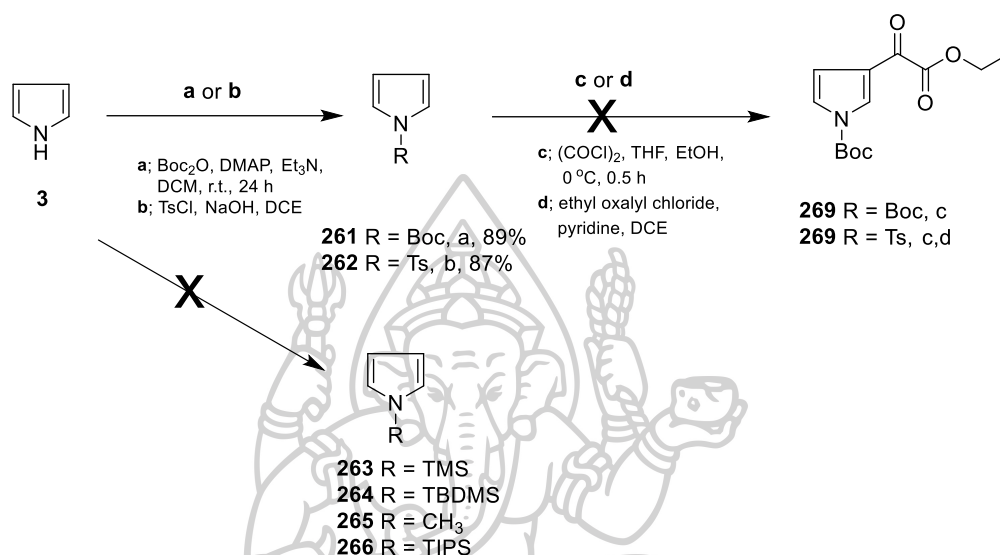
To study the substituent group at carbon and nitrogen of pyrrole that effect on the plant growth regulation, the first synthetic route was started from pyrrole (**3**) which was treated with oxalylchloride to produce keto-ester (**267**). The structure was confirmed by COSY NMR spectrum, the correlation of the proton on pyrrole ring at position 4 (6.35 ppm, dd, $J = 3.6, 2.1$ Hz, 1H) was coupled with proton at position 3 (7.20 ppm, s, 1H) and position 5 (7.39 ppm, dd, $J = 3.9, 1.2$ Hz, 1H) (Scheme 28).



Scheme 28. Acylation of pyrrole (**3**)

The substitution at position 2 can be explained by the highest degree of stability of protonated intermediate. However, in the case of IAA that have ethanoic acid at position 3 on pyrrole ring of indole. Thus, substitution on the 3-position might be important for the activity. Therefore, in order to achieve 3-substitution of the pyrrole ring, the researchers attempted to add the substitution group at the nitrogen atom for increasing the nucleophilicity of the pyrrole. The *N*-substitution was proceeded with various protecting group, however, the product of *N*-Boc and *N*-Ts substitutions were obtained while the other protecting groups were not success. The ¹H NMR of CH₃ proton of the Boc group in compound **261** was occurred as a singlet at 1.63 ppm (9H). While, the ¹H NMR of CH₃ proton of the tosyl group in compound **262** was occurred as singlet at 2.39 ppm (3H) and aromatic proton of the tosyl group was occurred as the doublet at

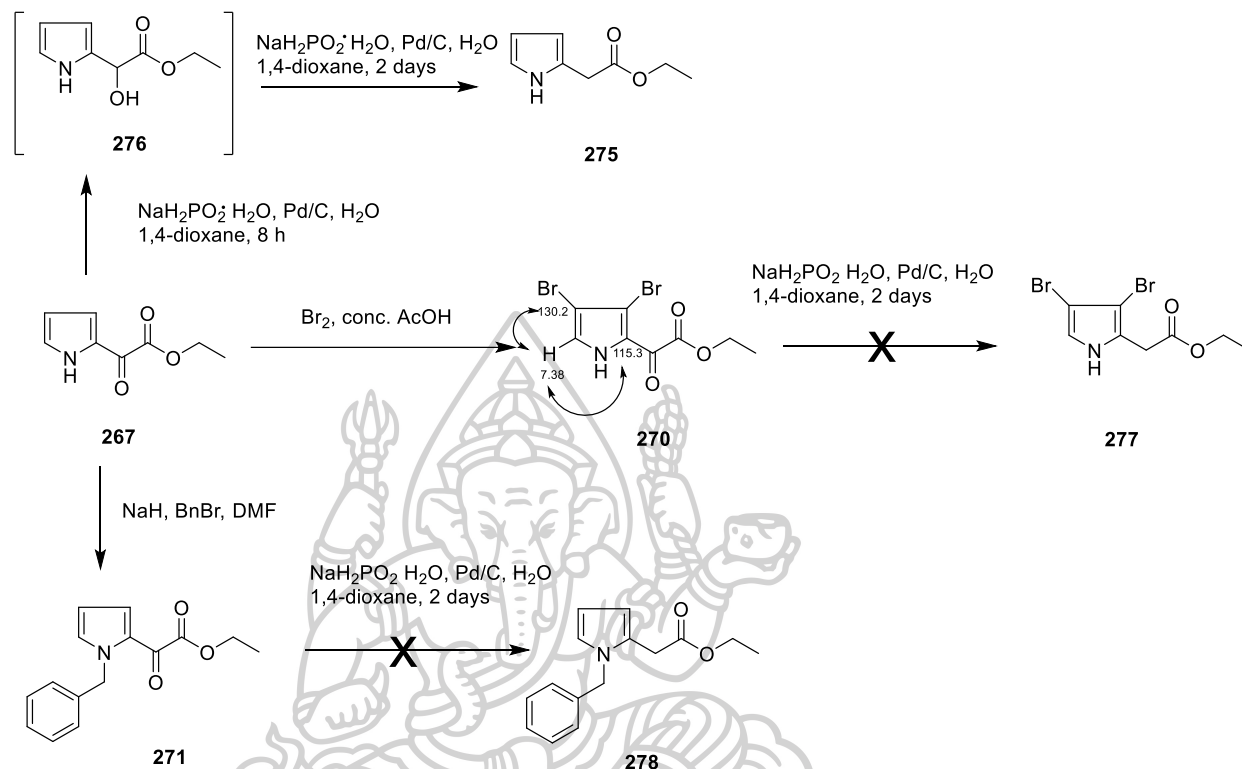
7.73 (2H) and 7.28 ppm (2H). Next, the compounds **261** and **262** were treated with oxalyl chloride via the same procedure for the synthesis of compound **267**, this reaction was unsuccessful because of the steric effect of boc and tosyl protecting groups. (Scheme 29).



Scheme 29. Preparation of N-substituted pyrrole keto-ester derivatives

The chlorinated analogue of the IAA auxin, 4-chloroindole-3-acetic acid (4-Cl-IAA) that was found as a potent auxin generally showing more activity than IAA in standard biological assays such as stimulation of growth of excised tissue of pea, oat, wheat and mung bean, increasing roots initiation and ethylene evolution in pea shoot cutting and the effective on the growth of intact plant organs include wheat, cucumber and tomato (Reinecke, 1999), therefore, the substitution of halogen atom on pyrrole ring was designed. Bromination of compound **267** produced di-substituted bromine (**270**). The ^1H NMR showed only a singlet of aromatic region at 7.38 ppm. The HMBC NMR showed that proton at 7.38 ppm was correlated with carbon 2 at 115.3 and carbon 3 at 130.2 ppm. At the same time, *N*-benzylation of compound **267** with benzylchloride gave *N*-benzylated product **271**. The chemical shift of ^1H NMR was occurred at 5.54 ppm as a

singlet for 2H of CH₂-benzyl group, multiplet for 2H at 7.14-7.11 ppm of aromatic benzyl group and multiplet for 3H at 7.30-7.19 ppm of aromatic benzyl group (Scheme 30).

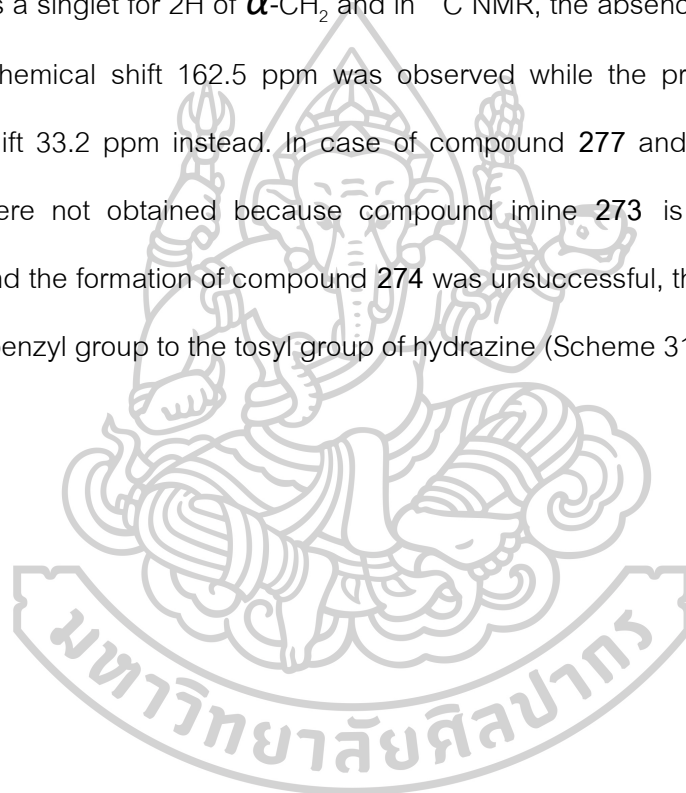


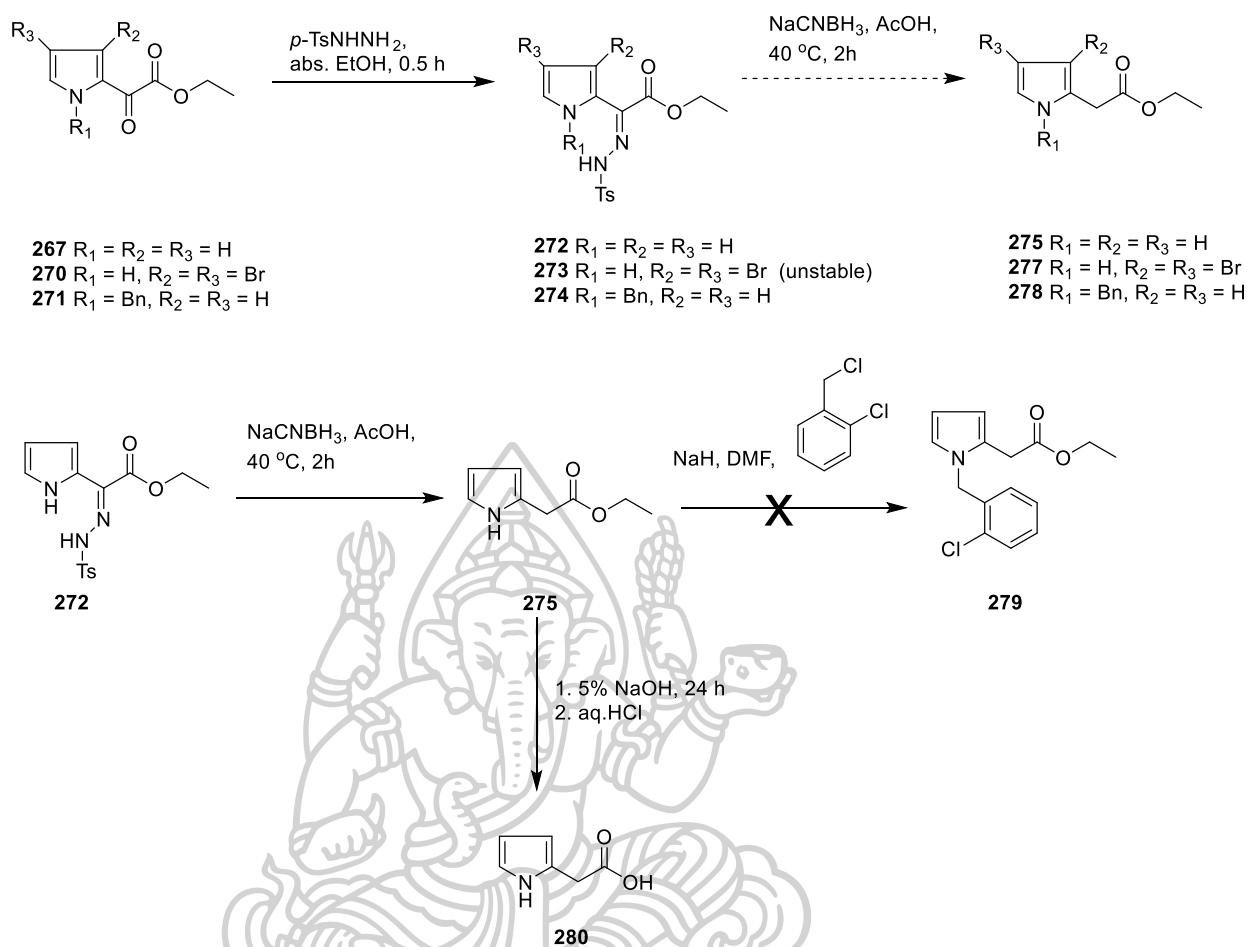
Scheme 30. Reduction of pyrrole keto-ester derivatives.

Then, the α -keto group of keto-acid (267) was reduced to CH₂ by using the procedure of triethylsilane as a reducing agent under acidic condition and procedure of Clemmensen reduction, However the product was not observed. Compound 267 was then reduced by using the Pd/C/NaH₂PO₂·H₂O to afford compound 275 in 5 %yield when the reaction was proceeded for 2 days. However, this procedure was afforded hydroxy compound 276 in 29 % yield when refluxing for 8 h. The ¹H NMR that showed the chemical shift at 5.25 ppm of singlet 1H of α -(CH)-OH (Scheme 31).

Compound 275 was attempted to increasing yield. The reduction of ketone to provide the methylene group via tosylhydrazone reduction was previously reported in good yield (Taylor & Djerassi, 1976). This procedure was proceeded through two step

syntheses. The imine formation at α -keto position of compound **267** with *p*-provided compound **272** in 75 % yield. The tosyl hydrazine chemical shift in ^1H NMR of product **272** was observed at 11.54 ppm as singlet for 1H of NH, 7.84 and 7.30 ppm as doublet for 2H of aromatic benzene and 2.42 ppm as singlet for 3H of CH_3 . Next, imine **272** was reduced by using NaCNBH_3 as a reducing agent under acidic condition to provide the reduced product **275**, in 8 % overall yield. The ^1H NMR was occurred at chemical shift 3.66 ppm as a singlet for 2H of $\alpha\text{-CH}_2$ and in ^{13}C NMR, the absence of carbon carbonyl ketone at chemical shift 162.5 ppm was observed while the presence of $\alpha\text{-CH}_2$ at chemical shift 33.2 ppm instead. In case of compound **277** and **278**, these reduced products were not obtained because compound imine **273** is unstable for further reduction and the formation of compound **274** was unsuccessful, this may be due to the bulk of the benzyl group to the tosyl group of hydrazine (Scheme 31).

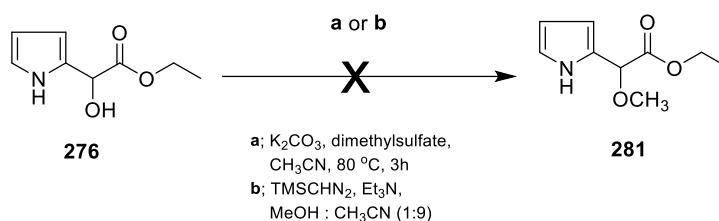




Scheme 31. Reductive elimination of pyrrole keto-ester derivatives.

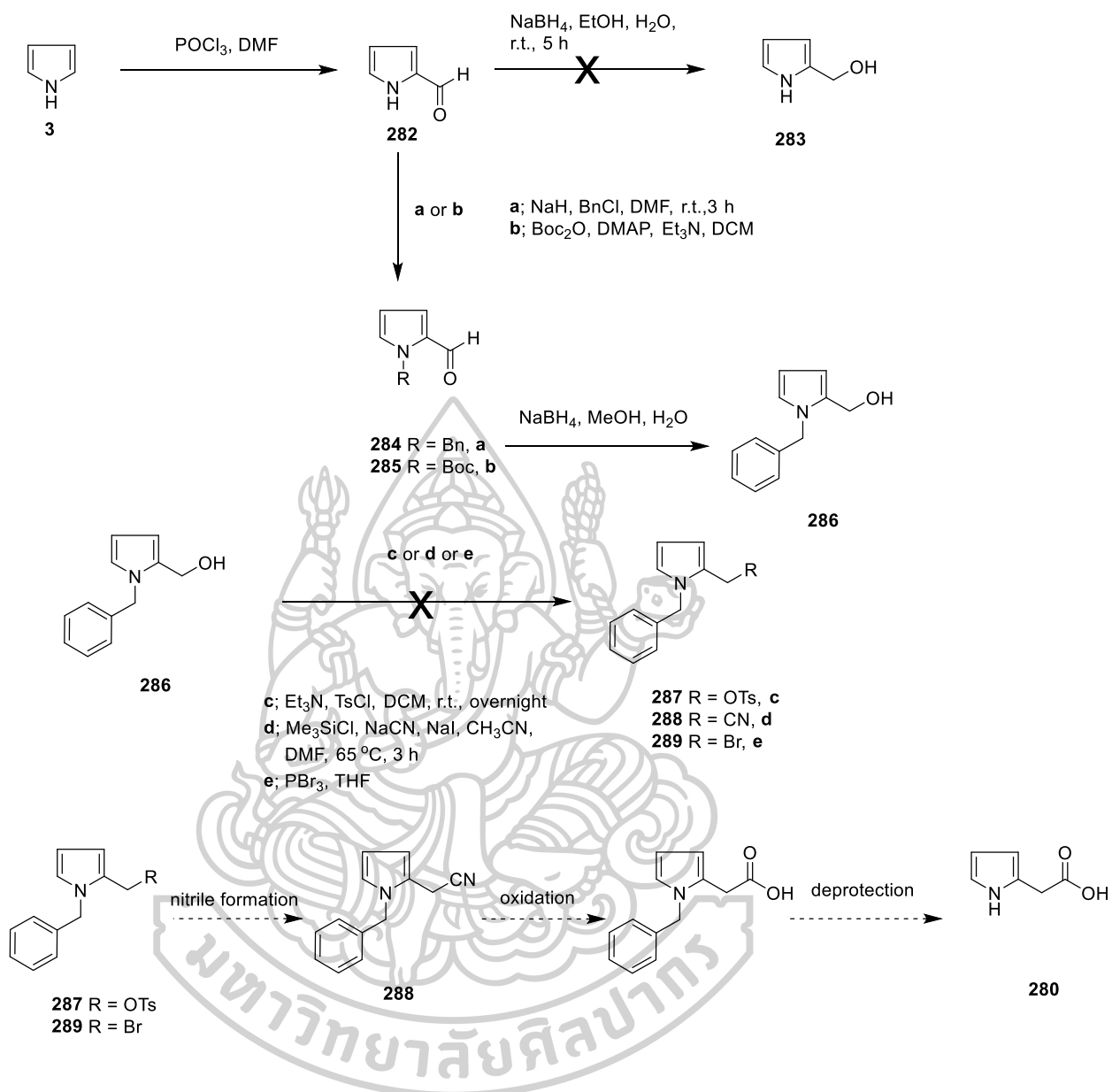
Then, the attempted synthesis of compound **279** by using *N*-substitution of compound **275** with a chlorobenzyl group was also unsuccessful. Ester compound **275** was hydrolysed to carboxylic acid **280** in 10% yield. The structure was confirmed by the ^1H and ^{13}C NMR, the absence of chemical shifts at 4.17, 1.27 ppm and 51.1, 14.1 ppm of the ethyl group while the presence of a carboxylic group in ^{13}C NMR at a chemical shift of 157.9 ppm was observed in compound **280** (Scheme 31).

Attempts to convert the hydroxy group of **276** to a good leaving group by using *O*-methylation with dimethyl sulfate or trimethylsilyldiazomethane. However, the reaction was unsuccessful (Scheme 32).



Scheme 32. Methylation of compound 276.

Subsequently, attempts to increase the percentage yield of compound 279 was planned as shown in scheme 33. Vilsmeier-Haack reaction of pyrrole (3) with phosphorus oxychloride and DMF provided product 282 in 88 % yield. The ¹H NMR of aldehyde of product 282 was confirmed with previous literature (de Groot et al., 1981). The aldehyde was reduced with NaBH₄, the product was not observed but the polymerization of compound 283 was occurred. Therefore, aldehyde 282 was protected with benzyl and Boc group to give products 284 and 285, respectively. Then, only the reduction of 283 was succeeded to give the alcohol 286. The CH₂-OH proton NMR of product 285 was occurred at chemical shift 5.12 as a singlet (2H). The attempted to transformation of hydroxy group to nitrile via O-tosyl, TMS- and bromine group for increasing the ability of leaving group were unsuccessful (Scheme 33).

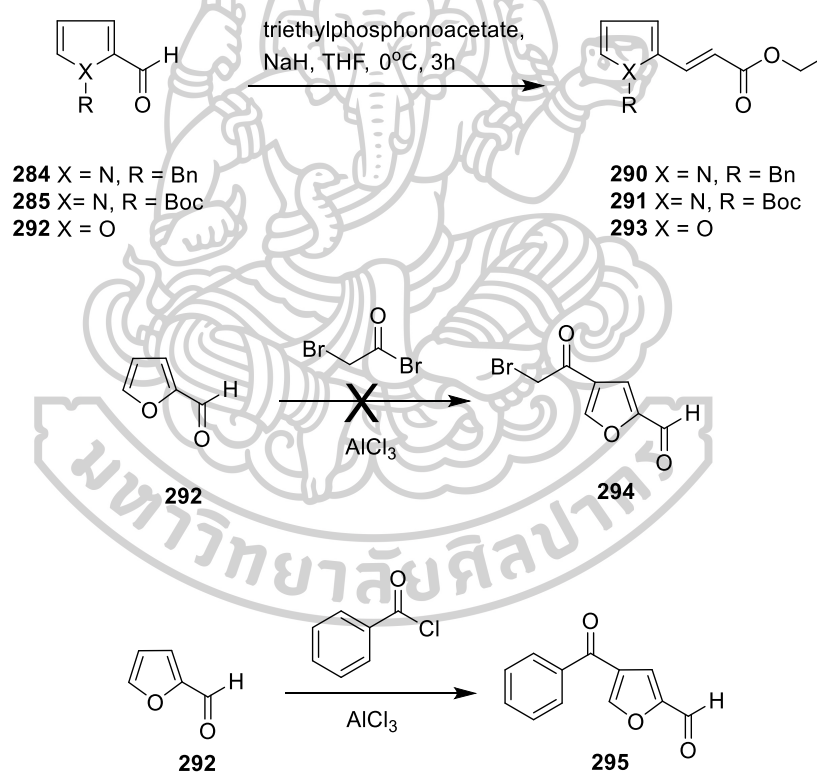


Scheme 33. Preparation of pyrrole-2-acetic acid.

2. The second synthetic route of pyrrole and furan derivatives

The synthetic route 2 is the synthesis of disubstituted of pyrrole and furan derivatives. The synthesis was started from Wittig reaction of triethylphosphonoacetate with the commercial 2-furaldehyde **292**, compound **284** and **285** (Scheme 34). Compound **293** was obtained as a single product while compound **290** and **291** were obtained as a mixture with starting materials in ration 1:1. The proton NMR spectrum of compound **291** was confirmed by occurring of two doublet peaks (1H) of olefin position

at chemical shift 7.43 and 6.30 ppm and quartet peak (2H), triplet peak (3H) of ethyl ester position at chemical shift 4.24 and 1.32 ppm, respectively. These spectrum pattern were also showed in ^1H NMR spectrum of compound **290** and **291**. The compound **294** and **295** were attempted to prepare by using Friedel-Craft reaction between 2-furaldehyde with bromo acetyl bromide or benzoyl chloride. The results showed that compound **294** was unsuccessful due to the unactive reagent while compound **295** was obtained in 8.1 %yield which ^1H NMR of benzoyl group showed chemical shift at 8.11 (2H), 7.62 (1H) and 7.48 (2H) ppm as a one doublet peak and two triplet peaks, respectively (Scheme 34).



Scheme 34. Preparation of 2,4-disubstituted heterocyclic derivatives.

3. Results of Identification of *Boesenbergia rotunda* Actinomyces crude extract.

The EtOAc crude extract of *Boesenbergia rotunda* Actinomyces (IP-M01) was received in 2.45 g from 200 petri disc. The crude extract was used to evaluate antibacterial activity against *B. subtilis* by using bioautography assays. The clear zone

around TLC was not clear. It was summarized that this crude extract did not have active purified compound.

4. Results of the synthesis of Lansai C and D derivatives

4.1 Extraction, purification and structure elucidation of Lansai compounds.

Lansai A-D (**26-29**) were obtained in 45.5, 5.4, 39.2 and 2.6 mg, respectively, from 750 mg of crude EtOAc extract. The structures of the Lansai A-D (**26-29**) were compared with previous report (Tuntiwachwuttikul et al., 2008).

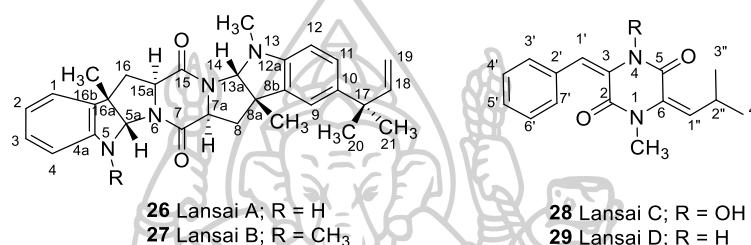
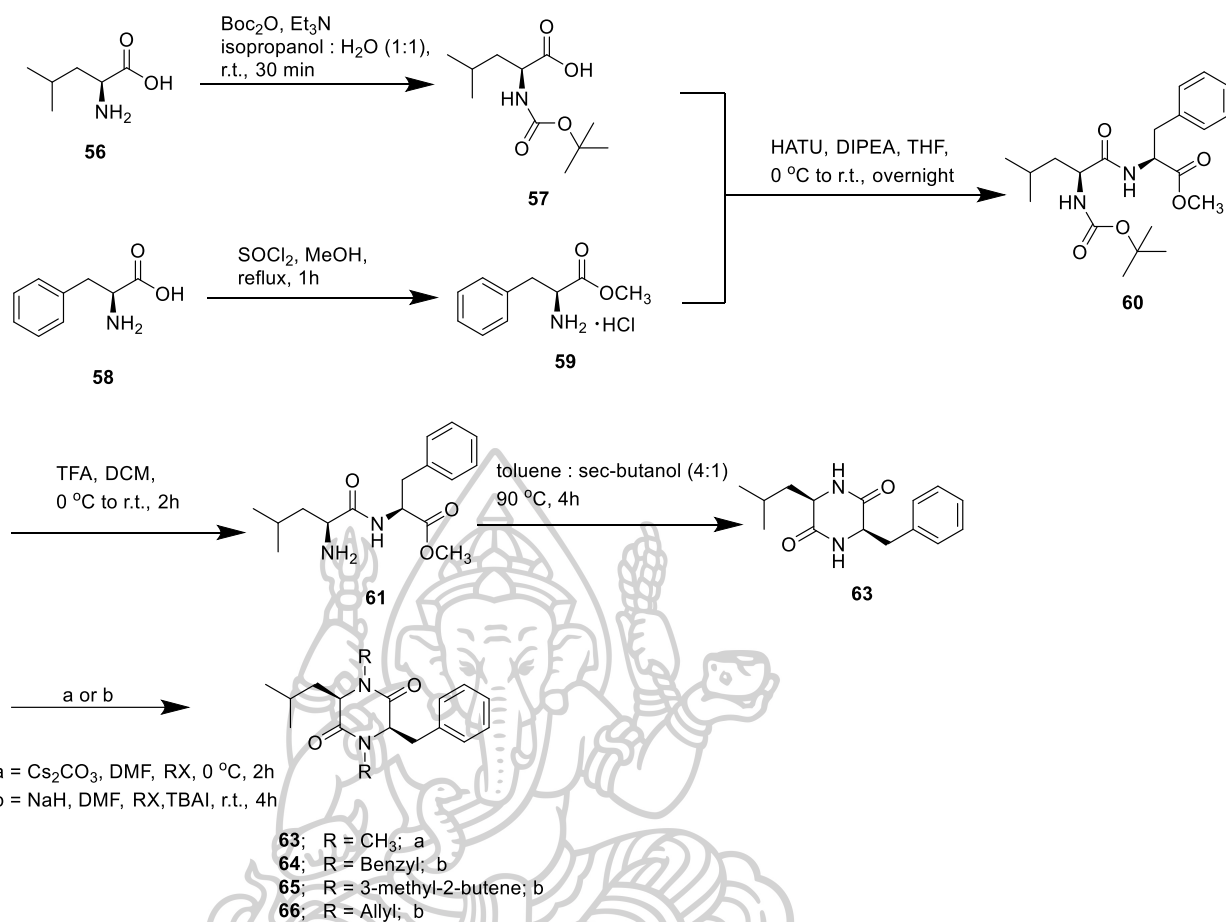


Figure 12. Structural elucidation of Lansai A-D (**26-29**).

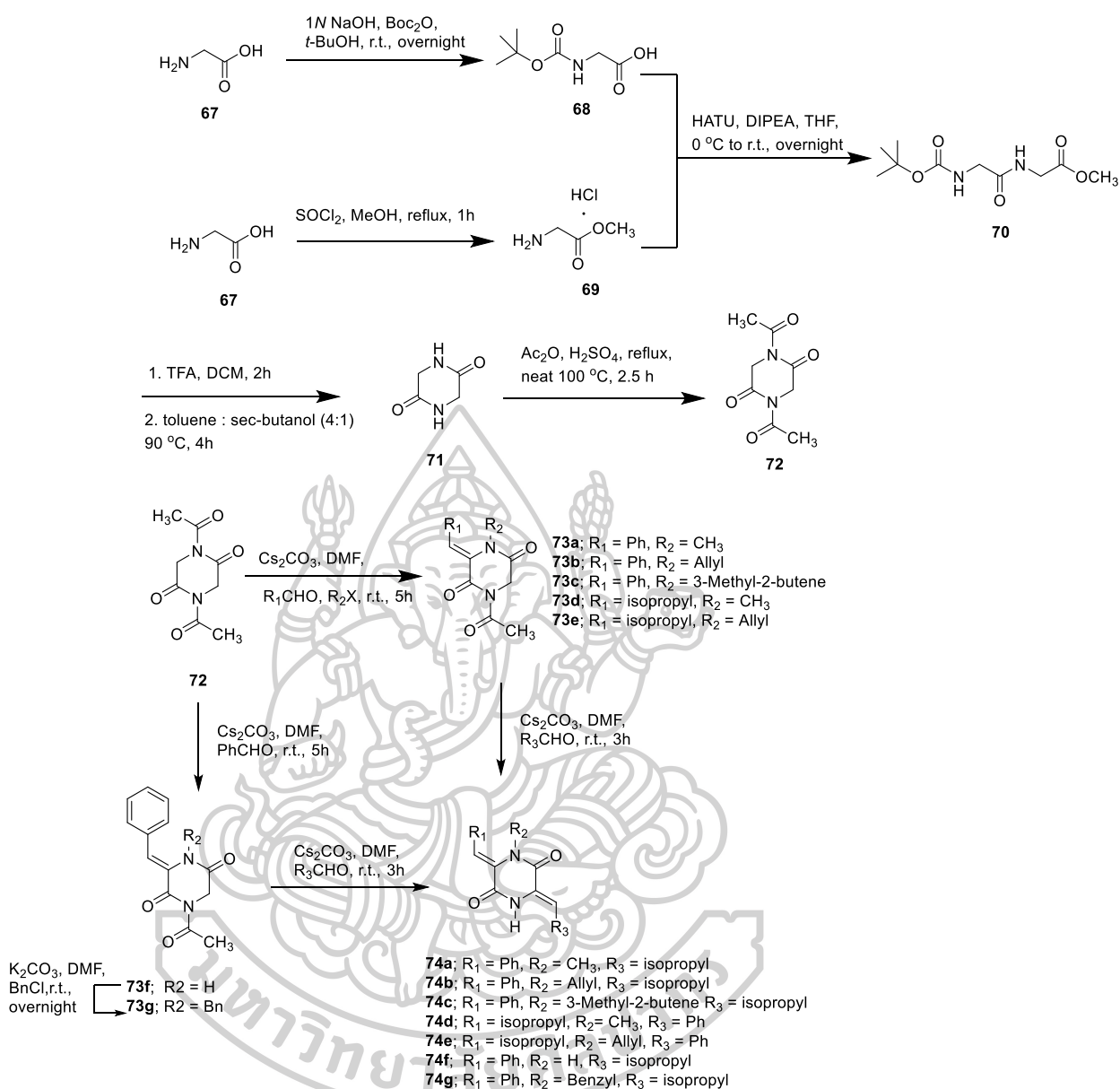
4.2 The synthesis of Lansai C and D derivatives.

The synthesis of tetrasubstituted 2,5-DKP derivatives started from dipeptide **60**, which was prepared from *N*-Boc-Leucine **57** and Phenylalanine methyl ester **59** by using HATU as amide coupling reagent in the presence of DIPEA as base. The ¹³C NMR of amide in compound **60** was occurred at chemical shift 155.5 ppm. Then, the deprotection of the Boc group followed by ring formation by using thermal reaction to obtain 2,5-DKP derivative **62**. The *N*-substitution of compound **62** with methyl iodide was employed the reaction with Cs₂CO₃ at 0 °C to afford compound **63**. Compound **64-66** was achieved via the reaction of compound **62** with benzyl chloride, 1-chloro-3-methyl-2-butene and allyl bromide in the presence of catalyst amount of TBAI and using NaH as base, provided the formation of tetrasubstituted 2,5-DKP derivatives **64-66** (Scheme 35) in fair yields.



Scheme 35. Synthesis of tetrasubstituted 2,5-DKP derivatives **63-66**.

The synthesis of Lansai C and D derivatives was started from the formation of 2,5-DKP ring, glycine anhydride **71**, from inexpensive material by using the same procedure for the synthesis of compound **63**. The 1,4-diacetyl-2,5-diketopiperazine **72** was synthesized from compound **71** using reflux in acetic anhydride. Compound **72** underwent Aldol addition–acetyl migration–elimination cascade with Cs_2CO_3 , alkyl halide, and various aldehydes (Liao, Qin, Li, et al., 2014) to provide highly (*Z*)-stereoselective products **73a-e** (Scheme 36).



Scheme 36. Synthesis of 2,5-DKP derivatives.

This reaction was explained by using the Zimmerman–Traxler model, which was reported by Balducci and co-worker (Balducci et al., 2012), the (*Z*)-Aldol intermediate was generated through transition state A, in which the interaction between the R substituent on the aldehyde and acetyl groups was minimized (Figure 13).

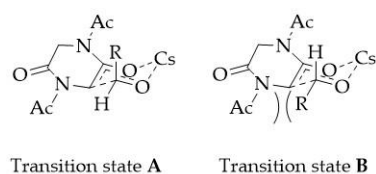
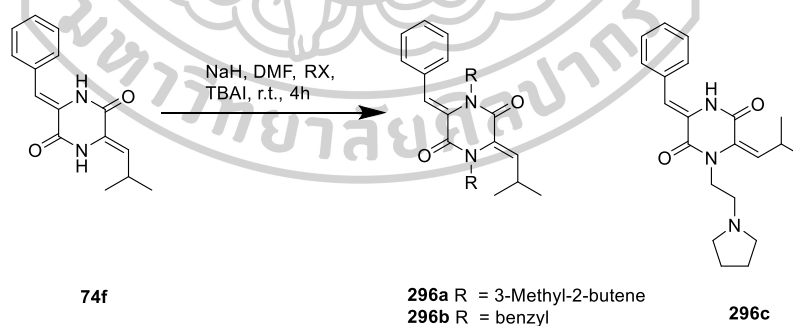


Figure 13. Zimmerman–Traxler model.

In the case of *N*-benzyl derivative **73g**, the cascade reaction using benzyl chloride failed to provide the desired product probably because of the steric hindrance with the benzylidene substituent. Thus, the benzylidene derivative **73f** was further benzylated to provide compound **73g**. Then, the next aldol condensation was accomplished to provide trisubstituted 2,5-DKP derivatives (**74a-g**). However, the yields obtained in this syntheses were poor because of the solubility of the products (Ando et al., 2011). Compound **74f** was known as Albonoursin, a natural product from *Streptomyces noursei* (Lautru et al., 2002). *N*-alkylation of compound **74f** with NaH, benzyl chloride, and 1-chloro-3-methyl-2-butene provided disubstituted products **296a** and **296b**. However, only monosubstituted product **296c** was obtained when using the bulkier 1-ethyl pyrrolidine chloride, and propylidene was converted to *E*-configuration probably because of the steric hindrance (Scheme 37).



Scheme 37. *N*-alkylation of 2,5-DKP derivatives.

The configuration of the double bond was confirmed by NMR spectroscopy. Fairhurst and co-worker (Fairhurst et al., 2018) compared the proton NMR spectrum between *Z*- and *E*-isomers of proton on an alkylidene double bond (C=CH) in complex *tert*-butyl-3-(2-methylpropylidene)-2,5-dioxopiperazine-1-carboxylate at 6.14 and 5.42

ppm, respectively. In this research, each proton NMR spectrum of the C=CH double bond in 6-(2-methylpropylidene) occurred at 6.01-6.13 ppm, which might indicate (6*Z*)-configuration. The NOEDIFF spectra of compound **73e** showed that the proton on the alkylidene double bond (C=CH) only enhanced the proton of isopropyl moiety. Thus, the alkylidene double bond of compound **73e** was characterized as (*Z*)-configuration. Another NOEDIFF analysis of compound **74d** showed that 4-NH and H-11 enhanced Ar-H of benzylidene moiety and 1-*N*-CH₃, respectively. Thus, compound **74d** was characterized as (3*Z*,6*Z*)-3-benzylidene-6-(2-methylpropylidene)-1-methyl-2,5-diketopiperazine (Figure 21). Other results showed steric hindrance between the proton of the aromatic ring and the carbonyl and steric repulsion between hydrogen atoms in benzylidene and the *N*-alkylated group, which might be due to (3*Z*)-selectivity. Further NOESY analysis was used to confirm the stereochemistry of (6*E*)-configuration in compound **296c**. An NOE enhancement from H-7 to H-18, H-19, H-21, H-22, H-23, and H-24 was observed, whereas an NOE enhancement of H-8 was not found. This result indicated (6*E*)-configuration (Figure 14).

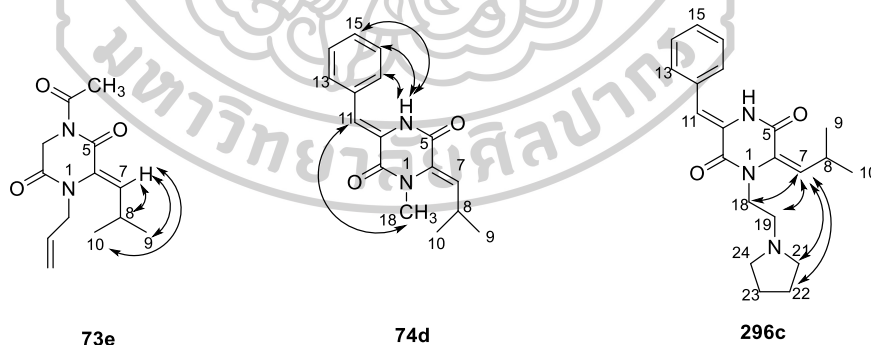


Figure 14. NOEDIFF and NOE contracts for stereoisomers of compounds **73e**, **74d**, and **296c**.

5. Results of the Biological activities

5.1 Cytotoxicity activity

Lansai A-D (**26-29**) were studied *in vitro* for their cytotoxic activities by MTT assay on Hela cancer cell line and LLC-MK2 normal cell line. All of IC₅₀ were shown in

Table 1. From all of tested compounds were low cytotoxicity in cancer cell line and moderately toxicity in normal cell line which Lansai C (28) has more active against Hela cancer cell line and lower toxicity against LLC-MK2 normal cell line than another tested compounds.

Table 1. The cytotoxicity of Lansai A-D (26-29) against Hela cancer cell line and LLC-MK2 normal cell line.

Compounds	IC ₅₀ (µg/mL)	
	Hala	LLC-MK2
26	403.90	287.65
27	262.70	353.51
28	183.70	507.84
29	448.60	437.33
Doxorubicin	1.95	98.92

5.2 Antiviral activity

5.2.1 Virus propagation inhibition assay

The efficacy of Lansai C (28), Lansai D (29), and its derivative to influenza virus (H5N2) propagation inhibition was evaluated at various concentrations in embryonated chicken eggs. A hemagglutination test was performed to estimate virus propagation. The summary result is displayed in Table 2. The result showed that Lansai C (28) inhibited virus propagation at a concentration of 25 µg/mL, whereas Lansai D (29) could not inhibit virus propagation at a high concentration (100 µg/mL). Therefore, *N*-substitutions are essential for the activity. However, compound 74d, which has opposite double bond configuration to Lansai D (29), showed an activity of influenza virus (H5N2) propagation inhibition at a concentration of 25 µg/mL. Thus, either *N*-substitution or double bond configuration affected the activity. The unprotected nitrogen

or protected nitrogen with electrostatic groups such as allyl and 3-methyl-2-butene adjacent to (*Z*)-benzylidene might influence the activity in compounds Lansai C (**28**), **74b-d**, and **296c**. However, the benzyl substituent **74g** had a different impact on the activity. The substitution on nitrogen adjacent to *iso*-propylidene should be small or none if the isopropylidene is in *Z*-configuration to possess the activity. Moreover, the presence of a double bond was important for the activity in compounds **63-66**.

Table 2. Summary of influenza virus (H5N2) propagation inhibition in embryonated chicken eggs of Lansai C (**28**), Lansai D (**29**), and its derivatives detected by hemagglutination assay.

Compounds	Concentrations ($\mu\text{g/mL}$)		
	100	50	25
	HA titer		
Control	1:1.5	1:1.5	1:1.5
28	Negative	Not test	Negative
29	1:12	Not test	1:24
63	1:48	1:12	1:6
64	Negative	1:6	1:6
65	1:24	1:1.5	1:3
66	Negative	1:6	1:24
74a	Negative	Negative	1:1.5
74b	Negative	Negative	Negative
74c	Negative	Negative	Negative
74d	Negative	Negative	Negative
74e	1:24	1:1.5	1:6
74g	1:6	1:1.5	1:384

296a	1:12	1:786	1:6
296b	1:24	1:6	1:1.5
296c	Negative	Negative	Negative

5.2.2 Molecular docking studies

The molecular docking studies were investigated the possible binding between enzymes involved in antiviral activities and compounds which serve as virus propagation inhibitor (Lansai C (**28**), compound **64**, compound **66**, and compounds **74a-74d**) as shown in figure 15, all of studied compounds bound in the active site of HGPRT and H5N2, whereas only five of studied compounds bound in the active site of SARS-CoV-2 3CLpro and SARS-CoV-2 RBD with ACE2.

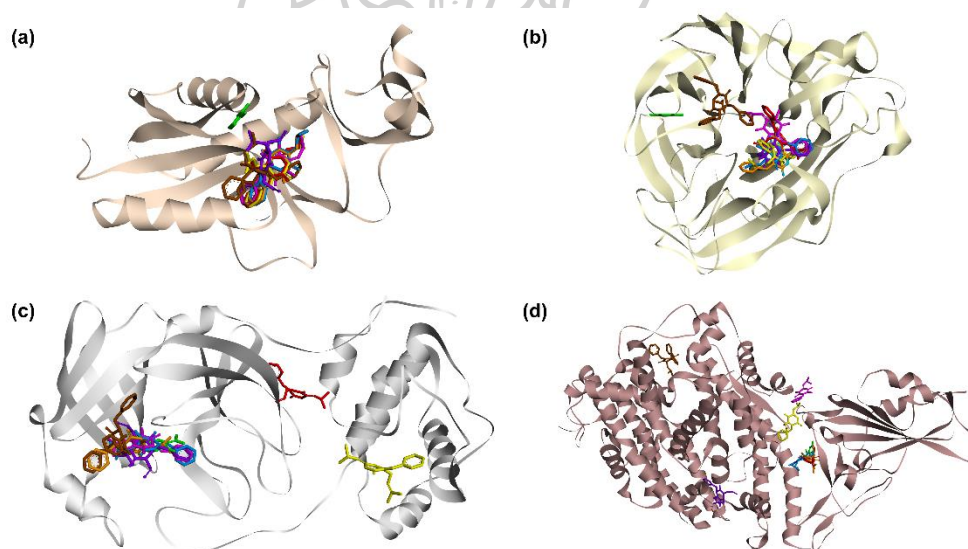


Figure 15. Comparison of the binding position of Favipiravir (green), Lansai C (**28**) (pink), compound **64** (brown), compound **66** (purple), compound **74a** (orange), compound **74b** (red), compound **74c** (yellow), and compound **74d** (blue) in the cavity of (a) human hypoxanthine-guanine phosphoribosyltransferase (HGPRT), (b) neuraminidase from H5N2 avian influenza virus, (c) SARS-CoV-2 3CL main protease, and (d) SARS-CoV-2 spike receptor-binding domain bound with ACE2.

The binding energies of our compounds bound in the cavity of four enzymes are demonstrated in Table 5. Compound **74a**, compound **74d**, and Lansai C (**28**) can bound in the active site of all four interested enzymes; however, only compound **74d** and Lansai C (**28**) can form H-bonds with the amino acids in the active site of the enzymes (Table 3 and Figure 16). Moreover, compound **74d** and Lansai C (**28**) bound in SARS-CoV-2 3CL main protease with lower binding energies (-92.90 and -98.31 kcal/mol, respectively) than Favipiravir (-81.43 kcal/mol). Interestingly, compound **74d** in H5N2 had lower binding energy (-101.86 kcal/mol) than Favipiravir (-88.51 kcal/mol), whereas Lansai C (**28**) had lower binding energy (-84.84 kcal/mol) than Favipiravir (-80.92 kcal/mol). Furthermore, hydrogen bond interactions were found between the substituent group (particularly the carbonyl group) on the 2,5-DKP ring of our compounds and amino acids in the active site of all four enzymes tested in this study, indicating that the 2,5-DKP scaffold of our compounds could be the key to bind and inhibit the enzyme involved in antiviral activities (Figure 16).

Table 3. Summary of binding energies, amino acid interaction, and hydrogen bond length of Favipiravir and 2,5-diketopiperazine derivatives in molecular docking studies.

Proteins	Compounds	Binding energy (kcal/mol)	Amino acid residues	H-bond length (Å)
Human hypoxanthine-guanine phosphoribosyltransferase	64	-85.45	LYS68	2.42
	66	-76.65	LYS68	1.93
	74a	-75.41	LYS68	1.73
	74b	-78.46	LYS68	2.06
	74c	-80.33	LYS68	2.27
	74d	-73.19	LYS68	1.73
	28	-78.29	ASP134	2.75

Proteins	Compounds	Binding energy (kcal/mol)	Amino acid residues	H-bond length (Å)
	Favipiravir	-88.29	GLY69, GLY70	2.70, 2.18
Avian influenza virus	64	-85.34	ASN249	1.84
	66	-77.18	ARG371	2.09
	74a	-85.09	-	-
	74b	-77.87	GLN432	1.87
	74c	-91.93	ARG371, ARG371	2.76, 2.18
	74d	-101.86	ARG371	2.24
	28	-81.02	ARG371	3.00
	Favipiravir	-88.51	GLY248, ALA250, HIS274, ILEE275, ASN294	2.79, 2.66, 1.63, 2.48, 2.61
COVID-19 3CL main protease	64	-75.90	THR26	2.00
	66	-70.29	SER144,CYS145	2.90,2.49
	74a	-74.81	-	-
	74d	-92.90	SER144, CYS145	2.89,1.63
	28	-98.31	SER144, CYS145	2.61,1.99
	Favipiravir	-81.43	HIS163	2.23
SARS-CoV-2 spike	74a	-84.40	-	-

Proteins	Compounds	Binding energy (kcal/mol)	Amino acid residues	H-bond length (Å)
receptor-binding domain bound with ACE2	74b	-80.47	-	-
	74c	-86.15	E: GLY504	2.67
	74d	-79.30	E: ARG403, E: ARG303, E: TYR505	1.55, 2.38, 2.63
	28	-84.84	A: ASN330, E: ASN439, E: GLN506	1.97, 2.70, 1.96
	Favipiravir	-80.92	A: HIS34, A: LYS353, E: TYR453, E: GLN493	3.09, 2.24, 2.45, 1.95

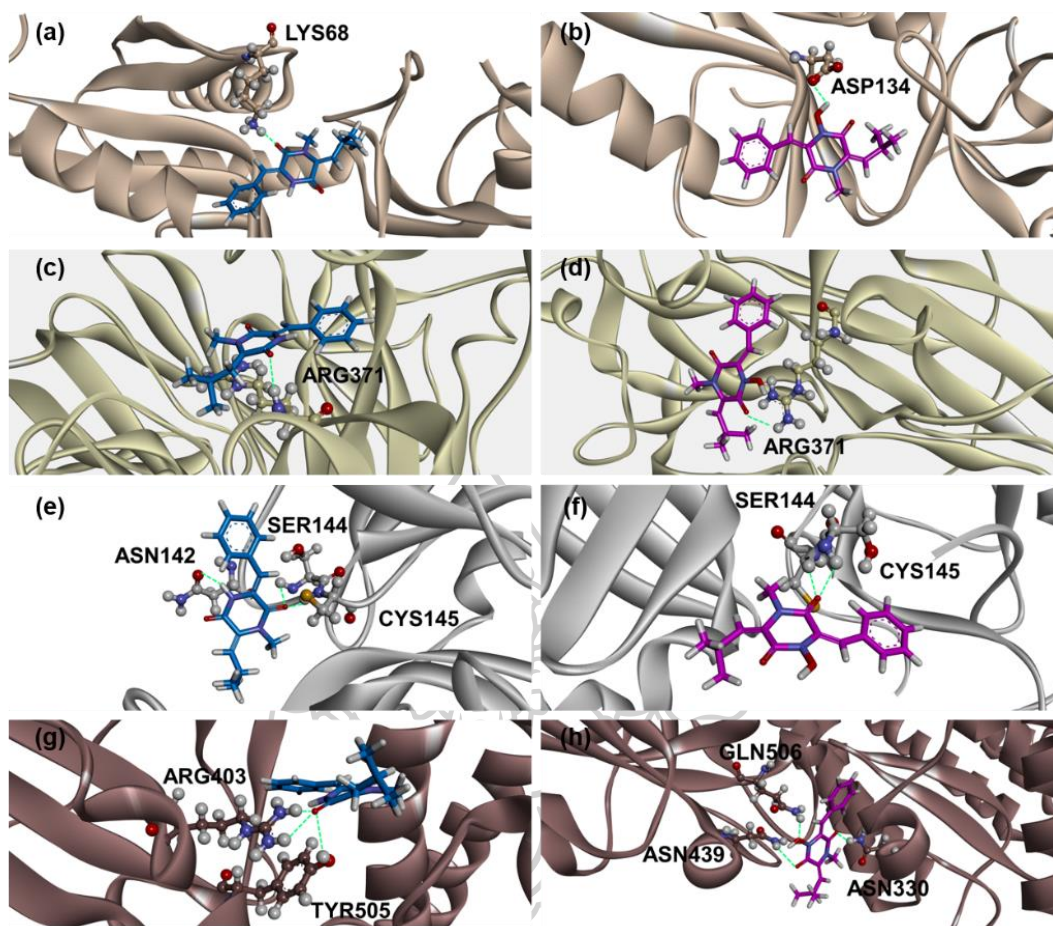


Figure 16. Hydrogen bond interactions of compound 74d (blue) and Lansai C (28) (pink) in the cavity of human hypoxanthine-guanine phosphoribosyltransferase (a,b), Avian influenza virus H5N2 (c,d), COVID-19 3CL main protease (e,f), and SARS-CoV-2 spike receptor-binding domain bound with ACE2 (g,h).

5.3 Antibacterial activity

The results of antibacterial activity of the Lansai C (28), Lansai D (29) and its derivatives (63-66, 74a-e, 74g, 296a-c) were determined against two bacterial strains that was shown in Table 4. All of tested compounds were showed low activities against *S. aureus* and *E. coli* (MIC > 512 $\mu\text{g/mL}$) (Table 4).

Table 4. The minimum inhibitory concentration (MIC) of antibacterial activity of Lansai C (28), Lansai D (29) and its derivatives (63-66, 74a-e, 74g, 296a-c)

Compounds	MIC ($\mu\text{g/mL}$)	
	<i>S. aureus</i>	<i>E. coli</i>
28	> 512	> 512
29	> 512	> 512
63	> 512	> 512
64	> 512	> 512
65	> 512	> 512
66	> 512	> 512
74a	> 512	> 512
74b	> 512	> 512
74c	> 512	> 512
74d	> 512	> 512
74e	> 512	> 512
74g	> 512	> 512
296a	> 512	> 512
296b	> 512	> 512
296c	> 512	> 512

CHAPTER 5

CONCLUSIONS

In conclusion of this studied, researcher attempted to synthesis pyrrole derivatives as serve as plant regulators. The first route was started from acylation of pyrrole (3) with oxalyl chloride to provide substitution at position 2 of pyrrole instead of position 3. The researcher attempted to provide the substitution at position 3 of pyrrole that same as position of IAA, Therefore, pyrrole was *N*-protected with boc, tosyl, trimethylsilyl, *tert*-butyldimethylsilyl, methyl and trisopropylsilyl group to reduce the nucleophilicity of pyrrole, provided only *N*-boc and *N*-tosyl pyrrole (261, 262) which further acylation with oxalyl chloride was unsuccessful. To study the substituent group at carbon and nitrogen of pyrrole to affective on the plant growth regulation, The disubstituted bromine 270 was synthesized from bromination of compound 267 and *N*-benzylation 271 was synthesized through the reaction with benzylchloride. Then, the reduction of α -keto of compound 267 to CH_2 was used the procedure of triethylsilane as a reducing agent under acidic condition and procedure of Clemmensen reduction which were not provided the product. The using of hydrogenolysis procedure with Pd/C/ $\text{NaH}_2\text{PO}_2 \cdot \text{H}_2\text{O}$ system afforded compound 275 in 5 %yield when the reaction was proceeded for 2 days while hydroxy compound 276 was received in 29 % yield when the reaction was proceeded for 8 h. To increasing of % yield, the using of reductive amination of compound 267, 270 and 271 were proceeded through two step synthesis, starting from imine formation at α -keto position by reacted with *p*-TsNHNH₂. The product 272 was received in good yield while product 273 is unstable for further reduction and the formation of compound 274 was unsuccessful. The imine 272 was

further reduced by using NaCNBH_3 as a reducing agent under acidic condition to provide the reduction of α -keto position to CH_2 completely, in 8 % overall yield. Ester compound **275** was hydrolysed to carboxylic acid **280**. Meanwhile, the methylation of hydroxy compound **276** was unsuccessful. The attempted the synthesis of compound **280** was proceeded through Vilsmeier-Haack reaction of pyrrole (**3**), *N*-protection, aldehyde reduction and nitrile transformation were unsuccessful. So, we were not successful to synthesize the pyrrole derivatives as plant growth regulators.

The synthetic route 2 is the synthesis of disubstituted of pyrrole and furan derivatives which was started from Wittig reaction of the commercial 2-furaldehyde **292**, compound **284** and **285** with triethylphosphonoacetate. These reactions were provided compound **293** as purified product only while product **290** and **291** were not separated from starting material. The compound **294** and **295** were attempted to prepare by using Friedel-Craft reaction between 2-furaldehyde with bromo acetyl bromide or benzoyl chloride, the product **294** was not obtained while compound **295** was obtained in very low yield. This synthetic route was unsuccessful.

The identification of EtOAc crude extract of *Boesenbergia rotunda Actinomyces* (IP-M01) was not success because this crude extract didn't have active purified compound which was analyzed by bioautography assay.

The isolation of Lansai A-D (**26-29**) from *Streptomyces* sp. SUC1 crude extract were obtained in 45.5, 5.4, 39.2 and 2.6 mg, respectively, from 750 mg of crude EtOAc extract.

The synthesis of tetrasubstituted 2,5-DKP derivatives started from the formation of 2,5-DKP ring from dipeptide followed by *N*-substitution with methyl iodide, benzyl chloride, 1-chloro-3-methyl-2-butene and allyl bromide, provided the formation of tetrasubstituted 2,5-DKP derivatives **63-66** in fair yields.

The synthesis of Lansai C and D derivatives was started from the formation of 2,5-DKP ring, glycine anhydride **71**, followed by *N*-acetylation and one-pot Aldol addition–acetyl migration–elimination cascade with alkyl halide, and various aldehydes to provide highly (*Z*)-stereoselective products **73a-e**. In the case of *N*-benzyl derivative **73g**, was provided through the benzylated of benzylidene derivative **73f**. The next Aldol condensation was accomplished to provide trisubstituted 2,5-DKP derivatives (**74a-g**). *N*-alkylation of compound **74f** with benzyl chloride, and 1-chloro-3-methyl-2-butene provided disubstituted products **296a** and **296b**. However, only monosubstituted product **296c** was obtained when using the bulkier 1-ethyl pyrrolidine chloride, and propylidene was converted to *E*-configuration.

The cytotoxicity of Lansai A-D were low cytotoxicity against Hela cancer cell line and LLC-MK2 normal cell line. Compounds Lansai C (**28**), **74b-d**, and **296c** showed an activity of influenza virus (H5N2) propagation inhibition. Compound Lansai C (**27**), **63**, **65**, and **74a-74d** could be bound in the active site of HGPRT and H5N2, whereas only five of studied compounds bound in the active site of SARS-CoV-2 3CLpro and SARS-CoV-2 RBD with ACE2. However, these results could be gainful for antiviral drug development in the future.

The antibacterial activity of the Lansai C (**28**), Lansai D (**29**) and its derivatives (**63-65**, **74a-e**, **74g**, **296a-c**) were low activities against *S. aureus* and *E. coli* (MIC > 512 µg/mL).

REFERENCES

- Ando, S., Grote, A. L., & Koide, K. (2011). Diastereoselective Synthesis of Diketopiperazine Bis- α,β -epoxides. *The Journal of Organic Chemistry*, 76(4), 1155-1158.
<https://doi.org/10.1021/jo102096d>
- Au - Brauer, R., & Au - Chen, P. (2015). Influenza Virus Propagation in Embryonated Chicken Eggs. *JoVE*(97), e52421. <https://doi.org/doi:10.3791/52421>
- Balducci, D., Conway, P. A., Sapuppo, G., Müller-Bunz, H., & Paradisi, F. (2012). Novel approach to the synthesis of aliphatic and aromatic α -keto acids. *Tetrahedron*, 68(36), 7374-7379. <https://doi.org/https://doi.org/10.1016/j.tet.2012.06.078>
- Barakat, F., Vansteelandt, M., Triastuti, A., Jargeat, P., Jacquemin, D., Graton, J., Mejia, K., Cabanillas, B., Vendier, L., Stigliani, J. L., Haddad, M., & Fabre, N. (2019). Thiodiketopiperazines with two spirocyclic centers extracted from *Botryosphaeria mamane*, an endophytic fungus isolated from *Bixa orellana* L. *Phytochemistry*, 158, 142-148. <https://doi.org/10.1016/j.phytochem.2018.11.007>
- Borthwick, A. D. (2012). 2,5-Diketopiperazines: Synthesis, Reactions, Medicinal Chemistry, and Bioactive Natural Products. *Chemical Reviews*, 112(7), 3641-3716.
<https://doi.org/10.1021/cr200398y>
- Bray, B. L., Mathies, P. H., Naef, R., Solas, D. R., Tidwell, T. T., Artis, D. R., & Muchowski, J. M. (1990). N-(Trisopropylsilyl)pyrrole. A progenitor "par excellence" of 3-substituted pyrroles. *The Journal of Organic Chemistry*, 55(26), 6317-6328.
<https://doi.org/10.1021/jo00313a019>
- Brindisi, M., Cavella, C., Brogi, S., Nebbioso, A., Senger, J., Maramai, S., Ciotta, A., Iside, C., Butini, S., Lamponi, S., Novellino, E., Altucci, L., Jung, M., Campiani, G., & Gemma, S. (2016). Phenylpyrrole-based HDAC inhibitors: synthesis, molecular modeling and biological studies. *Future Medicinal Chemistry*, 8(13), 1573-1587.
<https://doi.org/10.4155/fmc-2016-0068>
- Chen, X., Si, L., Liu, D., Proksch, P., Zhang, L., Zhou, D., & Lin, W. (2015). Neoechinulin B and its analogues as potential entry inhibitors of influenza viruses, targeting viral

- hemagglutinin. *Eur J Med Chem*, 93, 182-195.
<https://doi.org/10.1016/j.ejmech.2015.02.006>
- David, B., Sévenet, T., Thoison, O., Awang, K., Pais, M., Wright, M., & Guénard, D. (1997). Hemisynthesis of rhazinilam analogues: structure - activity relationships on tubulin-microtubule system. *Bioorganic & Medicinal Chemistry Letters*, 7(17), 2155-2158.
[https://doi.org/https://doi.org/10.1016/S0960-894X\(97\)00391-0](https://doi.org/https://doi.org/10.1016/S0960-894X(97)00391-0)
- de Groot, J. A., Gorter-La Roy, G. M., van Koeveringe, J. A., & Lugtenburg, J. (1981). MILD PREPARATION OF PYRROLE-2-CARBOXALDEHYDES. *Organic Preparations and Procedures International*, 13(2), 97-101.
<https://doi.org/10.1080/00304948109356102>
- Dudhe, P., Venkatasubbaiah, K., Pathak, B., & Chelvam, V. (2020). Serendipitous base catalysed condensation-heteroannulation of iminoesters: a regioselective route to the synthesis of 4,6-disubstituted 5-azaindoles [10.1039/C9OB02657F]. *Organic & Biomolecular Chemistry*, 18(8), 1582-1587. <https://doi.org/10.1039/C9OB02657F>
- Fairhurst, M. E., Zeeshan, M., Haug, B. E., & Bayer, A. (2018). Aldol Condensations on a 3-Alkylidene-2,5-diketopiperazine: Synthesis of Two Marine Natural Products. *Synlett*, 29(10), 1303-1306.
- Fu, Z., Hou, Y., Ji, C., Ma, M., Tian, Z., Deng, M., Zhong, L., Chu, Y., & Li, W. (2018). Design, synthesis and biological evaluation of anti-pancreatic cancer activity of plinabulin derivatives based on the co-crystal structure. *Bioorg Med Chem*, 26(8), 2061-2072. <https://doi.org/10.1016/j.bmc.2018.03.005>
- Gomez-Monterrey, I., Campiglia, P., Carotenuto, A., Stiuso, P., Bertamino, A., Sala, M., Aquino, C., Grieco, P., Morello, S., Pinto, A., Ianelli, P., & Novellino, E. (2008). Spiro[(dihydropyrazin-2,5-dione)-6,3'-(2',3'-dihydrothieno[2,3-b]naphtho-4',9'-dione)]-based cytotoxic agents: structure-activity relationship studies on the substituent at N4-position of the diketopiperazine domain. *Journal of medicinal chemistry*, 51(10), 2924-2932. <https://doi.org/10.1021/jm7013056>
- Hu, D. X., Withall, D. M., Challis, G. L., & Thomson, R. J. (2016). Structure, Chemical Synthesis, and Biosynthesis of Prodiginine Natural Products. *Chem Rev*, 116(14),

7818-7853. <https://doi.org/10.1021/acs.chemrev.6b00024>

Jassem, A. M., Dhumad, A. M., & Almashal, F. A. K. (2020). Synthesis of New Drug-Like Piperazine-2,5-diones by the Ugi/Tandem Process Catalyzed by TMSOTf and Their Molecular Docking. *Russian Journal of General Chemistry*, 90(11), 2181-2188. <https://doi.org/10.1134/s1070363220110262>

Kassab, A. E., Gedawy, E. M., Hamed, M. I. A., Doghish, A. S., & Hassan, R. A. (2021). Design, synthesis, anticancer evaluation, and molecular modelling studies of novel tolmetin derivatives as potential VEGFR-2 inhibitors and apoptosis inducers. *J Enzyme Inhib Med Chem*, 36(1), 922-939. <https://doi.org/10.1080/14756366.2021.1901089>

Katritzky, A. R., Fan, W.-Q., Szajda, M., Li, Q.-L., & Caster, K. C. (1988). Conjugated systems derived from piperazine-2,5-dione [<https://doi.org/10.1002/jhet.5570250243>]. *Journal of Heterocyclic Chemistry*, 25(2), 591-597. <https://doi.org/https://doi.org/10.1002/jhet.5570250243>

Kimura, T., Tajima, A., Inahashi, Y., Iwatsuki, M., Kasai, H., Mokudai, T., Niwano, Y., Shiomi, K., Takahashi, Y., Omura, S., & Nakashima, T. (2018). Mumiamicin: Structure and bioactivity of a new furan fatty acid from *Mumia* sp. YSP-2-79. *J Gen Appl Microbiol*, 64(2), 62-67. <https://doi.org/10.2323/jgam.2017.06.004>

Labriere, C., Kondori, N., Caous, J. S., Boomgaren, M., Sandholm, K., Ekdahl, K. N., Hansen, J. H., & Svenson, J. (2018). Development and evaluation of cationic amphiphilic antimicrobial 2,5-diketopiperazines. *J Pept Sci*, 24(7), e3090. <https://doi.org/10.1002/psc.3090>

Lautru, S., Gondry, M., Genet, R., & Pernodet, J.-L. (2002). The Albonoursin Gene Cluster of *S. noursei*: Biosynthesis of Diketopiperazine Metabolites Independent of Nonribosomal Peptide Synthetases. *Chemistry & Biology*, 9(12), 1355-1364. [https://doi.org/https://doi.org/10.1016/S1074-5521\(02\)00285-5](https://doi.org/https://doi.org/10.1016/S1074-5521(02)00285-5)

Liao, S., Qin, C., Yao, P., Li, J., Zhou, X., Wang, J., Huang, Z., & Liu, Y. (2014). One-Pot Synthesis of Polysubstituted 3-Amino-2-oxo-2,7-dihydro-1H-azepines. *Synthesis*, 46(05), 621-628.

- Liao, S., Qin, X., Li, D., Tu, Z., Li, J., Zhou, X., Wang, J., Yang, B., Lin, X., Liu, J., Yang, X., & Liu, Y. (2014). Design and synthesis of novel soluble 2,5-diketopiperazine derivatives as potential anticancer agents. *European journal of medicinal chemistry*, 83, 236-244. <https://doi.org/10.1016/j.ejmech.2014.06.030>
- Liao, S. R., Qin, X. C., Wang, Z., Li, D., Xu, L., Li, J. S., Tu, Z. C., & Liu, Y. (2016). Design, synthesis and cytotoxic activities of novel 2,5-diketopiperazine derivatives. *Eur J Med Chem*, 121, 500-509. <https://doi.org/10.1016/j.ejmech.2016.06.002>
- Lohmann, J. S., von Nussbaum, M., Brandt, W., Mülbradt, J., Steglich, W., & Spiteller, P. (2018). Rosellin A and B, two red diketopiperazine alkaloids from the mushroom *Mycena rosella*. *Tetrahedron*, 74(38), 5113-5118. <https://doi.org/10.1016/j.tet.2018.06.049>
- Mai, A., Valente, S., Nebbioso, A., Simeoni, S., Ragno, R., Massa, S., Brosch, G., De Bellis, F., Manzo, F., & Altucci, L. (2009). New pyrrole-based histone deacetylase inhibitors: binding mode, enzyme- and cell-based investigations. *Int J Biochem Cell Biol*, 41(1), 235-247. <https://doi.org/10.1016/j.biocel.2008.09.002>
- Martínez, R., & Villarreal, C. (2010). Synthesis of Novel Furo-, Thieno-, and Pyrroloazepines. *Synthesis*, 2010(19), 3346-3352. <https://doi.org/10.1055/s-0030-1257910>
- Mollica, A., Costante, R., Fiorito, S., Genovese, S., Stefanucci, A., Mathieu, V., Kiss, R., & Epifano, F. (2014). Synthesis and anti-cancer activity of naturally occurring 2,5-diketopiperazines. *Fitoterapia*, 98, 91-97. <https://doi.org/10.1016/j.fitote.2014.07.010>
- Nijampatnam, B., Nadkarni, D. H., Wu, H., & Velu, S. E. (2014). Antibacterial and Antibiofilm Activities of Makaluvamine Analogs. *Microorganisms*, 2(3), 128-139. <https://doi.org/10.3390/microorganisms2030128>
- Nishiuchi, K., Ohashi, H., Nishioka, K., Yamasaki, M., Furuta, M., Mashiko, T., Tomoshige, S., Ohgane, K., Kamisuki, S., Watashi, K., & Kuramochi, K. (2022). Synthesis and Antiviral Activities of Neoechinulin B and Its Derivatives. *J Nat Prod*, 85(1), 284-291. <https://doi.org/10.1021/acs.jnatprod.1c01120>

- Nitecki, D. E., Halpern, B., & Westley, J. W. (1968). Simple route to sterically pure diketopiperazines. *The Journal of Organic Chemistry*, 33(2), 864-866.
<https://doi.org/10.1021/jo01266a091>
- Niu, S., Liu, D., Shao, Z., Proksch, P., & Lin, W. (2017). Eutypellazines A–M, thiodiketopiperazine-type alkaloids from deep sea derived fungus *Eutypella* sp. MCCC 3A00281 [10.1039/C7RA05774A]. *RSC Advances*, 7(53), 33580-33590.
<https://doi.org/10.1039/C7RA05774A>
- Reinecke, D. M. (1999). 4-Chloroindole-3-acetic acid and plant growth. *Plant Growth Regulation*, 27(1), 3-13. <https://doi.org/10.1023/A:1006191917753>
- Saavedra, C. J., Cuevas, F., Romero-Estudillo, I., & Boto, A. (2020). Synthesis of Diketopiperazine Scaffolds with Tailored N- and α -Chains by Selective Modification of Customizable Units [<https://doi.org/10.1002/adsc.202000470>]. *Advanced Synthesis & Catalysis*, 362(15), 3158-3169.
<https://doi.org/https://doi.org/10.1002/adsc.202000470>
- Serra Moreno, J., Agas, D., Sabbieti, M. G., Di Magno, M., Migliorini, A., & Loreto, M. A. (2012). Synthesis of novel pyrrolyl-indomethacin derivatives. *Eur J Med Chem*, 57, 391-397. <https://doi.org/10.1016/j.ejmech.2012.09.008>
- Shan, T., Jiang, W., Liu, X., Wang, C., Gao, S., Yan, P., Sun, B., & Miao, L. (2020). Alkaloids including two rare variecoloritides from the fungus *Aspergillus ruber*. *Tetrahedron*, 76(24). <https://doi.org/10.1016/j.tet.2020.131258>
- Shin, C.-g., Chigira, Y., Masaki, M., & Ohta, M. (1969). Synthesis of Albonoursin. *Bulletin of the Chemical Society of Japan*, 42(1), 191-193. <https://doi.org/10.1246/bcsj.42.191>
- Singh, A., Patel, V. K., & Rajak, H. (2021). Appraisal of pyrrole as connecting unit in hydroxamic acid based histone deacetylase inhibitors: Synthesis, anticancer evaluation and molecular docking studies. *Journal of Molecular Structure*, 1240. <https://doi.org/10.1016/j.molstruc.2021.130590>
- Taechowisan, T., Wanbanjob, A., Tuntiwachwuttikul, P., & Liu, J. (2009). Anti-inflammatory activity of lansais from endophytic *Streptomyces* sp. SUC1 in LPS-induced RAW 264.7 cells. *Food and Agricultural Immunology*, 20(1), 67-77.

<https://doi.org/10.1080/09540100902730064>

Taechowisan, T., Wanbanjob, A., Tuntiwachwuttikul, P., & Liu, J. (2010). Anti-inflammatory effects of lansai C and D cause inhibition of STAT-1 and NF- κ B activations in LPS-induced RAW 264.7 cells. *Food and Agricultural Immunology*, 21(1), 57-64.

<https://doi.org/10.1080/09540100903419592>

Taylor, E. J., & Djerassi, C. (1976). Mechanism of the sodium cyanoborohydride reduction of α,β -unsaturated tosylhydrazones. *Journal of the American Chemical Society*, 98(8), 2275-2281. <https://doi.org/10.1021/ja00424a046>

Tuntiwachwuttikul, P., Taechowisan, T., Wanbanjob, A., Thadaniti, S., & Taylor, W. C. (2008). Lansai A–D, secondary metabolites from *Streptomyces* sp. SUC1. *Tetrahedron*, 64(32), 7583-7586.

<https://doi.org/https://doi.org/10.1016/j.tet.2008.05.104>

Valente, S., Conte, M., Tardugno, M., Massa, S., Nebbioso, A., Altucci, L., & Mai, A. (2009). Pyrrole-based hydroxamates and 2-aminoanilides: histone deacetylase inhibition and cellular activities. *ChemMedChem*, 4(9), 1411-1415.

<https://doi.org/10.1002/cmdc.200900082>

Wang, H., & Reisman, S. E. (2014). Enantioselective Total Synthesis of (–)-Lansai B and (+)-Nocardioazines A and B [<https://doi.org/10.1002/anie.201402571>]. *Angewandte Chemie International Edition*, 53(24), 6206-6210.

<https://doi.org/https://doi.org/10.1002/anie.201402571>

Wang, P., Xi, L., Liu, P., Wang, Y., Wang, W., Huang, Y., & Zhu, W. (2013).

Diketopiperazine derivatives from the marine-derived actinomycete *Streptomyces* sp. FXJ7.328. *Marine drugs*, 11(4), 1035-1049.

<https://doi.org/10.3390/md11041035>

Wei, B., Chen, C., You, C., Lv, H., & Zhang, X. (2017). Efficient synthesis of (S,R)-Bn-Yanphos and Rh/(S,R)-Bn-Yanphos catalyzed asymmetric hydroformylation of vinyl heteroarenes [10.1039/C6QO00641H]. *Organic Chemistry Frontiers*, 4(2), 288-291.

<https://doi.org/10.1039/C6QO00641H>

Yu, L., Ding, W., Wang, Q., Ma, Z., Xu, X., Zhao, X., & Chen, Z. (2017). Induction of cryptic

bioactive 2,5-diketopiperazines in fungus *Penicillium* sp. DT-F29 by microbial co-culture. *Tetrahedron*, 73(7), 907-914. <https://doi.org/10.1016/j.tet.2016.12.077>

Zhao, H., Yang, A., Zhang, N., Li, S., Yuan, T., Ding, N., Zhang, S., Bao, S., Wang, C., Zhang, Y., Wang, X., & Hu, L. (2020). Insecticidal Endostemonines A-J Produced by Endophytic *Streptomyces* from *Stemona sessilifolia*. *J Agric Food Chem*, 68(6), 1588-1595. <https://doi.org/10.1021/acs.jafc.9b06755>

Zubia, A., Ropero, S., Otaegui, D., Ballestar, E., Fraga, M. F., Boix-Chornet, M., Berdasco, M., Martinez, A., Coll-Mulet, L., Gil, J., Cossio, F. P., & Esteller, M. (2009). Identification of (1H)-pyrroles as histone deacetylase inhibitors with antitumoral activity. *Oncogene*, 28(11), 1477-1484. <https://doi.org/10.1038/onc.2008.501>



APPENDIXES

APPENDIX A NMR spectrum

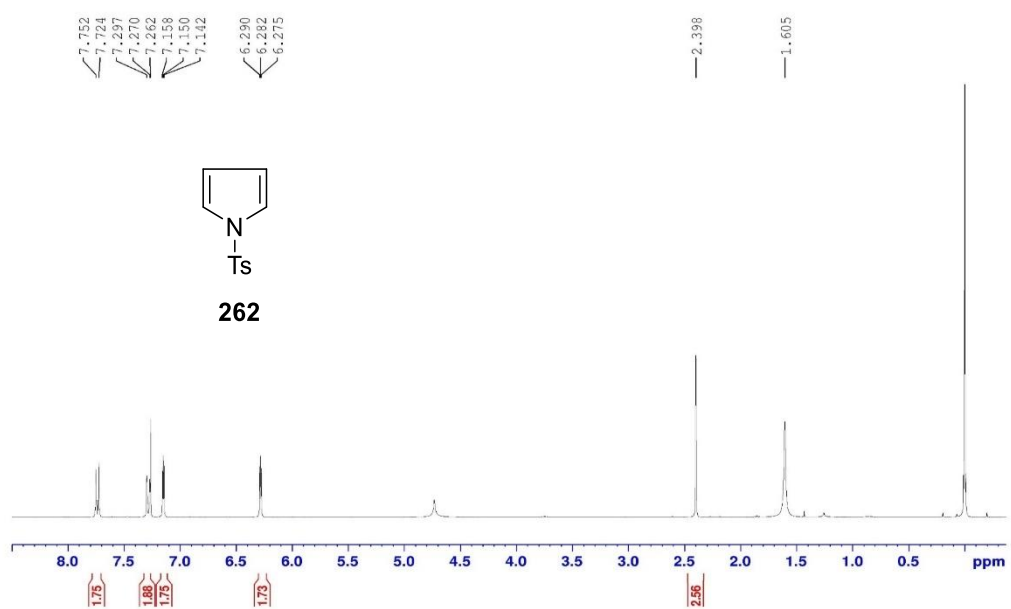
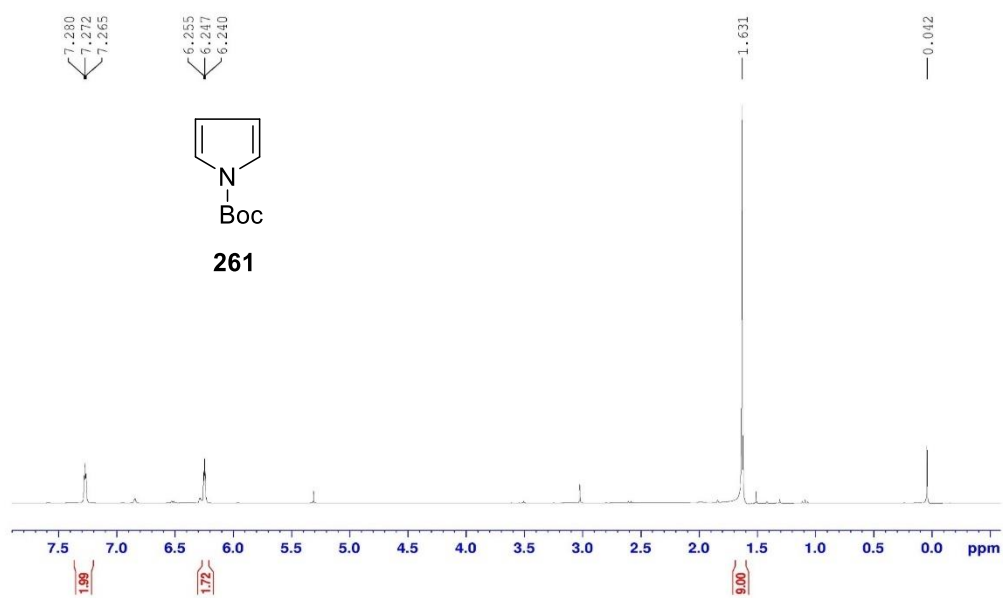
APPENDIX B MTT assay of cytotoxicity activities

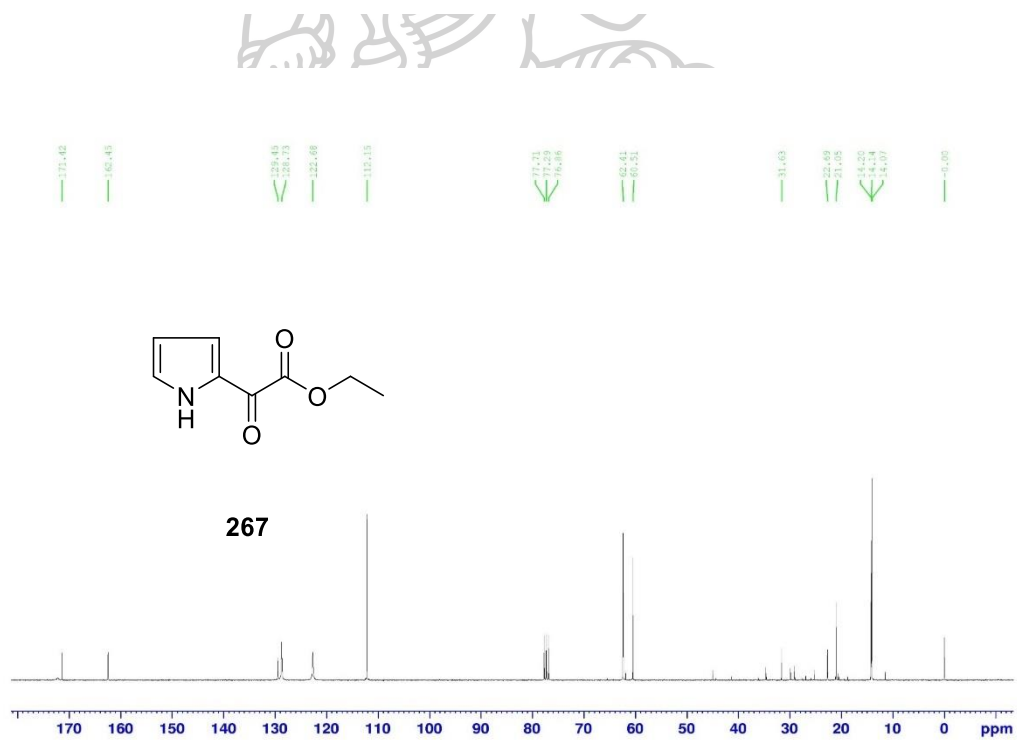
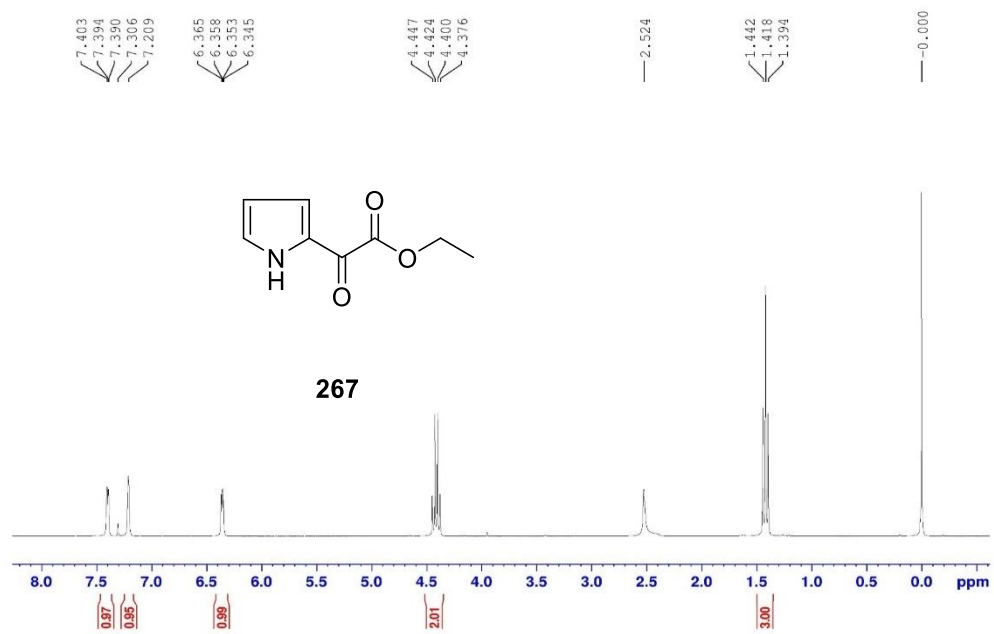
APPENDIX C Hemaagglutination assay

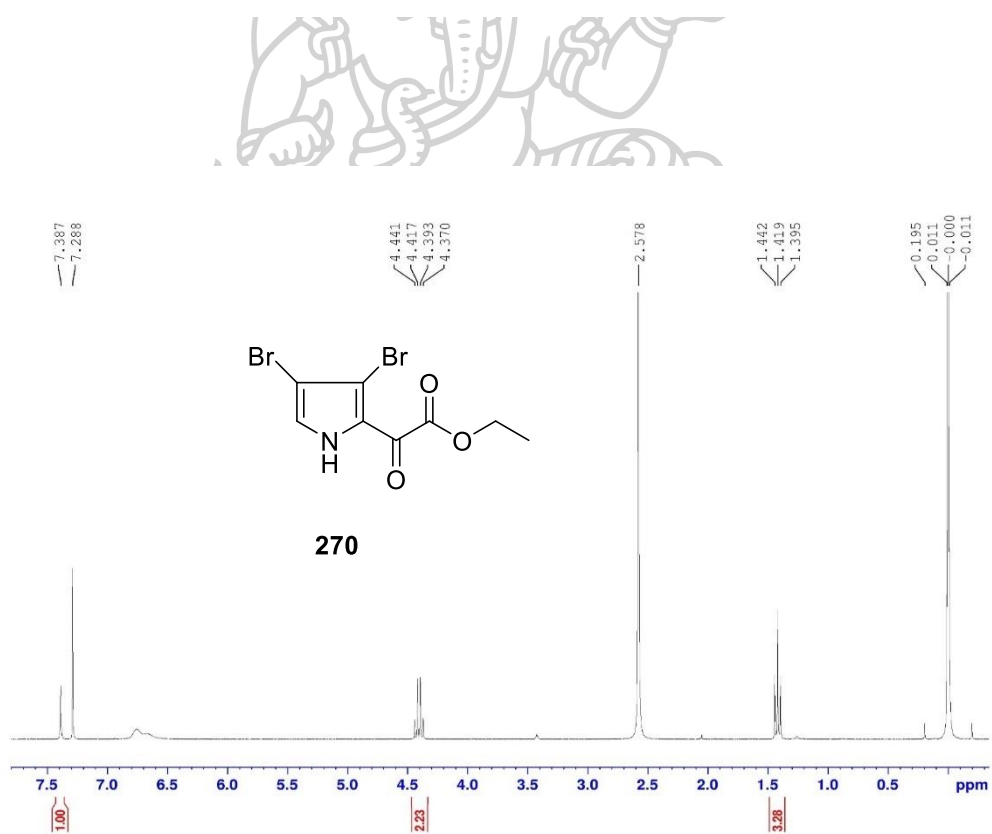
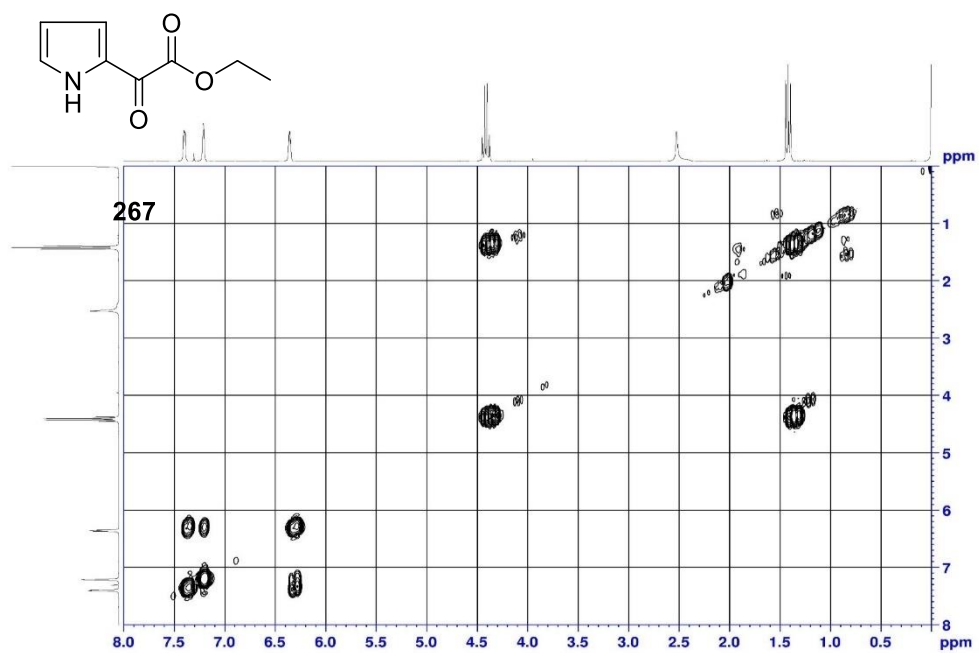


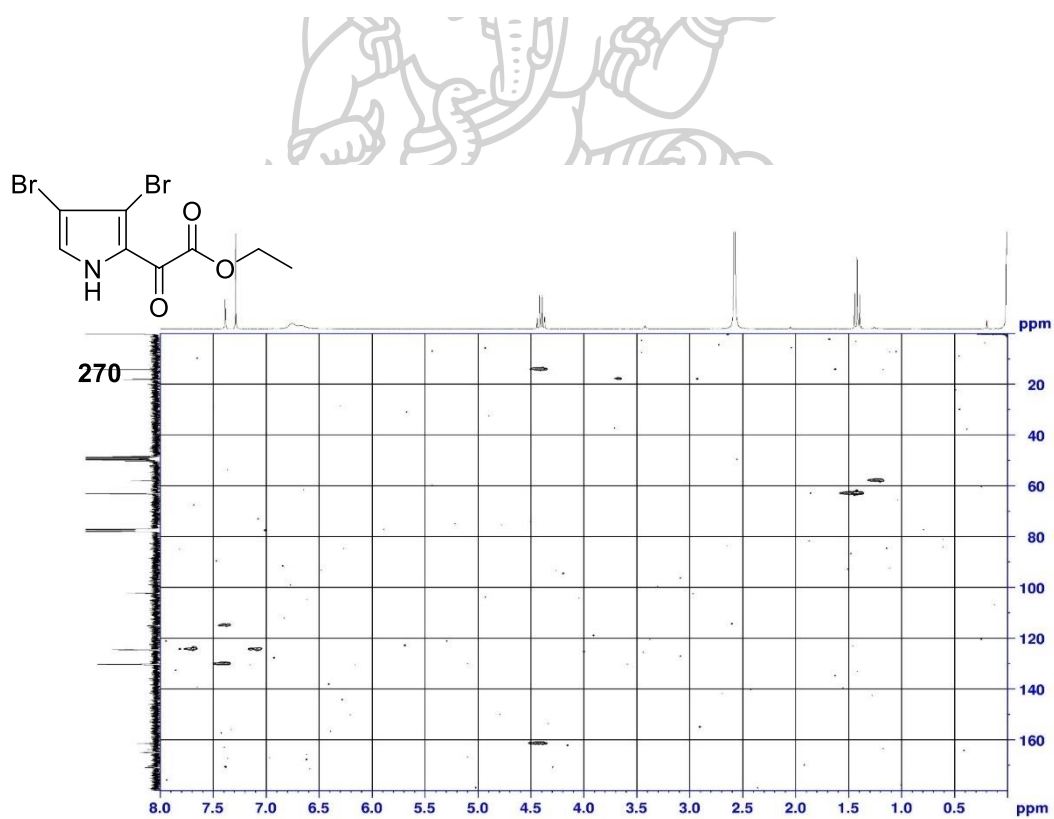
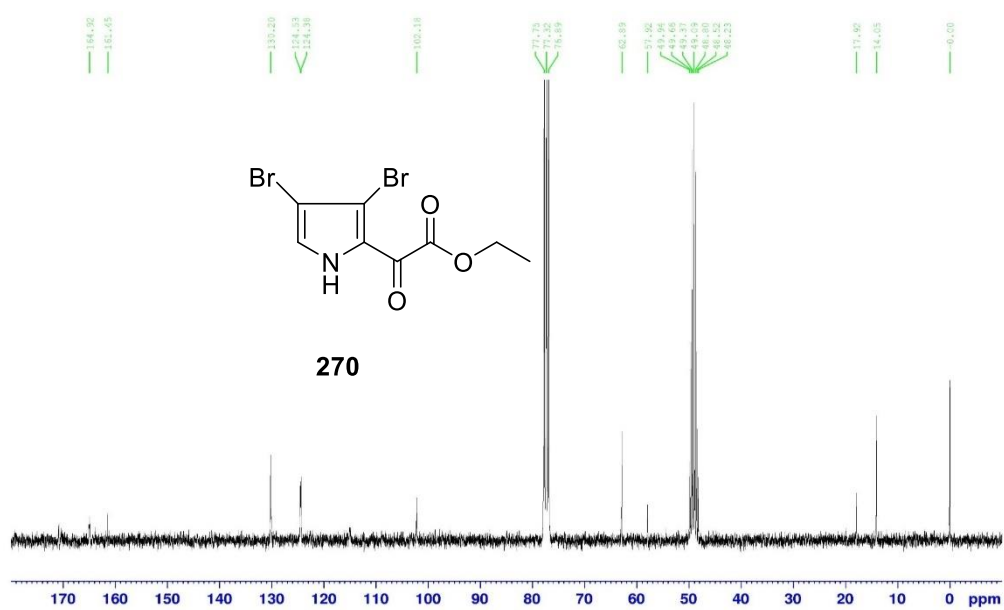


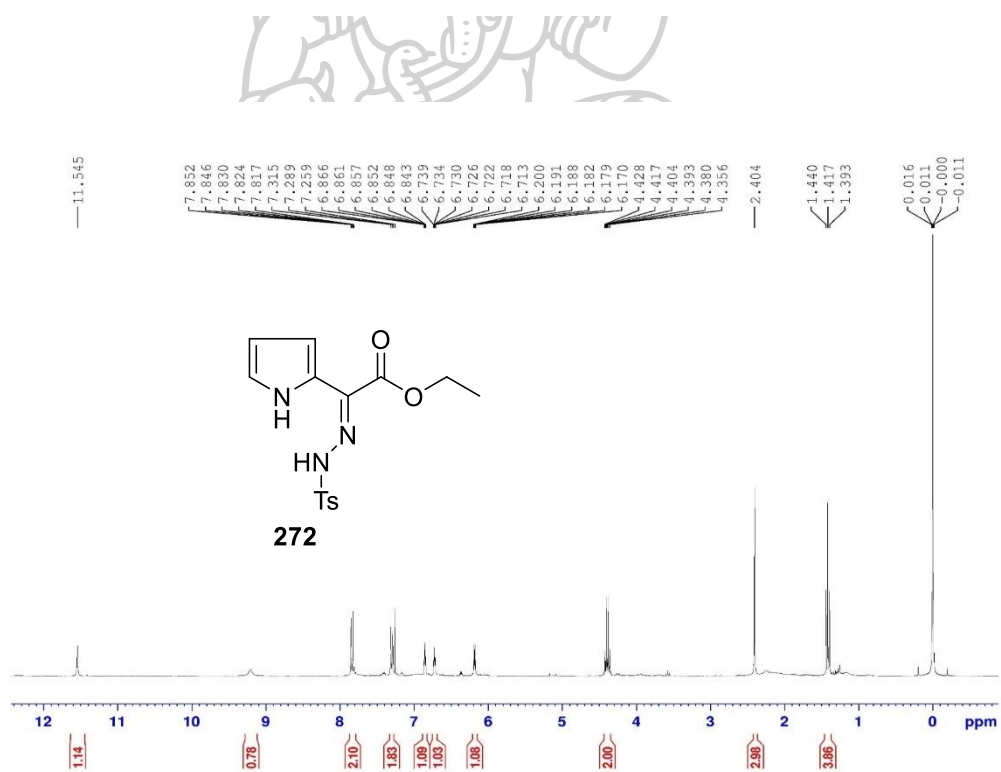
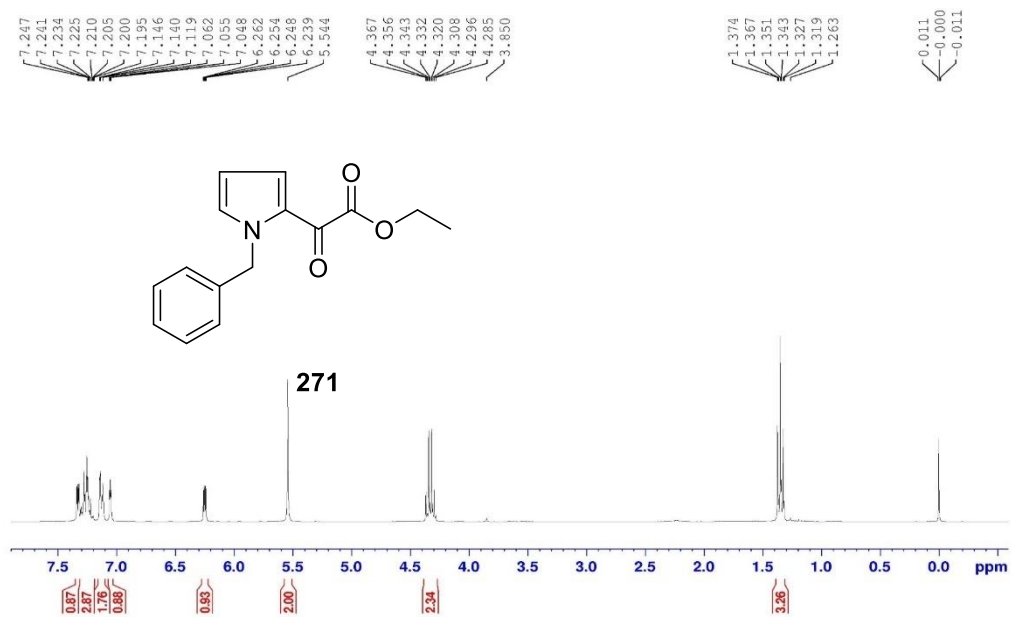
APPENDIX A
NMR spectrum

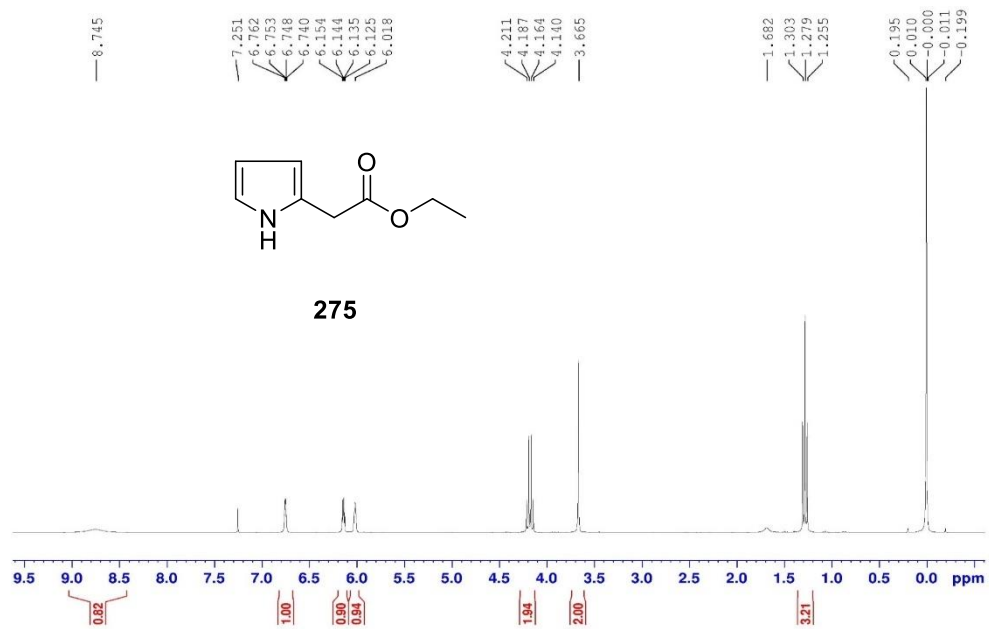
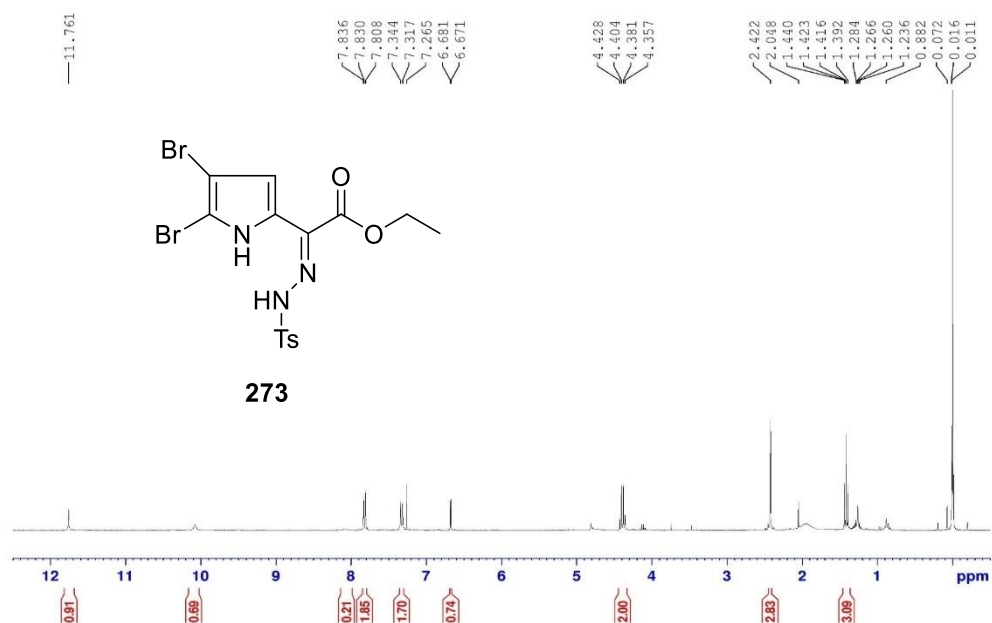


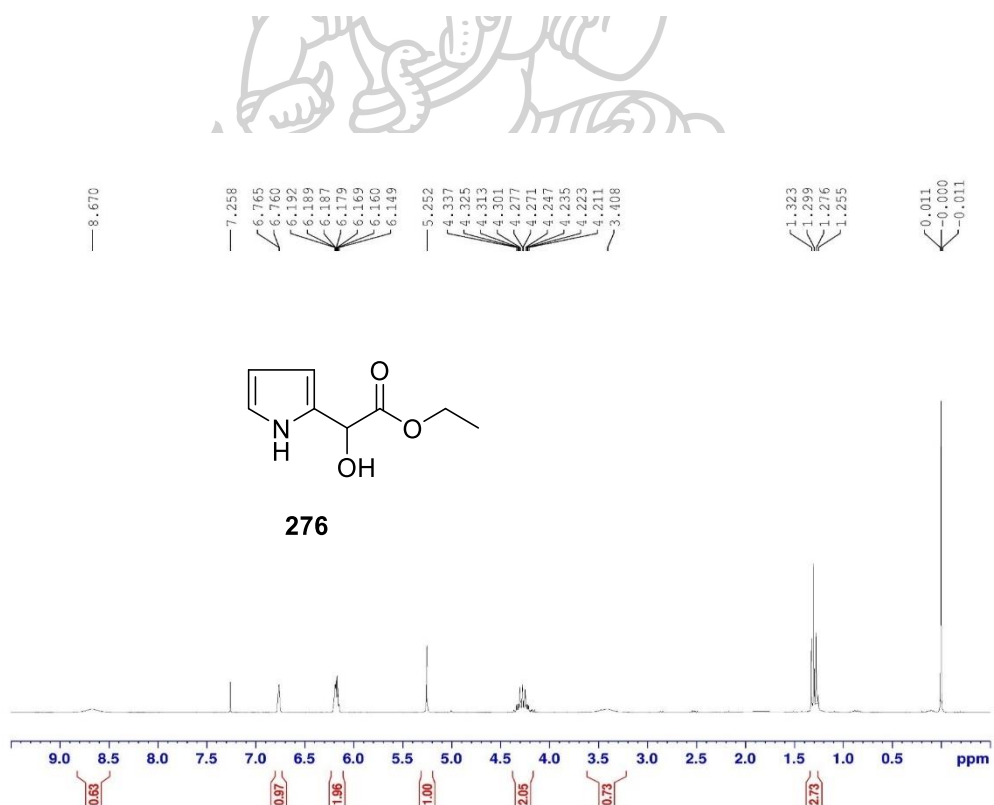
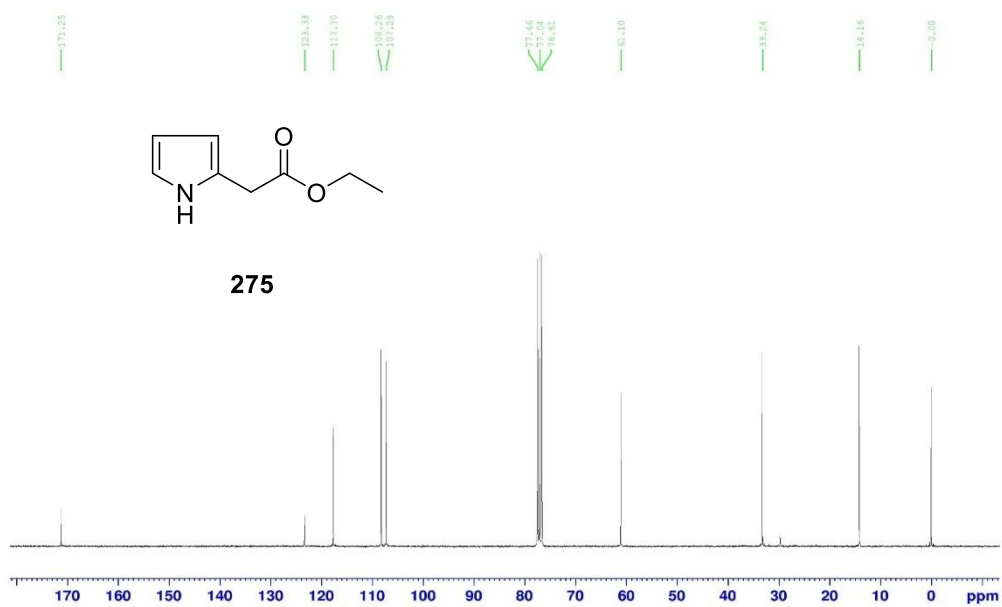


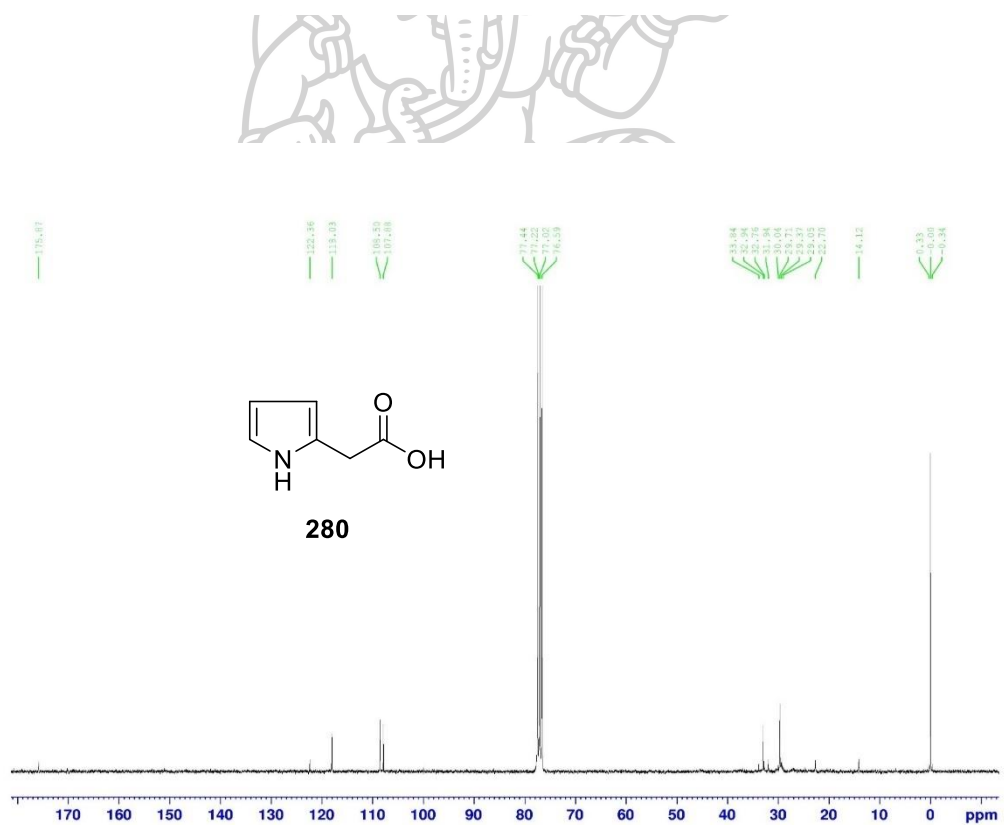
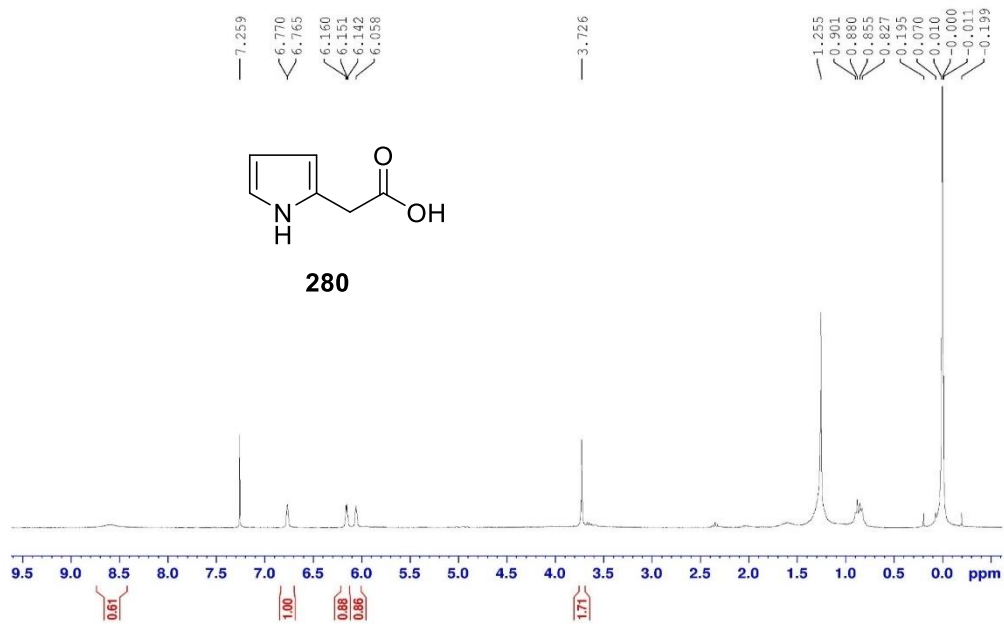


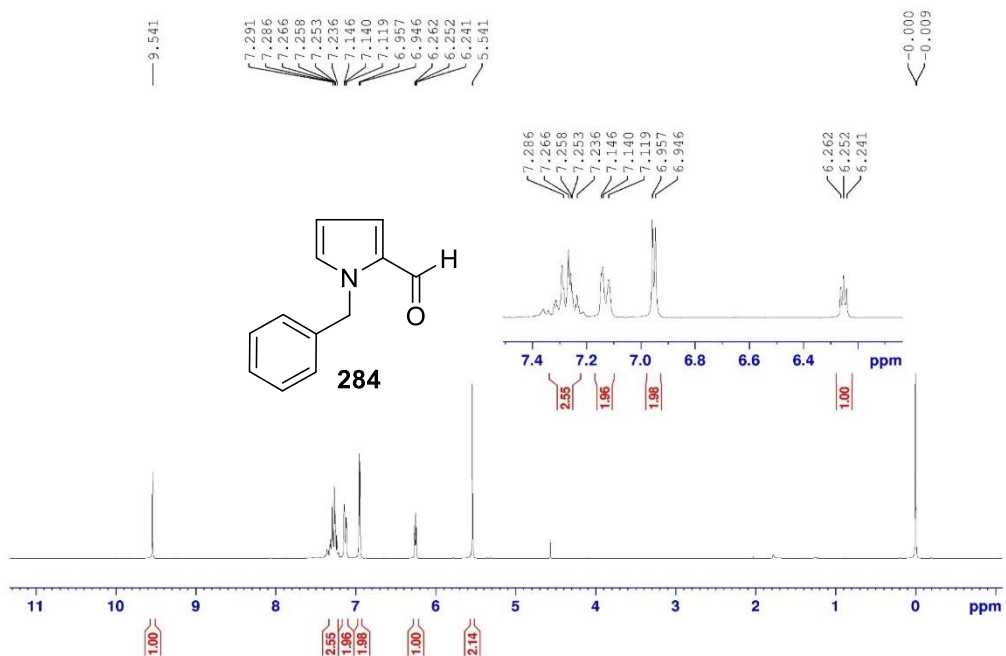
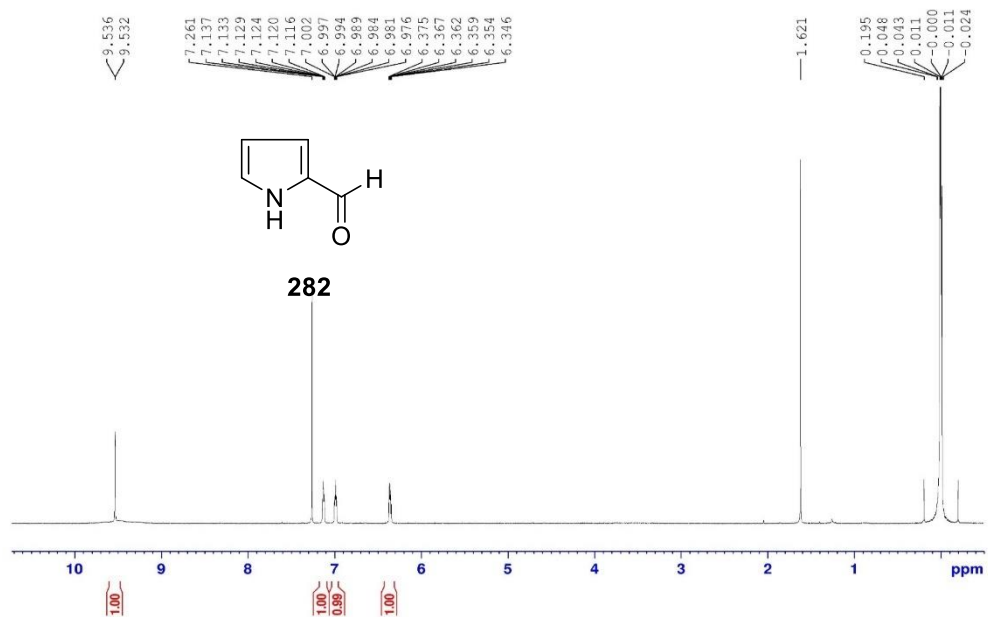


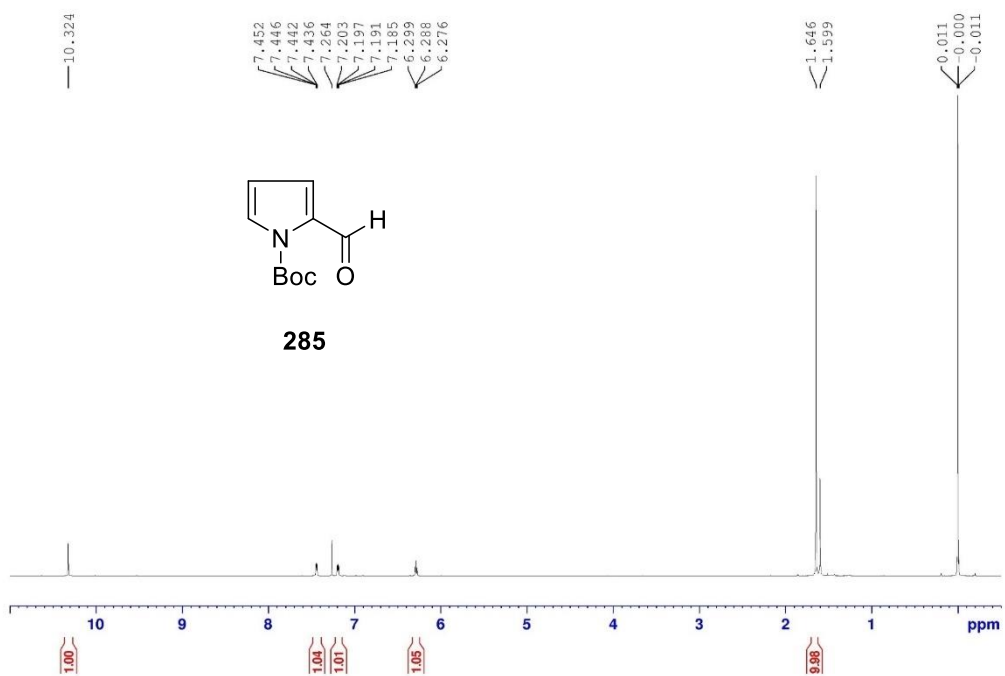
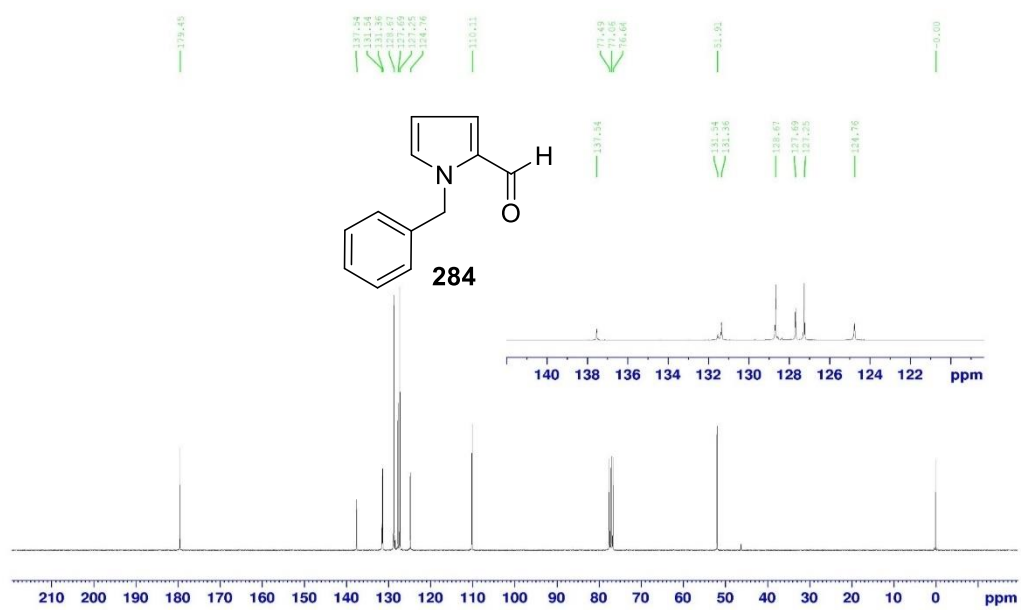


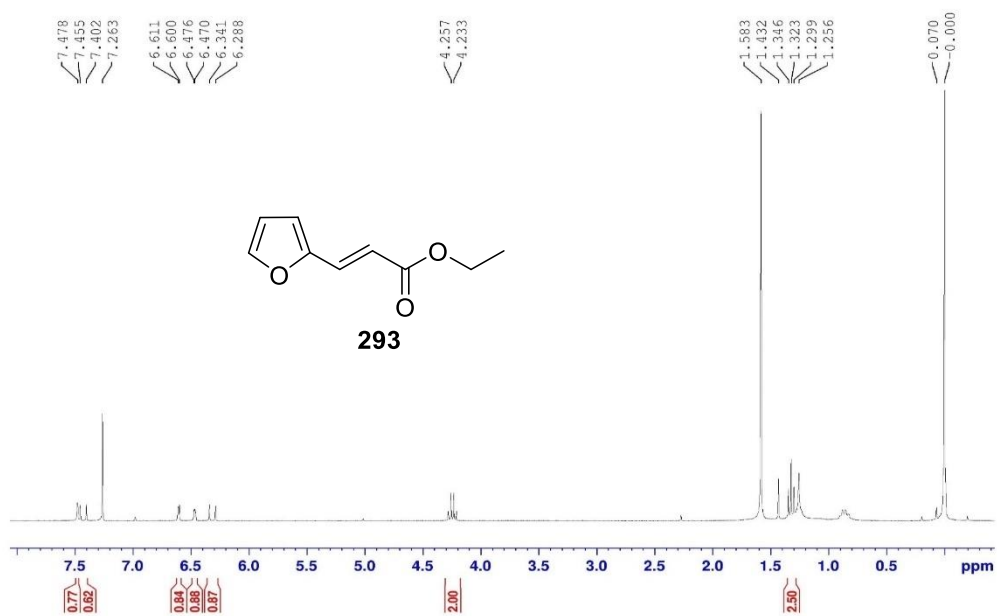
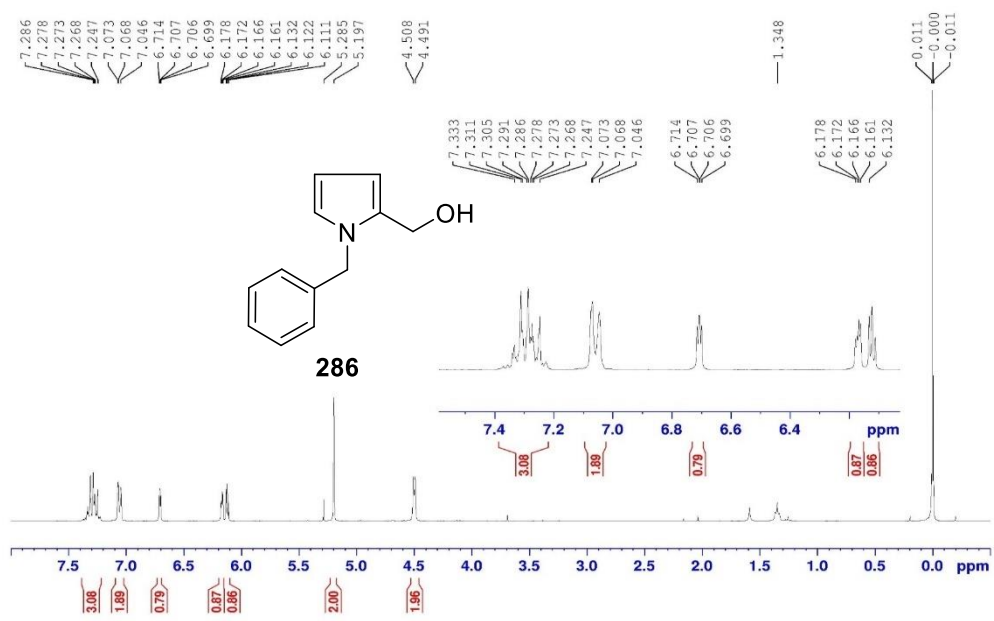


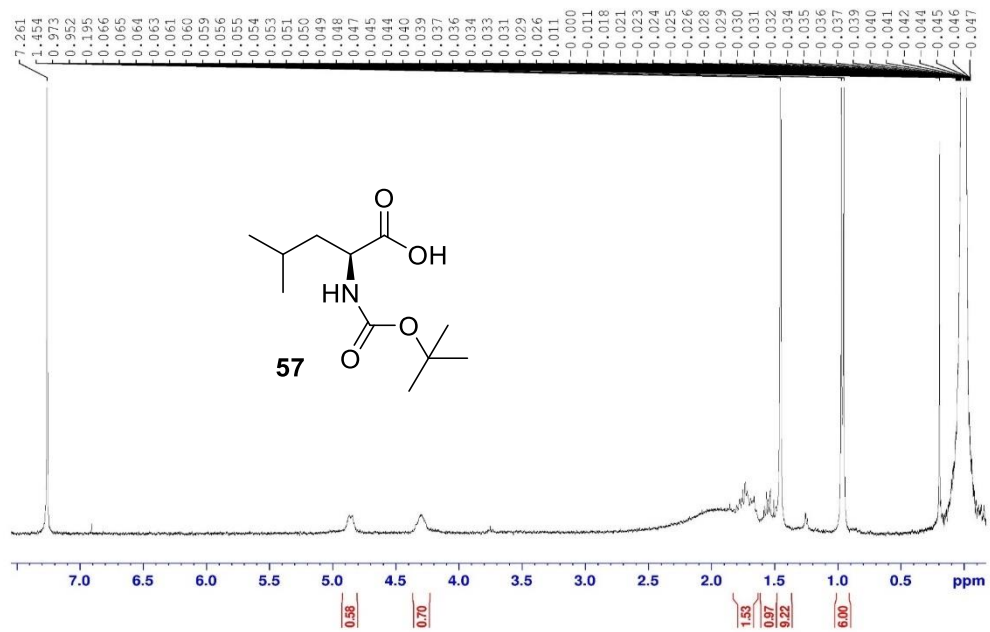
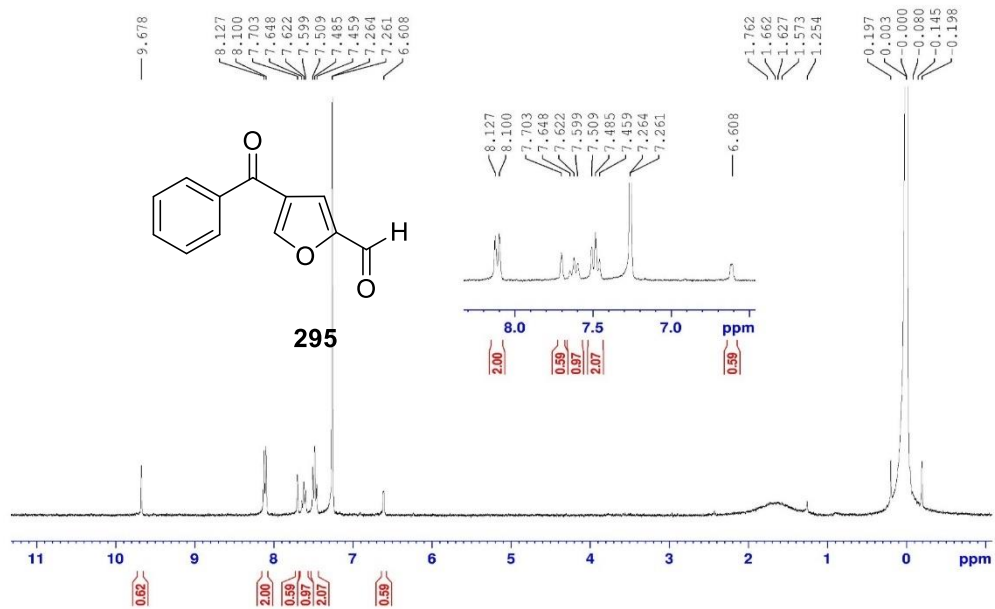


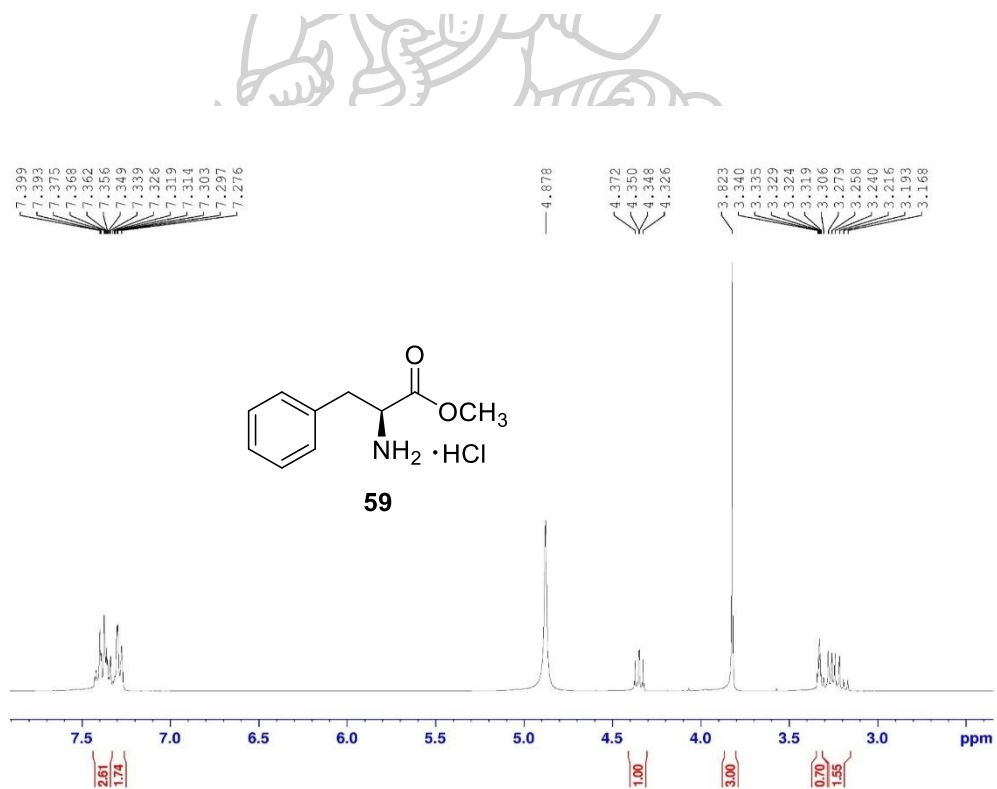
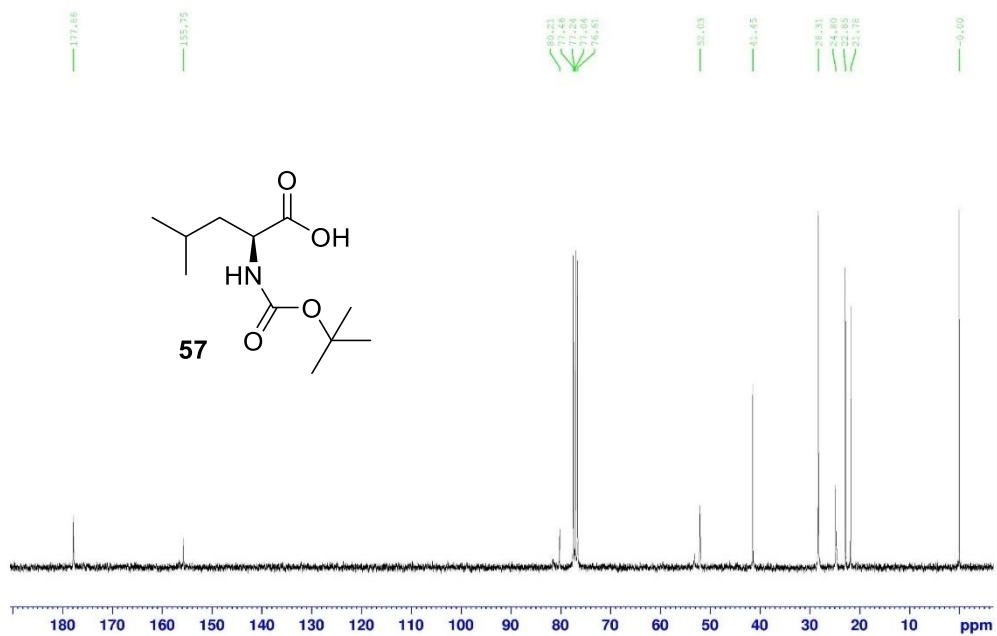


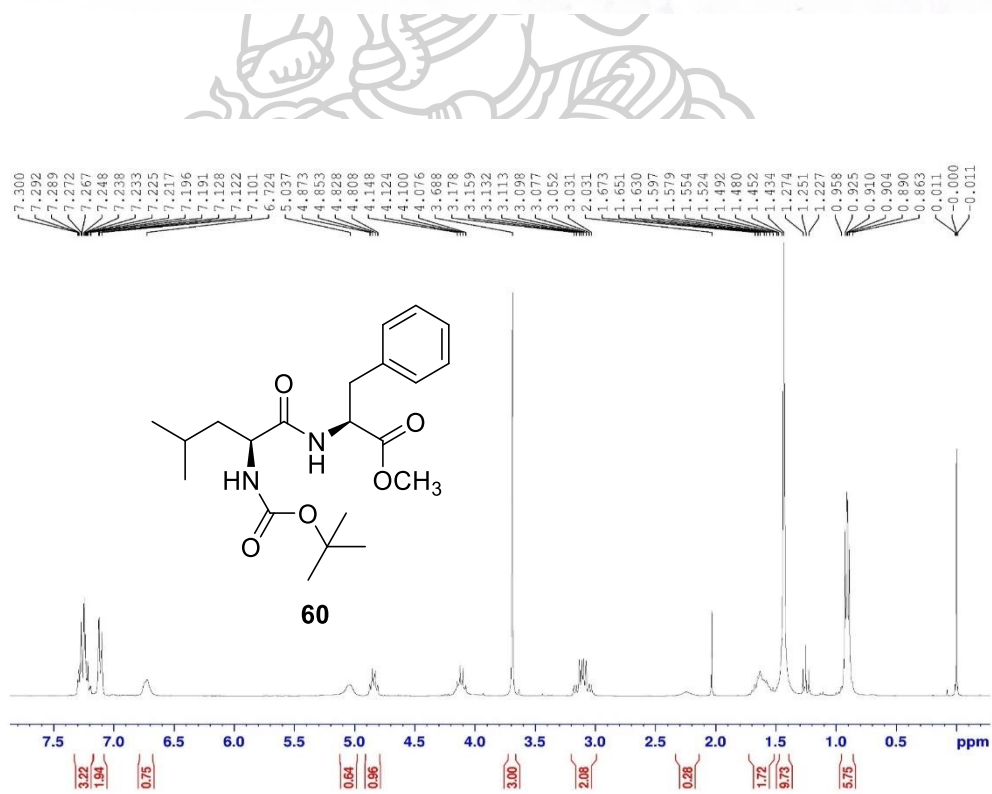
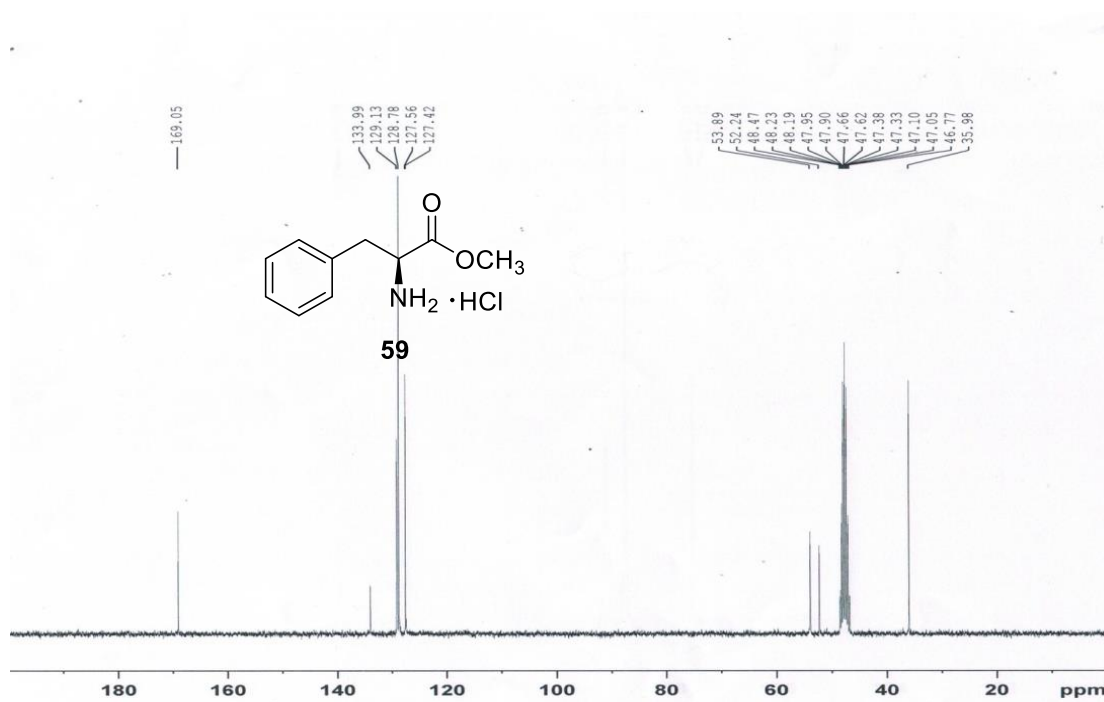


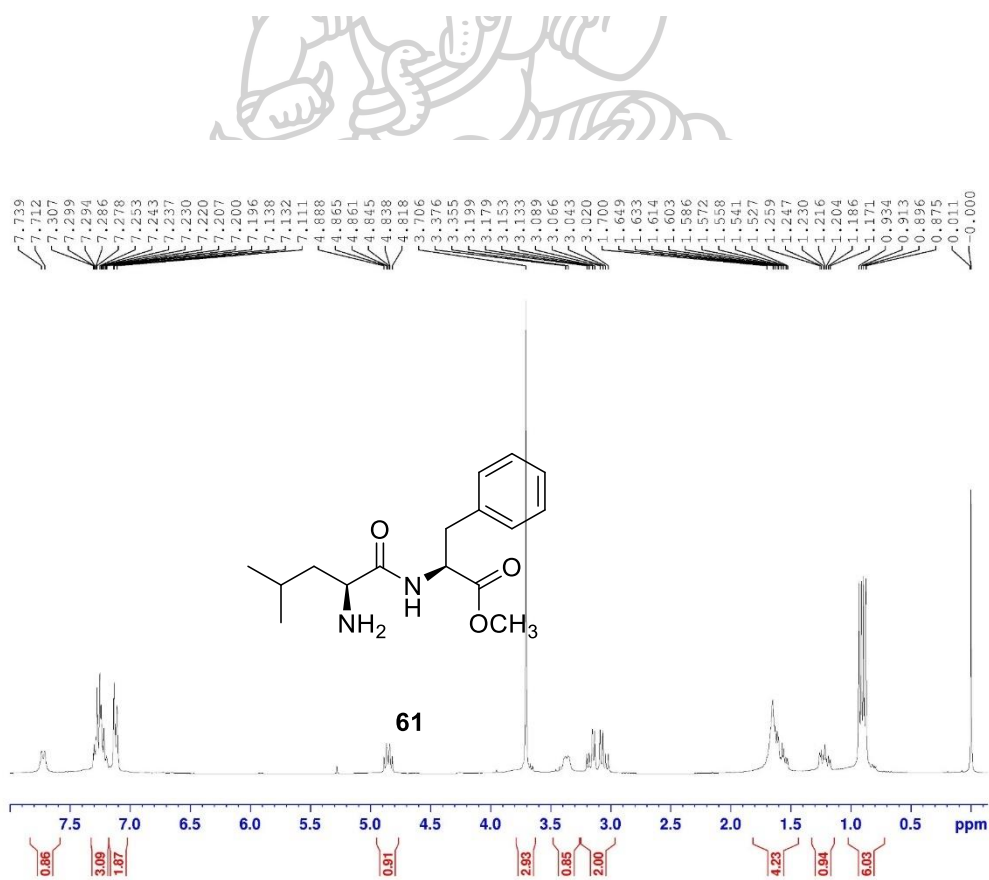
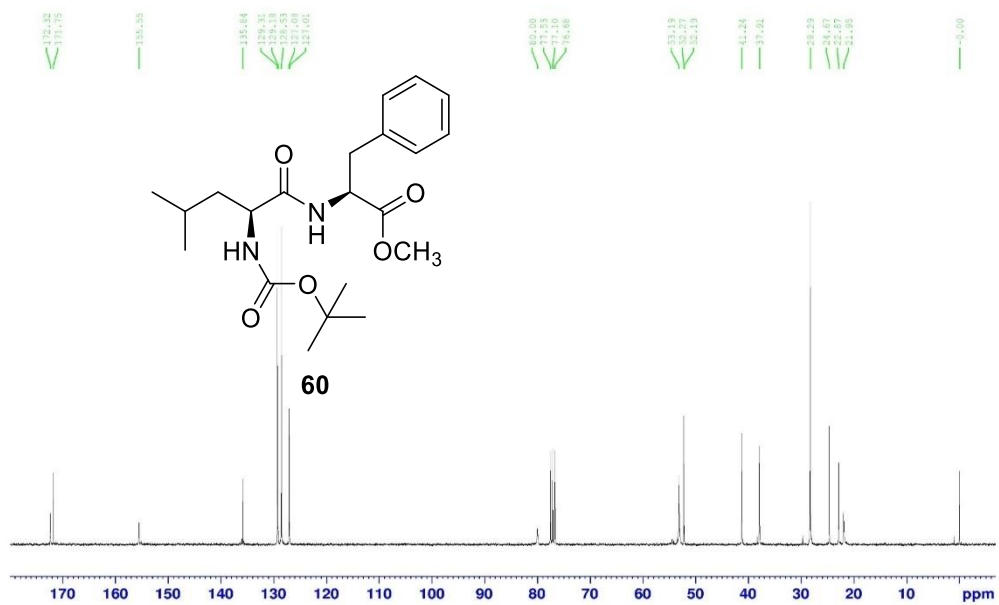


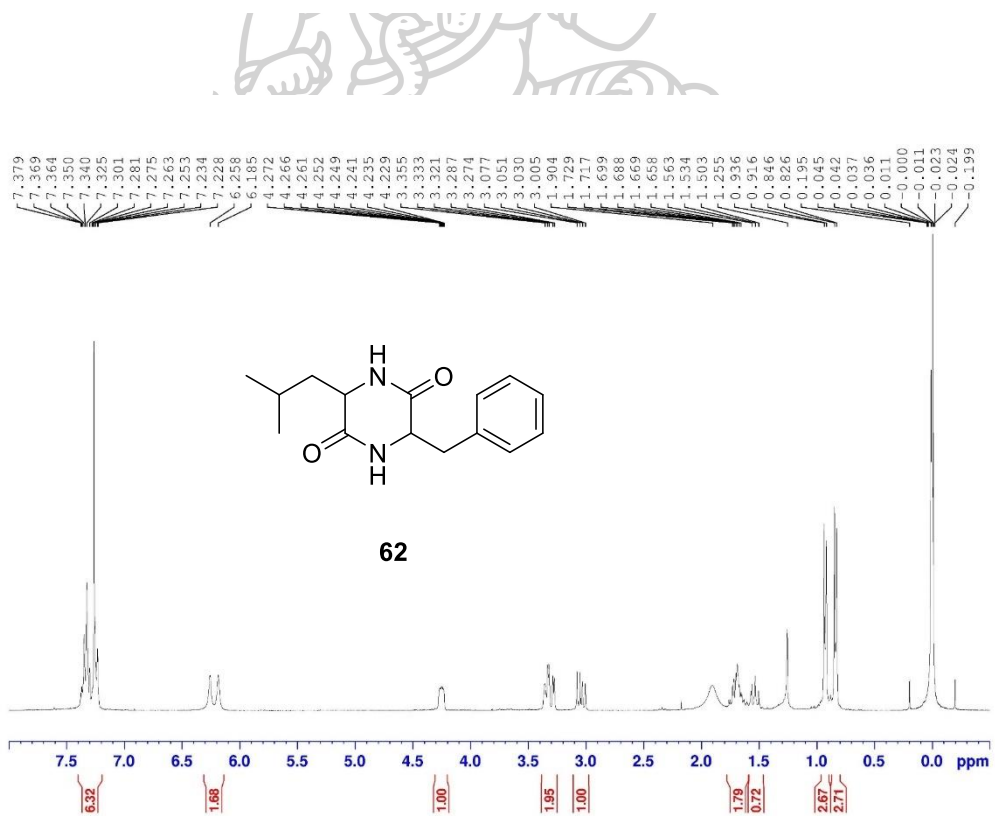
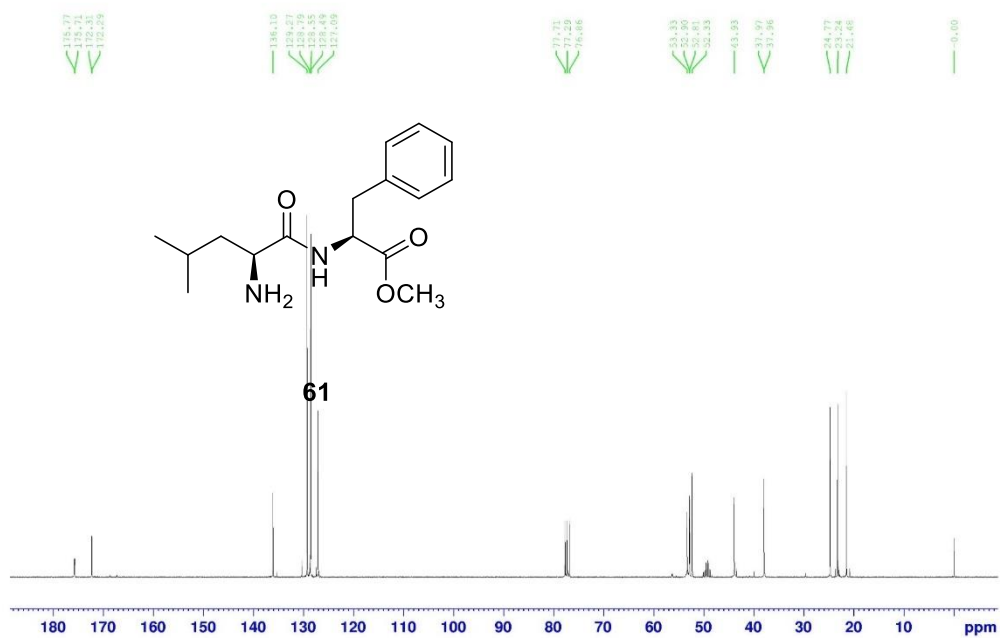


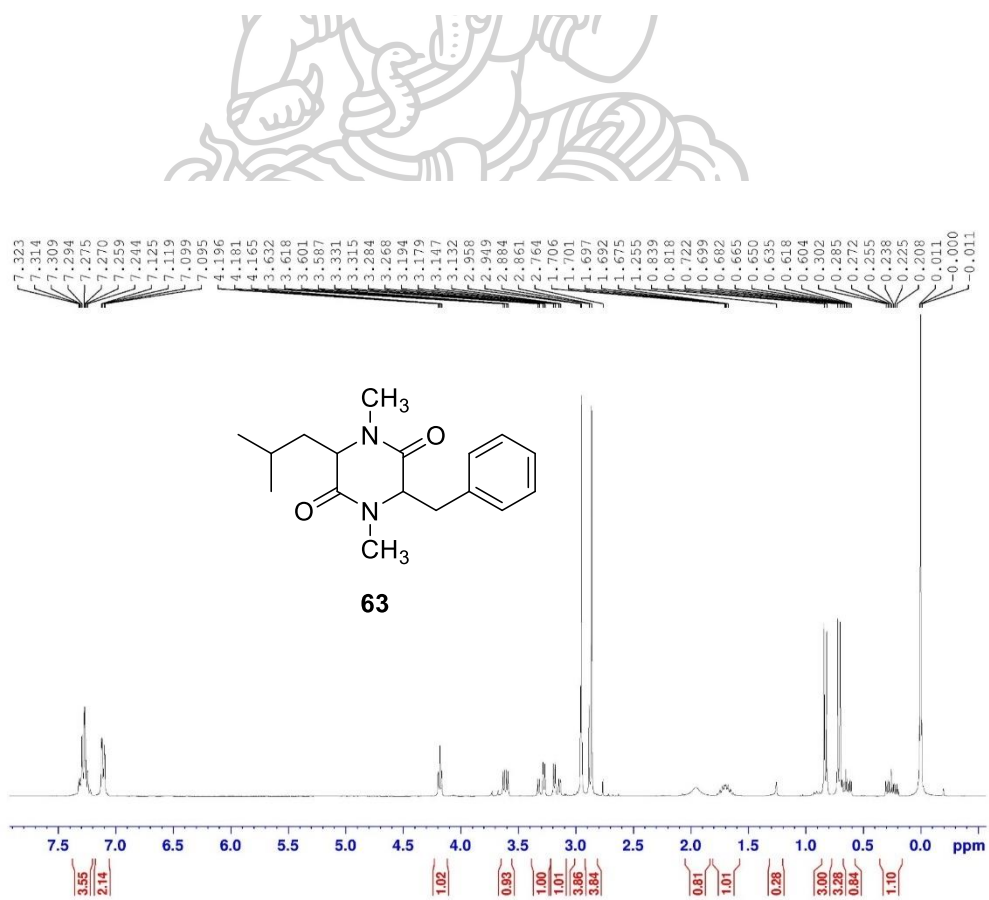
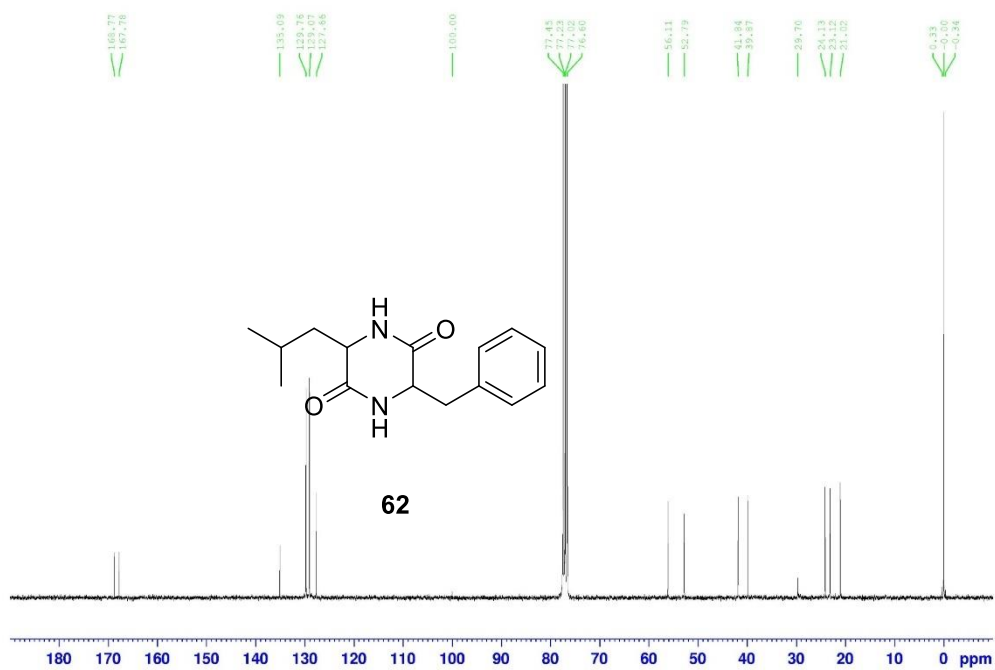


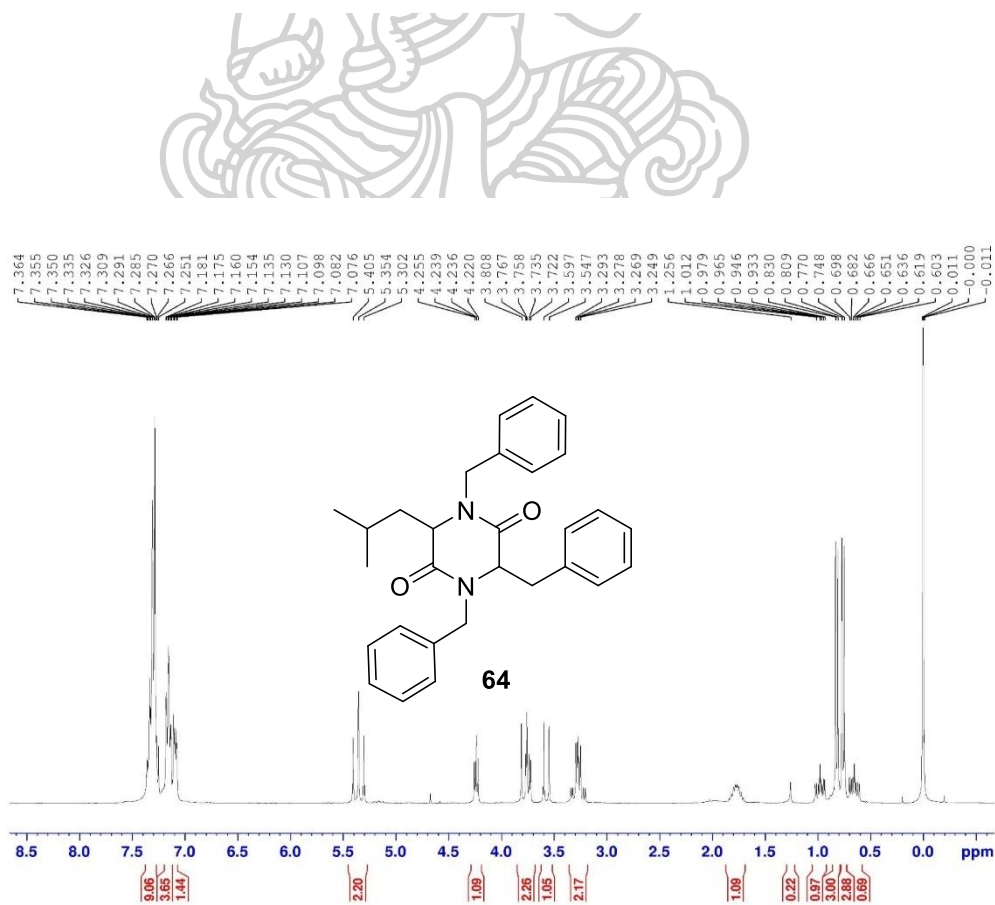
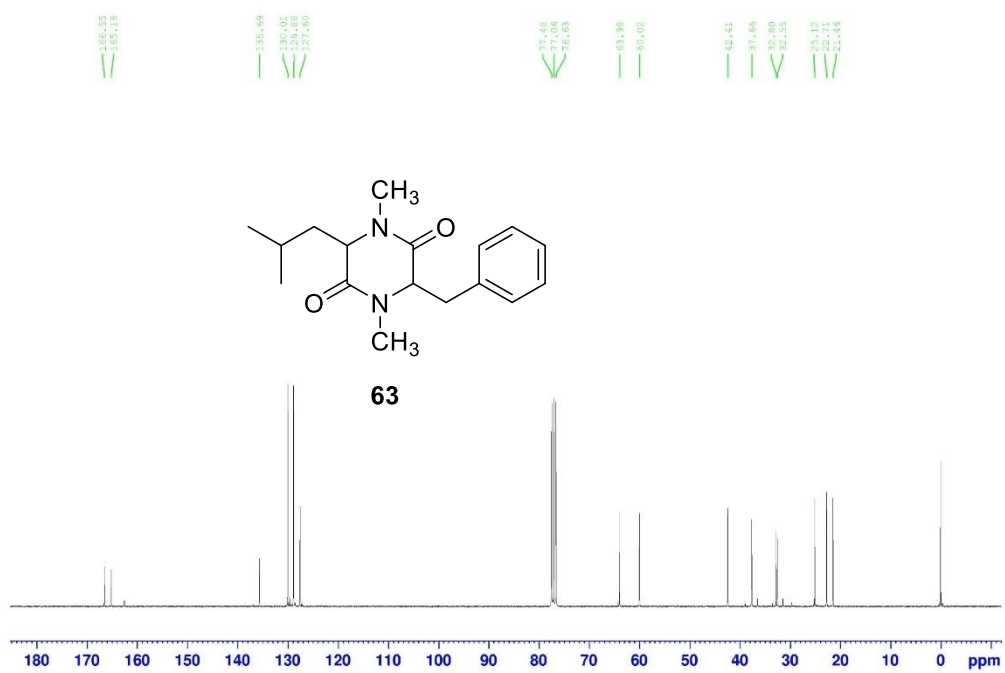


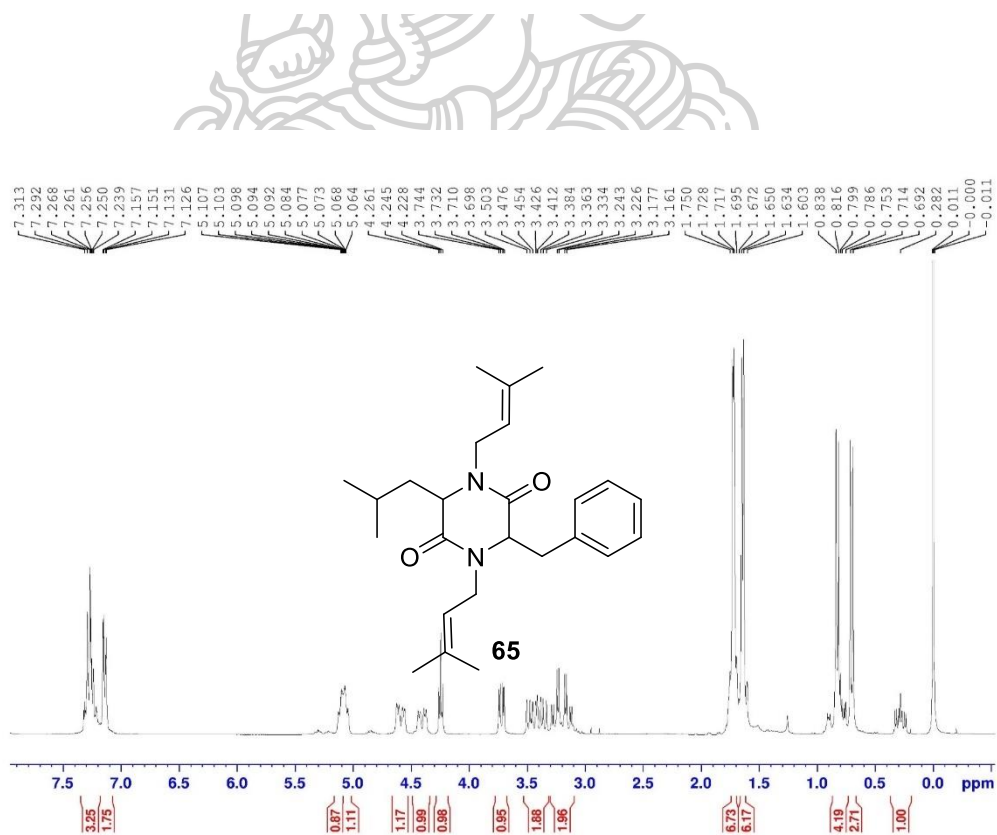
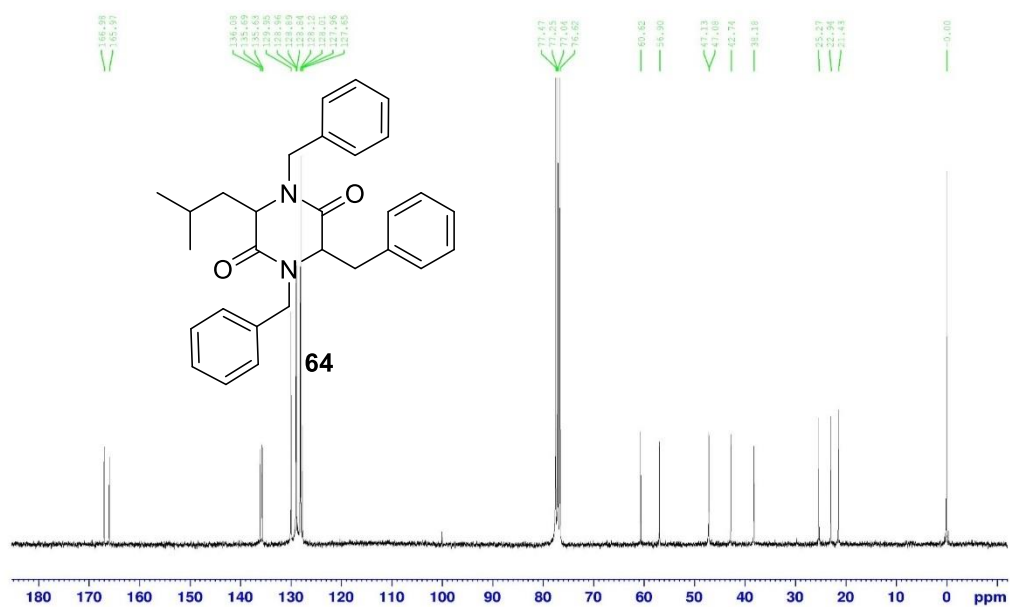


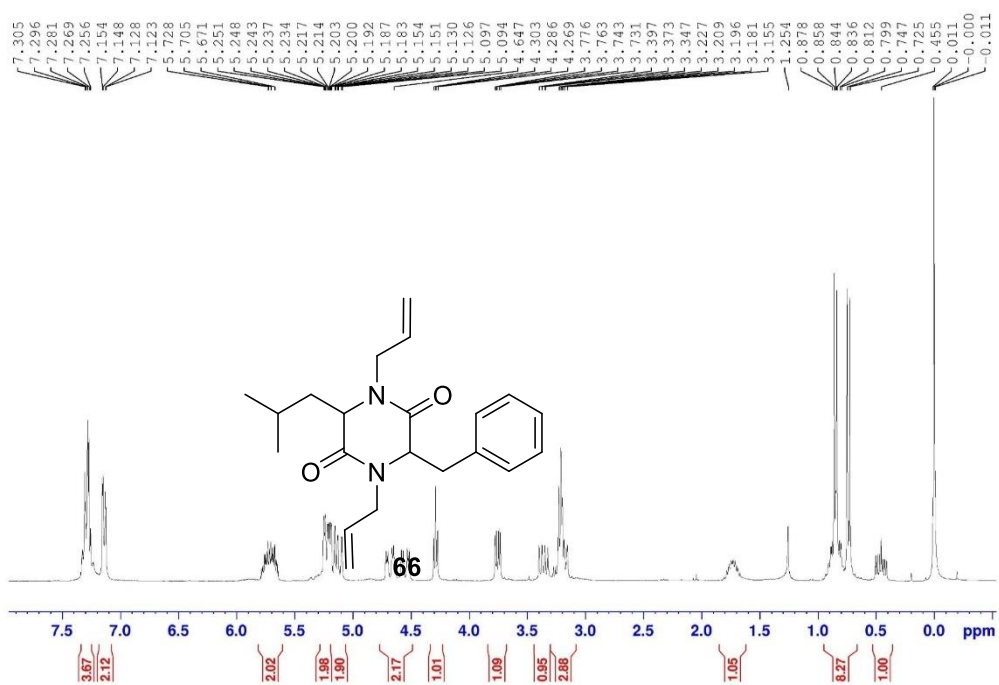
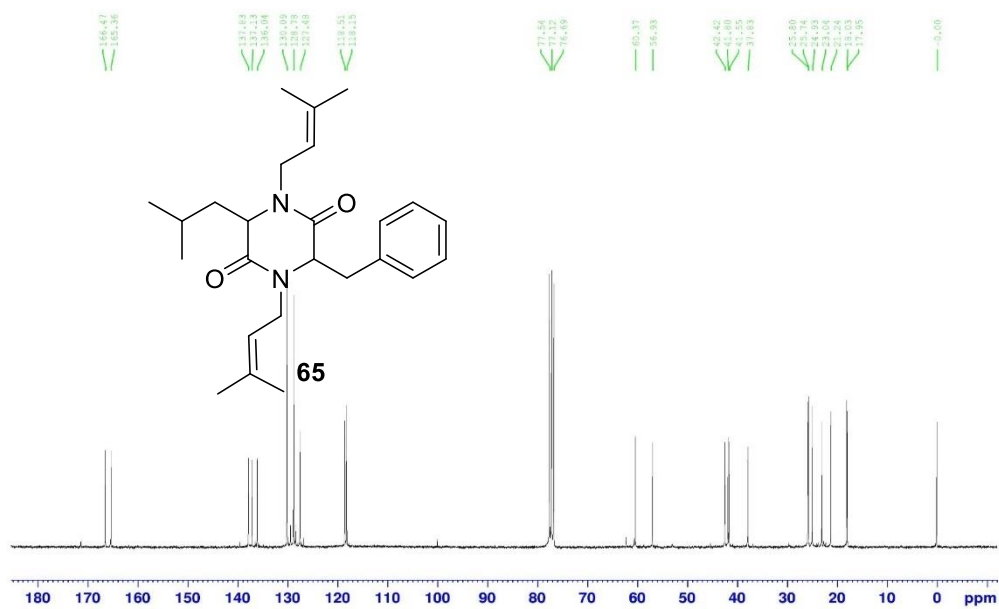


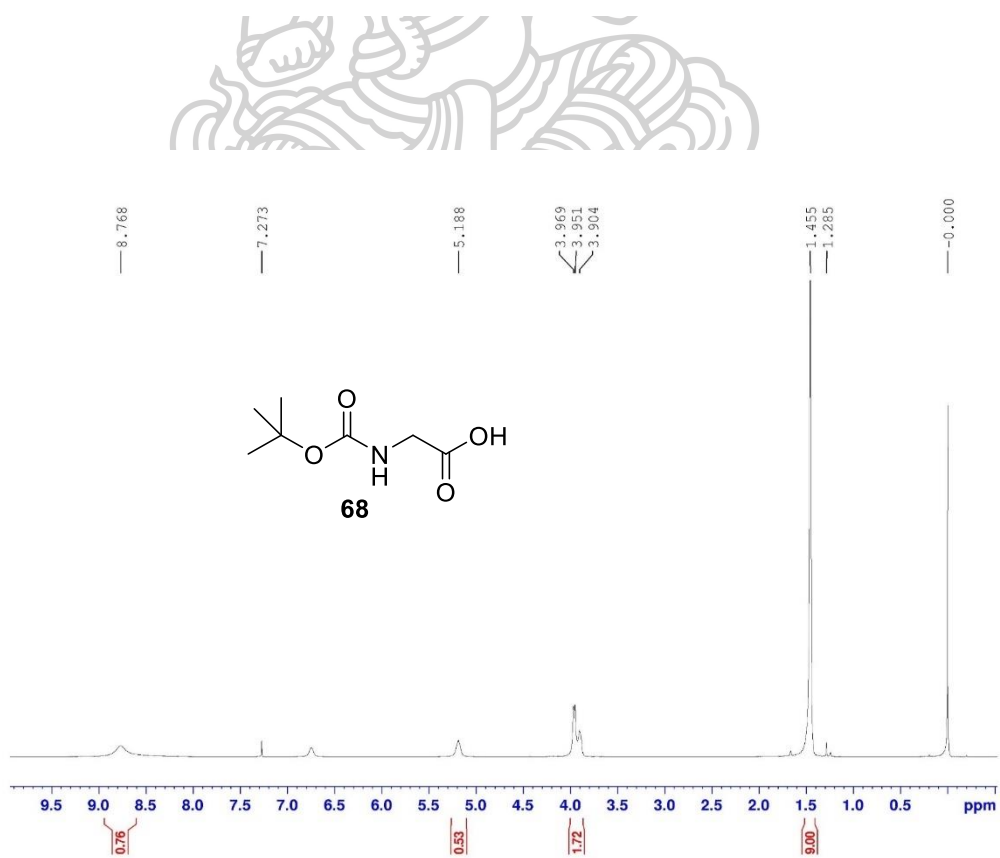
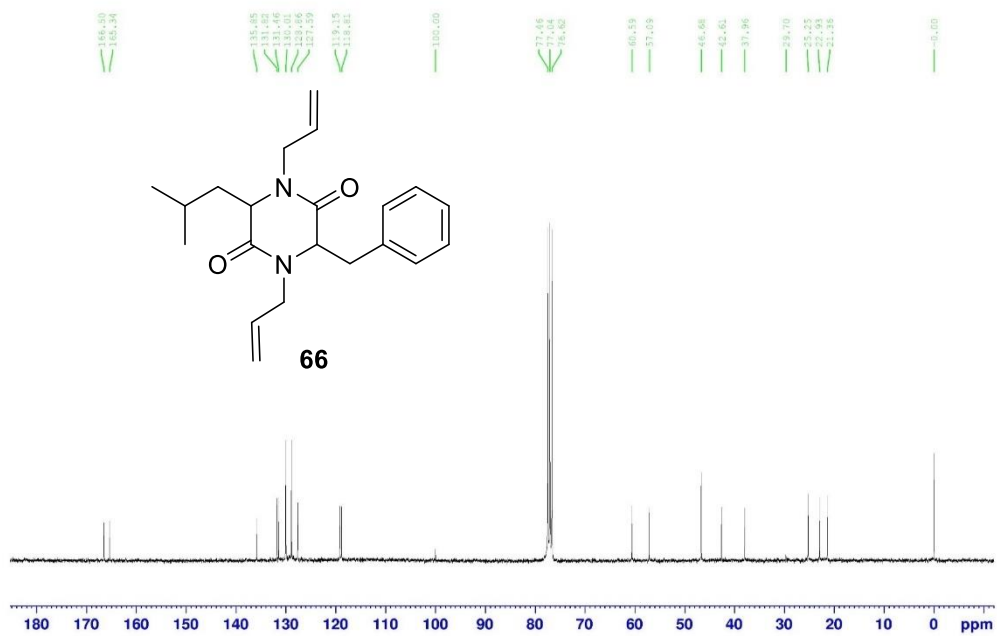


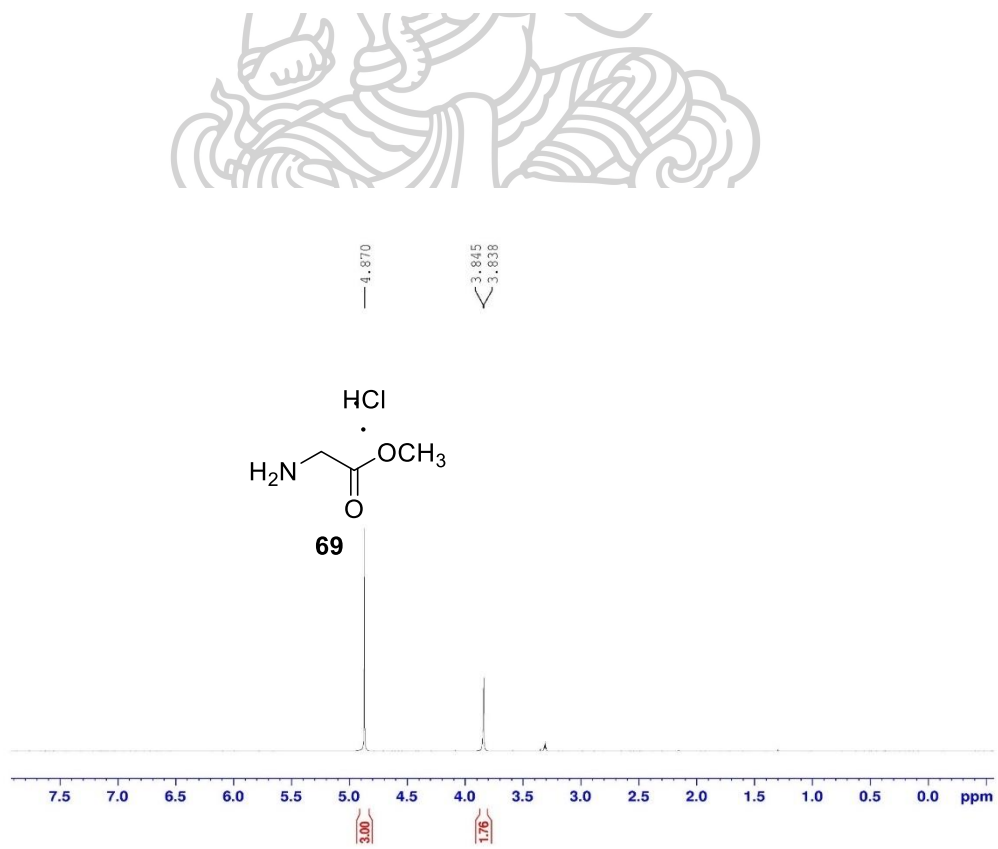
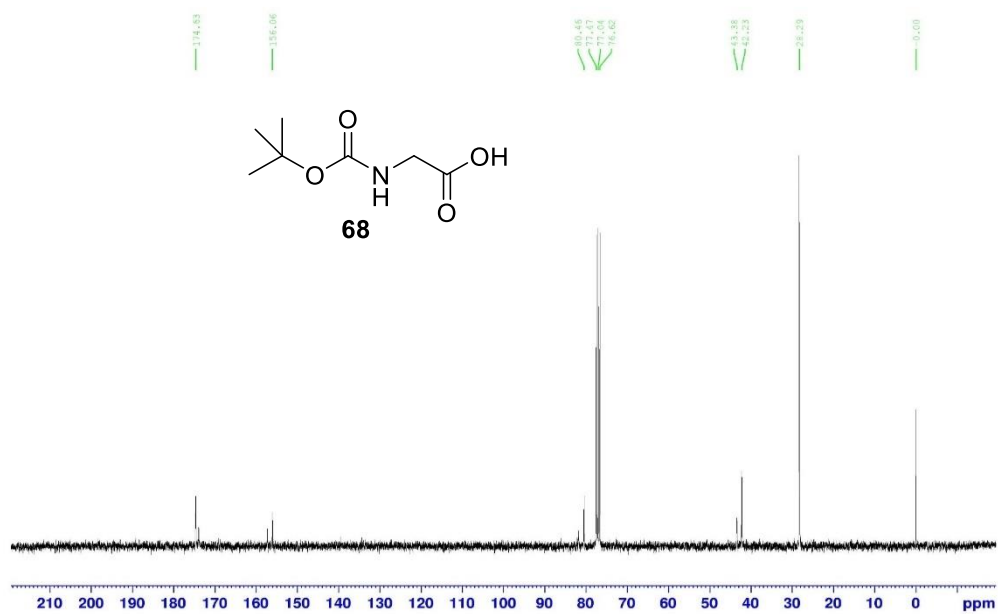


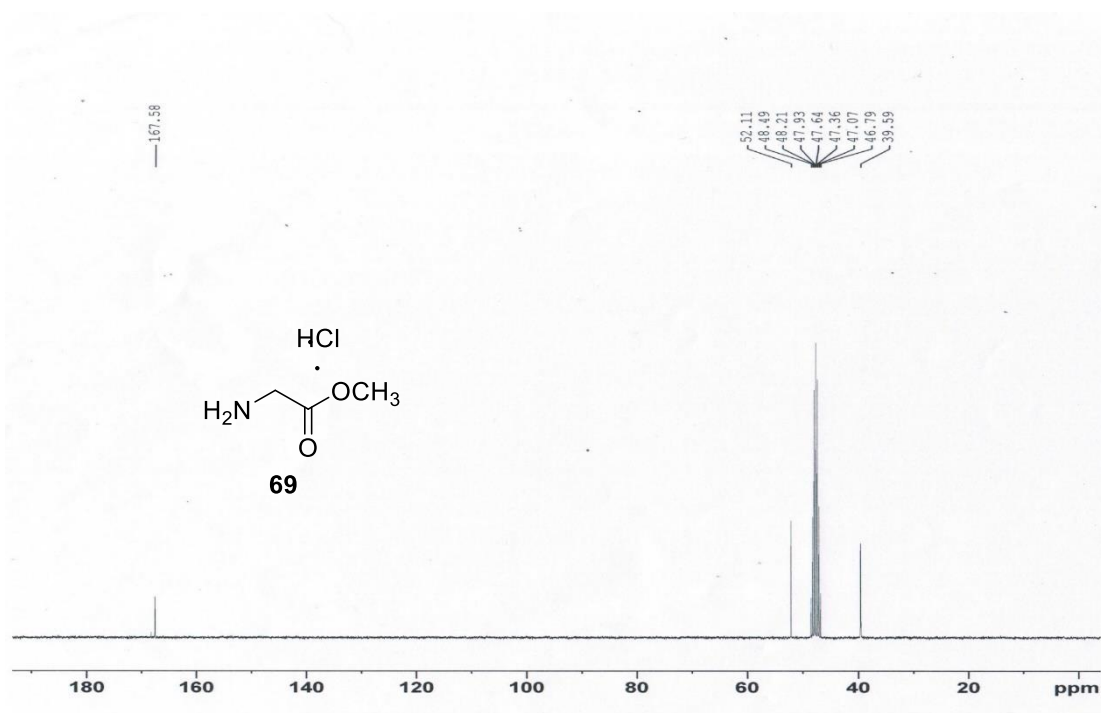


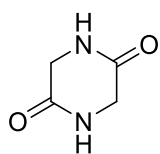




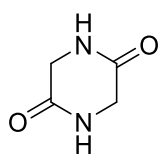
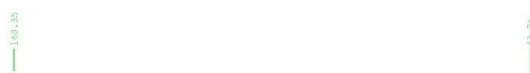
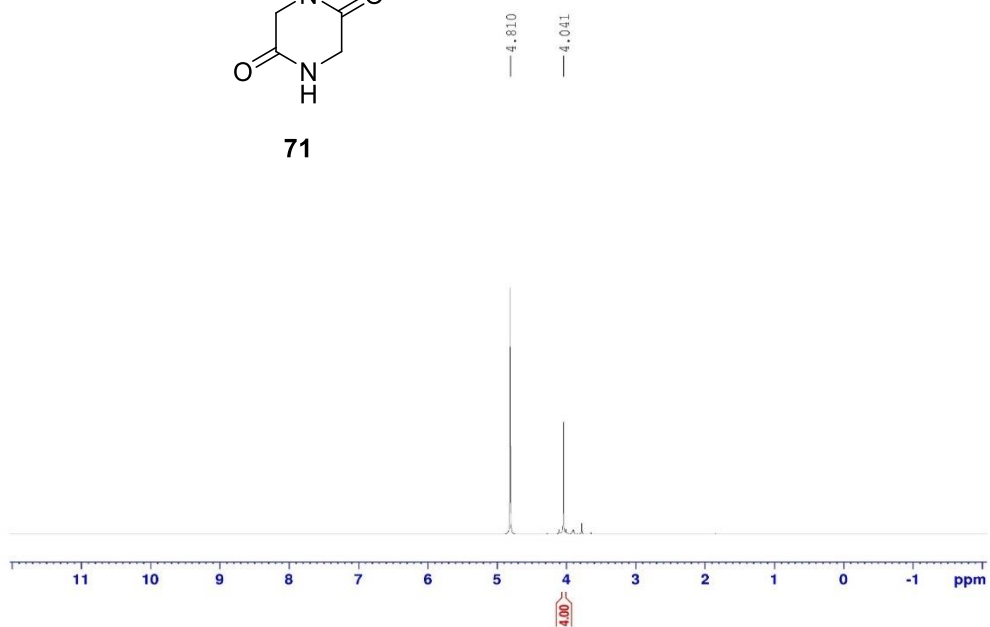




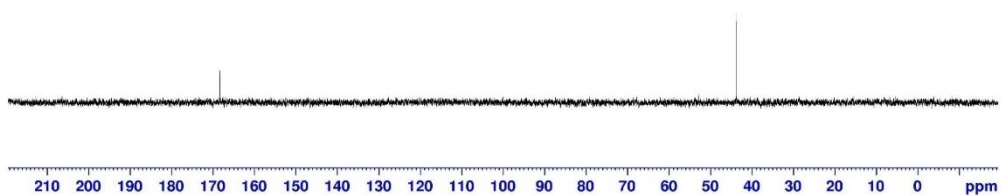


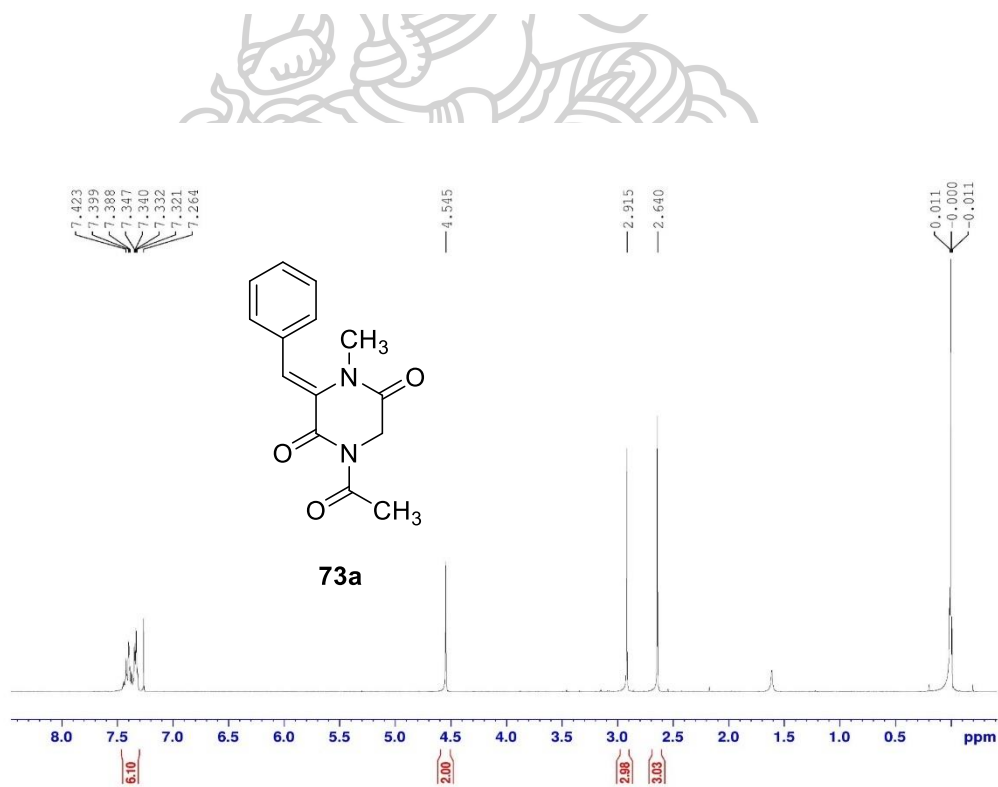
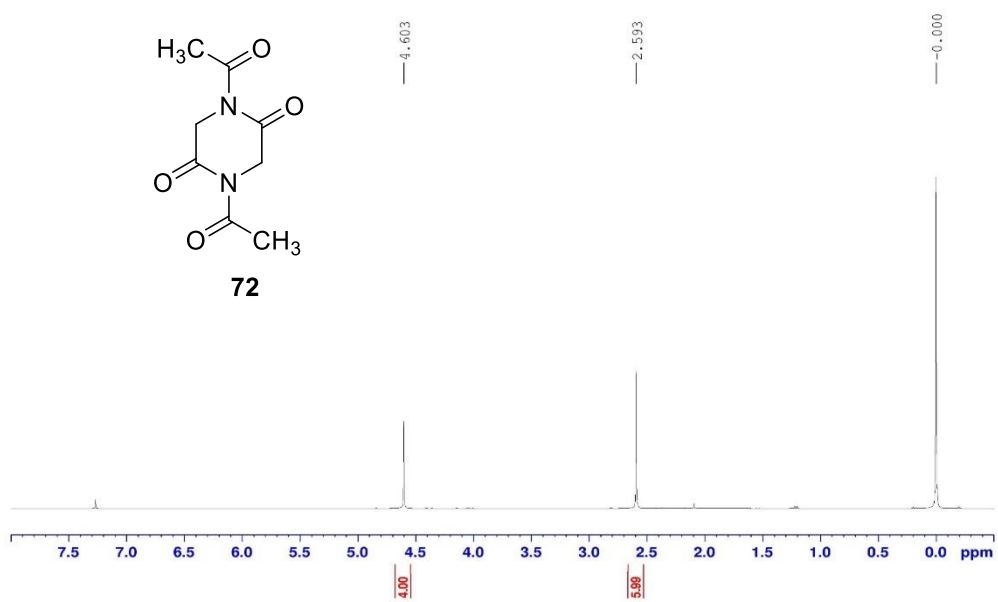


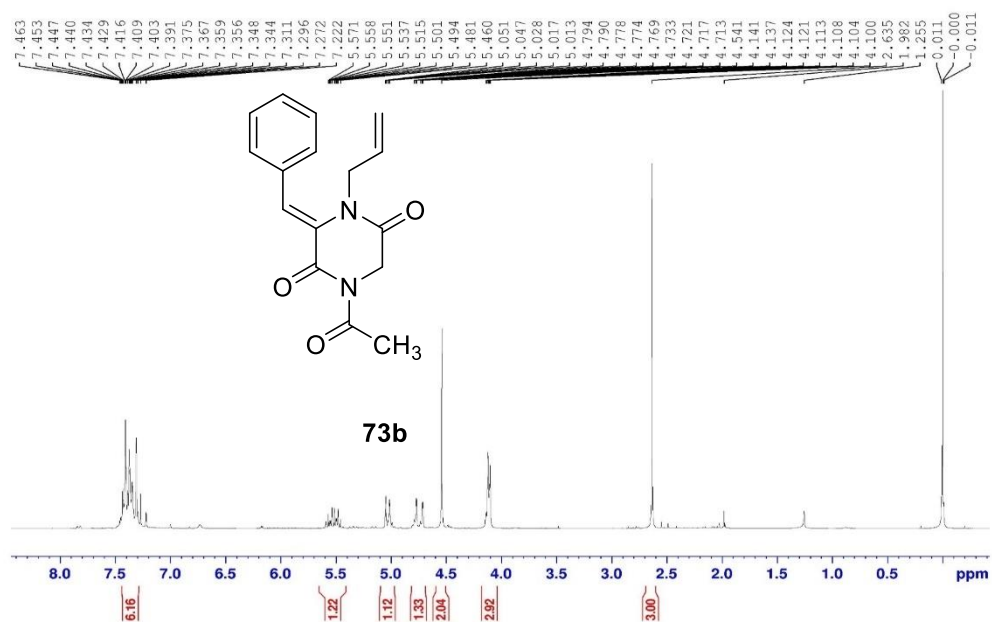
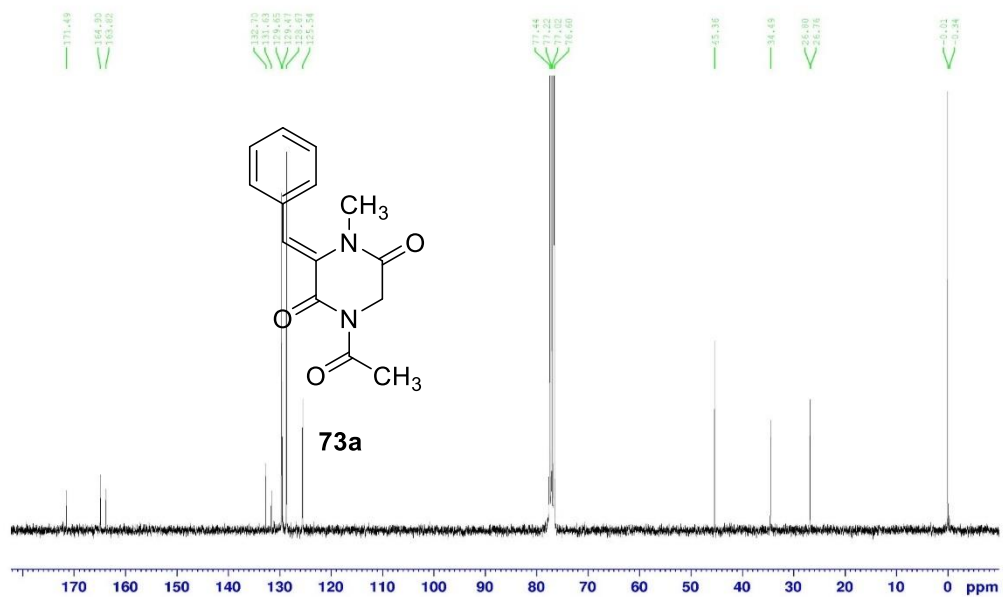
71

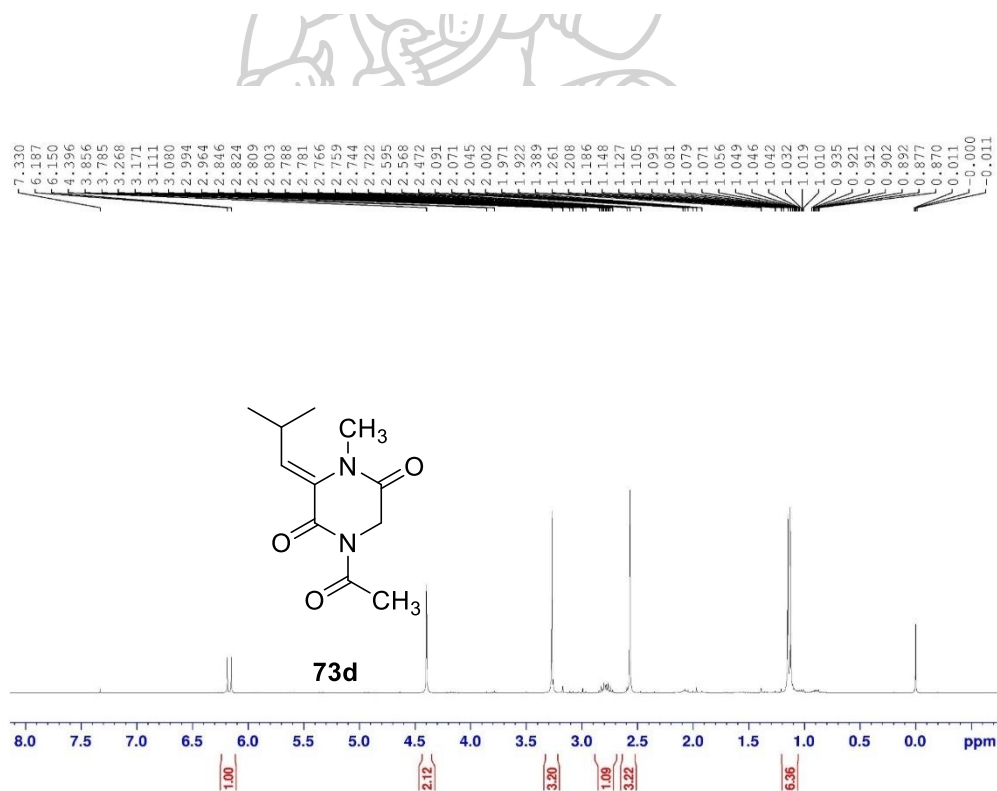
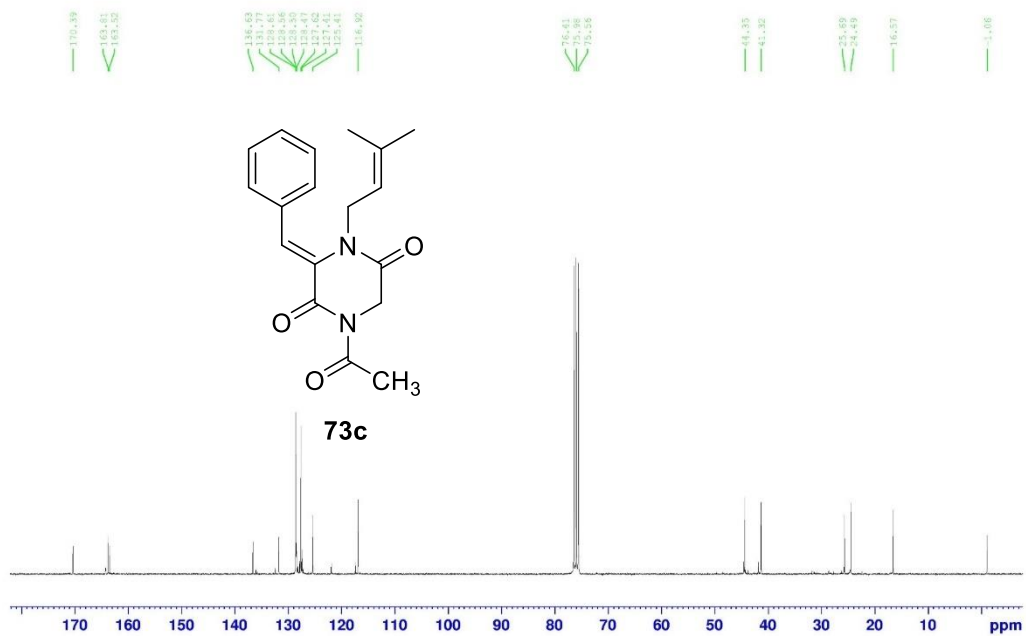


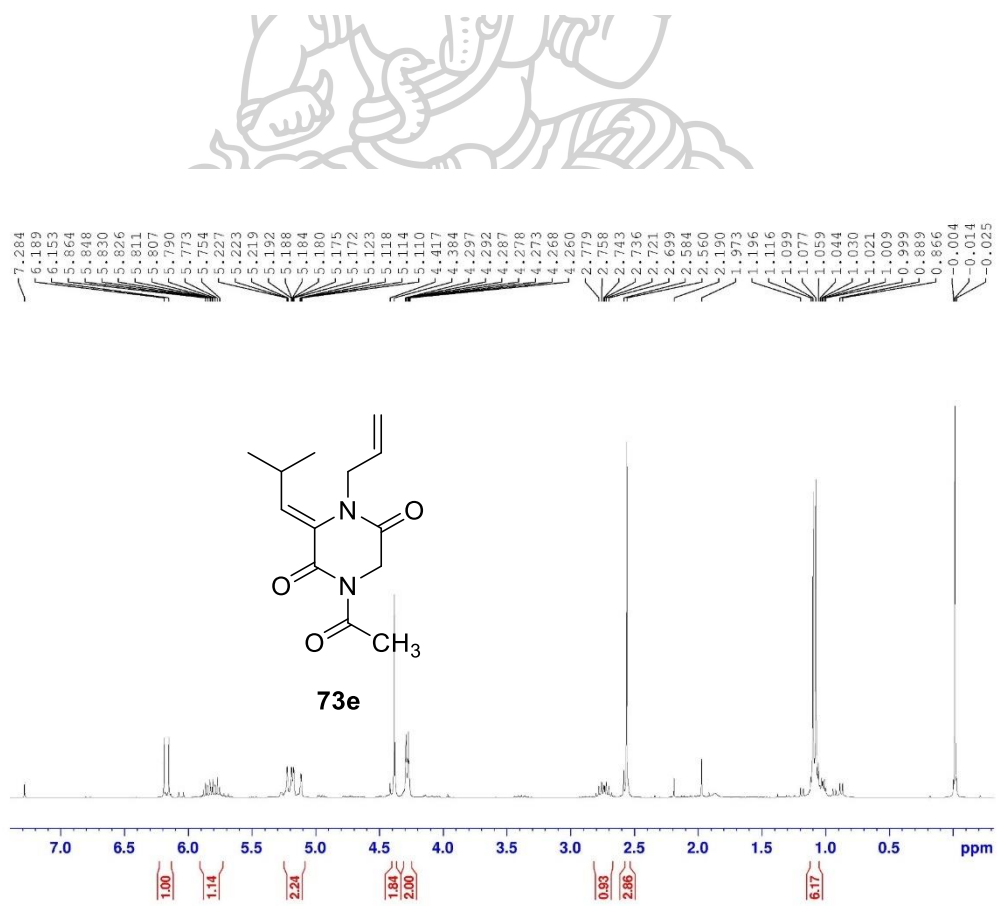
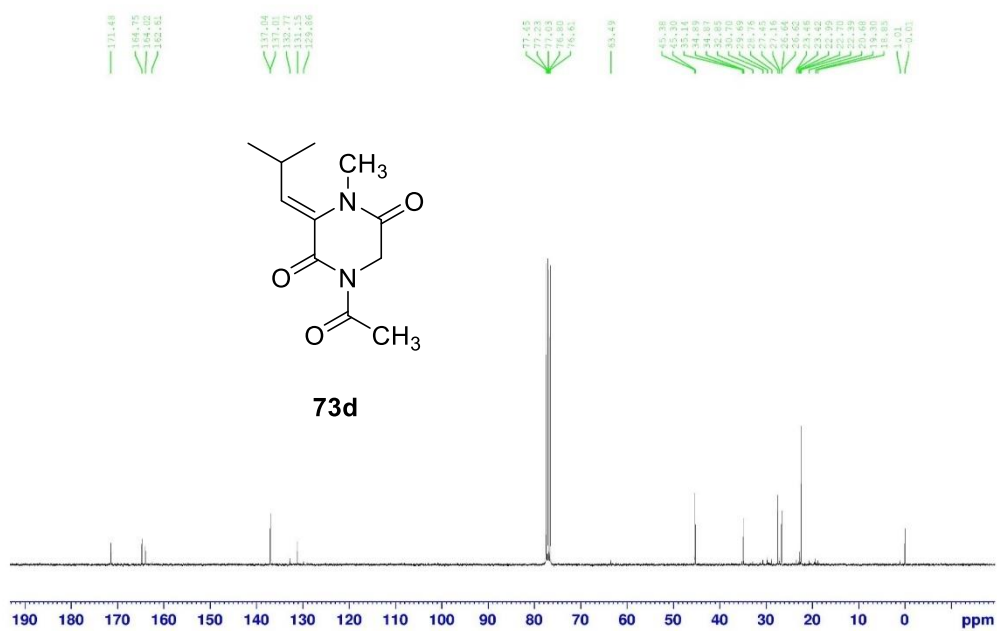
71

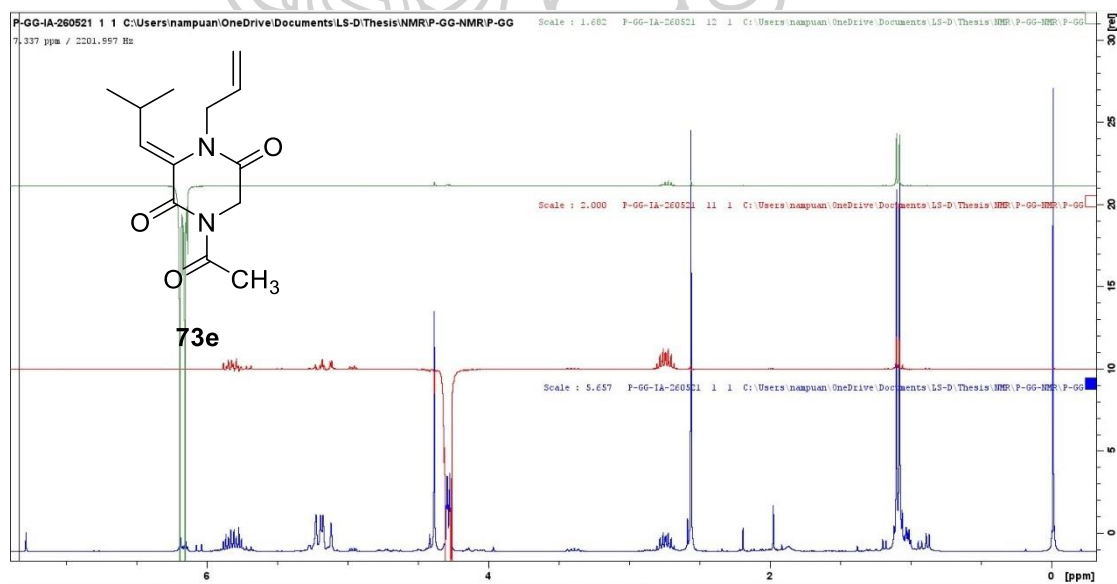
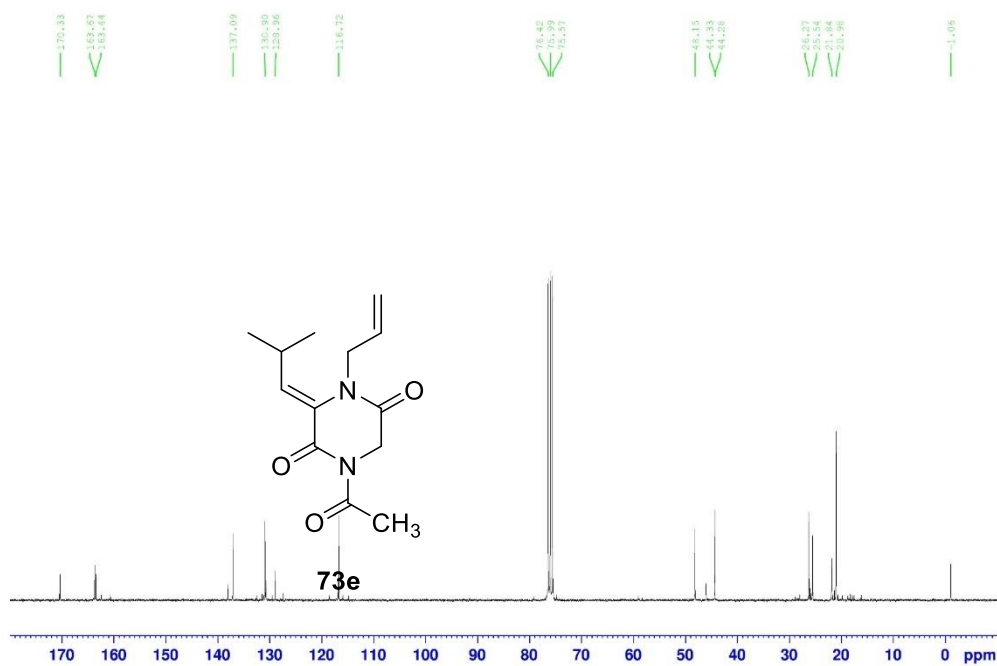


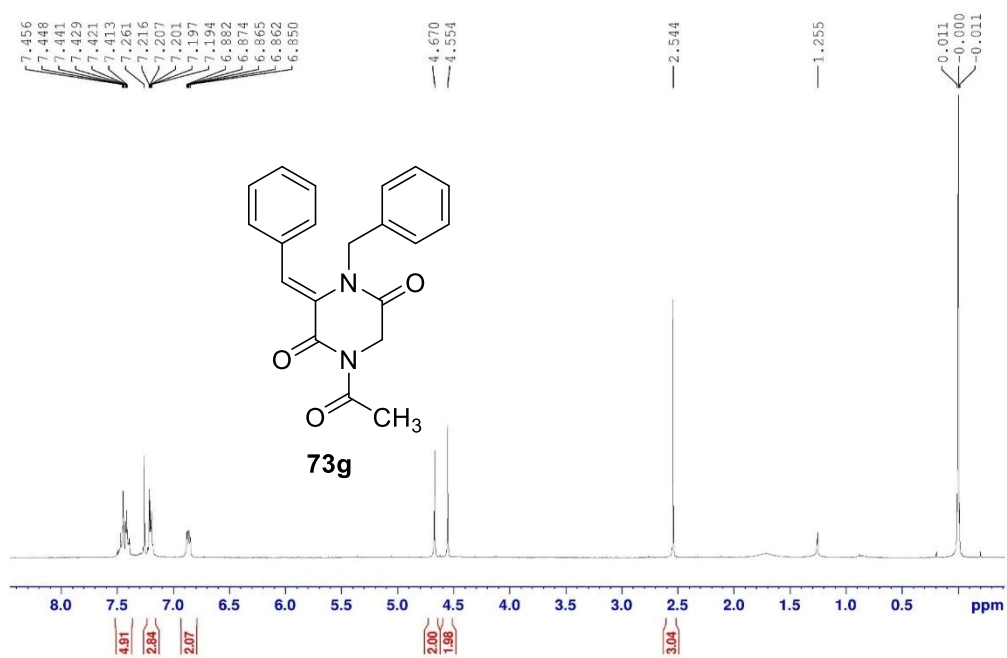
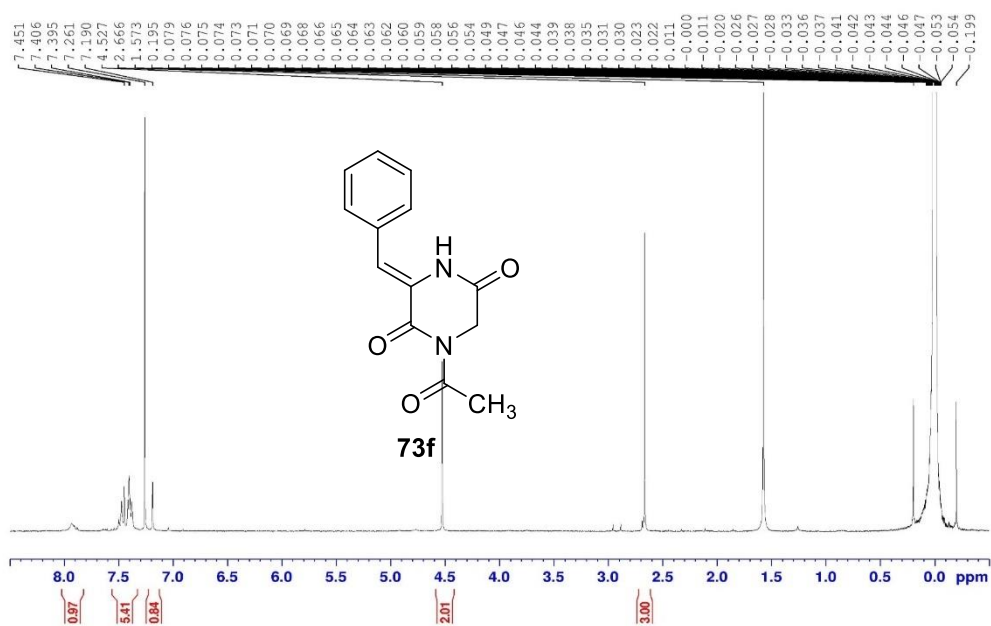


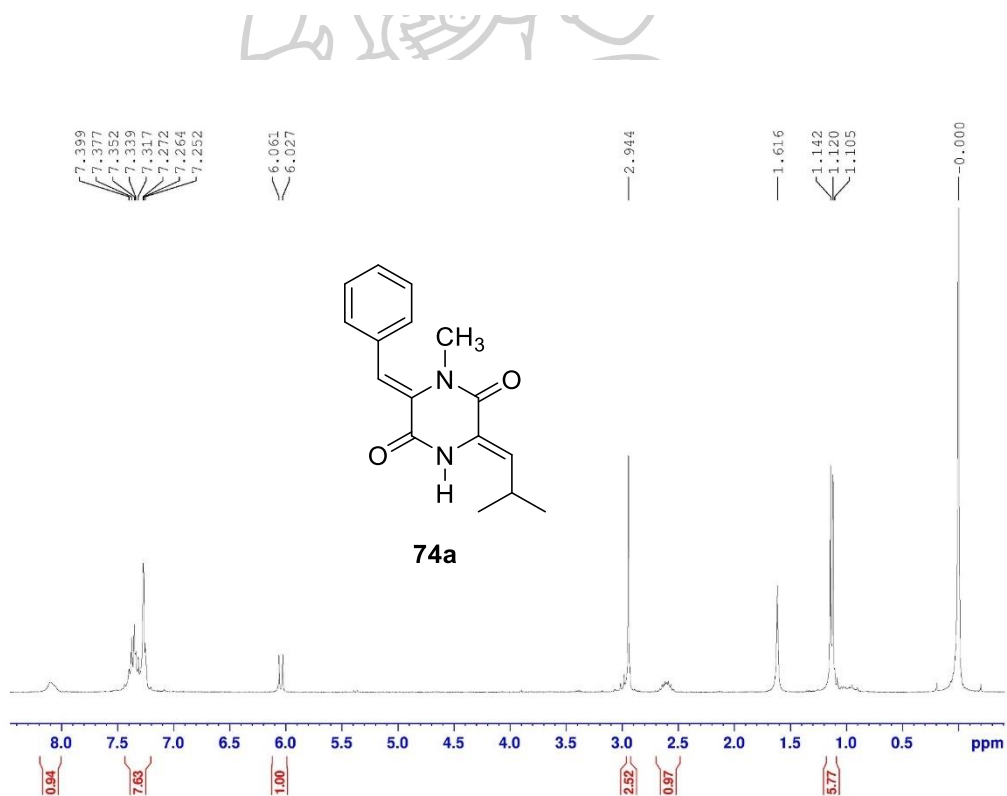
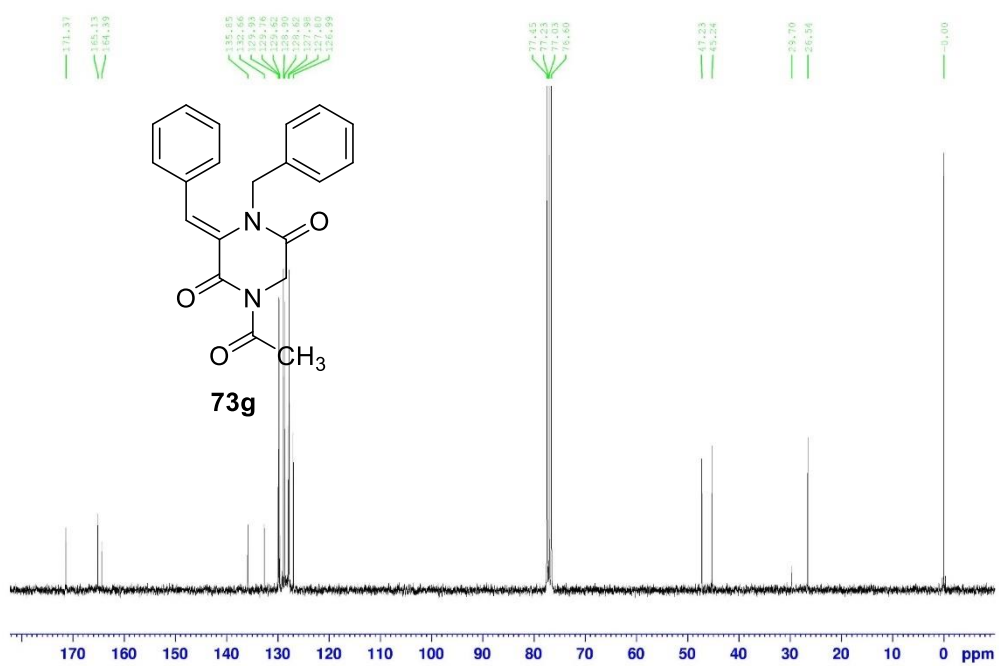


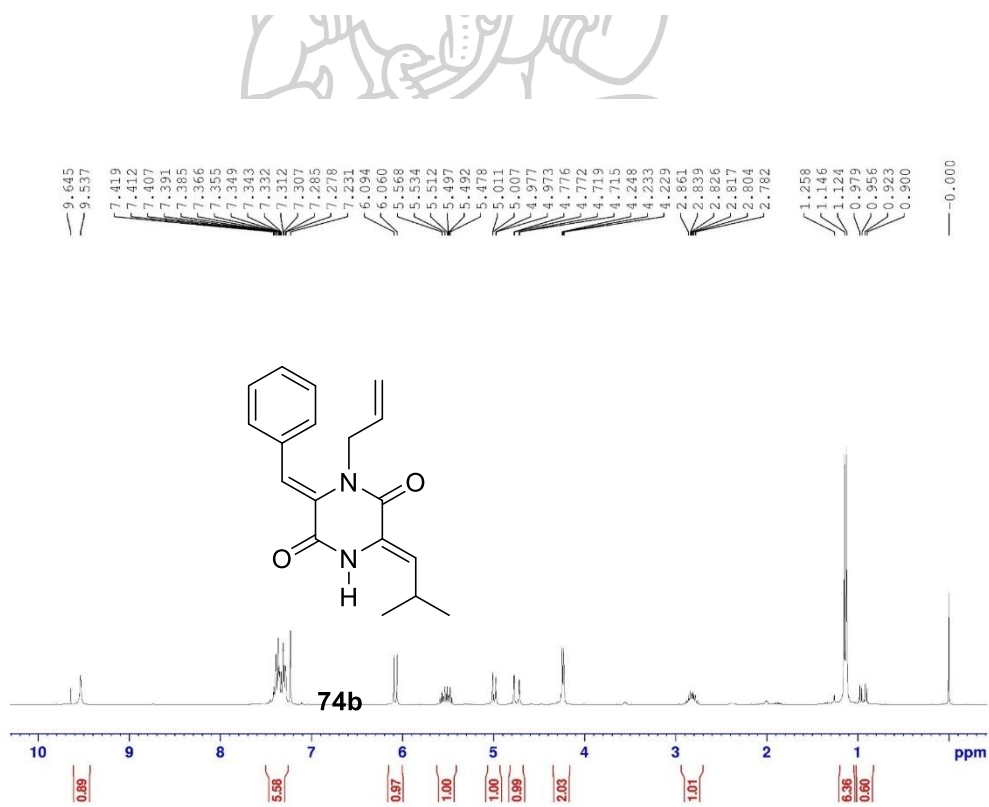
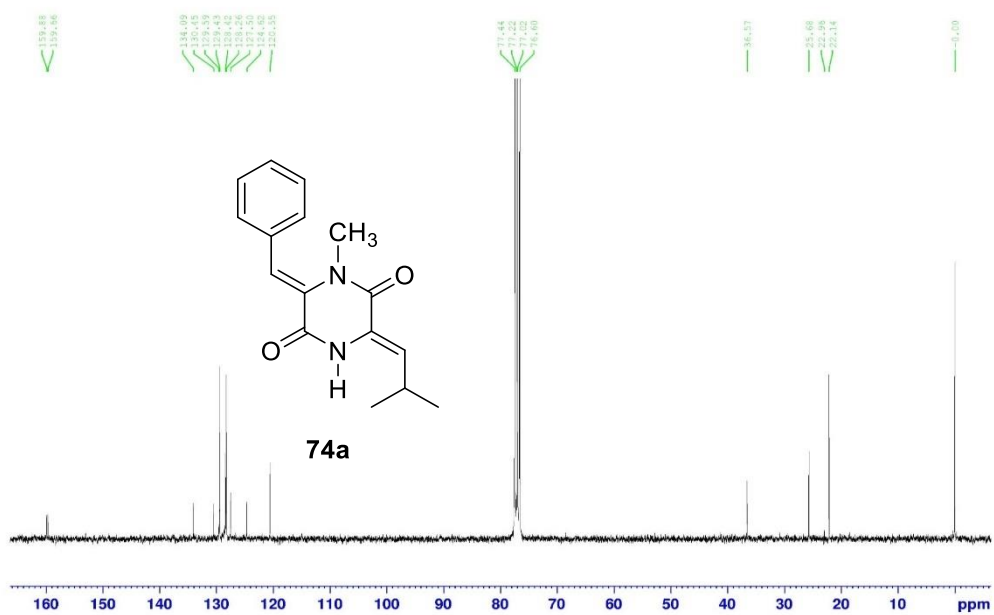


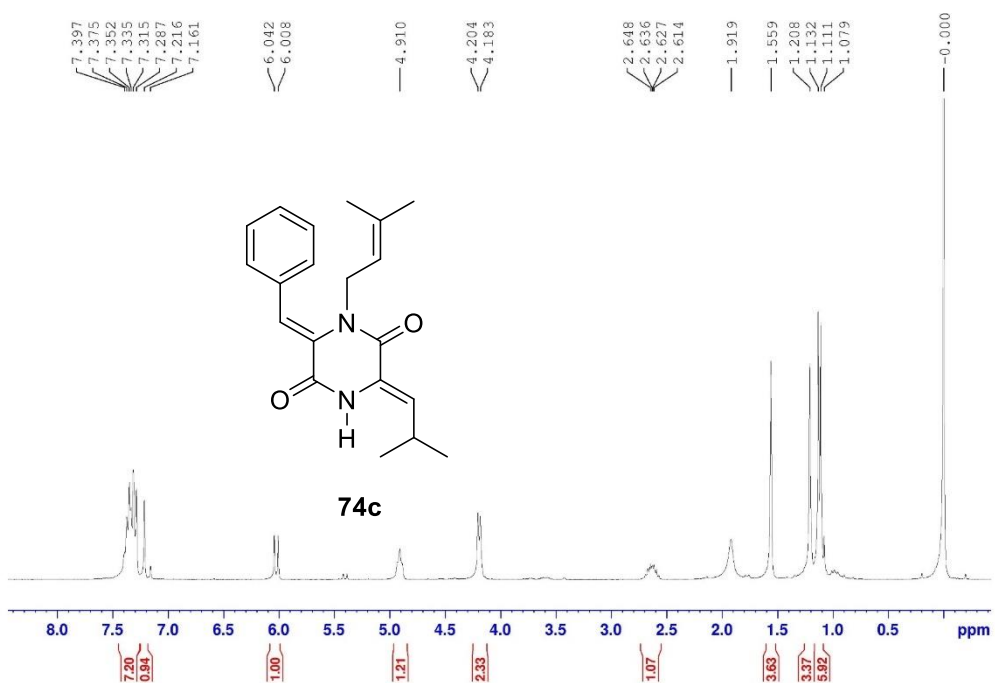
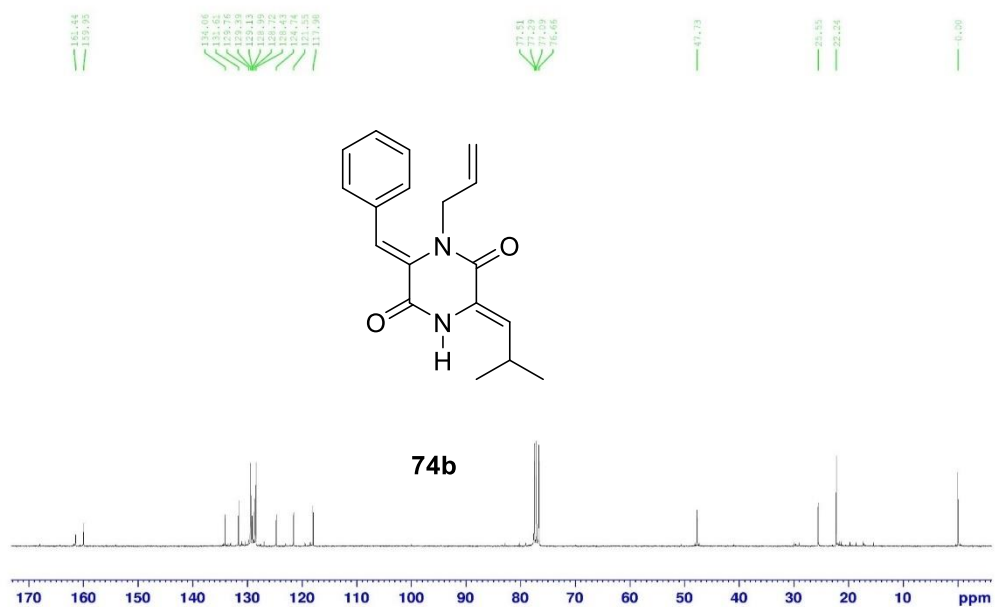


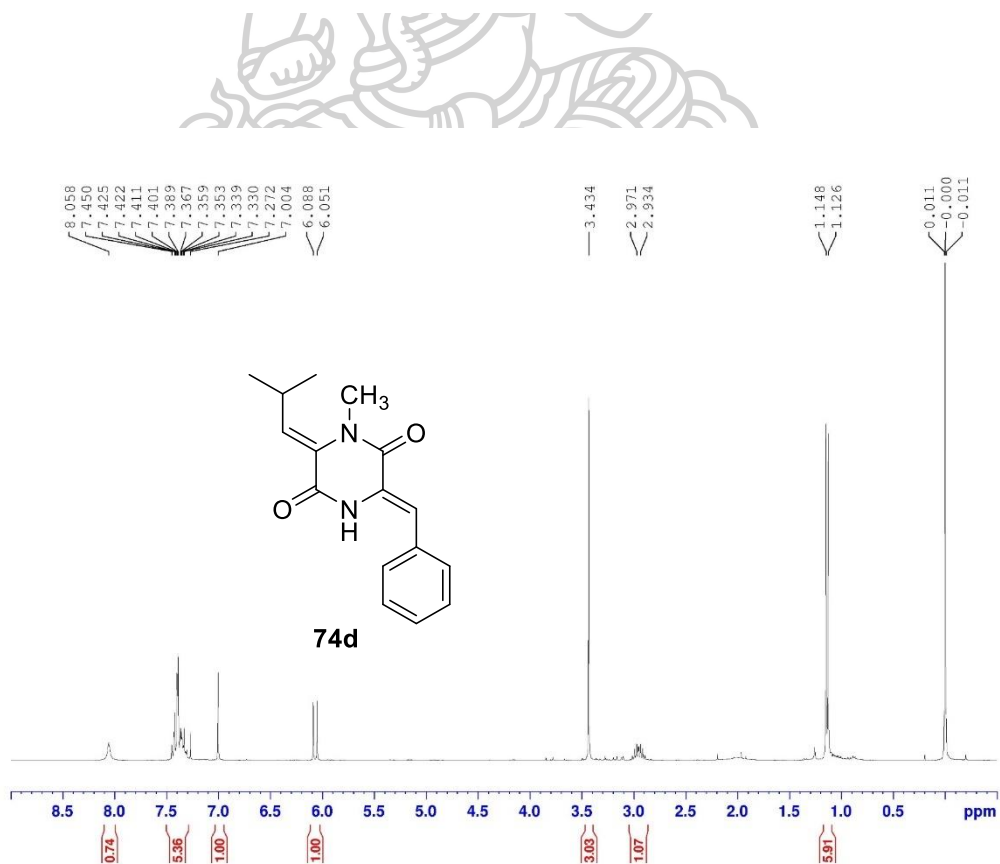
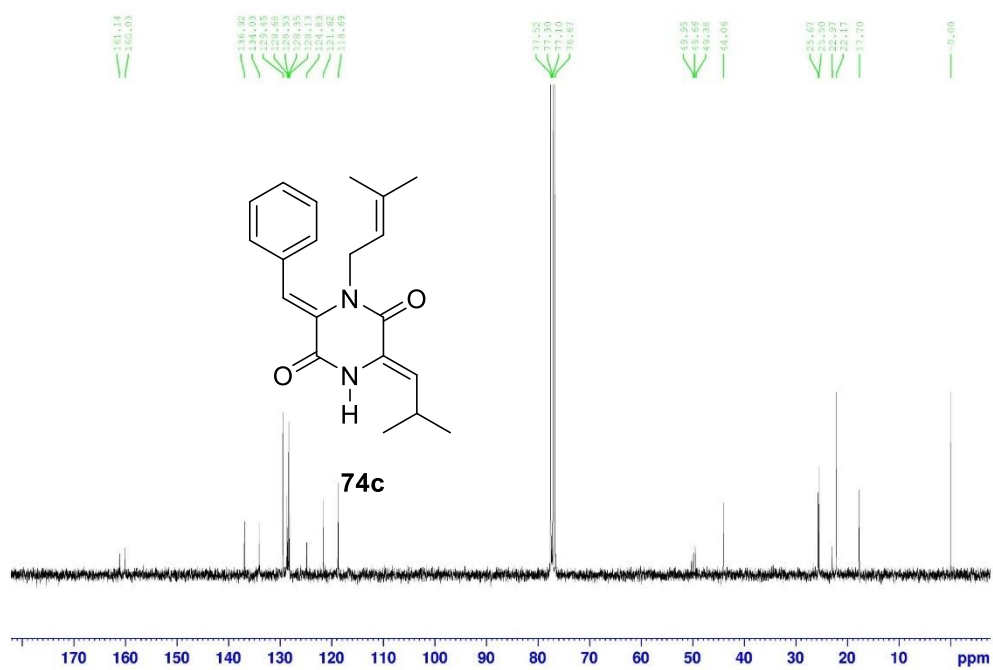


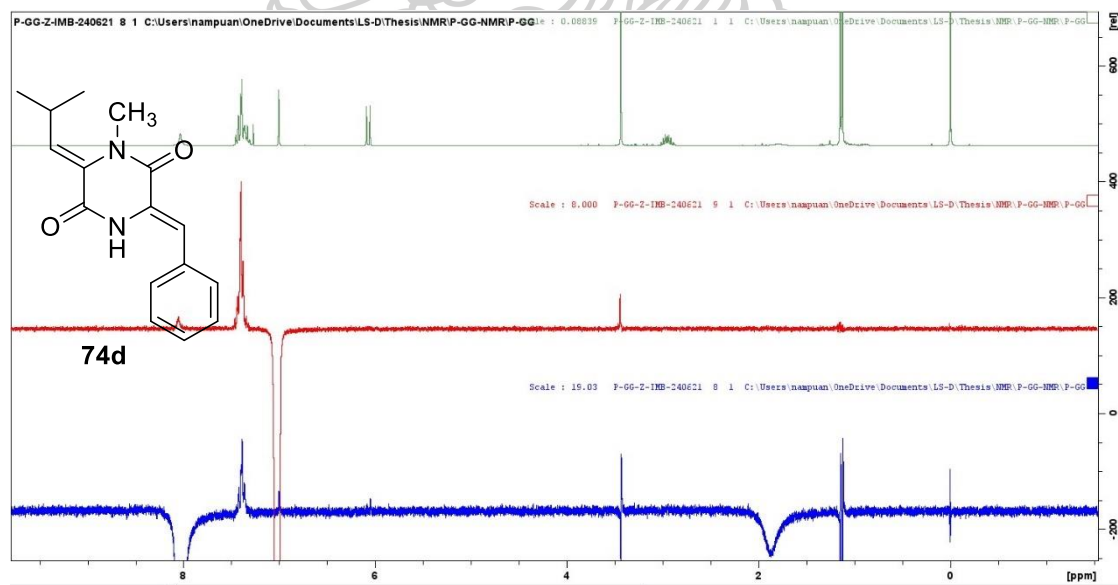
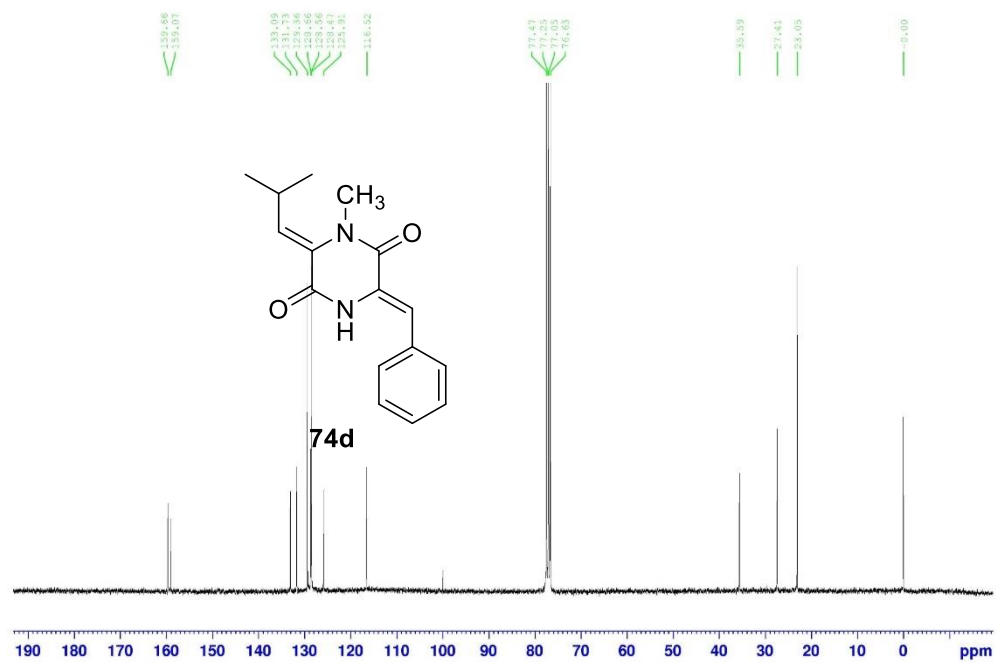


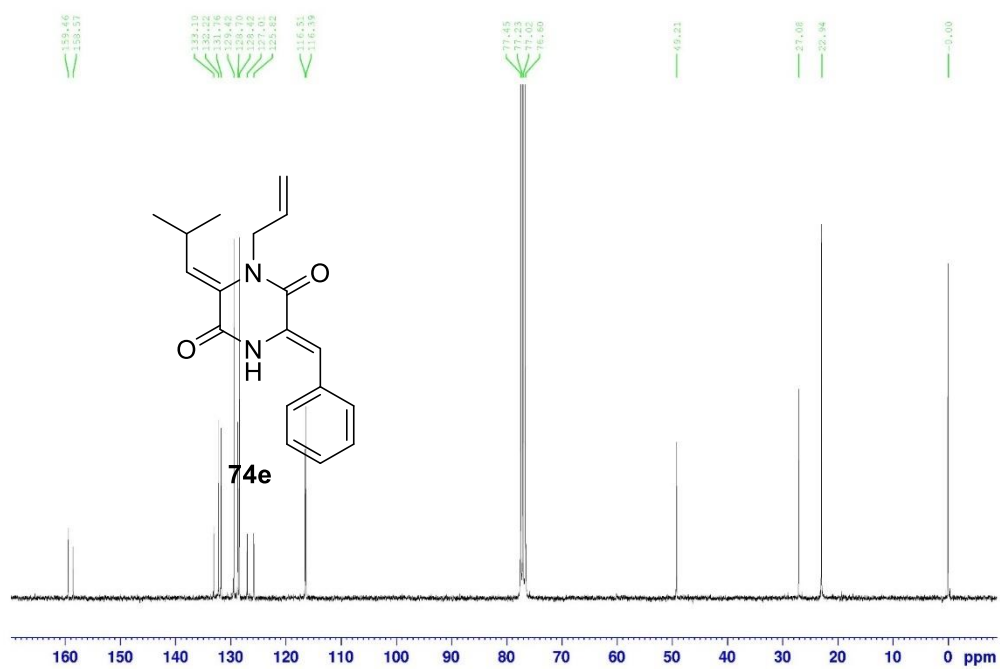
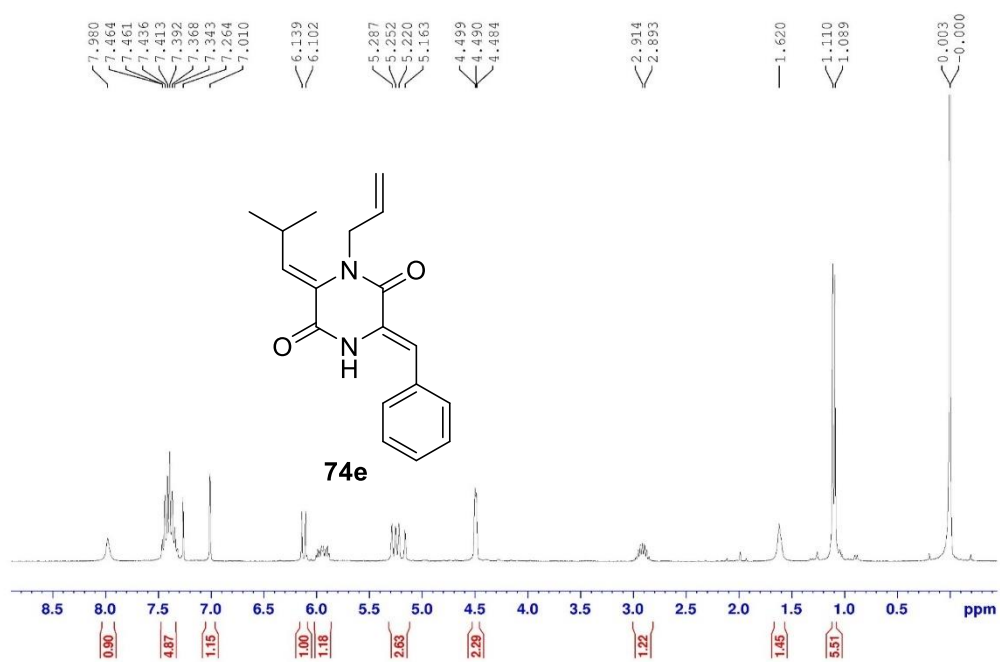


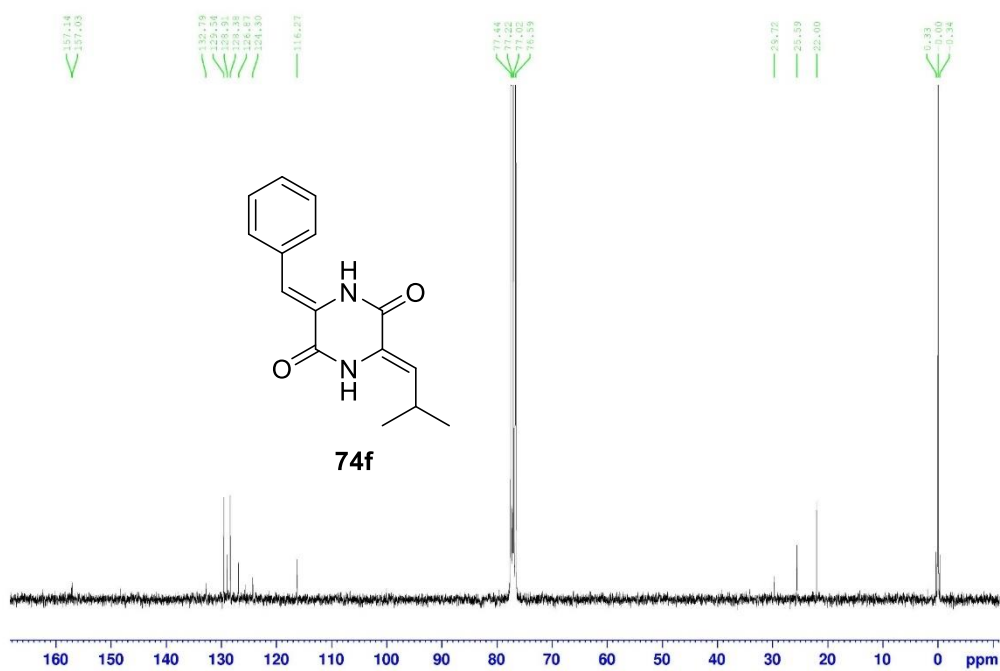
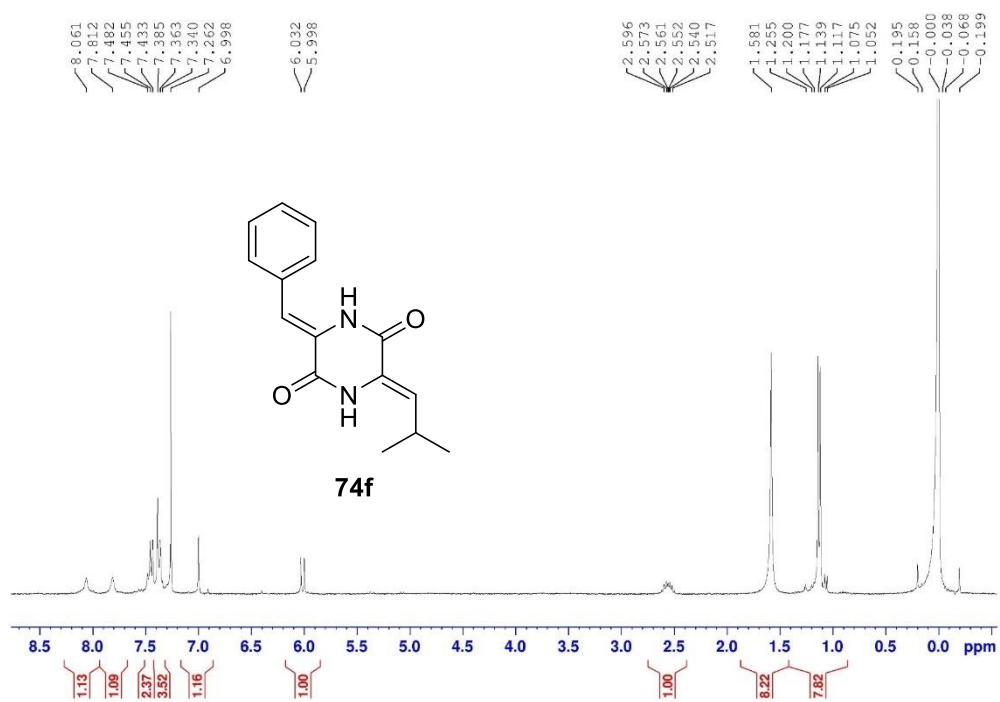


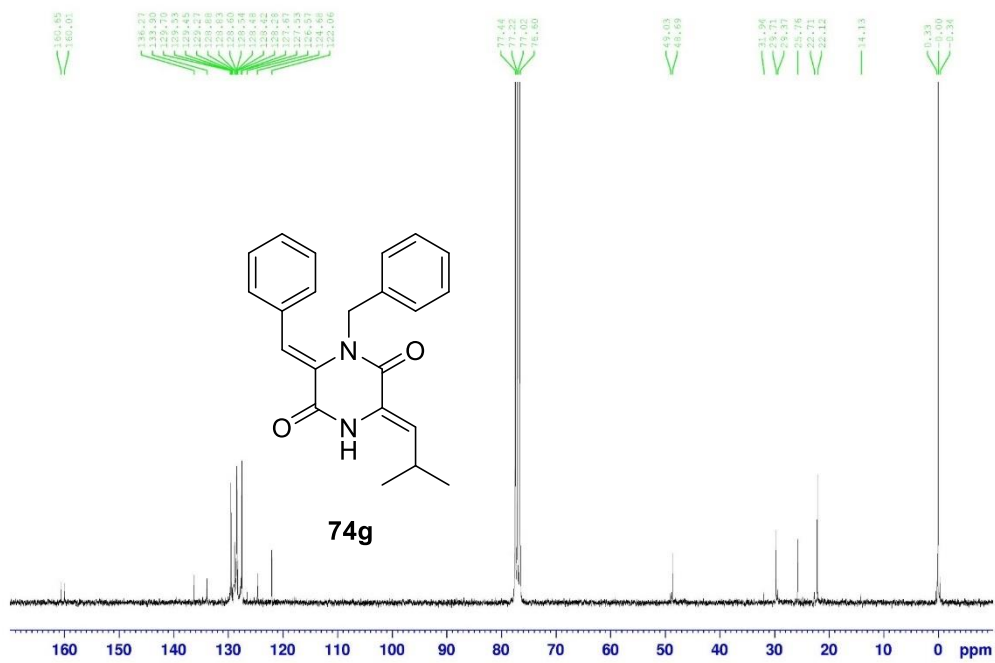
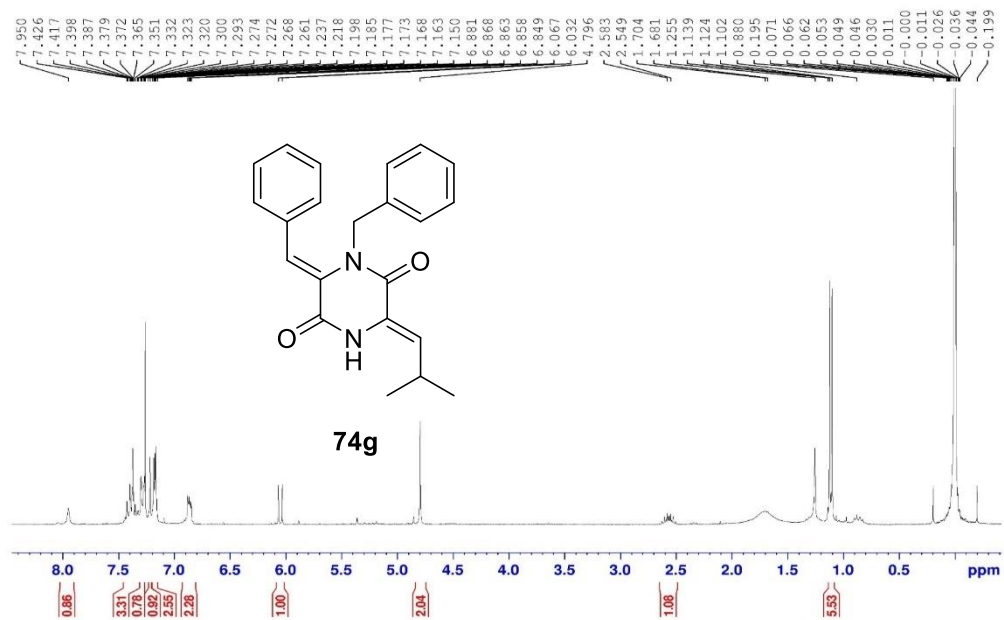


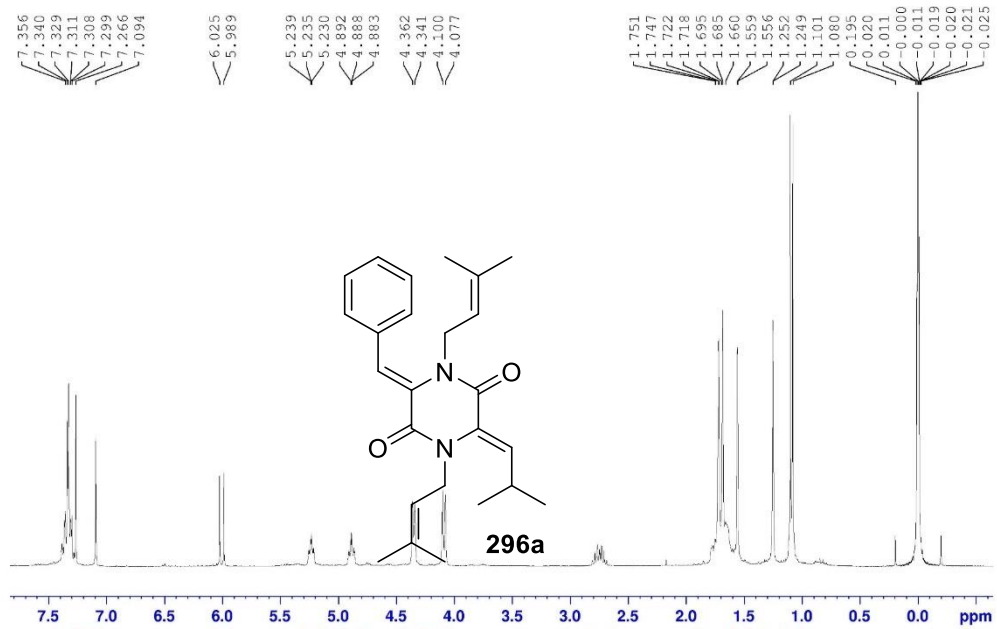


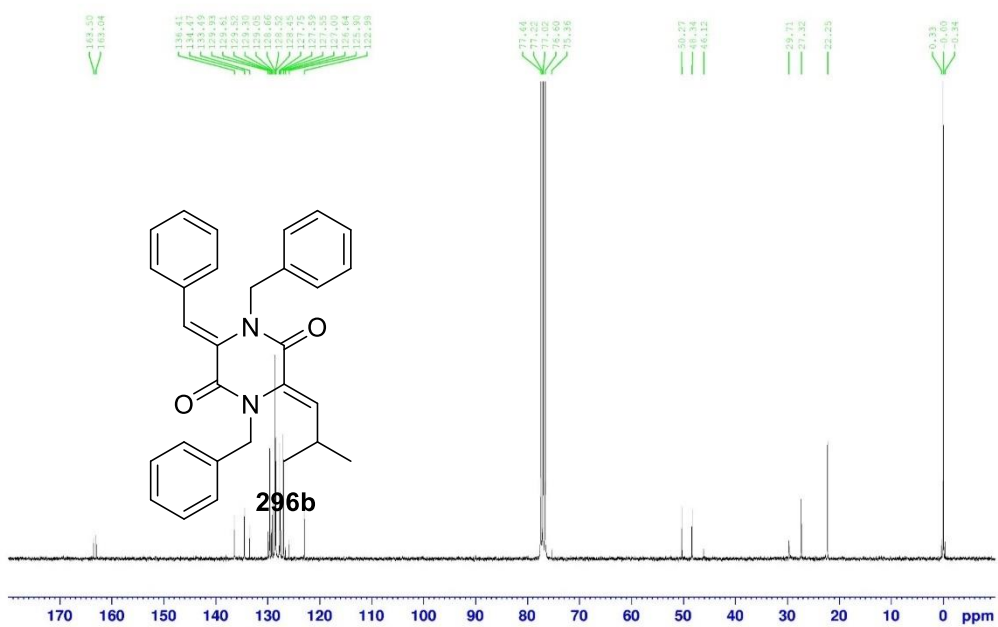
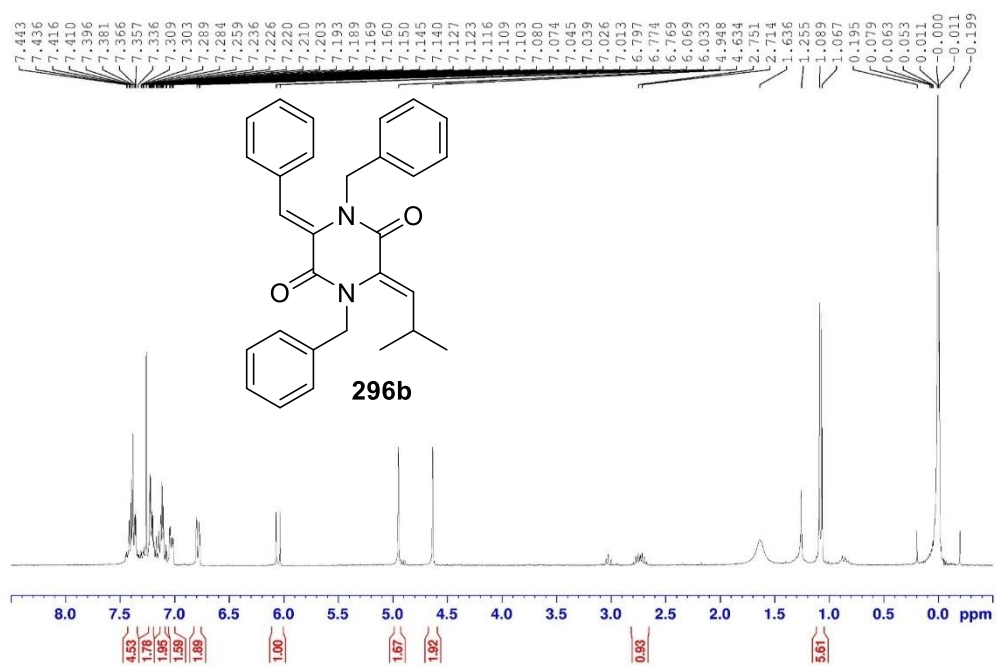


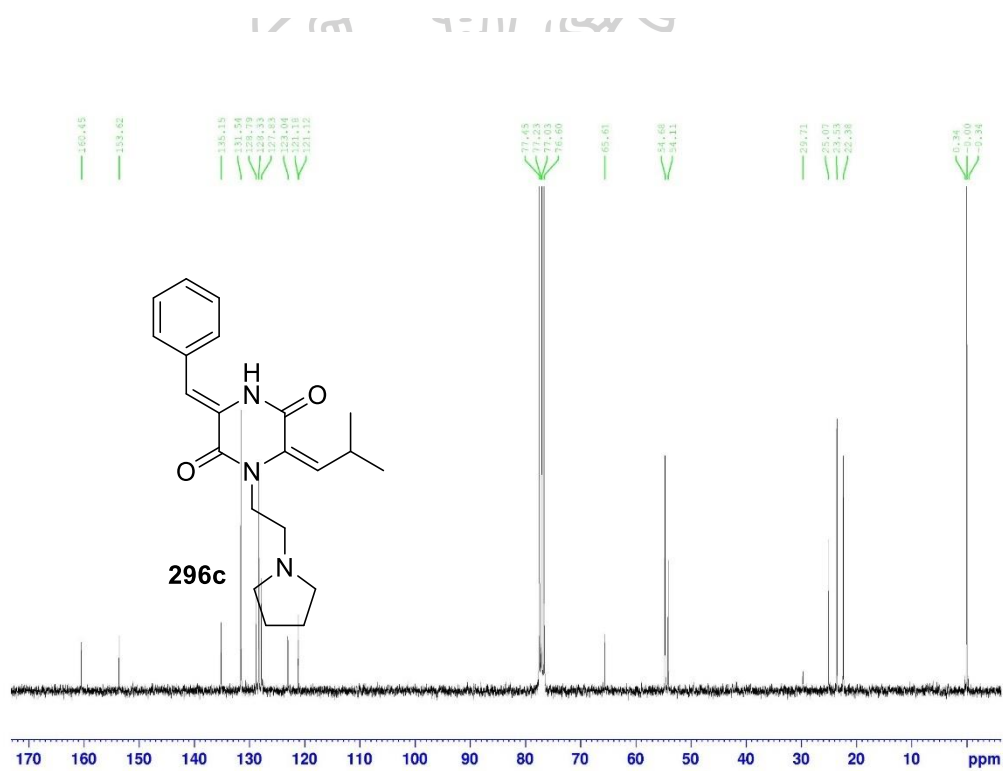
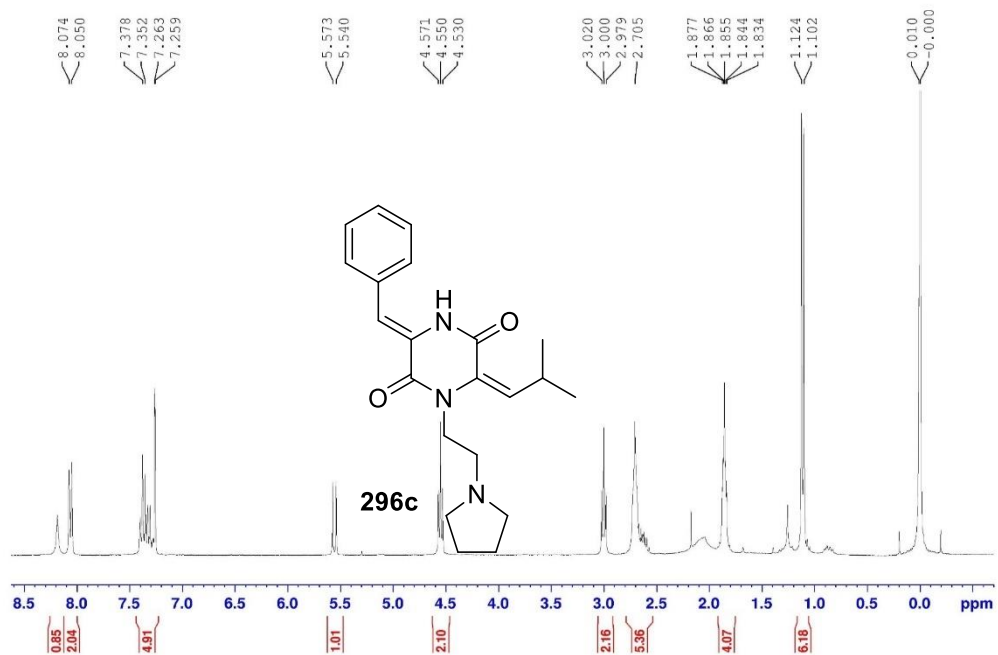


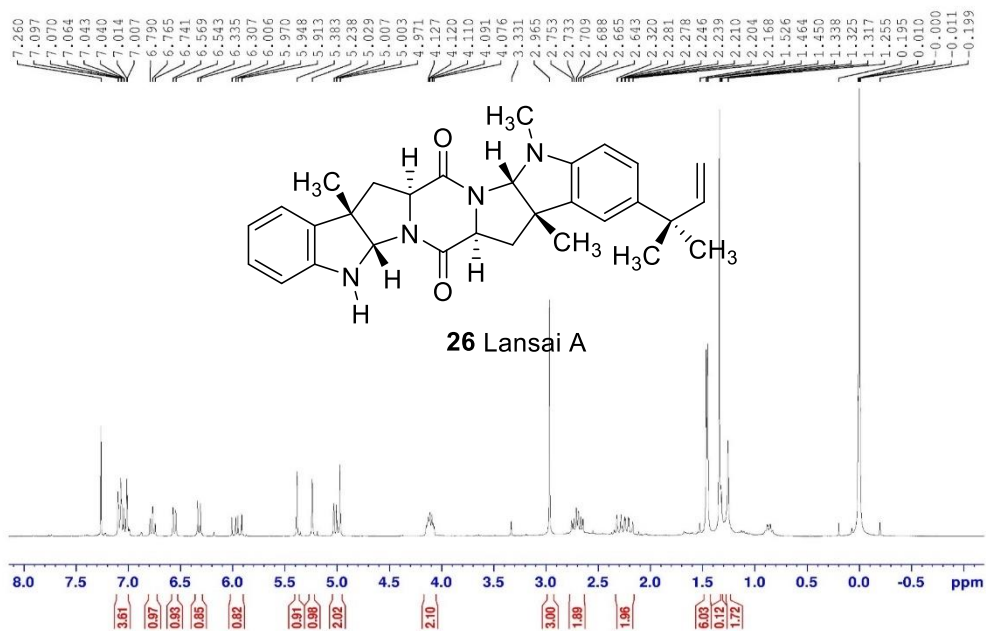
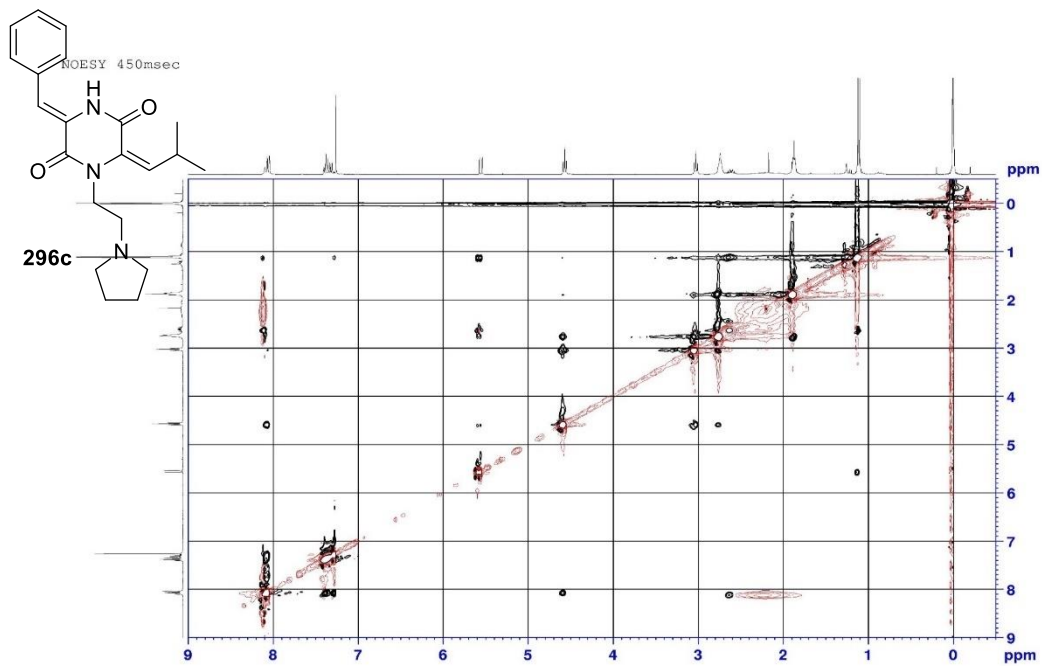


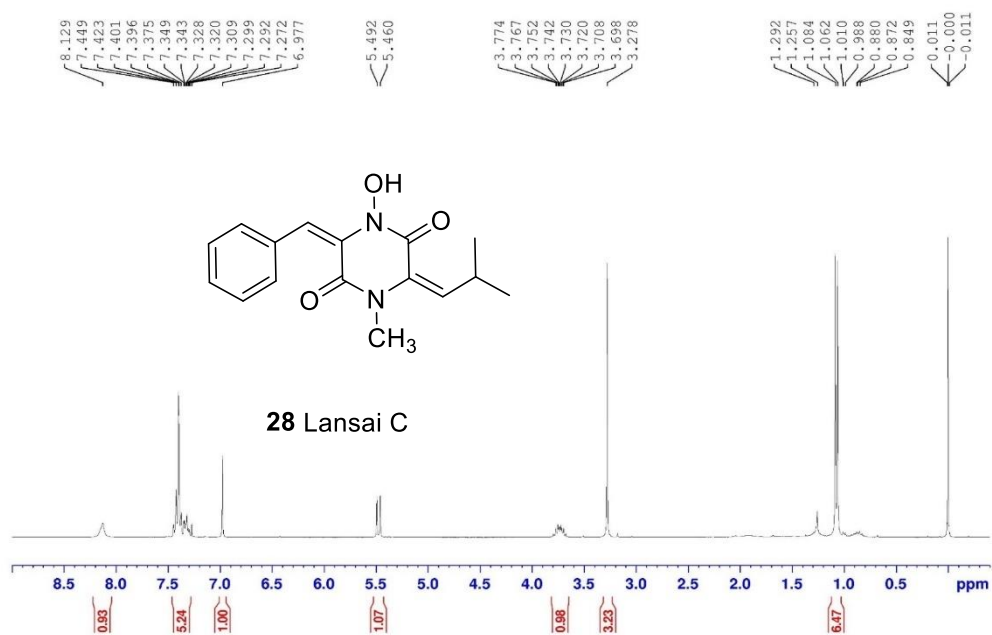
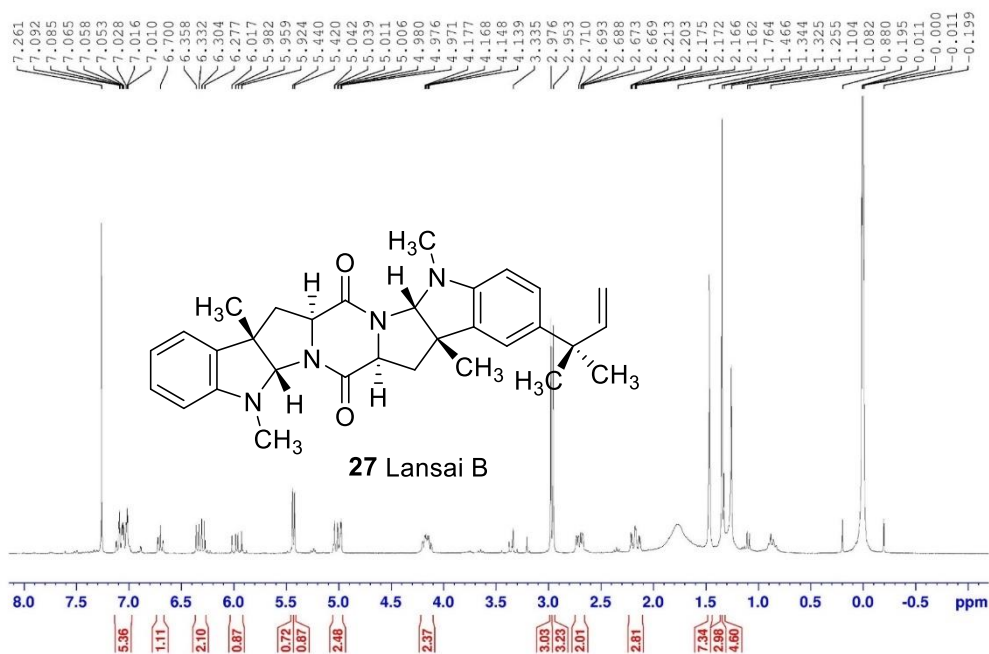


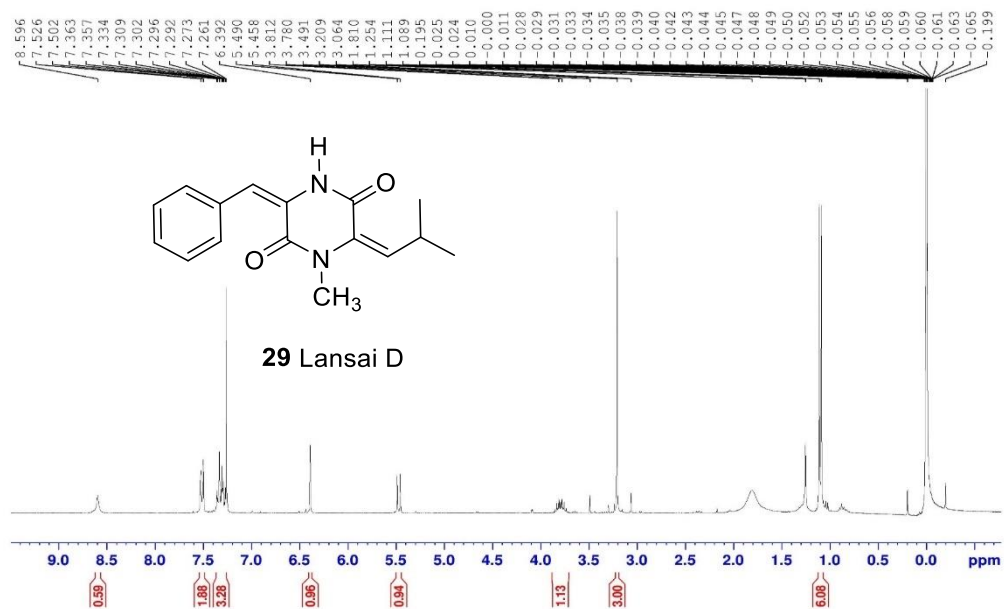


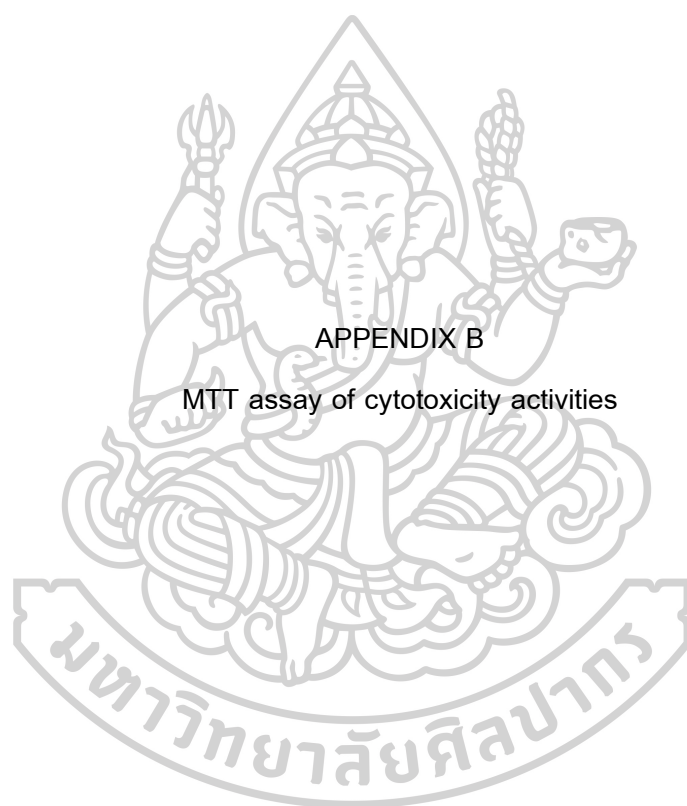












APPENDIX B

MTT assay of cytotoxicity activities

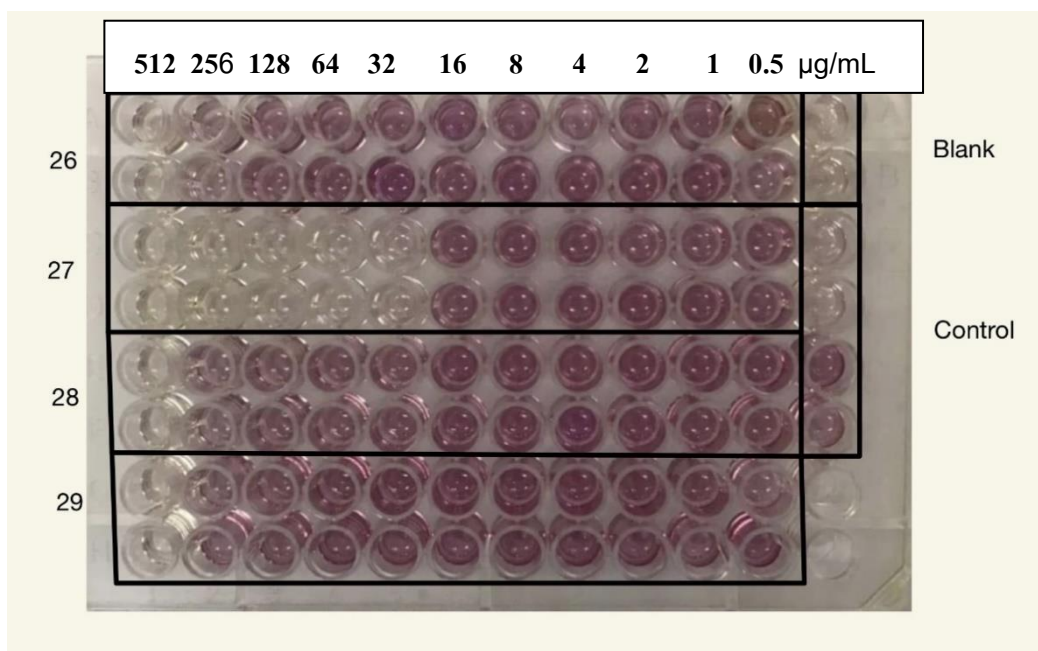


Figure 17. The results of cytotoxicity against human cervical cancer cells (HeLa).

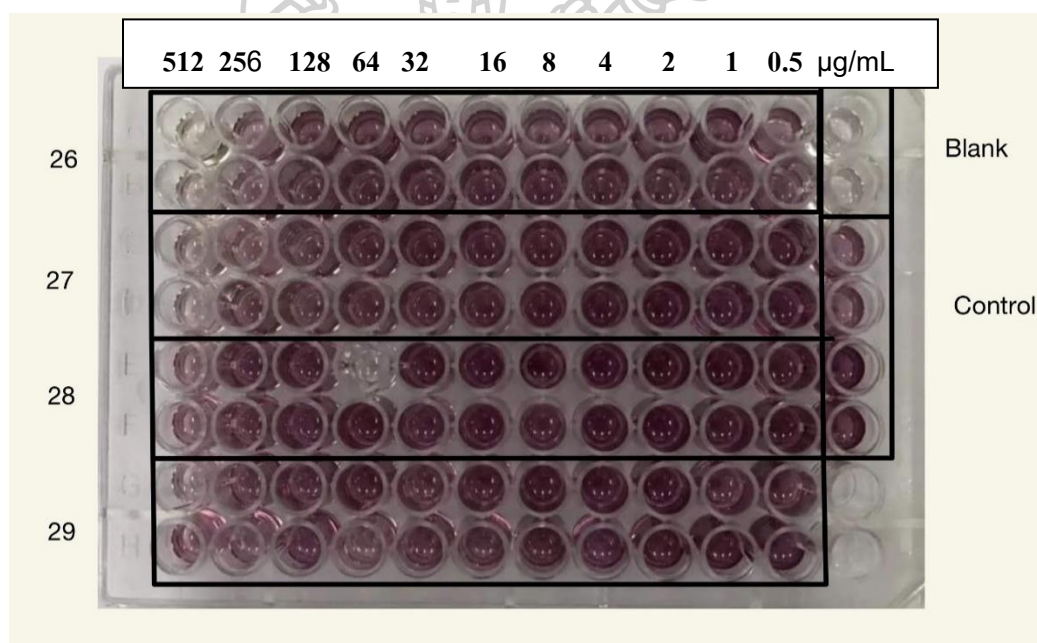
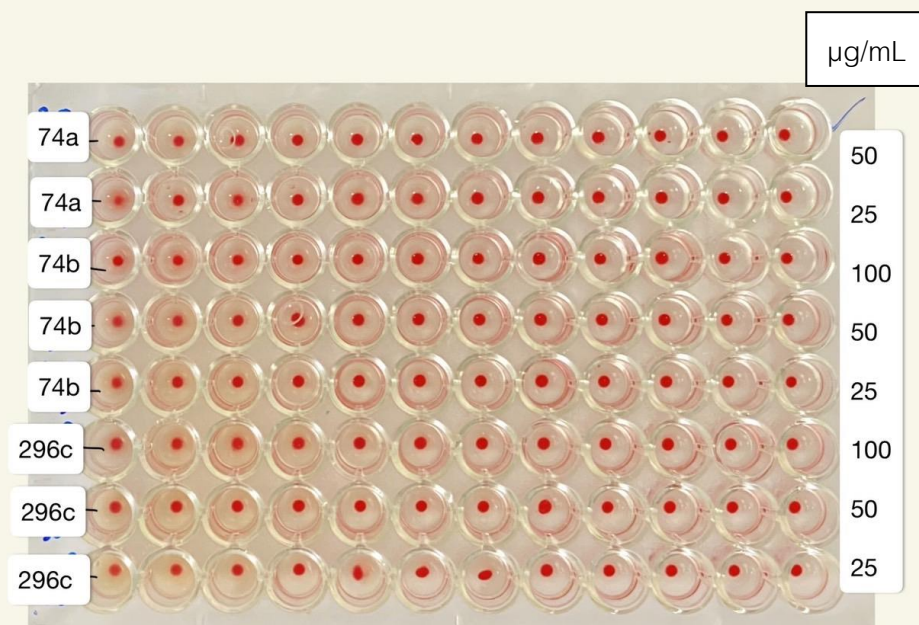
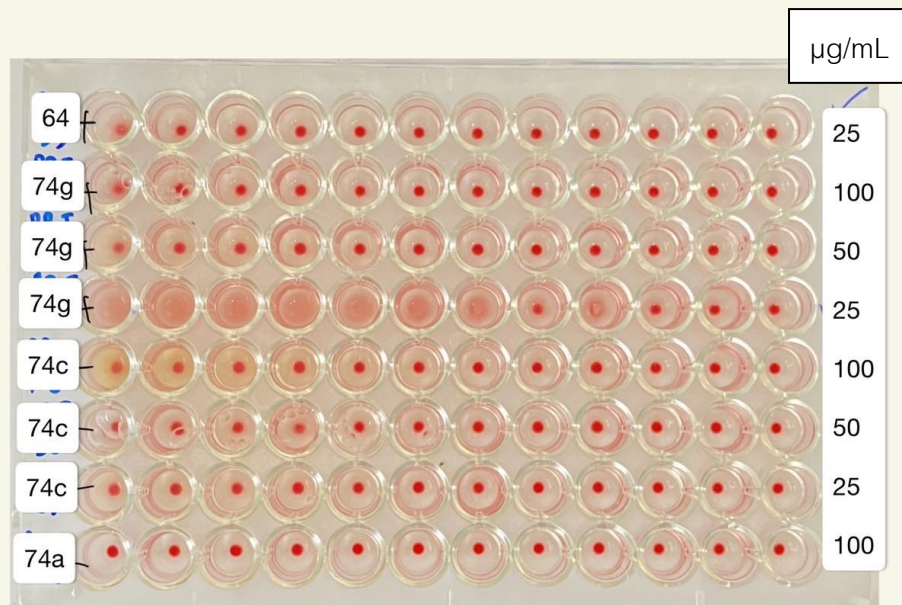
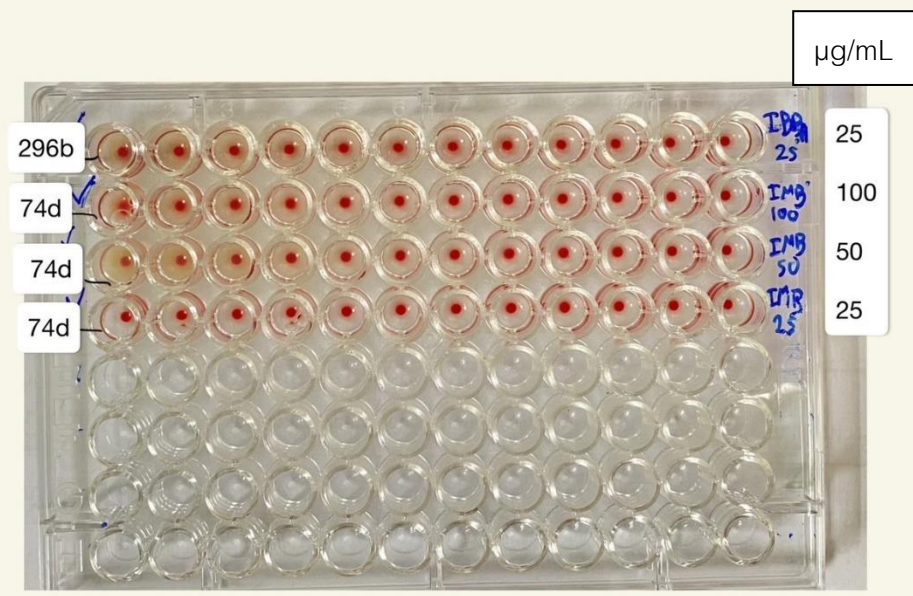
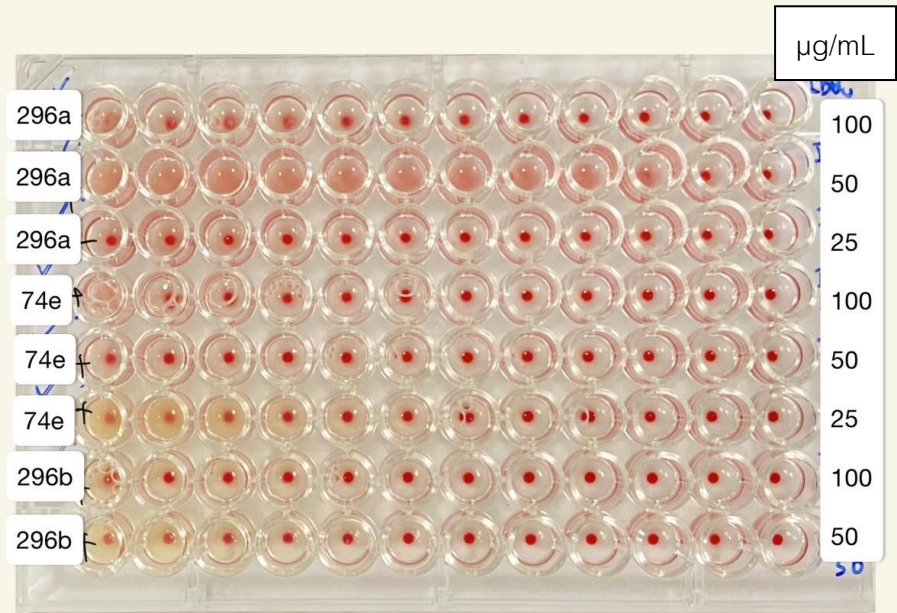


Figure 18. The results of cytotoxicity against Rhesus monkey kidney cells (LLC-MK2).



APPENDIX C
Hemaagglutination assay





VITA

NAME CHANAKAN WINYAKUL

DATE OF BIRTH 05 March 1988

PLACE OF BIRTH Phetchabun

HOME ADDRESS 83/44 Sadiang subdistrict Muang district Phechabun 67000

PUBLICATION Phutdhawong, W., Winyakul, C., Phutdhawong, W.S. (2014).
Synthesis of 3-indolylacetamide derivatives and evaluation
of their plant growth regulator activity. Maejo Int. J. Sci.
Technol., 8, 181-189.
- Poster Presentation
Winyakul, C., Phutdhawong, W., Phutdhawong, W.S. (2012),
Synthesis and antibacterial evaluation of 6,7-dihydro-12H-
benzo[2,3'oxepino[4,5b]indole derivatives, Pure and
Applied Chemistry International Conference (PACCON
2012), 11-13 January 2012, Chiangmai, Thailand.
Winyakul, C., Phutdhawong, W., Phutdhawong, W.S. (2013),
Synthesis and plant growth regulatory activity of indole-
fused seven-membered ring derivatives and
indolecarboxylic acid derivatives, Pure and Applied
Chemistry International Conference (PACCON 2013), 23-25
January 2013, Chonburi, Thailand.